

Dissertation zur Erlangung des Doktorgrades
der Fakultät für Chemie und Pharmazie
der Ludwig-Maximilians-Universität München

Scale-Up of Liposome Manufacturing:
Combining High Pressure Liposome Extrusion
with Drying Technologies



Michael Wiggernhorn
aus Kranenburg

Juli 2007

Erklärung

Diese Dissertation wurde im Sinne von § 13 Abs. 3 bzw. 4 der Promotionsordnung vom 29. Januar 1998 von Herrn Prof. Dr. Gerhard Winter betreut.

Ehrenwörtliche Versicherung

Diese Dissertation wurde selbstständig, ohne unerlaubte Hilfe erarbeitet.

München, am 05. Juli 2007

(Michael Wiggenhorn)

Dissertation eingereicht am 05. Juli 2007

1. Gutachter: Prof. Dr. Gerhard Winter

2. Gutachter: Prof. Dr. Wolfgang Frieß

Mündliche Prüfung am 30. Juli 2007

Acknowledgements

The presented thesis has been investigated and written at the Department of Pharmacy, Pharmaceutical Technology and Biopharmaceutics at the Ludwig-Maximilians-University (LMU) in Munich (Bavaria) under the supervision of Prof. Dr. Gerhard Winter.

First of all, I want to express my greatest gratitude to Prof. Dr. Gerhard Winter, who welcomed me with an open mind and provided me the opportunity to further strengthen my research education in his working group. I am very thankful for his outstanding professional and enthusiastic guidance and for giving me the freedom required for the success of this scientific project. Through all phases I always had the feeling to be in good hands with an overall encouragement. Thanks for this!

Prof. Dr. Wolfgang Frieß, I not only want to say thank you for taking over the co-referee, but particularly for being the second scientific and personal advisor in the last years. The outstanding collaboration between him and Prof. Dr. Winter made practical-working and sharing of ideas to a tremendous resource of knowledge for me. I am very pleased about being part of it.

Many thanks go to Prof. Dr. Geoffrey Lee, from the Department of Pharmaceutical Technology at the Friedrich-Alexander University in Erlangen-Nuernberg, at first for the possibility to use his technical equipment for several times, and also for joining my defence and being part of the oral examination commission.

I deeply appreciate the MediGene AG (Martinsried) for the initiation of this interesting project and the friendly financial support over the last 2 ½ year. Especially, I would like to thank Dr. Heinrich Haas for the supervision of this project from MediGene side and for the many fruitful discussions, numerous inspirations and the freedom to operate in many technical fields. Also, I like to say gratefully thank you to Dr. Klaus Drexler for managing the whole project from the real beginning. Thank you to Dr. Andreas Geissler for the successful collaboration in the patent field.

The other colleagues from MediGene AG in Martinsried and in Neuried, a special acknowledgement belongs to you all, for the assistance in the production and many analytical considerations. It was a pleasure for me to work with you in this straightforward collaboration, which simplified practical things. All of you should be mentioned Armin Bareth, Dr. Brita Schulze, Christina Fingerhut, Dr. Frank Zettl, Dr. Gabriela Kosuthova, Dr. Harald Meissner, Jürgen Seifert, Melanie Reiter, Dr. Michael Rankl, Ursula Fattler, Tawanda Muzorewa, Dr. Georg Belke-Louis and all the colleagues who contributed directly or indirectly to this thesis.

Part of this work was done at Delft University of Technology (The Netherlands) at the Process and Energy Department of Prof. Dr. P. J. Jansens and Prof. Dr. G. J. Witkamp. Thank you very much for providing the possibility and the access to the equipment.

Without my friends from FeyeCon B.V. (Weesp, The Netherlands) the supercritical part of the work would not have been feasible at all. Therefore, my deep thankfulness belongs to you all. Especially to Hubert Pellikaan, who was directly dedicated from the very beginning and Dr. Bas Vermeulen for the assistance at the apparatus. Dr. Andréanne Bouchard for the interesting discussions and the "Separex" considerations. Dr. Vanesa Fernández Cid and Dr. Gerard Hofland for discussions and the careful correction, as well as Dr. Geert Woerlee who supported the project.

From the Department of Pharmaceutical Chemistry at the LMU in Munich, I would like to thank Dr. Holger Lerche for the collaboration with the installation of the Static Headspace Gas Chromatography.

Also I want to appreciate the friendship over the last years to my former lab-colleagues Patricia Plath and Ahmed Youssef and close to the next door Jan Zillies and Klaus Zwioerek. Many thanks go to all other (former-) colleagues and friends from the research groups of Prof. Winter and Prof. Frieß. Especially, to Cornelius, Fritz, Gabi, Dr. Gerhard Simon, Kathrin, Matthias, Richard, Sandra, Silke, Stefan, Tim and Roland. For their quick proof reading I want to thank Lars Schiefelbein and Frank Schaubhut. Two students should be mentioned as well Andrea and Sarah you did a good job.

I would like to thank all my friends at home, in the Netherlands and here in Munich for their friendship and encouragement during the last years. Achim, Christiane, Christoph, Gerrit, Guido, Graham, Hildegard, Jens, Jörg, Jürgen, Kathrin, Ludger, Peter, Petra, Prashant, Roman, Sascha, Simon, Volker, Wouter, and all other.

Finally, and most important I want to appreciate my family and especially my parents for their dedicative encouragement over the last 10 years of studying. My brother Thomas with Kerstin, my sister Elisabeth with Ludger (Simon, Johannes and let´s see) and finally my sister Maria, thank you for being a part of me.

Andrea, you and your love are the best things I will take from Munich. Thanks for being around me and the help for my work, especially in the last month with proof-reading of the thesis.

For my parents / Für meine Eltern

TABLE OF CONTENTS

Chapter 1

Introduction and Objective of the Thesis

1. INTRODUCTION	2
2. LIPOSOMAL PREPARATION	3
3. LIPOSOMAL FORMULATIONS CONTAINING PACLITAXEL	5
4. STABILIZING OF LIPOSOMAL FORMULATIO	6
5. OBJECTIVE OF THE THESIS	8
6. REFERENCES	12

Chapter 2

Optimizing the Freeze-Drying Process of Liposomal Paclitaxel Formulation

1. INTRODUCTION	16
2. MATERIAL AND METHODS	18
2.1 Liposome Preparation.....	18
2.2 Freeze-Drying Method.....	18
2.3 Lipid Analysis.....	19
2.4 Paclitaxel Analysis	19
2.5 Residual Moisture	19
2.6 Differential Scanning Calorimetry Analysis.....	19
2.7 Analysis of Cake Morphology	20
2.8 Size Measurements of Liposomes.....	20
2.9 Residual Ethanol Content.....	20
3. RESULTS AND DISCUSSION	21
3.1 Freeze-Drying Method with Modified Cake Geometry.....	21
3.2 Determination of the Glass Transition Temperature (T_g)	22
3.3 Studies to Optimize the Freeze-Drying Cycle for Placebo Formulations.....	22
3.4 Increasing the Filling Volume to Optimize the FD Process	24
3.4.1 Primary-drying time and residual moisture	25
3.4.2 Cake morphology	26
3.4.3 Liposome properties with increased filling volume	27
3.5 Investigation of the Optimized Filling Volume	28
3.5.1 Characterization of primary-drying.....	28
3.5.2 Residual moisture and organic solvent content.....	30
3.5.3 Cake morphology and effects on storage stability	33
3.5.4 Liposome properties at increased filling volume	35
3.5.5 Effect of filling volume and process parameters on the lipid recovery	37
3.5.6 Effect of the filling volume on the Paclitaxel recovery.....	38
4. CONCLUSIONS.....	40
5. REFERENCES	41

Chapter 3

Spray Freeze-Drying of Liposome Paclitaxel Formulations

1. INTRODUCTION	44
2. MATERIAL AND METHODS	45
2.1 Liposome Preparation.....	45
2.2 Spray-Freezing Methods	45
2.3 Freeze-Drying Method	46
2.4 Freeze-Drying Velocity	47
2.5 Analysis of Pellet Morphology	47
3. RESULTS AND DISCUSSION	48
3.1 Particle Formation processes	48
3.2 Drying velocity.....	49
3.3 Particle Yield and Residual Solvent Content	49
3.4 Particle Size Distribution.....	50
3.5 Residual Moisture	51
3.6 Particle Morphology	52
3.7 Liposome Characterization	53
3.8 Lipid and Paclitaxel Recovery	54
4. CONCLUSIONS.....	55
5. REFERENCES	56

Chapter 4

Development of a Percolative Vacuum-Drying Process

1. INTRODUCTION	59
2. MATERIAL AND METHODS	60
2.1 Liposome Preparation.....	60
2.2 Fluorescence Spectroscopy	60
2.3 Percolative-Drying Method	61
3. RESULTS AND DISCUSSION	62
3.1 The Percolative Drying Concept	62
3.2 Residual Moisture	64
3.3 Particle Morphology	65
3.4 Liposome Properties And Drug Loading	65
3.5 Lipid Recovery	66
4. CONCLUSIONS.....	67
5. REFERENCES	68

Chapter 5

Evaluation of Spray-Drying as a Stabilizing Technique for Liposomes

1. INTRODUCTION	70
2. MATERIAL AND METHODS	71
2.1 Liposome Formation	71
2.2 Spray-Drying Method with Büchi Mini Spray-Dryer	71
2.3 Spray-Drying Method with a Niro SD-Micro.....	72
2.4 Vacuum-Drying	73
2.5 Analysis of Particle Morphology.....	73
2.6 Viscosity Measurements	74
2.7 Light Obscuration	74
2.8 Zeta-Potential	74
3. RESULTS AND DISCUSSION	75
3.1 Feasibility Study of Liposome Spray-Drying.....	75
3.1.1 Particle morphology	75
3.1.2 Product temperature during the process	75
3.1.3 Particle size distribution.....	77
3.1.4 Residual moisture content.....	78
3.1.5 Particle yield	79
3.1.6 Liposome recovery	80
3.1.6.1 Liposome size and polydispersity	80
3.1.6.2 Liposome zeta-potential	83
3.1.7 Physico-chemical characterization	83
3.1.8 Lipid recovery	85
3.2 Spray-Drying of Paclitaxel Formulations.....	85
3.2.1 Particle properties	86
3.2.2 Liposome recovery	87
3.2.3 Paclitaxel recovery.....	87
3.2.4 Particle contamination.....	88
4. CONCLUSIONS.....	89
5. REFERENCES	90

Chapter 6

New Liposome Preparation Technique by Single Pass Extrusion

1. INTRODUCTION	93
2. MATERIAL AND METHODS	95
2.1 Development of the High Pressure Liposome Preparation Method.....	95
2.2 Determination of Density.....	96
2.3 Determination of Surface tension.....	96
3. RESULTS AND DISCUSSION	97
3.1 Liposome Formation using the Conventional Extrusion Process.....	97
3.2 High Pressure Liposome Formation.....	98
3.2.1 Liposome preparation using an orifice nozzle	98
3.2.2 Liposome Preparation using a porous device and the orifice nozzle	102
3.2.2.1 Liposome preparation using a porous device.....	102
3.2.2.2 Considerations on liposome preparation using a porous device.....	103
3.2.2.3 Liposome preparation using a porous device and the orifice nozzle	104
3.3 High Pressure Liposome Formation at High Ethanol Concentrations.....	107
3.3.1 Liposome preparation by ethanol injection	107
3.3.2 Liposome preparation using an orifice nozzle	108
3.3.3 Liposome preparation using a porous device and the orifice nozzle	110
4. CONCLUSIONS.....	113
5. REFERENCES	114

Chapter 7

Preparation and Spray-Drying of Liposomes using a Single-Step Process

1. INTRODUCTION	118
2. MATERIAL AND METHODS	118
2.1 Liposome Preparation and Drying Process	118
3. RESULTS AND DISCUSSION	120
3.1 Particle Formation Process	120
3.2 Particle Morphology	121
3.3 Process Temperatures.....	123
3.4 Particle Yield and Residual Moisture.....	124
3.5 Liposome characterization	126
3.5.1 Using the orifice nozzle	126
3.5.2 Using the porous device and the orifice nozzle	126
3.6 Lipid recovery	127
3.7 Drug loading studies	128
4. CONCLUSIONS.....	131
5. REFERENCES	132

Chapter 8

Inert Spray-Drying using High Organic Solvent Concentrations for the Preparation and Drying of Liposomes

1. INTRODUCTION	134
2. MATERIAL AND METHODS	135
2.1 Liposome Preparation.....	135
2.2 Inert Spray-Drying Method	135
3. RESULTS AND DISCUSSION	137
3.1 Inert Spray-Drying of Multilamellar Suspensions	137
3.1.1 Influence of ethanol concentration on powder yield	137
3.1.2 Influence of ethanol concentration on particle morphology and size	138
3.1.3 Effect of ethanol on residual moisture and residual solvent content	139
3.1.4 Morphological characterization of the inert-spray-dried products.....	141
3.1.5 Liposome Properties.....	142
3.1.5.1 Effect of ethanol on liposome size using the orifice nozzle.....	142
3.1.5.2 Effect of ethanol on liposome size using the porous device / orifice nozzle ...	143
3.1.5.3 Effect of drying temperature on liposome size using the orifice nozzle	143
3.1.6 Lipid recovery after inert spray-drying	144
3.1.7 Drug loading studies	145
3.1.7.1 Using Nile Red as model compound.....	145
3.1.7.2 Drug loading using Coumarin	148
3.2 Inert Spray-Drying of Clear Lipid-Trehalose Solutions	148
3.2.1 Influence of initial ethanol concentration on powder yield	148
3.2.2 Influence of ethanol concentration on particle morphology and size	149
3.2.3 Particle formation model.....	150
3.2.4 Effect of ethanol on residual moisture and residual solvent content	151
3.2.5 Effect of drying temperature on liposome size using the orifice nozzle	153
3.3 Inert Spray-Drying using other Co-Solvents	153
3.3.1 Effect of solvents on residual moisture and residual solvent content.....	153
3.3.2 Effect of other solvents on the liposome size	154
4. CONCLUSIONS.....	155
5. REFERENCES	157

Chapter 9

Liposome Drying using Subcritical- and Supercritical Fluids

1. INTRODUCTION	159
1.1 Thermodynamic Behavior of Supercritical Fluids (SCF)	161
1.2 Ternary System Carbon Dioxide / Ethanol / Water	163
1.3 Particle Formation and Drying Process under Subcritical Conditions	165
1.4 Experimental Outline	166
2. MATERIAL AND METHODS	166
2.1 Material	166
2.2 Methods	167
2.2.1 Liposome Preparation	167
2.2.2 Particle Formation Methods	167
2.2.2.1 Supercritical Spray-Drying Methods	167
2.2.2.2 Subcritical Spray-Drying Method	170
3. RESULTS AND DISCUSSION	170
3.1 Particle Formation and Drying Studies	170
3.1.1 Particle morphology	173
3.1.1.1 Residence tube	173
3.1.1.2 Orifice atomization nozzle	173
3.1.1.3 Gravity feed nozzle	174
3.1.1.4 Concentric coaxial nozzle	175
3.1.2 Particle size distribution	176
3.1.2.1 Residence tube	176
3.1.2.2 Orifice atomization nozzle	177
3.1.2.3 Gravity feed nozzle	177
3.1.2.4 Concentric coaxial nozzle	178
3.1.3 Yield and residual moisture	179
3.1.3.1 Residence tube	179
3.1.3.2 Gravity feed nozzle	180
3.1.3.3 Concentric coaxial nozzle	181
3.1.4 Residual solvents	182
3.1.4.1 Gravity feed nozzle	182
3.1.4.2 Concentric coaxial nozzle	183
3.1.5 X-ray powder diffraction	184
3.2 Liposome Size and Lipid Solubility	185
3.2.1 Liposomes dried by the residence tube	185
3.2.2 Liposomes dried by the gravity feed nozzle	185
3.2.2.1 Liposomes size at varied pressure	185
3.2.2.2 Lipid recovery at varied pressure	186
3.2.2.3 Liposomes size and lipid recovery at varied trehalose concentration	187
3.2.3 Liposomes dried by the concentric coaxial nozzle	188
3.2.3.1 Liposomes size at varied co-solvent flow rate	188
3.2.3.2 Lipid recovery at varied co-solvent flow rate	188

3.3 Phase Diagrams for Methanol, Ethanol, Isopropanol and Acetone.....	189
3.3.1 Particle morphology	190
3.3.2 Particle size distribution.....	191
3.3.3 Yield and residual moisture	192
3.3.4 Residual solvents.....	192
3.3.5 DSC and X-ray powder diffraction	193
3.3.6 Liposome size an lipid recovery	194
3.4 Particle Formation Without a Co-Solvent	195
3.4.1 Particle morphology	196
3.4.2 Particle size distribution.....	196
3.4.3 Yield and residual moisture	197
3.4.4 DSC and X-ray powder diffraction	197
3.4.5 Liposomes size and lipid recovery	198
3.5 Particle Formation Without a Co-Solvent under Different Pressures	198
3.5.1 Particle morphology	199
3.5.2 Particle size distribution.....	200
3.5.3 Yield and residual moisture	201
3.5.4 Liposome size and lipid recovery.....	201
3.6 Particle Formation using Subcritical Conditions.....	202
3.6.1 Particle morphology	202
3.6.2 Particle size distribution.....	202
3.6.3 Yield and residual moisture	203
3.6.4 DSC and X-ray powder diffraction	203
3.6.5 Liposome size and lipid recovery.....	204
3.7 Drug Loading Studies.....	204
3.7.1 Drug loading gravity feed nozzle.....	205
3.7.2 Drug loading without co-solvents	205
3.7.3 Drug loading at subcritical conditions	206
4. CONCLUSIONS.....	208
5. REFERENCES	209

Chapter 10

Summary of the Evaluated Drying Technologies

1. NEW LIPOSOME FORMATION TECHNIQUE	215
2. SCALABILITY AND INDUSTRIAL USE OF THE EVALUATED DRYING TECHNIQUE	215
3. COMPARISON OF THE EVALUATED DRYING TECHNOLOGIES.....	216
3.1 Freeze-Drying	217
3.2 Spray Freeze-Drying	217
3.3 Percolative Vacuum-Drying	217
3.4 Spray-Drying using a Two-Fluid Nozzle	218
3.5 Spray-Drying with an Orifice Nozzle	218
3.6 Inert Spray-Drying with an Orifice Nozzle.....	218
3.7 Subcritical and Supercritical Fluid Drying.....	219
4. CONCLUSIONS.....	219

CHAPTER 1

Introduction and Objective of the Thesis

Abstract:

Liposomes have been studied more than 40 years for various applications. Industrial liposomal products entered the cosmetic field first and several years later the field of tumor therapy. The favorable properties of these colloidal drug carriers include active targeting, ability for drug loading and biocompatibility. Many techniques are used to prepare liposomes also in an industrial production process. However, stabilization and storage problems are still major concerns for the development and approval of such products. Nowadays numerous liposomal products are available on the market either as suspensions or as lyophilized dosage forms. If storage as a liquid form is not feasible due to stability problems, a drying process is required. So far, all dry products are lyophilized due to the lack of sophisticated alternatives. There is a need to further develop new stabilization technologies for large scale production of liposomes to circumvent the time and cost intensive freeze-drying process which is limited in scalability.

1. INTRODUCTION

Liposomes are artificial membranes, in most cases composed of phospholipids like phosphatidylcholines (PC), phosphatidylethanolamines (PE) and phosphatidylserines (PS), enclosing an aqueous compartment. They form spontaneously when phospholipids are placed in an aqueous environment, because of their dual preference to solvents, which was first described by Bangham and Horne in 1962 [1]. Amphiphilic lipids consist of one lipophilic part that is soluble in nonpolar solvents and a hydrophilic part soluble in polar solvents. Liposomes can be classified according to their structural properties or to their preparation method [2,3].

Table 1: Overview of commercially available liposomal products [4]

trade name (FDA approval) product/drug substances	type of dosage form	phospholipids and drug/lipid ratio	liposome type particle size
Abelcet® (1995) Amphotericin B	liposomal suspension	DMPC:DMPG 7:3 molar ratio drug/lipid 1:1 molar ratio	MLV < 5 µm
AmBisome® (2001) Amphotericin B	freeze-dried liposomes	213 mg hyd. soy phosphatidylcholine 84 mg distearoylphosphatidylglycerol 52 mg cholesterol, 0.64 mg α tocopherol drug/lipid 1:1 [w/w]	SUV < 100 nm
DaunoXome® (1996) Daunorubicin citrate	liposomal suspension	distearylphosphatidylcholine/ cholesterol, 2:1 molar ratio lipid/drug 18.7:1 [w/w]	SUV ~ 45 nm
Doxil® (1999) Doxorubicin liposomes	liposomal suspension ready to use	3.19 ml/ml MPEG-DSPE 9.58 mg/ml HSPC 3.19 mg/ml cholesterol drug/lipid 1:6 [w/w]	LUV 100 nm
Myocet® (2006) Doxorubicin liposomes	liposomal suspension	Egg-Pc/cholesterol 1:1 molar ratio drug/lipid 1:1 molar	OLV 180 nm
Visudyne® (2001) Verteporfin® for injection Benzoporphyrin liposomes	freeze-dried liposomes	Egg phosphatidyl glycerol Dimyristoyl phosphatidylcholine Ascorbyl palmitate and butylated hydroxytoluene, 15 mg DS/vial DS/PL 1:7.5-15 weight ration	SUV ~ < 100nm
Junovan® (expected 2007) Muramyltripeptidephosphatidy l-ethanolamine (MTP-PE)	freeze-dried	POPC/DOPS 7:3 [w/w] DS/lipid 1:250 [w/w] tert. butanol	MLV 2-5 µm

An advantage, making liposomes an efficient drug delivery system, is the possibility that both hydrophilic and lipophilic molecules can be entrapped either into the aqueous core or into the lipid bilayer [5]. Due to their structure and the employed lipid molecules, liposomes are biocompatible, biodegradable and relatively non-toxic [6]. The application

of liposomes as drug carriers and pharmaceutical products depends on their colloidal stability, chemical composition, microencapsulating and surface properties. A classification of liposomal products ranges from drug-dosage forms [7] over cosmetic formulations [8] to diagnostics [9] and various applications in the food industry [10]. In drug delivery applications they have been extensively investigated for the delivery of anti-tumor substances [11], antimicrobial agents for treatments of bacterial [12], viral [13] and parasitic induced diseases [14], as well as for the use as immunological adjuvants for vaccines [15]. Other studies demonstrated the entrapment of genes [16] and DNA [17] into liposomal systems. Currently, many clinical studies for liposomal preparations are under investigations and several products have already entered the market (Tab 1).

2. LIPOSOMAL PREPARATION

Since the introduction of liposomes as drug delivery vehicles in the 1970s a comprehensive knowledge on strategies improving stability and on interaction characteristics between drugs and lipid membranes has been gained. The cosmetic industry was the first to launch a product containing liposomes in 1986. It took almost ten more years until the first pharmaceutical product Abelcet[®] reached the market in 1995. Although the successful development of many products has been achieved and extensive investigations have been made over decades, the production and stabilization of liposomal formulations for long term storage is still a major concern.

Particularly the industrial manufacturing of liposomes at a large scale is very challenging, as the production process is complex and consists of several steps. The procedure is based on several production steps, which are varying in complexity and are generally well described. Figure 1 provides an overview on a standard large scale production process for liposomes. As a first step the compounds will be dissolved in an appropriate solvent depending on the properties of the used lipids and drugs. The residual solvent concentration in the formulation must be reduced by an elimination step before continuing the processing of the liposomal formulation. A variety of hydration and homogenization steps can be used. Finally, the sterilization step and the stabilization are important to achieve a stable product. For invasive administration in humans by the parenteral route a sterilization of the liposomal formulations is essential. The most common method is sterile filtration using a 0.2 µm membrane [18]. Also gamma-irradiation [19], heat sterilization of the end product by autoclaving at 121°C [20] or steam sterilization [21] has been used for the sterilization of liposomes.

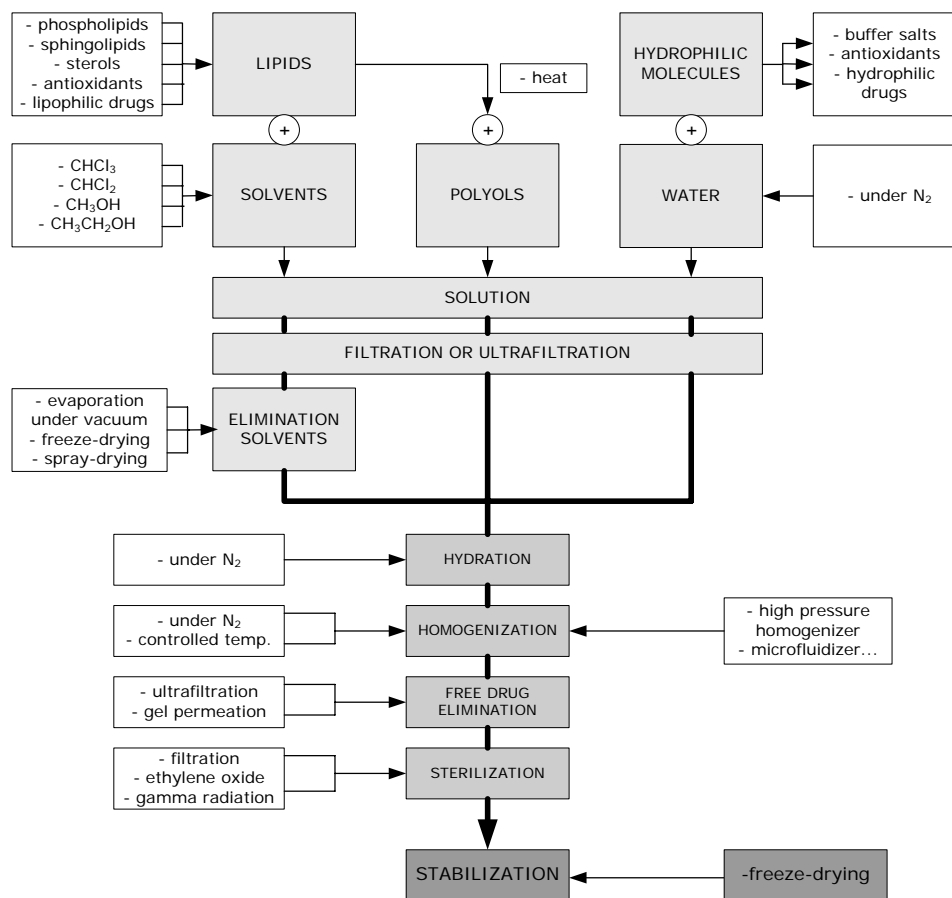


Figure 1: Schematic diagram for a large-scale liposome facility. Adopted from Redziniak et al. 1995 [22].

During the last two decades many of these process steps were further investigated and optimized. One approach described in literature is the introduction of new components or solvents for the preparation of solutions during the production of liposomes [23]. Organic solvents are often employed in liposomal production processes to solubilize either the lipids or the drug. The elimination of such organic solvents and the removal of non-encapsulated drugs are often required for the purification of the final product. In several cases this represents the limiting factor for scalability of the process. Additionally, to avoid stability problems like sedimentation or leakage of liposomes over the storage time the manufacturing with uniform liposomal size distributions by homogenization is particularly important [24]. For certain applications it is necessary to achieve certain liposome sizes e.g. multi-lamellar (MLV), small uni-lamellar (SUVs), large uni-lamellar (LUVs) or multi-vesicular vesicles (MVVs). The effect of liposome size can be important in respect of drug loading [25] or the circulation time accumulation behavior after application to the patient [26].

A simplification of the homogenization method has been another optimization goal within the last years. Therefore, preparation techniques were optimized for example the use of supercritical gases as solvents [27]. Based on the ethanol injection technique new approaches to control the local lipid concentration at the injection point were developed which result in spontaneous formation of homogenous liposomes [28]. Furthermore, new techniques like the jet disperser were introduced to optimize the homogenization step [29].

Another issue, which has to be overcome, is the prevention of physical or chemical reactions occurring during manufacturing or long term storage. Chemical stability is directly dependent on the composition of the liposomes. Lipid peroxidation and hydrolysis are the most common processes of chemical degradation. Physical processes can be the loss of bilayer compounds due to desorption, leakage of entrapped material, vesicle fusion and aggregation. A possible approach to stabilize the liposomal formulations is the removal of water and the production of a dried formulation. Only freeze-drying was used so far as dehydration process for approved products on the market.

3. LIPOSOMAL FORMULATIONS CONTAINING PACLITAXEL

Paclitaxel is an antineoplastic drug used in the treatment of breast and ovarian cancer [30] derived from the bark of *Taxus brevifolia* a natural complex diterpene with an extended side chain necessary for activity on C13 [31]. The major concern of Paclitaxel in formulation development is its low solubility of 1 µg/ml in aqueous media, which makes its formulation challenging [32]. The commercially available formulation Taxol[®] contains 6 mg Paclitaxel, dissolved in 527 mg of the surfactant Cremophor[®] EL (polyethoxylated castor oil) and is finally filled up with water-free ethanol ad 1 ml [33]. Cremophor[®] EL and ethanol are used to improve the solubility of Paclitaxel. A further dilution step with a physiological solution is necessary as described by Straubinger et al. (1995) prior to administration, which often results in a Paclitaxel precipitation [34]. To circumvent irritations for the patient by precipitated material, a filter is placed between the infusion bag and the injection port. Additionally, serious side effects are known for Paclitaxel in combination with Cremophor[®] EL because of an increased toxicity and hypersensitivity reactions [35]. Studies to overcome this drawback by using the solubility enhancer Pluronic[®], a block co-polymer [36], or by the preparation of emulsions [37] revealed no advantages with respect to precipitation and crystallization. The approach of an oral administration of Paclitaxel (Paxene[®]) failed, due to the low absorption and the reduced bioavailability [38]. As an alternative to Cremophor[®] EL based formulations,

liposomal preparations were developed to overcome some of these drawbacks which are summarized by Haas (2005) [39] and Holvoet et al. (2007) [40].

The formulation EndoTAG[®]-1, which is used for our studies is based on cationic liposomes developed as delivery system for neovascular targeting of Paclitaxel inserted into the lipid bilayer [41]. For this formulation the solubility and loading approach was extensively discussed by Gruber in 2004 [42]. The lipid complex is composed of the two lipids N-[1-(2,3-Dioleoyloxy)propyl]-N,N,N,-trimethylammonium chloride (DOTAP-Cl) and 1,2-Dioleoyl-sn-glycero-3-phosphatidyl choline (DOPC). DOTAP-Cl is a synthetic lipid with a positively charged headgroup, whereby DOPC is a zwitterionic natural phospholipids. The mechanism of action in the neovascular cancer therapy of the so called vascular-disrupting agents (VDA) can be described as a specific targeting of blood vessels [43]. In this way the tumor tissue compartment and the newly formed endothelial tumor vasculature are affected. This lead to thrombus formation with a subsequent occlusion of the tumor blood vessel, which may cause a reduction or even a collapse of such vessels [44]. The consequence is a reduced or even hindered tumor supply with nutrients and oxygen [45]. The lipids used for EndoTAG[®]-1 exhibit an overall positive surface charge of the liposome. Due to the negatively charged surface of proliferating or activated endothelial cells in the tumor blood vessels and the positive charge of the liposomes a certain targeting effect of the Paclitaxel loaded liposomes can be achieved [46]. This specific charged phospholipid headgroup of the liposomes itself interacts through electrostatic interactions with negative charges of phospholipid headgroups, which are preferentially expressed on the tumor endothelial cells [47]. The intracellular uptake may occur via endocytosis and/or membrane fusion, but it is not yet fully understood as described by Michaelis and Haas (2007). To approve the unique mode of action, clinical phase II studies are currently carried out [48].

4. STABILIZING OF LIPOSOMAL FORMULATION

In early studies up to the 1990s typically large multi-lamellar vesicles in the micrometer range were employed. More recent investigations revealed an advantage of homogenous uni-lamellar vesicles in the size range of 50 to 200 nm. Liposome stability decreases with increasing size and shows an optimum at a size between 80 and 200 nm. The selection of an appropriate size is always a compromise between loading efficiency, which increases with liposome size, and the resulting decline in stability [49]. Physical and chemical stability of liposomes can be strengthened by choosing a homogenous size, the optimum encapsulation efficiency and by the addition of diverse excipients like antioxidants (e.g. alpha- or gamma tocopherhol) or chelating agents (e.g. like ethylenediaminetetraacetic

acid (EDTA) or diethylene triamine pentaacetic acid (DTPA)). Furthermore, by the optimization of the size and the formulation conditions, liquid formulations can be stable for several years like DauXome[®], Doxil[®] or Myocet[®]. With the addition of appropriate cryoprotectants and lyoprotectants, liquid formulations can also be frozen or lyophilized to enhance the stability. As already mentioned, freeze-drying is exclusively employed as dehydration process for industrial manufacturing and stabilization of approved liposomal products up to the present. Freeze-drying (FD) is extensively discussed as a standard method to stabilize liposomal formulations [50,51,52] and will be discussed more in depth in chapter 2 of this thesis. Besides the commercial Paclitaxel containing liposomal formulations AmBisome[®] and Visudyne[®] are freeze-dried. Other techniques like spray-drying (SD) of liposomal products have been demonstrated to be feasible in several publications for regular manufacturing of dried liposomal formulations especially for the stabilization of lipophilic drugs [53,54,55,56].

The current manufacturing process of the Paclitaxel loaded liposomal formulation EndoTAG[®]-1 was described by Michaelis and Haas (2007). The formulation comprises 3 mol% Paclitaxel in a 10 mM DOTAP-Cl/DOPC lipid matrix dissolved in ethanol. Polydisperse liposomes are formed during the ethanol injection of the Paclitaxel containing lipid stock solutions into an aqueous trehalose phase. The size of the liposomes is adjusted to 200 nm using consecutive extrusion steps through a membrane with pore size of 0.2 μm followed by a sterile filtration step. However, the liquid formulation is not suitable for long term storage over several months due to the crystallization tendency of Paclitaxel. To achieve sufficient storage stability and to avoid Paclitaxel crystallization the formulation is finally lyophilized. This process was developed by Gruber (2004) to achieve a stable product for at least two years.

The major goal of this thesis was to overcome the limitations related to the liposome formation process and the freeze-drying cycle during the preparation of the EndoTAG[®]-1 formulation. Several extrusion cycles are necessary to achieve homogenous liposomes. The blocking of the membrane is a frequent problem related to the extrusion process especially at large scale and can only be overcome by an exchange of the blocked membrane. With filling volumes of 25 ml in a single vial the freeze-drying process takes about one week. For the application to the patient a large volume of the EndoTAG[®]-1 needs to be injected and therefore, several vials are combined to achieve the application volume. Instead of the classical lyophilized cake, free flowable bulk material would be beneficial to simplify the dosing for the patient. A scale-up of the so far used production process is related to tremendous difficulties. Due to the mentioned obstacles in the current production process of the EndoTAG[®]-1 formulation, alternative large scale

production methods for liposome formation and drying of bulk particles should be investigated.

5. OBJECTIVE OF THE THESIS

In this thesis alternative techniques that can be scaled up to industrial scale for the drying and stabilization of the liposomal Paclitaxel formulation EndoTAG[®]-1 should be explored and compared for their ability to achieve an ideal stabilizing effect. The primary goal was to identify possible techniques to preserve the physical and chemical stability of the liposomes and to study the effect of process parameters on the product without performing major changes in the formulation. Furthermore, we focused on particulate drying processes to benefit from the advantages of the free flowing bulk material and flexibility in dosing. The combination of the engineering part, designing new processes with the product quality after the drying was the major task. Several drying techniques were included into the thesis, all with the same liquid formulations but with different approaches to achieve a dry product (Fig 2). Furthermore, to overcome the complex preparation of liposomes a new technique should be developed that allows the formation of homogeneous liposomes within a single process step. With such a process some of the preparation steps described in figure 1 could be replaced and the complexity of an industrial process could be reduced.

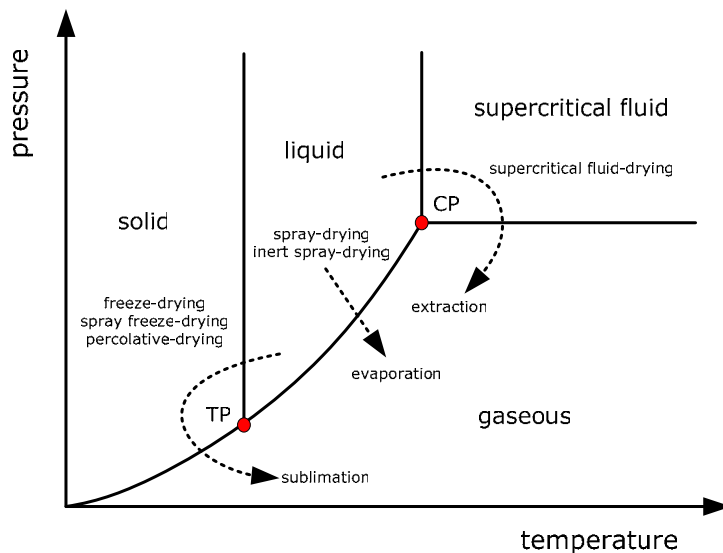


Figure 2: Schematic pressure-temperature diagram with the triple point (TP) and the critical point (CP) and the different phases. The investigated drying pathways from the liquid phase over solid (freeze-drying, spray freeze-drying, percolative vacuum-drying) and supercritical phase (supercritical fluid-drying) and the direct evaporation (spray-drying and inert spray-drying) are shown.

To gain further information on the existing formulation and production process, the freeze-drying (FD) process should be studied and optimized in **chapter 2**. Although freeze-drying is the accepted production technique the process is very time consuming. Therefore, we wanted to increase the efficiency of the lyophilization process by different approaches. One approach was to shorten the drying process by optimizing the sublimation rate. Furthermore, the approach to increase the filling volume for an enhanced productivity was to be tested. Finally, the cake geometry should be varied to investigate the heat and mass transfer properties.

In **chapter 3** spray freeze-drying (SFD) should be evaluated as a method to stabilize liposomes in free flowable dry granules. As no SFD equipment is available at our department, suitable set-ups should be planned and technically implemented, which allow the controlled production of different particle sizes. The impact of process conditions on the particle properties like size and morphology, as well as the liposomal integrity and the drying speed compared to the conventional freeze-drying process should be studied.

In **chapter 4** a new drying method the percolative vacuum-drying (PVD), which combines several aspects of spray freeze-drying, vacuum-drying and atmospheric freeze-drying should be tested as an approach to further enhance the drying process, with special focus on a decrease in drying time. The first task was the implementation of a technical set-up for this non standard process. Generally, the limitations for the sublimation of water are the relatively low driving force of heat and mass transfer resulting in very time consuming processes. The idea was to overcome these limitations and to enhance the sublimation rate by the introduction of a percolation gas streaming through the particle layer. The process parameter should varied to gain deeper knowledge of this new drying-method

Processes like spray-drying (SD) require high drying temperatures but result in a rather quick evaporation of the aqueous content. Therefore, in **chapter 5** such a fast technique should be tested for the manufacturing of small and dry particles from the liposomal formulations. Variations in the solid content and process parameters, like liquid flow rate, nozzle type or temperature and the related physico-chemical properties of the dried powder, as well as the liposomal integrity should be evaluated. These experiments should give insight into the overall preservation of the liposomal integrity during spray drying. An important goal was to perform first studies with Paclitaxel loaded liposomes to test the integrity of Paclitaxel formulations after SD.

During the evaluation of the spray-drying process the idea of using the shear forces of a nozzle to prepare homogenous liposomes originated with the aim to avoid a consecutive extrusion process of multi-lamellar vesicles (MLV). While atomizing the liquid feed by a conventional two-fluid nozzle, the shear forces not only induced a droplet break-up but also exhibited the ability to reduce the size of the liposomes. Based on this assumption we wanted to develop a new liposome preparation technique to obtain small and homogeneously distributed liposomes in a single step by an inline extrusion at high pressure followed by an atomization step. The development of such a process, as well as underlying mechanistic explanations are described in **chapter 6**.

Furthermore, our aim was to transfer the single step liposome formation of chapter 6 into a conventional pilot scale spray-drying apparatus, to subsequently stabilize the formed liposomes by drying. A feasibility study to investigate the liposomal formation in combination with the drying step should be performed, which is the topic of **chapter 7**. By testing several drying conditions an optimum working range, which results in appropriate particle properties and liposomal qualities should be identified.

The results from spray-drying revealed that the temperature exposure during the drying step was in some cases too high resulting in degradation products. For the reduction of the heat capacity necessary to dry the liposomal formulations our intention was to evaluate the addition of organic solvents to the aqueous formulation, which is described in **chapter 8**. Spray-drying of formulations with more than 10 % organic solvent requires special equipment due to the risk of explosion. A closed inert loop spray-drying system allows the processing of organic solvents at all selected temperature. Different organic solvents should be employed to reduce the drying temperature and their impact on the liposomes quality should be analyzed. The idea of the single step liposome formation as described in chapter 5 should be tested in this set-up as well. Furthermore, our aim was to use a molecular disperse solution of lipids and excipients to overcome the spontaneous polydisperse liposome formation by ethanol injection and to further simplify the production method.

The relatively new and promising technology of sub- and supercritical fluids should be tested to dry aqueous liposomal suspension. The main advantages of these techniques are the gentle drying conditions at low temperature around the critical point (**chapter 9**). Several technical set-ups and the impact of the working conditions like pressure, flow rate and co-solvents on the particle characteristics and the liposomal integrity should be

tested. The solubility of lipids in supercritical fluids was an additional challenge to be overcome in order to preserve the integrity of the liposome.

One of the main objectives of the thesis was to finally compare all developed and tested processes for their feasibility to function as an alternative optimized production method for the EndoTAG[®]-1 formulations. In **chapter 10** we therefore intended to give a comprehensive comparison of the processes with respect to product quality and scalability as well as an outlook into necessary investigations.

6. REFERENCES

-
- [1] Bangham, A.D., Horne, R.W., Action of saponin on biological cell membranes, *Nature*, 196: 952-953 (1962).
- [2] New, R.R.C., Influence of liposome characteristics of their properties and fate, in: *Liposomes as tools in basic research and industry*, p: 3-20, Eds. Philippot, J.R., Schuber, F., CRC Press (1995).
- [3] Brandl, M.M., Bachmann, D., Drechsler, M., Bauer, K.H., Liposome preparation using high-pressure homogenizers, in: *Liposome Technol. (2nd Ed.)*, vol 1 p: 49-65, Ed. Gregoriadis, G., CRC Press (1993).
- [4] Van Hoogevest, P., *Liposomal Parenteral Products – Status Anno 2005*, APV Focus group drug delivery newsletter, 1: 4-8 (2006)
- [5] Walde, P., Preparation of vesicles (liposomes), *Encycl. Nanosci. Nanotech.*, vol. 9: 43-79, Eds. Nalwa, H.S., APS (2004).
- [6] Shek, P.N., Barber, R.F., Liposomes: a new generation of drug and vaccine carriers, *Mod. Med. Can.* 41: 314–326 (1986).
- [7] Vemuri, S., Rhodes, C.T., Preparation and characterization of liposomes as therapeutic delivery systems: a review, *Pharm. Acta Helv.*, 70(2): 95-111 (1995).
- [8] Handjani-Vila, R.M.; Ribier, A.; Vanlerberghe, G., Liposomes in the cosmetics industry, in: *Liposome Technol. (2nd Ed.)*, vol 2 p: 201-213, Ed. Gregoriadis, G., CRC Press (1993).
- [9] Phillips, W.T., Delivery of gamma-imaging agents by liposomes, *Adv. Drug Delivery Rev.*, 37(1-3): 13-32 (1999).
- [10] Kirby, C.J., Controlled delivery of functional food ingredients: Opportunities for liposomes in food industry, in: *Liposome Technol. (2nd Ed.)*, vol 2: 215-232, Ed. Gregoriadis, G., CRC Press (1993).
- [11] Lasic, D.D., Papahadjopoulos, Cancer therapy, in *Medical application of liposomes*, p: 221-275, Eds. Lasic, D.D., Papahadjopoulos, Elsevire (1998).
- [12] Agrawal, A.K., Gupta, C.M., Tuftsin-bearing liposomes in treatment of macrophage-based infections, *Adv. Drug Delivery Rev.*, 41(2): 135-146 (2000).
- [13] Lasic, D.D., Novel application of liposomes, *Trends Biotechnol.* 16(7): 307-321 (1998).
- [14] Crommelin, D.J.A., Nassander, U.K., Peeters, P.A.M., Steerenberg, P.A., De Jong, W.H., Eling, W.M.C., Storm, G., Drug-laden liposomes in antitumor therapy and in the treatment of parasitic diseases, *J. Cont. Rel.*, 11(1-3): 233-43 (1990).
- [15] Owais, M., Masood, A.K., Agrewala, J.N., Bisht, D., Gupta, C.M., Use of liposomes as an immunopotentiating delivery system: In perspective of vaccine development, *Scand. J. Immunol.*, 54(1/2): 125-132 (2001).
- [16] Gao, X, Huang, L., Potentiation of cationic liposome - mediated gene delivery by polycations, *Biochemistry*, 35(3): 1027-1036 (1996).
- [17] Gregoriadis, G., Bacon, A., Caparros-Wanderley, W., McCormack, B., A role for liposomes in genetic vaccination, *Vaccine*, 20(Suppl. 5): B1-B9 (2002).
- [18] Ostro, M.J., Industrial application of liposomes: what does that mean?, in: *Liposomes as Drug Carriers*, p: 855-862, Ed. Gregoriadis, G., Wiley&Sons (1988).
- [19] Zuidam, N.J., Lee, S.S.L., Crommelin, D.J.A., Gamma-irradiation of non-frozen, frozen, and freeze-dried liposomes, *Pharm. Res.*, 12(11): 1761-1768 (1995).
- [20] Zuidam, N.J., Lee, S.S., Crommelin, D.J.A., Sterilization of liposomes by heat treatment, *Pharm. Res.*, 10(11): 1591-1596 (1993).
- [21] Tardi, C., Drechsler, M., Bauer, K.H., Brandl, M., Steam sterilization of vesicular phospholipid gels, *Int. J. Pharm.*, 217(1-2): 161-172 (2001).

-
- [22] Redziniak, G., Perrier, P., Marechal, C., Liposomes at the industrial scale, p: 59-67 in: Liposomes as tools in basic research and industry, Eds. Philippot, J.R., Schuber, F., CRC Press (1995).
- [23] Walde, P., Namani, T., Morigaki, K., Hauser, H., Formation and Properties of Fatty Acid Vesicles (Liposomes), in: Liposome Technol. (3rd Ed.), vol 1 p: 1-20, Ed, Gregoriadis, G., informa (2007).
- [24] New, R.R.C., Preparation of Liposomes, in: Liposomes a practical approach, p: 33-104, Ed. New, R.R.C., IRL Press (1990).
- [25] Kulkarni, S.B., Betageri, G.V., Singh, M., Factors affecting microencapsulation of drugs in liposomes, *J. Microencaps.*, 12(3): 229-246 (1995).
- [26] Litzinger, D.C., Buiting, A.M.J., van Rooijen, N., Huang, L., Effect of liposome size on the circulation time and intraorgan distribution of amphipathic poly (ethylene glycol)-containing liposomes, *Biochim. Biophys. Acta, Biomem.* 1190(1): 99-107 (1994).
- [27] Frederiksen, L., Anton, K., van Hoogvest, P., Keller, H.R., Leuenberger, H., Preparation of liposomes encapsulating water-soluble compounds using supercritical carbon dioxide, *J. Pharm. Sci.*, 86(8): 921-928 (1997).
- [28] Wagner, A., Platzgummer, M., Kreismyr, G., Quendler, H., Stiegler, G., Ferko, B., Vecera, G., Vorauer-Uhl, K., Katinger, H., GMP production of liposomes – a new industrial approach, *J. Lip. Res.*, 16(3): 311-319 (2006).
- [29] Klinksiak, B., Schleenstein, D., Hovestad, W., vom Felde, M., Adjustable jet disperser for producing aqueous two-component polyurethane paint emulsions, EP1203036 (2002).
- [30] Wiseman, L.R., Spencer, C.M., Paclitaxel. An update of its use in the treatment of metastatic breast cancer and ovarian and other gynaecological cancers, *Drugs & aging*, 12(4), 305-334 (1998).
- [31] Straubinger, R.M., Sharma, A., Sharma, U.S., Balasubramanian, S.V., Pharmacology and antitumor effect of novel paclitaxel formulations, in: Taxane anticancer agents: basic science and current status, p: 111-123, Eds. Georg, G.I., Chen, T.T., Ojima, I., Vyas, D.M., ACS Symposium Series 583 (1995).
- [32] Adams, J.D., Flora, K.P., Goldspiel, B.R., Wilson, J.W., Arbuck, S.G., Finley, R., Taxol: A history of pharmaceutical development and current pharmaceutical conditions, *J. Nat. Cancer Inst. Mono.*, 15: 141-147 (1993).
- [33] Sharma, A., Mayhew, E., Bolcsak, L., Cavanaugh, C., Harmon, P., Janoff, A., Bernacki, R.J., Activity of Paclitaxel liposome formulations against human ovarian tumor xenografts, *Int. J. Cancer*, 71(1): 103-107 (1997).
- [34] Balasubramanian, S.V., Straubinger, R.M., Taxol-lipid interaction: Taxol-dependent effects on the physical properties of model membranes, *Biochem.*, 33(30): 8941-8947 (1994).
- [35] Straubinger, R.M., Sharma, A., Murray, M., Mayhew, E., Novel Taxol formulations: Taxol – containing liposomes, *J. Nat. Cancer Inst. Monographs* (15): 69-78 (1993).
- [36] Tarr, B.D., Yalkowsky, S.H., A new parenteral vehicle for the administration of some poorly water soluble anti-cancer drugs, *J. Par. Sci. Tech.*, 41(1): 31-33 (1987).
- [37] Tarr, B.D., Sambandan, T.G., Yalkowsky, S.H., A new parenteral emulsion for the administration of taxol, *Pharm. Res.*, 4(2): 162-165 (1987).
- [38] Meerum-Terwoght, J.M., Malingre, M.M., Beijnen, J.H., Ten Bokkel Huinink, W.W., Rosing, H., Koopman, F.J., Van Tellingen, O., Swart, M., Schellens, J.H.M, Coadminstration of oral cyclosporin A enables oral therapy with paclitaxel, *Clin. Cancer Res.*, 5(11): 3379-3384 (1999).
- [39] Haas, H., Entwicklungen neuer Taxan-Formulierungen: Herausforderung an die Galenik, *Pharmazie in unserer Zeit*, 34(2): 2-8 (2005).
- [40] Holvoet, C., van der Heyden, Y., Lories, G, Plaizier-Vercammen, J., Preparation and evaluation of paclitaxel-containing liposomes, *Pharmazie*, 62(2): 126-132 (2007).

-
- [41] Michaelis, U., Haas, H., Targeting of Cationic Liposomes to Endothelial Tissue, in: *Liposome Technol.* (3rd Ed.), vol 3 p: 151-170, Ed. Gregoriadis, G., informa (2007).
- [42] Gruber, F., Untersuchung zur Encapsulierung von Paclitaxel in kationischen Liposomen, Dissertation (2004).
- [43] Siemann, D.W., Bibby, M.C., Dark, G.G., Dicker, A.P., Eskens, F.A.L.M., Horsman, M.R., Marme, D., Lorusso, P.M., Differentiation and definition of vascular- targeted therapies, *Clinical Cancer Res.*, 11(2 Pt 1): 416-420 (2005).
- [44] Tozer, G.M., Kanthou, C., Baguley, B.C., Disrupting tumour blood vessels, *Nature reviews; Cancer*, 5(6): 423-435 (2005).
- [45] Krasnici, S., Werner, A., Eichhorn, M.E., Schmitt-Sody, M., Pahernik, S.A., Sauer, B., Schulze, B., Teifel, M., Michaelis, U., Naujoks, K., Dellian, M., Effect of the surface charge of liposomes on their uptake by angiogenic tumor vessels, *Int. J. Cancer*, 105(4): 561-567 (2003).
- [46] Schmitt-Sody, M., Strieth, S., Krasnici, S., Sauer, B., Schulze, B., Teifel, M., Michaelis, U., Naujoks, K., Dellian, M., Neovascular Targeting Therapy: Paclitaxel Encapsulated in Cationic Liposomes Improves Antitumoral Efficacy, *Clin. Cancer Res.*, 9(6): 2335-2341 (2003).
- [47] Thurston, G., McLean, J.W., Rizen, M., Baluk, P., Haskell, A., Murphy, T.J., Hanahan, D., McDonald, D.M., Cationic liposomes target angiogenic endothelial cells in tumors and chronic inflammation in mice, *J. Clin. Inv.*, 101(7): 1401-1413 (1998).
- [48] <http://www.medigene.de/deutsch/ProjektEndo.php> 06/03/07, 9.00pm (2007).
- [49] Lasic, D.D., Novel application of liposomes, *Trends Biotechnol.*, 16(7): 307-321 (1998).
- [50] Crowe, J.H., Crowe, L.M., Preservation of liposomes by freeze-drying, in: *Liposome Techn.* (2nd Ed.), vol. 1 p: 229-252, Ed. Gregoriadis, G., CRC Press (1993).
- [51] Vanleberghe, G., Handjani, R.M., Storage stability of aqueous dispersions of spherules, GB2013609 (1979).
- [52] Crowe, J.H., Leslie, S.B., Crowe, L.M., Is vitrification sufficient to preserve liposomes during freeze-drying?, *Cryobiology*, 31(4): 355-366 (1994).
- [53] Kikuchi, H., Yamauchi, H., Hirota, S., A spray-drying method for mass-production of liposomes, *Chemical and Pharmaceutical Bulletin*, 39(6): 15-22-1527 (1991).
- [54] Goldbach, P., Borchart, H., Stamm, A., Spray-Drying of Liposomes for a Pulmonary Administration. II. Retention of Encapsulated Materials, *Drug. Dev. Ind. Pharm.*, 19(19): 2623-2636 (1993).
- [55] Lu, D., Hickey, A.J., Liposomal dry powders as aerosols for pulmonary delivery of proteins, *AAPS PharmSciTech*, 6(4): E641-648 (2005).
- [56] Lo, Y-L., Tsai, J-C., Kuo, J-H., Liposomes and disaccharides as carries in spray-dried powder formulations of superoxide dismutase, *J. Cont. Rel.*, 94(2-3): 259-272 (2004).

CHAPTER 2

Optimizing the Freeze-Drying Process of Liposomal Paclitaxel Formulation

Abstract :

The aim of the study was to optimize the existing lyophilization process for a liposomal Paclitaxel formulation and to reduce the drying time by improving the process parameters, increasing the filling volume and changing the cake geometry. The effect of freezing rate, shelf temperature and pressure on primary-drying time was investigated. Furthermore, the filling volume was increased from 25 to 80 ml and the cake geometry, as well as surface structure was modified. By selecting a freezing shelf temperature below the T_g (-47.0°C) and shelf temperatures between -10 and 0°C during the primary drying, the drying time could be significantly reduced compared to the existing lyophilization process, without any quality loss of liposomal properties. Changes of the lyophilization protocol decreased the primary-drying time by about 20 hours. Increasing the filling volume was feasible at least up to 50 ml without causing lipid or Paclitaxel degradation.

1. INTRODUCTION

Freeze-drying (FD) is a well established standard method for the stabilization of liposomal formulations [1,2,3]. However, the time consuming and expensive freeze-drying processes are the major drawbacks. To develop an economical freeze-drying process the formulations need to be optimized to withstand a high temperature during drying, which can reduce the drying time [4]. Many approaches are feasible for developing and optimizing a conventional freeze-drying cycle, e.g. changes in the excipient composition, use of different primary packaging material, variations of filling volumes or changes in the process conditions. Freeze-drying comprises three different stages, beginning with the freezing procedure, followed by the removal of the frozen water (ice) at low temperatures and high vacuum via sublimation (primary-drying) [5]. Finally, absorbed water is further removed at ambient temperature and low vacuum (secondary-drying) [6]. The success and efficiency of each stage of the freeze-drying cycle depends on process variables such as pressure, shelf-temperature and duration [7]. Changing the freezing process can play a major role in determining the product quality. The ice formation process is impacted by several factors like shelf temperature, ramp rate, composition of the formulation in the vial, concentration, fill volume/depth and the interior surface properties of the vial itself. By altering the ice crystal size, the ice distribution pattern across fill volume, the ice interconnection and ice crystal habit, the progress of the subsequent drying steps, as well as the final product appearance can be influenced [8]. Liposome bilayer membranes can be damaged during the freezing step, by mechanical stress during ice crystal formation or chemical stress due to the increased solute concentration. Cryoprotectants have been shown to prevent vesicle fusion and leakage induced by the described processes and to ensure the physical integrity of the liposomes during storage [9]. Non-crystallizing cryoprotectants form amorphous matrices upon freezing. During freezing the transition from a viscous gel to a hard glass with a reduced molecular mobility is referred to as the glass transition temperature of the maximally freeze-concentrated solution. During freeze-drying the product needs to be frozen below T_g' . Accordingly, when amorphous matrices have to be dried, the product temperature during primary drying needs to be kept below T_g' , which consequently can lead to longer drying cycles. The macroscopic collapse temperature of the formulation (T_c) is the temperature above which the freeze-dried cake loses macroscopic structure and collapses during freeze-drying. T_c is usually about 2°C higher than T_g' . The collapse temperature equals the eutectic temperature (T_{eu}), if solutes are crystallizing in the frozen solution. In order to produce an acceptable freeze-dried product, it is in most cases required to freeze-dry a formulation at a product temperature below T_c .

Trehalose is used as cryoprotector in the formulation with the advantage of having a high collapse temperature that allows faster drying rates at higher product temperatures [10]. For the protection of liposomes sugars like trehalose or sucrose are employed in a concentration between 5 and 20 %. They protect the liposomes by interacting directly with the lipid membranes, probably via hydrogen bonding [11]. In order to develop an economical freeze-drying cycle, it is crucial to minimize the process time, especially the primary-drying step. Thereby, the ice sublimation rate is the most important parameter. The sublimation rate is a direct result of the selected parameters (freezing process, temperature, pressure, etc.). First, the freezing process has a deep impact on the surface area of the freeze-dried product and with it the sublimation rate [12]. The ice crystal formation and growth occurs spontaneously and is hard to predict. In general, fast freezing leads to smaller ice crystals, whereas slow freezing results in larger crystals and pores. The larger porosity leads to higher sublimation rates during primary-drying. During primary-drying the solvent is removed from the product and transferred to the condenser. Limitations during lyophilization are mainly induced by the mass transfer through the dried cake structure under high vacuum. Other aspects like stopper and chamber resistance can be neglected. During the last stage of the lyophilization cycle, the secondary-drying step, adsorbed water will be removed and the optimum residual moisture content for long time storage is adjusted. Higher shelf temperatures for a short time should be preferred because of the drastic water desorption deceleration over time [13].

Within in this study the formulation was kept constant and only changes in process parameters, filling volume and cake geometry were evaluated. The current standard freeze-drying process used for the drying of the liposomal Paclitaxel formulation is very time consuming: the primary-drying requires about 90 hours. For storage stability and product quality reasons residual moisture contents below 3 % have to be reached and maintained during storage. Various process conditions for freezing and drying were used in this study and their impact on primary-drying time and product quality was evaluated. Furthermore, the influence of cake structure and filling volume was investigated. Drying of high fill volumes presents additional challenges, due to longer cycle times, which can result in heterogeneity of the cake and non-elegant cake appearance. Another approach evaluated within the study was to modify the cake geometry and with it the resulting surface area with the goal to improve the freeze-drying process.

2. MATERIAL AND METHODS

2.1 LIPOSOME PREPARATION

The ethanol injection technique was used for preparing placebo and drug containing liposomes. Briefly, for the placebo formulation a lipid stock solution of 400 mM DOTAP-Cl (1,2-dioleoyl-3-trimethylammonium-propane-chloride) and DOPC (1,2-dioleoyl-*sn*-glycero-3-phosphocholine) in ethanol was prepared (Merck, Darmstadt, Germany). 25 ml of this lipid stock solution were subsequently injected under stirring into 975 ml 10.5 % [w/v] trehalose solution to result in a total final lipid concentration of 10 mM. The ethanol injection was followed by five cycles of extrusion through a 0.2 μm polycarbonate membrane. The liposomal Paclitaxel containing formulation consisted of molar concentrations 50/47/3 of DOTAP-Cl/DOPC/Paclitaxel (Natural Pharmaceuticals Inc., Beverly, MA, USA) and was prepared in the same way. The liposomal suspension was filled into 100H vials (Schott, Mainz, Germany) with a filling volume between 25 and 80 ml.

2.2 FREEZE-DRYING METHOD

Lyophilization was performed with the freeze-dryer Epsilon 2-12D special (Martin Christ, Osterrode, Germany). The refrigeration system consists of two 4 KW (5.5 hp) generators with an ice capacity of 12 kg. The ice condenser capacity is limited with 10 kg per 24 hours and a minimum ice condenser temperature of -85°C can be reached. The ice condenser has a volume of 35 liters and the drying chamber a size of 350 * 450 * 420 mm and a volume of 150 liters. The vacuum pump has a specific power of 20 m^3/h . For each run a total number of 108 100H vials filled with volumes between 25 and 80 ml were dried. Two of the three shelves were used with a total size of 0.472 m^2 . Several lyophilization cycles were investigated and compared with the conventional lyophilization process for vial freeze-drying (Fig. 1).

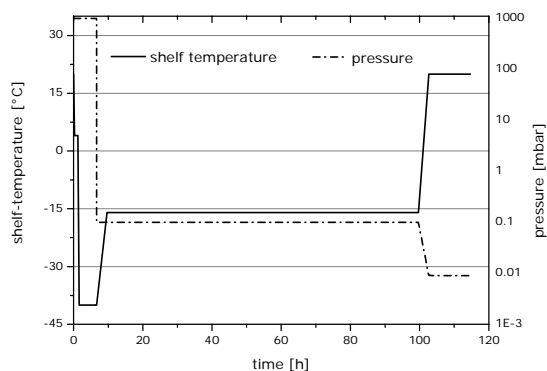


Figure 1: Standard freeze-drying cycle used so far for the liposome drying.

2.3 LIPID ANALYSIS

The concentration of the lipids DOTAP-Cl and DOPC was analyzed by a gradient RP-HPLC using UV/VIS detection at 205 nm. Separation and quantification of the components was carried out using a C8 Luna 5 μ m 100 RP-selected A column (150 x 2 mm). The mobile phase consisted of acetonitrile with 0.1 % TFA and water with 0.1 % TFA (Merck, Darmstadt, Germany). Aliquots of the samples were diluted 1:3 with acetonitrile:water mixtures prior the measurement. The flow rate was set to 0.4 ml/min at an oven temperature of 45°C.

2.4 PACLITAXEL ANALYSIS

Paclitaxel content was analyzed by RP-HPLC using UV/VIS detection at 229 nm. Separation and quantification of the drug was carried out using a LiChroCart 250-4 LiChrospher 60, RP-select B (5 μ m) column. The mobile phase of Acetonitril/THF/Ammoniumacetat 32/12/56 (v/v/v) 2 mM was adjusted to pH 5 with acetic acid (Merck, Darmstadt, Germany). Aliquots of the samples were diluted 1:3 with 2 mM Acetonitril/THF/Ammoniumacetat 48/18/34 (v/v/v) and the pH was adjusted to 5 with acetic acid prior the measurement. The flow rate was set to 1 ml/min at an oven temperature of 35°C.

2.5 RESIDUAL MOISTURE

Residual moisture in freeze-dried cakes was determined by a coulometric Karl Fischer titrator with a Head-Space oven (Analytic Jena AG, Jena, Germany). Sealed dried samples were heated in the oven chamber to 80°C. The vaporized water from the particles was transported into the Karl Fischer chamber via a needle-flexible tube system.

2.6 DIFFERENTIAL SCANNING CALORIMETRY ANALYSIS

DSC was used to study T_g' and T_g of the formulations. Approximately 20 mg of the solution were analyzed in crimped Al-crucibles. For T_g' the samples were cooled down from 20°C to -70°C and reheated to 20°C with a scanning rate of 10 K/min in a Netzsch DSC 204 Phoenix® (Selb, Germany), calibrated with Indium. For the glass transition temperature DSC was preformed using a scanning rate of 10 K/min over an appropriate temperature range. T_g' and T_g (onset and point of inflection) and crystallization (onset, peak and enthalpy) of the excipients were determined during the heating scan.

2.7 ANALYSIS OF CAKE MORPHOLOGY

Wide angle X-ray powder diffraction (XRD) was used to study the morphology of the lyophilized products at the Angstrom scale. The X-ray diffractometer XRD 3000 TT (Seifert, Ahrensburg, Germany) equipped with a copper anode (40 kV, 30 mA, wavelength 0.154178 nm) and a scintillation counter was used. About 10 to 30 mg of the freeze-dried product was placed in the sample carrier and analyzed in the angular range from 5-40 ° 2- θ , with steps of 0.05 ° 2- θ and duration of 2 s per step.

2.8 SIZE MEASUREMENTS OF LIPOSOMES

For each measurement a complete vial was reconstituted with the necessary amount of water to reach the starting concentration. The particle size (z-average) and polydispersity index (PI) of the liposomes was analyzed by photon correlation spectroscopy (PCS) using a Malvern Zetasizer Nano (Malvern Instruments; UK). Each sample was diluted 1:10 with a sterile filtered 10.5 % [w/v] trehalose solution and measured after an equilibration time of 3 minutes. A viscosity of 1.3 cP and refractive index of 1.348 was used for the aqueous phase. The Zetasizer Nano is operating with a 4 mW He-Ne-Laser at 633 nm and non invasive back-scatter technique (NIBS) at a constant temperature of 25°C. The measurements were conducted in the manual mode using 20 sub runs of 10 seconds. The size distribution by intensity and volume was calculated from the correlation function using the multiple narrow mode of the Dispersion Technology Software version 4.00 (Malvern, Herrenberg, Germany). Thereby, the resulting size distributions show the hydrodynamic diameter.

2.9 RESIDUAL ETHANOL CONTENT

The residual ethanol content was determined using a DANI 6000 static headspace gas chromatography (HS-GC) equipped with a HS 850 automated headspace sampler and a flame ionization-detector (FID) (DANI, Monza, Italy). All data were acquired with a HP 3396 series integrator. A DB-WAX (J&W) capillary column 60 m * 0.32 mm i.d. and 0.5 μ m film thickness was used (Agilent Technologies, Waldbronn, Germany). The carrier gas was helium at a flow rate of 5.0 ml/min. Injection was carried out in split mode, with a total split of 1 ml/min (1:1). The injector temperature was 160°C and the detector temperature was set to 240°C. The oven temperature remained constant at 60°C. All samples were provided in a 20 ml headspace vial conditioned in the headspace oven at 80°C under continuous gentle shaking for 2 h. The loop temperature was 110°C with a transfer line temperature of 120°C. Pressurization time for the vial, loop equilibrium and

the injection time were adjusted to 0.16 min. For the quantification methanol was used as internal standard. Furthermore, a calibration curve of 6 reference solutions containing ethanol was set up at the beginning of each run. The calibration curve was calculated by the least square method using the relative areas of ethanol.

3. RESULTS AND DISCUSSION

3.1 FREEZE-DRYING METHOD WITH MODIFIED CAKE GEOMETRY

During the development of the formulation the optimization of the freeze-drying protocol is often neglected. For the given liposomal formulation diverse filling volumes were investigated to identify the optimum between the drying process parameter and the filling volume inside a single vial (Fig 2, (A)). Another technical approach to improve the efficiency of the lyophilization process is to raise the filling volume inside the vials with the same or even longer drying cycles. However, the increased load per drier may overcompensate the process time increase and lead to an optimized economical process with a higher throughput. Freeze-drying of such products usually requires a longer cycle time and can result in product quality problems due to a higher intravial heterogeneity during freezing and drying and unaesthetic cake appearance [14]. Additionally, the cake geometry was modified, because it is obvious that the filling height and the cake thickness have an impact on the drying time (Fig 2, (B)). The so formed thinner shells with a hollow centre could be compared to a sort of spin freezing [15]. By further variations of freezing temperature and freezing rate, the effect of ice crystal formation on product quality was investigated. Finally, the vacuum and the shelf temperature during primary-drying were varied to optimize the drying time. A reduced vacuum will allow the formulations to be dried at higher shelf temperatures and an enhanced heat transfer without compromising the cake appearance [16].

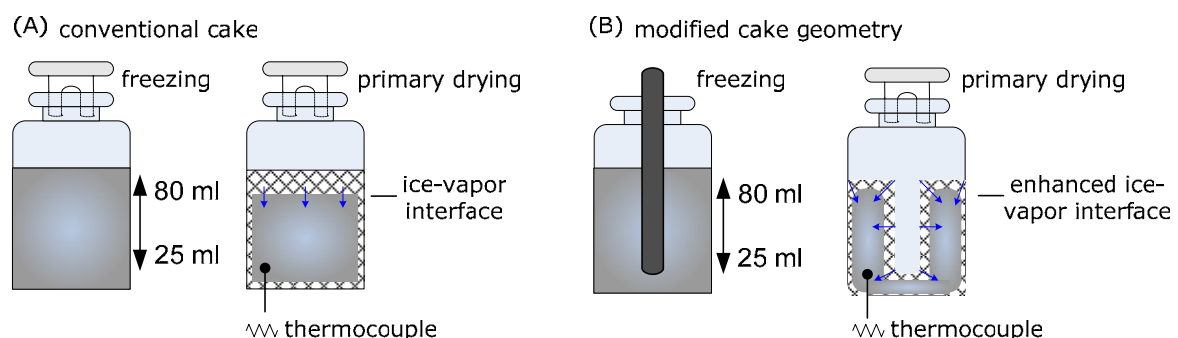


Figure 2: Model of freezing and drying behavior with the sublimation front of a conventionally filled vial (A) and of a vial with an increased surface area (modified cake) by using a removable stick during freezing (B).

3.2 DETERMINATION OF THE GLASS TRANSITION TEMPERATURE (T_g')

The T_g' of the formulations was measured by DSC. A 10.5 % [w/v] trehalose solution, trehalose liposome placebo and the Paclitaxel containing liposomal formulation with/without ethanol were investigated. During liposome formation the lipids were dissolved in ethanol and injected into the aqueous phase, which introduced a small amount of organic solvent into the formulations. To investigate the influence of ethanol on the glass transition, different ethanol concentrations were added to the formulation and the T_g' measured by DSC. At a scanning rate of 10°C/min the point of inflection, which marks the T_g' was -28.5°C for trehalose (Fig 3, left). The combination of trehalose with lipids and also with Paclitaxel itself had no influence on the T_g' . Ethanol however led to a significant reduction of T_g' from -28.5°C without ethanol, to -33.5°C with 2.0 g/l ethanol, to -43.5°C at 7.5 g/l ethanol and finally to -47.0°C at the standard concentration ethanol of 13.8 g/l (Fig 3, right).

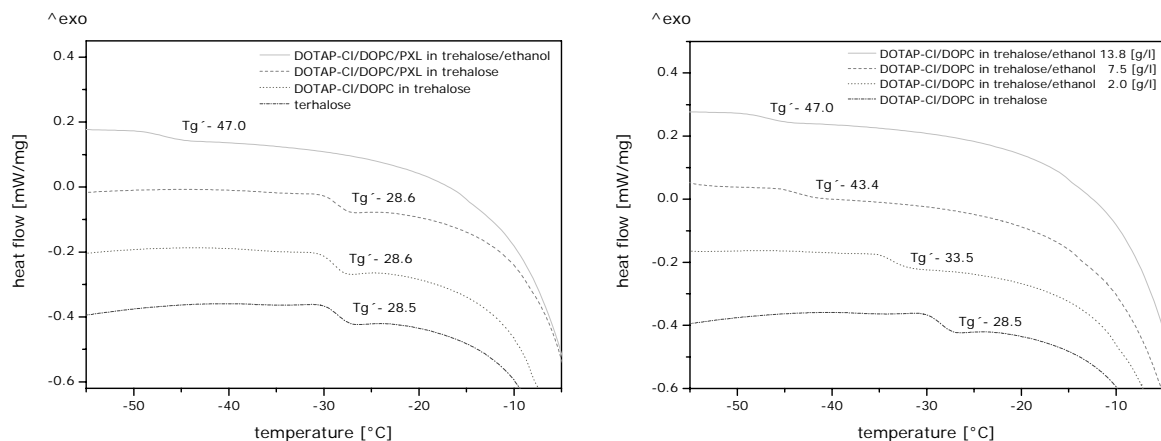


Figure 3: DSC heating scans of trehalose solution, lipid mixtures and lipid/drug mixture with ethanol (left) and the influence of the ethanol content on the T_g' (right).

During lyophilization it is important to freeze the solution below the T_g' to assure a complete solidification of the frozen matrix. The product temperature during the primary-drying has to be adjusted in this range, as well. Potential quality problems in the product can be seen for the used liposomal formulation relatively straightforward, as this would result in leakage and fusion of the liposomes and a variation in the size distribution

3.3 STUDIES TO OPTIMIZE THE FREEZE-DRYING CYCLE FOR PLACEBO FORMULATIONS

In the standard freeze-drying process used so far, the freezing shelf temperature of -40°C is held for 4 hours for 25 ml product. During primary-drying the shelf temperature is raised to -16°C at a chamber pressure of 0.1 mbar and kept for 95 hours. For the

secondary-drying step the shelf temperature is raised to 20°C at a vacuum of 0.009 mbar (Fig 1).

Based on the results of the T_g' determination by DSC, which revealed a T_g' of -47°C for Paclitaxel loaded liposomes, the shelf temperature during freezing was reduced to -50°C to assure complete freezing and solidification. The product temperature during primary-drying was kept below the T_g' by selecting a vacuum of 0.045 mbar. Further changes of the freezing, primary-drying (PD) and secondary-drying (SeD) temperatures are summarized in table 1. By the faster freezing ramp which is realized when the freezing temperature is set to -50°C instead of -40°C, faster primary-drying rates were achieved with a total primary-drying time of 87 hours. In combination with increased shelf temperature during primary-drying, enhanced heat transfer rates with respect to the higher vacuum during primary-drying resulted in faster sublimation rates [17].

Table 1: Summarized process conditions for the first optimization round.

drying run No.	freezing temp [°C]	freezing ramp [°C/min]	primary drying temp [°C]	vacuum PD [mbar]	product temp [°C]	secondary-drying temp [°C]	vacuum SeD [mbar]
1	-40	0.18	-16	0.1	-30	20	0.01
2	-65*	0.28	-16	0.1	-35	20	0.009
3	-50	0.30	-16	0.045	-34	20	0.009
4	-50	0.31	-10	0.045	-35	20	0.009
5	-50	0.31	-5	0.045	-35	20	0.009
6	-50**	0.30	-5	0.045	-34	20	0.009

* two step freezing to -50°C hold for two hours than down to -65°C; ** annealing step (-20°C / 2h)

When increasing the shelf temperature during primary-drying from -16°C to -5°C the lyophilization time could be reduced from 87 hours down to 68 hours without affecting liposome size and polydispersity (Fig 4, right). A higher vacuum during primary-drying results in an optimized pressure difference between the vapor pressure of ice and the partial pressure of water in the chamber [18]. A compromise between a high sublimation rate and a homogenous heat transfer was necessary, and a combination of higher shelf temperature and a higher vacuum was preferred. This could be achieved by freezing down to -50°C and increasing the shelf temperature during primary-drying from -16 to -10 and -5°C. The primary-drying time was reduced from 87 hours at -16°C to 68 hours at -5°C, a decline of 23 %. Additionally, with increasing the primary-drying shelf temperature the residual moisture decreased and reached the lowest value of 0.3 % at a shelf temperature of -10°C and a vacuum during PD of 0.045 mbar (Fig 4, left). During

secondary-drying the absorbed water is removed by the high vacuum of 0.009 mbar. The liposome properties after the different drying protocols are shown in figure 4 (right). Favorable liposome properties with polydispersity indices of 0.16 and 0.14 were obtained for the lyophilization cycle with a very low freezing temperature of -65°C (drying run no. 2) and the lyophilization cycle with a freezing temperature of -50°C and a shelf temperature primary-drying of -10°C (drying run no. 4). An annealing step resulted in liposomes with a high polydispersity index indicating fusion and aggregation of liposomes. Furthermore, more favorable liposome properties with a polydispersity index of 0.16 were obtained when drying at a reduced product temperature of -35°C compared to -30°C at a changed vacuum.

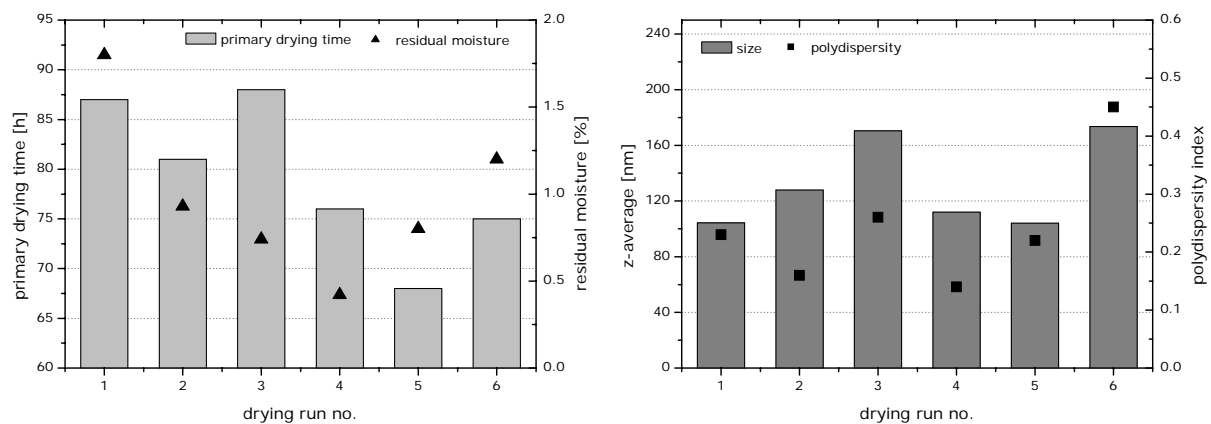


Figure 4: Primary-drying time and residual moisture (left) and the corresponding liposome size and polydispersity index (right) for the drying runs described in table 1.

The first optimization studies resulted in more advantageous process conditions regarding process time, compared to the conventional freeze-drying cycle. The combination of a decreased freezing temperature of -50°C and optimized mass transfer at higher vacuum of 0.045 mbar during primary-drying were responsible for the result [19,20]. The higher shelf temperature of -10°C or -5°C reduced the primary-drying time by about 14 respectively 20 hours. A further increase in shelf temperature can result in too high vaporization rates, at which the solvent permeates through the already dried layer above the solvent-vapor front [21].

3.4 INCREASING THE FILLING VOLUME TO OPTIMIZE THE FD PROCESS

As a second approach to increase the efficiency of the lyophilization cycle, experiments with increasing filling volume were conducted. The filling volume of the 100H vial was

raised from the initial 25 ml to 80 ml for placebo formulations and freeze-drying was performed with two different freezing procedures (Tab 2).

Table 2: Process conditions used for lyophilization of variable filling volumes of placebo formulation.

freezing temp. (F) [°C]	primary-drying temp. (PD) [°C]	vacuum PD [mbar]	secondary-drying temp. [°C]	vacuum SeD [mbar]	filling volume [ml]
-40	-5	0.045	20	0.009	25 – 80
-50	-5	0.045	20	0.009	25 – 60

3.4.1 Primary-drying time and residual moisture

The primary-drying time of the placebo formulations depends on the freezing temperature and on the filling volume of the vials (Fig. 5, left). When using the lower shelf temperature of -50°C during freezing, the primary-drying time was reduced by about 30 hours. This is indicative for an increased sublimation rate compared to the shelf temperature of -40°C . At -40°C the product is not completely solidified and the temperature increase during primary-drying resulted in unstable matrix with higher mobility and higher resistance, due to closed pores. With higher filling volumes, the duration of primary-drying increased drastically due to the rising dry layer resistance of the higher cakes. Although drying time increased with filling volume the processes were more efficient. When comparing the calculated time required to dry one ml of the formulation at different filling volumes (Fig 5, right) the higher efficiency of the process becomes obvious. For freezing down to -50°C an improvement of 20 % could be achieved compared to the conventional process.

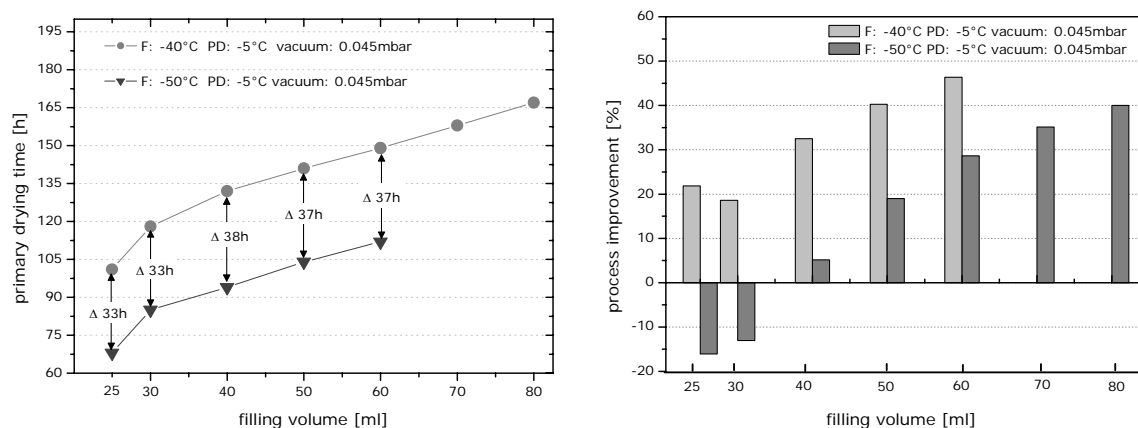


Figure 5: Duration of primary-drying with increasing filling volumes (left) and the process improvement compared to the conventional freeze-drying process (right) for freezing temperatures of -40 and -50°C and primary-drying at shelf temperature of -5°C and a vacuum of 0.045 mbar.

The residual moisture of the dried products ranged below 1.5 % for filling volumes up to 60 ml for both studied freezing protocols (Fig. 6). When the filling volume exceeded 60 ml the residual moisture level stepped up above 3 %. Additionally, at a higher freezing rate of 0.3°C/min, when setting the shelf temperature during freezing down to -50°C, larger ice crystals can form when crystal growth is more rapid than ice nucleation. Such a freezing procedure, especially at high filling volumes can create heterogeneity in solute distribution [22]. When the rate of the nuclei formation is greater than the ice crystal growth, nearly instantaneous ice crystal formation occurs throughout the sample, which leads to a uniform intravial distribution of solutes in the vial [23]. With a homogenous ice crystal distribution the sublimation was enlarged also for high filling volumes. So far the optimum can be described with a high freezing rate and filling volumes up to 50 ml.

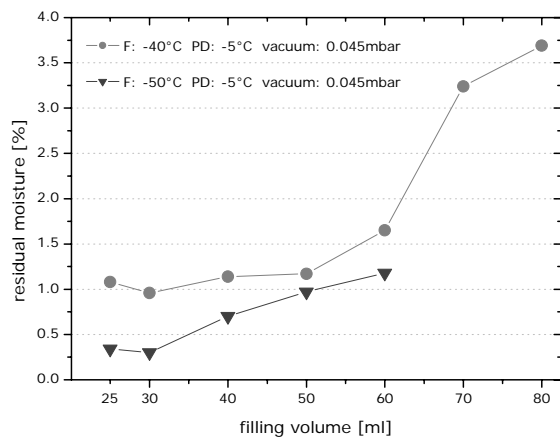


Figure 6: Residual moisture of the freeze-dried products dried with freezing temperatures of -40 and -50°C and primary-drying at a shelf temperature of -5°C and a vacuum of 0.045 mbar.

3.4.2 Cake morphology

The morphology of the dried placebo formulations was analyzed by powder X-ray diffraction. Amorphous samples were obtained for filling volumes up to 60 ml when using the freezing shelf temperature of -40°C and -50°C (data not shown) and primary-drying conditions of -5°C shelf temperature at a vacuum of 0.045 mbar (Fig 7, left). Only when the filling volume was increased to 70 and 80 ml distinct peaks of crystalline trehalose were detected. The crystallization can be attributed to the increased residual moisture level in these cakes, which can facilitate crystallization (Fig 7, right) [24].

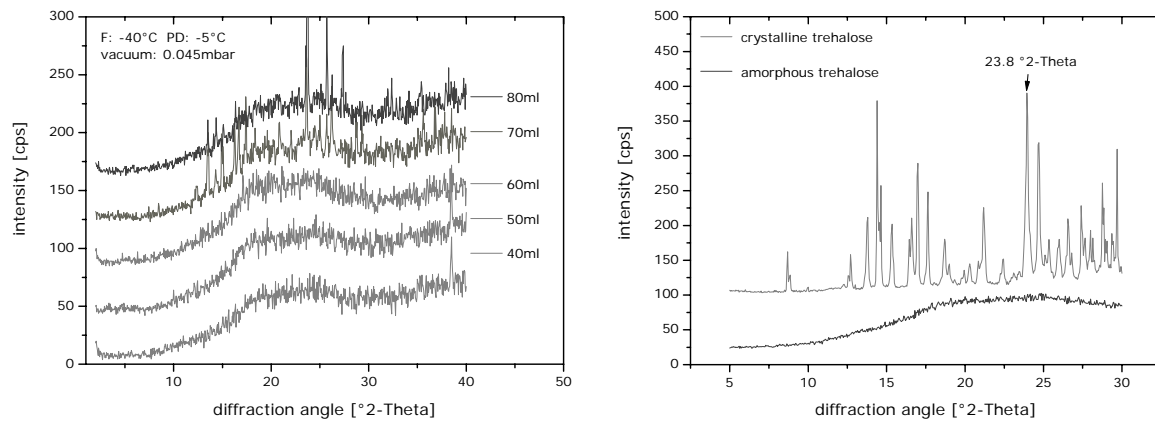


Figure 7: X-ray diffraction pattern of lyophilized placebo formulations using freezing shelf temperature of -40°C and primary-drying at -5°C at a vacuum of 0.045 mbar (left) and comparative X-ray diffraction pattern of crystalline and amorphous trehalose (right).

3.4.3 Liposome properties with increased filling volume

Liposome size and polydispersity in the placebo formulations were neither affected by the freezing-drying protocol nor by the filling volume (Fig. 8, left). The liposome size was about 100 nm with a polydispersity between 0.2 and 0.25, which was comparable to the values before lyophilization with a size of 120 nm and a PI of 0.19. After 12 months storage at 5°C , the liposome size of about 100 nm could be retained for both freezing protocols and all filling volumes (Fig. 8, right). The polydispersity on the other hand remained more stable for products using the freezing temperature of -50°C . No obvious disadvantage could be determined for the high filling volumes of 70 and 80 ml, although they exhibited higher residual moisture levels and crystallization after lyophilization.

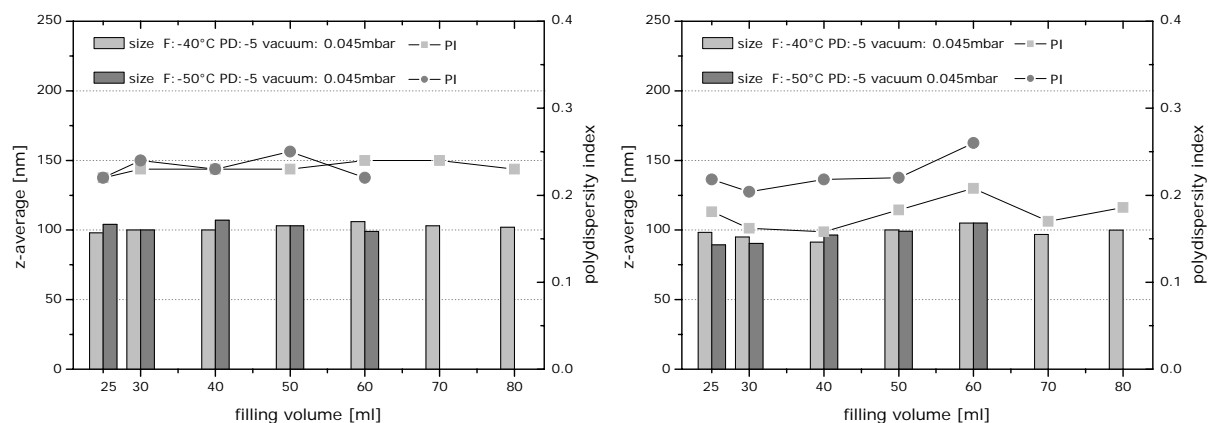


Figure 8: Liposome size and polydispersity for the reconstituted cakes at filling volumes between 25 and 80 ml after lyophilization using freezing shelf temperatures of -40°C and -50°C , primary-drying temperature of -5°C at a vacuum of 0.045 mbar (left) and after 12 months storage at 5°C (right).

3.5 INVESTIGATION OF THE OPTIMIZED FILLING VOLUME

To overcome the limitations of mass transfer in conventional cakes with high filling volumes a modified cake geometry was evaluated. An enlarged surface area could be assigned to the cakes with the modified geometry. This modification in cake geometry and the related change in drying behavior could help to clarify the impact of surface area on drying behavior and mass transfer. Moreover, it will be an alternative approach to optimize the lyophilization time. The filling volume of a 100H vial was raised from the initial 25 ml to 80 ml for a conventional cake and directly compared to the cakes with modified cake geometry for Paclitaxel loaded formulations (Tab 3)

Table 3: Process conditions: freezing temperature and shelf temperatures during primary- and secondary-drying with variable filling volumes of Paclitaxel formulation.

freezing temp (F) [°C]	primary drying temp (PD) [°C]	vacuum PD [mbar]	secondary-drying temp [°C]	vacuum SeD [mbar]	conventional cake filling volume [ml]	modified cake filling volume [ml]
-50	-10	0.045	20	0.009	25 - 80	-
-50	-5	0.045	20	0.009	25 - 80	30 - 80
-50	0	0.045	20	0.009	25 - 80	30 - 80
-50	0	0.009	20	0.009	25 - 80	30 - 80

The thermal contact and therefore the heat transfer between the shelf surface and the vial is known to be small, because only a limited area of the vial has direct contact with the shelf surface. Based on this consideration, Pikal et al. (1984) observed a preferential sublimation of ice from the wall of the vial into the centre [18]. With the additional cake surface the distribution and sublimation of ice would change and should result in an enhanced drying process.

3.5.1 Characterization of primary-drying

The product temperature profiles are exemplarily shown for the process with a freezing shelf temperature of -50°C , primary-drying temperature of 0°C at a vacuum of 0.045 mbar. The remarkable differences in the temperature profile between the processes when using the conventional cake (Fig 9, left) and when using the modified cake geometry (Fig 9, right) can be assigned to the changed drying behavior related to the different sublimation interface. Conventional cakes basically dry from the top to the bottom with simultaneous minor drying from the wall into the centre. The temperature

profiles obtained by the thermocouples reveal a constant temperature increase already at the beginning of the primary-drying step. With the modified cake an enlarged ice-vapor interface and a thinner layer were present leading to a later but steeper increase in product temperature.

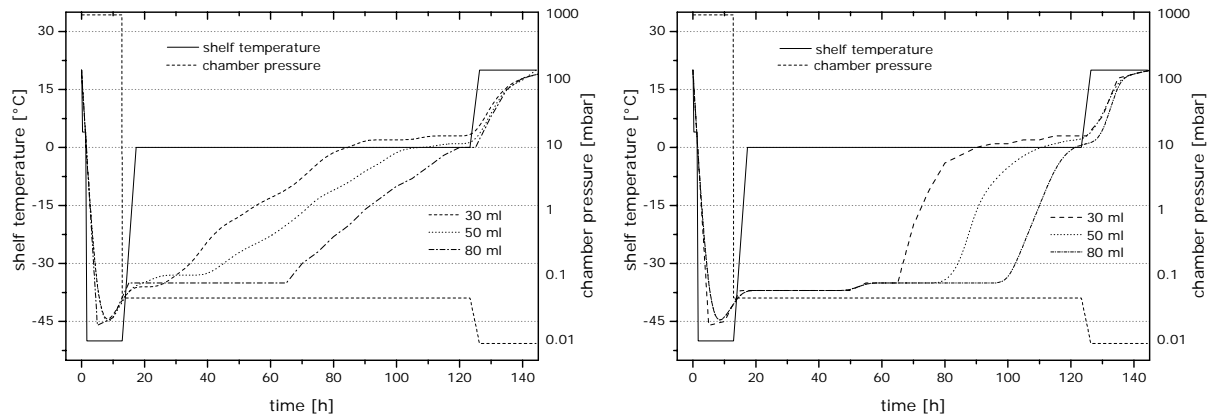


Figure 9: Freeze-drying process temperature profiles obtained from the same drying cycle with product temperature during the drying stages at filling volume of 30, 50 and 80 ml by the conventional cake (left) and the modified cake (right).

Depending on shelf temperature and chamber pressure the drying time increased with increasing filling volumes for the conventional cake structure at all conditions (Fig 10, left). Compared to the conventional drying process for almost all conditions and filling volumes the drying time could be reduced (Fig 10, right). Depending on vacuum and shelf temperature time savings up to 60 % were achieved. An optimum filling volume of 50 ml per vial could be suggested, because a further increase did not substantially improve the process efficiency.

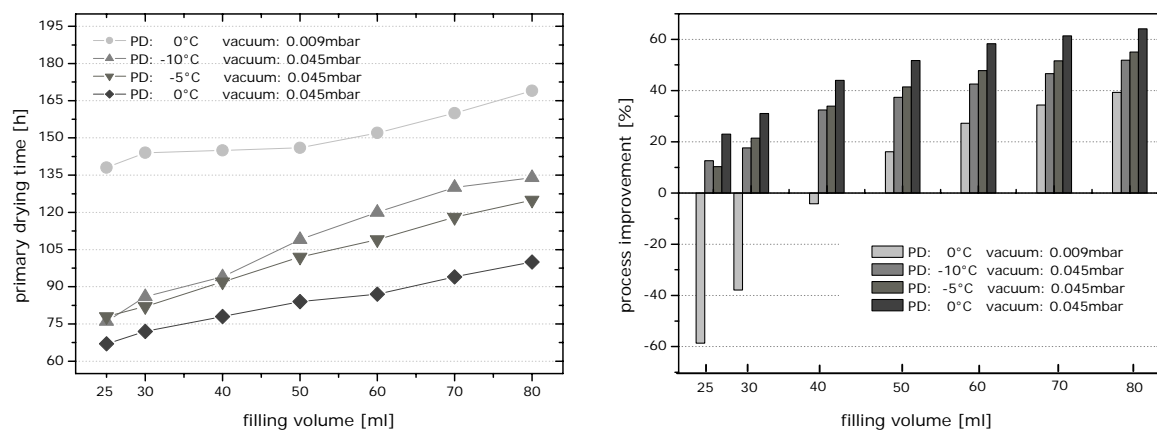


Figure 10: Primary-drying time of different processes for conventional cakes (left) and process improvement during primary-drying compared to the conventional process (right).

With the modified cake geometry the primary-drying time increased with filling volume comparable to the conventional cake structure (Fig 11, left). Only at a chamber pressure of 0.009 mbar a significant reduction of the primary-drying time was achieved for all filling volumes (Fig 11, right). At the other process conditions only a minor time saving could be achieved due to the additional surface area.

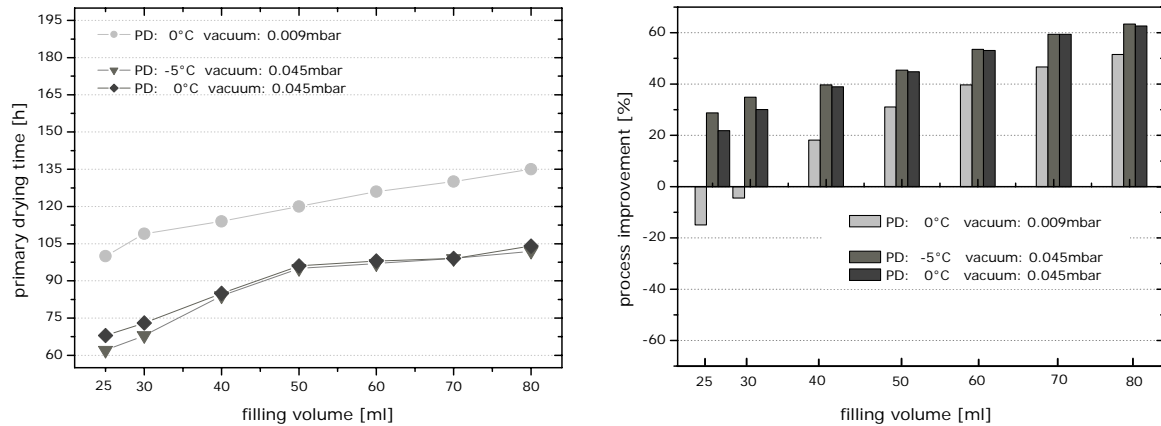


Figure 11: Primary-drying time of different processes for the modified cakes (left) and process improvement during primary-drying compared to the conventional process (right).

The primary-drying time is influenced by sublimation rate, heat and mass transfer. During the drying progress of a conventional cake, the heat transfer into the centre of the cake levels down because of the reduced heat conductivity of the dried regions [25]. With the introduction of the hole within the modified cake the maximum distance, which has to be overcome by the heat transfer is reduced with the consequence of a reduced primary-drying time. This effect is most pronounced when the sublimation rate is low e.g. at a high vacuum of 0.009 mbar or a low shelf temperature of -10°C . At sufficient high heat transfer rates at a shelf temperature of 0°C and a vacuum of 0.045 mbar primary-drying time was not reduced for the modified cakes. This indicates that the thickness of the drying layer does not primarily influence the sublimation rate, which is in agreement with Ybema et al. (1995) [26]. For this reason, the heat transfer and the heat conductivity are the more relevant factors for the drying speed of high filling volumes.

3.5.2 Residual moisture and organic solvent content

Generally, the residual moisture of a freeze-dried product should be as low as possible [27]. It became obvious when comparing the residual moisture levels of the dried products that water vapor transfer rates were affected by the cake geometry. The residual moisture content of the conventional cakes increased with the filling volume (Fig 12, left). For the cakes with modified cake geometry the residual moisture could be kept

below 0.5 % even for the higher filling volumes of 70 and 80 ml (Fig. 12, right), whereas residual moistures of about 1 % were obtained at regular conditions.

Considering the replacement theory by Tsvetkova et al. (1998) sugars can replace water molecules bound to the lipid headgroups after drying [28]. At a higher residual moisture content a larger amount of water molecules can still interact with the lipid headgroups. This can result in significantly improved storage stability and the assumption that a certain amount of water is beneficial, which is around 0.5 %.

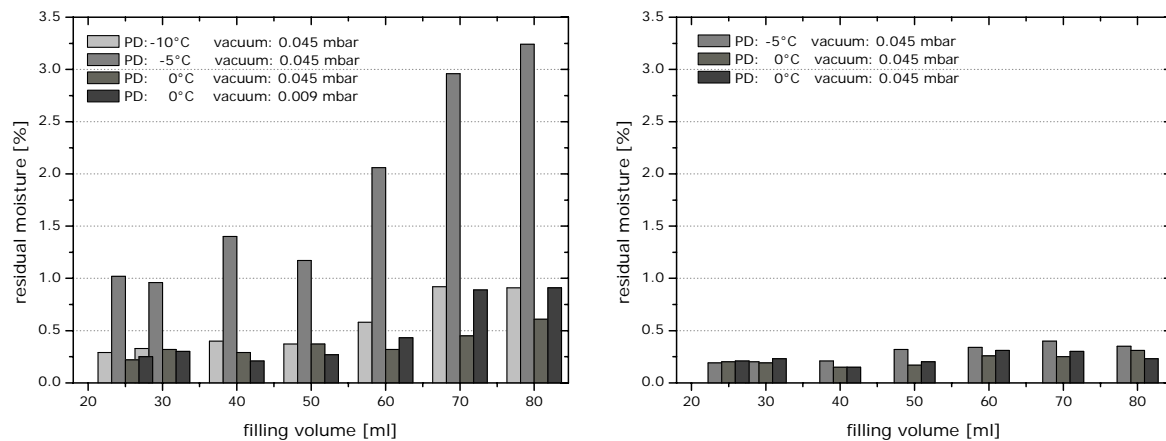


Figure 12: Residual moisture of products produced by different processes at conventional cake (left) and at conditions with modified cake geometry (right).

Since the liposomal formulations contain ethanol, it is important to determine the residual ethanol content after lyophilization. Organic solvents like ethanol are known for their incomplete evaporation from the freeze-dried product during secondary-drying [29,30]. According to the ICH Guidelines, ethanol is a class 3 solvent with low toxicity potential, but the solvent concentration should nevertheless as low as possible [31]. The residual amount of ethanol after freeze-drying was investigated for the different drying processes and cake geometries. The residual ethanol content was only marginally affected by freezing temperature, shelf temperatures or vacuum applied during the process. Apparently, a residual ethanol concentration of about 5500 ppm was retained in the lyophilized product for filling volumes between 25 and 80 ml (Fig 13, left). Moreover, different pressures during primary-drying and variations in secondary-drying could not reduce the retention of ethanol in the cake. For the residual ethanol content of the samples dried at a vacuum of 0.045 mbar and a shelf temperature of 0°C a reduction of the ethanol content to about 3500 to 4000 ppm was achieved by the modified cake geometry (Fig. 13, right). However, the residual ethanol content varied between 4500 and 6000 ppm within the conventional cake.

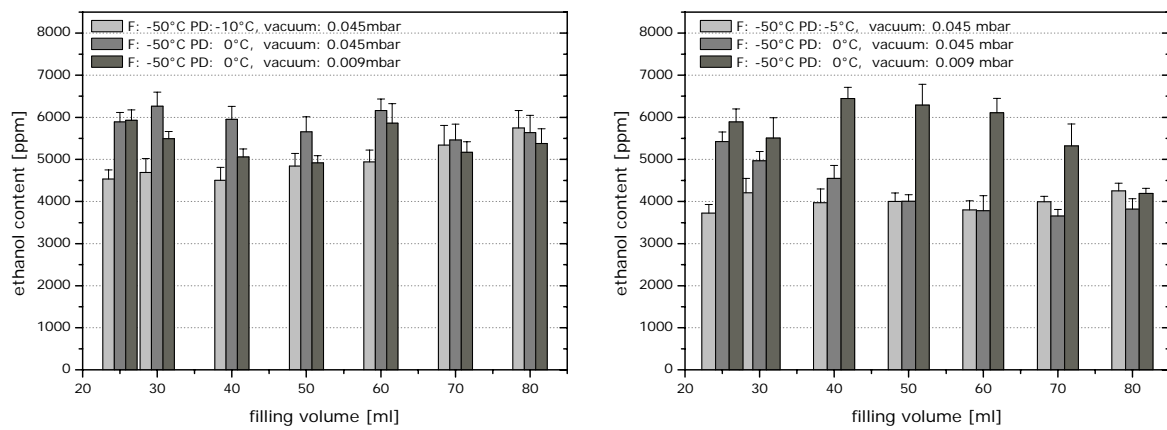


Figure 13: Residual ethanol content of products produced by different processes at the conventional cake (left) and at conditions with modified cake geometry (right).

The relatively high retention levels of ethanol after lyophilization indicate a specific binding of ethanol to the used excipients and components. Especially the high amount of trehalose in the lyophilized product can be responsible for this effect. The retention of ethanol in amorphous sugars is ascribed to intermolecular hydrogen bonding between the sugar molecules and ethanol during lyophilization [32]. To verify this assumption, trehalose formulations with increasing ethanol concentrations were lyophilized with the process shown in figure 14 (left). The data suggested that more ethanol remained bound to the amorphous trehalose when increasing the initial ethanol concentration (Fig 14, right). Furthermore, a saturation/retention level of ethanol was observed between 5000 and 10000 ppm, which was in agreement with the residual ethanol concentration measured for the varied drying processes. Even after grinding of freeze-dried material the organic volatiles remained entrapped in microregions [33]. However, it was feasible to also dry the high ethanol concentration (> 10 %) without any indications of collapse, although such formulations are known to be difficult to dry [34].

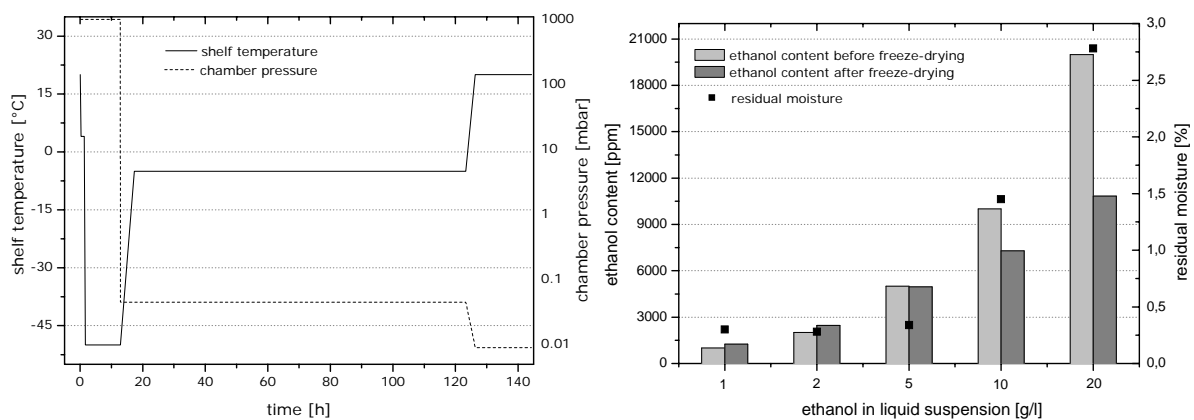


Figure 14: Freeze-drying process for varied ethanol concentrations (left) and the residual ethanol and moisture content of freeze-dried trehalose with increased ethanol content in the formulation (right)

3.5.3 Cake morphology and effects on storage stability

DSC and X-ray diffraction were used to characterize the morphology of the freeze-dried products. The morphology of the cakes was analyzed, as it can affect the storage stability of the formulations and affect liposome integrity and fusion [35]. To characterize the amorphous phase the glass transition temperature was determined by DSC for conventionally lyophilized cakes and cakes with modified geometry. The glass transition temperature was around 75°C for the majority of the studied formulations. With increasing filling volumes the T_g remained constant (Fig 15). Lower T_g values of about 40°C on the other hand were determined for conventional cakes dried at a shelf temperature of -5°C and a vacuum of 0.045 mbar due to the high residual moisture content.

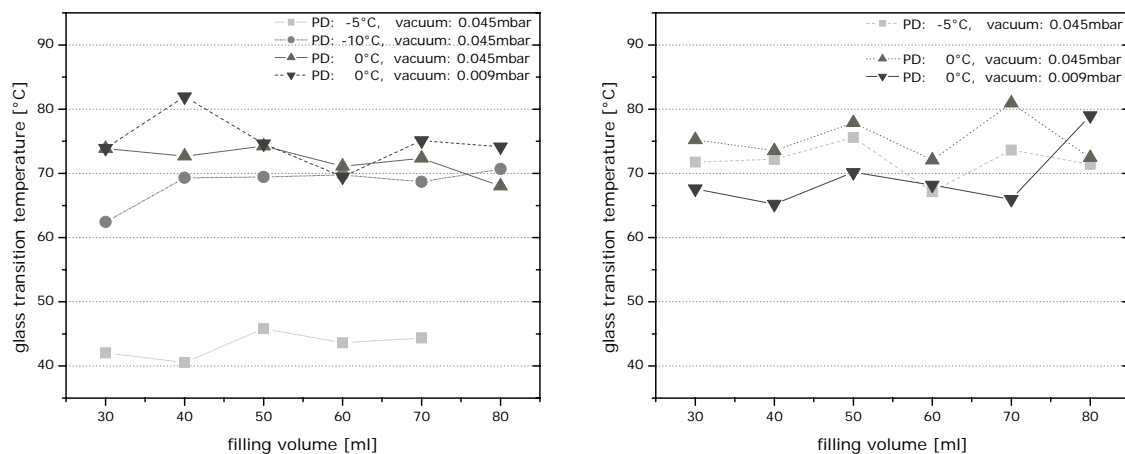


Figure 15: Glass transition temperature (T_g) of lyophilized conventional cakes (left) and at conditions with modified cake geometry (right).

To a great extent the amorphous state of the conventional cakes was assured after the studied processes (Fig. 16). The XRD diffraction pattern of a freeze-dried sample displayed a maximum in the range from 17 to 25° 2-Theta with the maxima at about 20 and 24° 2-Theta, corresponding to lattice spacings of about 4.4 and 3.7 Å, respectively. At a shelf temperature of -5°C and a vacuum of 0.045 mbar during primary-drying some peaks indicate the presence of crystalline trehalose (Fig 16, (B)). The higher residual moisture content resulted in a crystalline structure during the storage, especially at moisture content above 4 % (compare chapter 9).

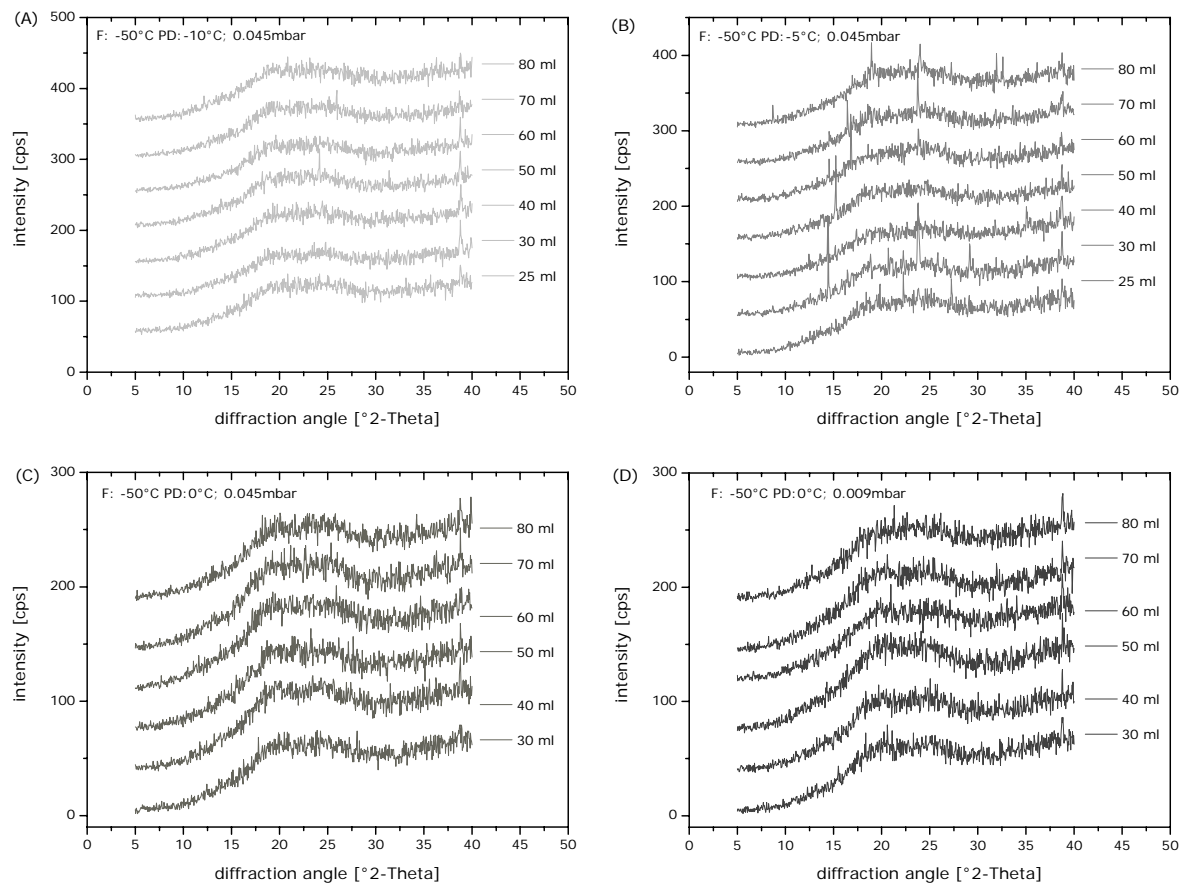


Figure 16: X-ray diffraction pattern of conventional lyophilized cakes at primary-drying of -10°C and a vacuum of 0.045 mbar (A), primary-drying of -5°C and a vacuum of 0.045 mbar (B), primary-drying of 0°C and a vacuum of 0.045 mbar (C) and primary-drying of 0°C and a vacuum of 0.009 mbar (D).

XRD confirmed the results from DSC. Overall amorphous structures were obtained for the cakes with the modified cake geometry (Fig 17). The presence of an amorphous halo and the absence of peaks of any other form of trehalose in the XRD patterns suggested an amorphous state. The DSC measurements already indicated amorphous structures by the high glass transition temperatures.

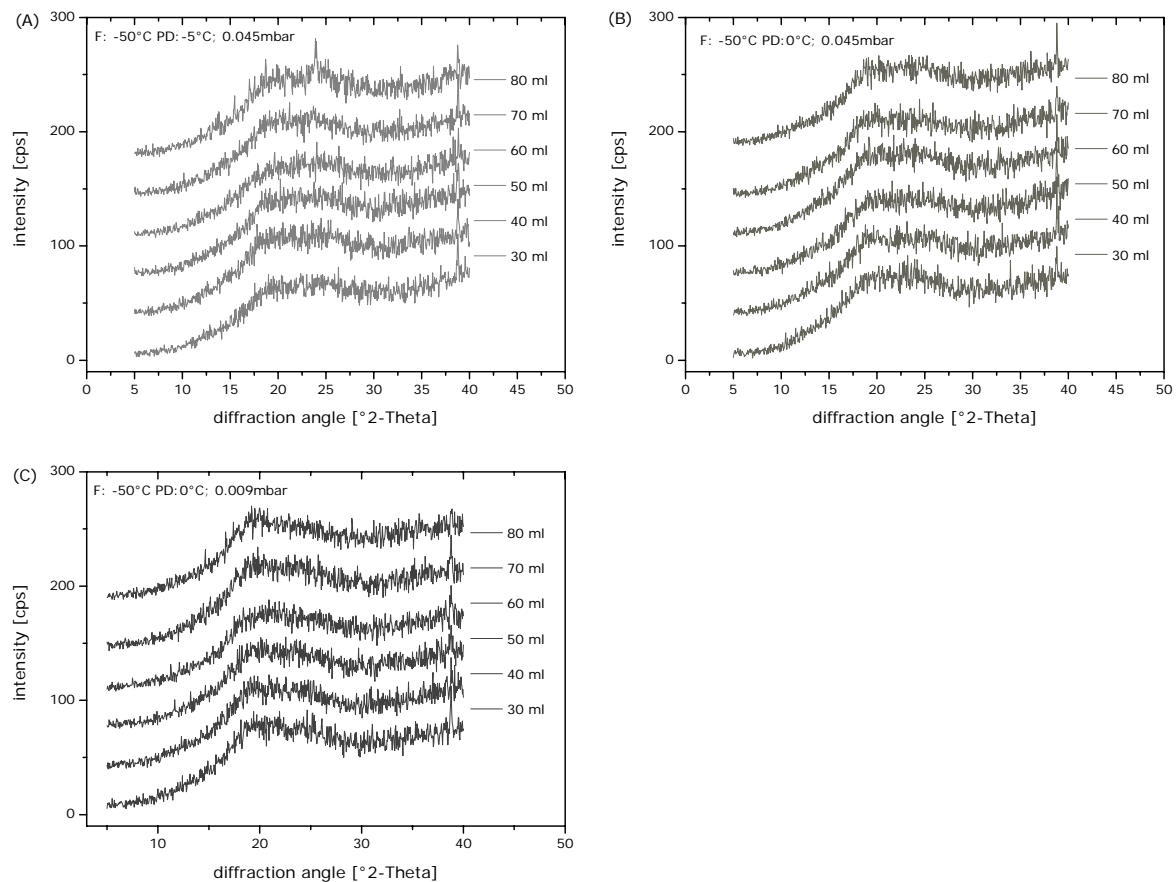


Figure 17: X-ray diffraction pattern of lyophilized cakes with modified cake geometry at primary-drying of -5°C and a vacuum of 0.045 mbar (A), primary-drying of 0°C and a vacuum of 0.045 mbar (B) and primary-drying of 0°C and a vacuum of 0.009 mbar (C).

3.5.4 Liposome properties at increased filling volume

Various process variables affect the efficiency of freeze-drying. Product temperature and mass transfer are the most important factors because the sublimation rate is generally faster at higher temperatures [36]. The appearance of the cake and the reconstitution behavior depend on the lyophilization cycle and the filling volume. With raised filling volumes and higher shelf temperatures of 0°C the cakes collapsed marginally from the wall and the top. Finally, the reconstitution time was slowed down slightly for such cakes (data are not shown).

The direct interaction of trehalose with lipid head groups is described to preserve the liposomes [37,3]. However, liposome size and polydispersity index in the conventional cakes were affected by the process parameters and the filling volume. The tendency of slightly increased liposome sizes at higher filling volumes was obvious for all tested conditions (Fig 18). Under the regular drying conditions and for the normal cake morphology the polydispersity index increased above 0.4 when the filling volume

exceeded 50 ml. This is indicative for a loss of structural integrity of the liposomes and a potential crystallization of Paclitaxel. The process of liposomal damaging was further induced by raising the shelf temperature from -10 to 0°C (Fig 18, (A to C)). Only at the most gentle drying conditions with a shelf temperature of 0°C and a vacuum of 0.009 mbar the polydispersity remained constant also for the filling volumes above 50 ml (Fig 18, (D)). The very time consuming and gentle process showed macroscopically a homogenous cake appearance. Due to the very high vacuum the product temperature and the heat transfer through the cake were reduced.

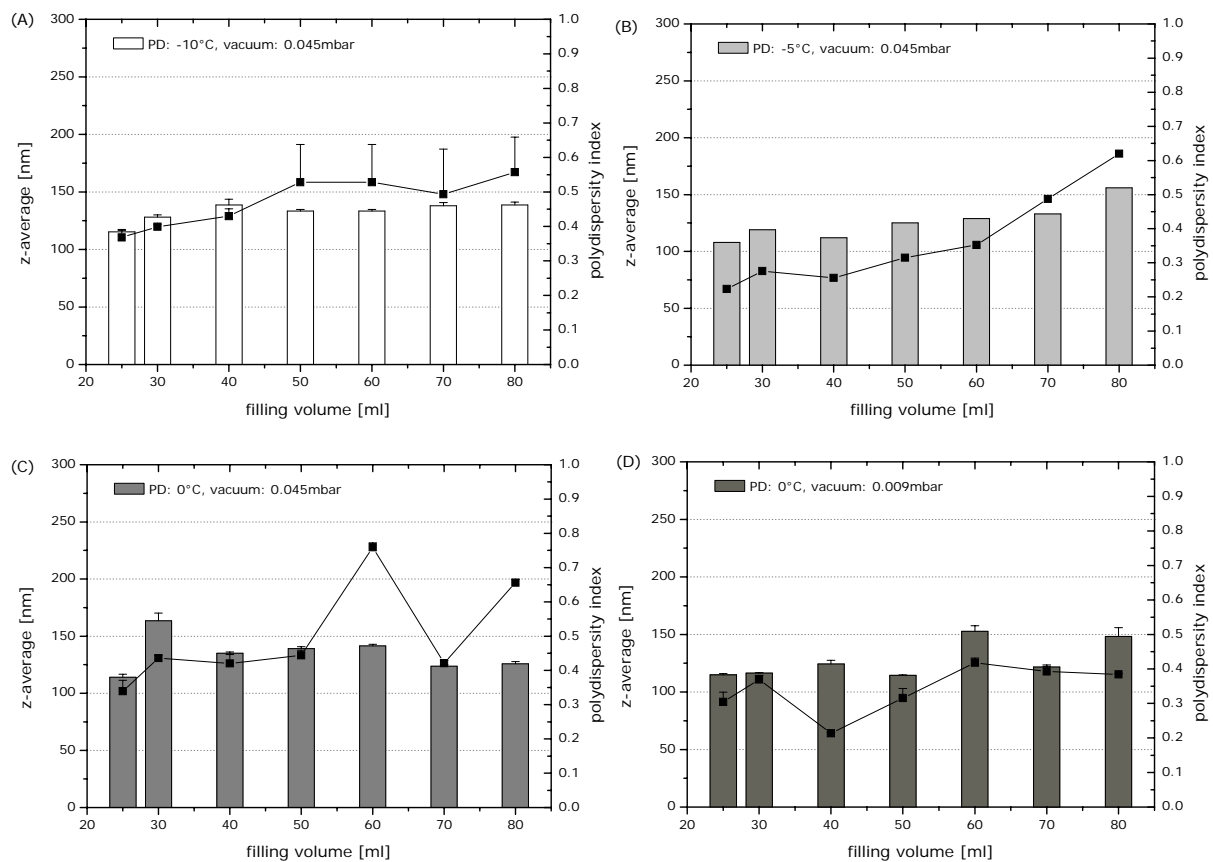


Figure 18: Liposome size and polydispersity index after reconstitution of conventional cakes at primary-drying of -10°C and a vacuum of 0.045 mbar (A), primary-drying of -5°C and a vacuum of 0.045 mbar (B), primary-drying of 0°C and a vacuum of 0.045 mbar (C) and primary-drying of 0°C and a vacuum of 0.009 mbar (D).

With the modified cake geometry, no change in cake appearance and no macroscopically collapsed structures were visible for all processes and filling volumes. The liposomes size and the polydispersity indices stayed constant for all investigated conditions. Here the liposome size varied between 120 and 150 nm with acceptable polydispersity indices around 0.4 (for Paclitaxel loaded liposomes) (Fig 19). Again the gentle and very time consuming drying process at a vacuum of 0.009 mbar resulted in the most favorable

liposome properties with a size of about 120 nm and polydispersity below 0.4. Compared to the conventional cake conditions the additional surface of the cakes and the related drying performance preserved the liposomal structure during the faster drying process and led to a reduced heat exposure due to the overall thinner layer thickness.

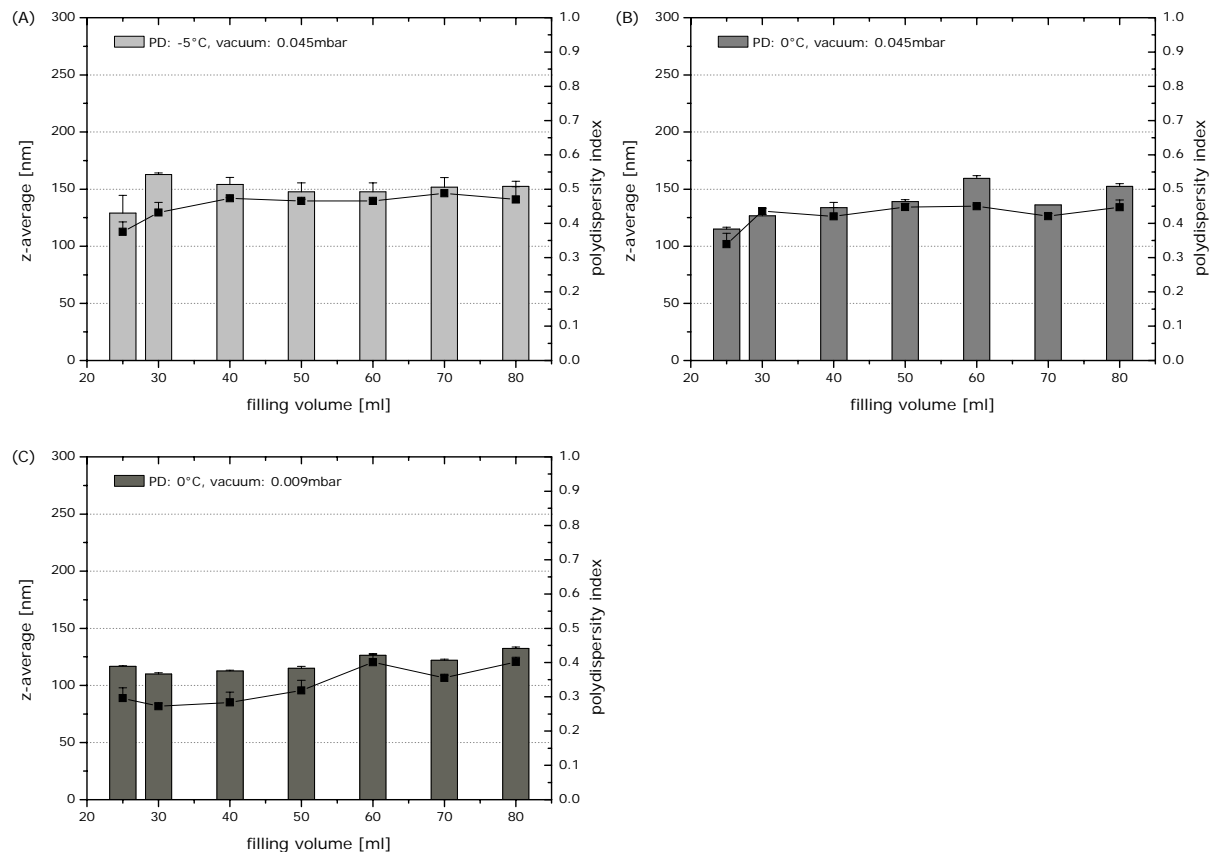


Figure 19: Liposome size after reconstitution of optimized cake conditions at primary-drying of -5°C and a vacuum of 0.045 mbar (A), primary-drying of 0°C and a vacuum of 0.045 mbar (B) and primary-drying of 0°C and a vacuum of 0.009 mbar (C).

3.5.5 Effect of filling volume and process parameters on the lipid recovery

Before lyophilization the formulation contained 5 mM DOTAP-Cl and 4.7 mM DOPC, which was determined by RP-HPLC. The lipid recovery of DOTAP-Cl and DOPC after the different freeze-drying processes remained constant. In addition no variations were found for the vials with increased filling volumes (Tab 4).

Table 4: Lipid recovery values for filling volumes between 25 and 80 ml prepared with the conventional cake structure at varied freeze-drying programs.

conventional cake	DOTAP-Cl recovery [mM]								DOPC recovery [mM]							
	before	filling volume [ml]							before	filling volume [ml]						
		25	30	40	50	60	70	80		25	30	40	50	60	70	80
F: -50°C PD: -10°C 0.045mbar	5.1	5.4	5.4	5.3	5.2	5.2	5.2	5.3	4.8	5.0	5.1	5.1	5.0	5.0	5.0	5.0
F: -50°C PD: -5°C 0.045mbar	5.0	-	5.0	4.9	-	-	-	4.8	4.7	4.6	-	4.7	4.7	-	-	-
F: -50°C PD: 0°C 0.045mbar	5.0	5.5	5.3	5.1	5.2	-	5.2	5.3	4.8	5.0	5.2	5.1	4.9	5.0	-	5.0
F: -50°C PD: 0°C 0.009mbar	5.0	4.8	5.0	5.0	5.0	4.9	4.9	4.9	4.7	4.5	4.8	4.7	4.7	4.7	4.7	4.7

The lyophilized vials with the changed cake geometry showed similar lipid recoveries as the conventional cakes. No decomposition or degradation of the lipids could be determined (Tab 5). The data revealed that lyophilization with high filling volumes and with harsher conditions e.g. shelf temperature of 0°C resulted in a good lipid recovery and the absence of degradation products.

Table 5: Lipid recovery values for filling volumes between 25 and 80 ml prepared with the additional surface cake structure at varied freeze-drying programs.

optimized cake	DOTAP-Cl recovery [mM]								DOPC recovery [mM]							
	before	filling volume [ml]							before	filling volume [ml]						
		25	30	40	50	60	70	80		25	30	40	50	60	70	80
F: -50°C PD: -5°C 0.045mbar	5.3	-	5.7	5.7	5.6	5.6	5.4	5.5	5.0	-	5.4	5.4	5.4	5.4	5.3	5.3
F: -50°C PD: 0°C 0.045mbar	5.0	5.3	5.4	5.3	5.3	5.1	-	5.2	4.8	5.0	5.1	5.0	5.0	4.8	-	5.0
F: -50°C PD: 0°C 0.009mbar	5.0	4.9	5.0	5.0	5.0	5.0	-	4.9	4.7	4.7	4.8	4.7	4.7	4.7	-	4.7

3.5.6 Effect of the filling volume on the Paclitaxel recovery

The Paclitaxel content after lyophilization and the content of the degradation product 7-Epipaclitaxel was determined for conventional cakes and cakes with modified geometry. The values determined for the products dried at the higher shelf temperature of 0°C were comparable for both cake geometries. The degradation and crystallization of Paclitaxel from lipid membranes is known to be very sensitive. However, no loss of Paclitaxel out of

the membrane occurred for both cake structures and during all drying processes (Fig 20). The different freeze-drying conditions and especially the high filling volumes did not lead to a crystallization of Paclitaxel.

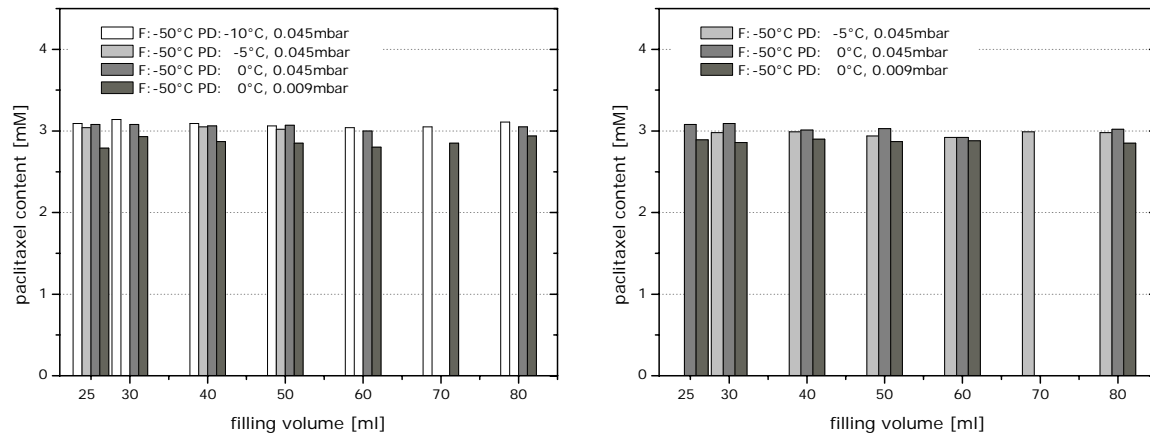


Figure 20: Paclitaxel recovery after varied freeze-drying conditions for the conventional cakes (left) and modified cake geometries (right).

Before lyophilization no 7-Epipaclitaxel was determined. The content of this degradation product after freeze-drying ranged between 1.3 to 2.2 % for all process conditions, for the conventional cakes and increasing filling volume (Fig 21, left). By using the modified cake geometry a significant reduction of the impurity below 1 % was obtained at the primary-drying temperature of -5°C and a vacuum of 0.045 mbar (Fig 21, right). The values determined for the products dried at the higher shelf temperature of 0°C were comparable for both cake geometries. Although the shelf temperature during primary-drying was increased up to 0°C and the heat transfer thereby enhanced, the degradation products remained in acceptable values below 3 %.

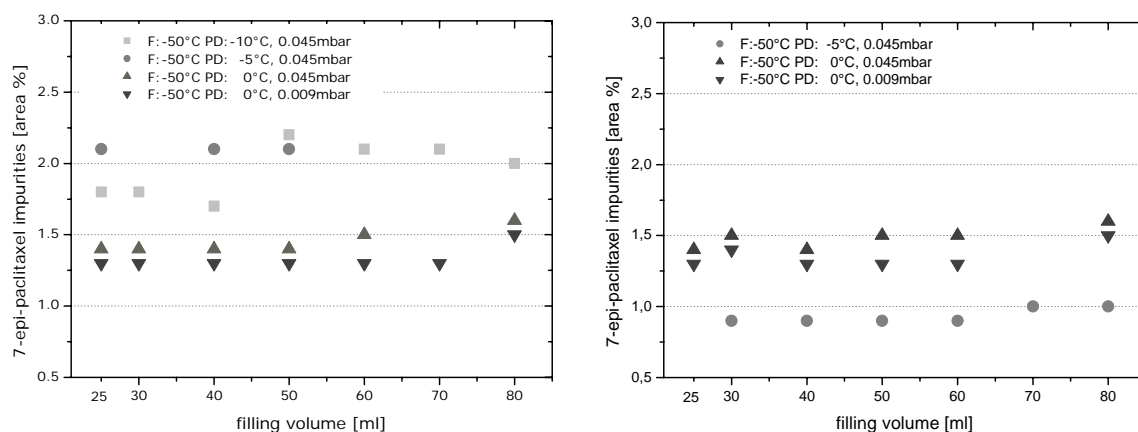


Figure 21: Impurities of 7-Epipaclitaxel after varied freeze-drying conditions for the conventional cakes (left) and modified cake geometry (right).

4. CONCLUSIONS

The goal to increase the efficiency of the lyophilization process was achieved either by reducing the process time, by increasing the filling volume or by changing the cake geometry to higher surfaces. The change of the freezing step to a freezing temperature below T_g' resulted in enhanced solidification of the products, which shortened the primary-drying step. This can be ascribed to enhanced sublimation rates, which resulted in a 10 to 25 % reduction in primary-drying time. Furthermore, the faster freezing ramp and the resulting formation of larger ice crystals can make primary drying more efficient. An increased shelf temperature of -5°C and higher vacuum of 0.045 mbar enhanced the difference in relative vapor pressure between the solvent in the product and the atmosphere above the sublimation front, intensifying the driving force for sublimation. However, compared to the lowering of the freezing temperature, the impact on primary drying time was less pronounced.

When using such an optimized lyophilization cycle the filling volume can be successfully raised to at least 50 ml per vial without cake shrinkage and collapse. The drying behavior of vials filled up to 80 ml, combined with modified cake geometry was studied for Paclitaxel loaded formulations. A process improvement saving up to 60 % time compared to the conventional process and filling volume of 25 ml could be achieved in this way.

With the modified cake geometry primary-drying could be shortened, especially for filling volumes up to 40 ml. The sublimation rate, which is generally limited by the heat transfer, was enhanced due to the additional surface. At filling volumes above 50 ml the additional surface did not improve the drying time as efficient as compared to the conventional cakes. Thus, it can be concluded that the heat transfer through the dry layer of the cake is a more limiting factor for sublimation than the product resistance. Up to a filling volume of 50 ml liposomal integrity, reflected in size and PI, as well as Paclitaxel loading was preserved for both, conventional cakes and those with modified geometry. Overall, the cakes with modified geometry exhibited lower moisture contents, more homogenous liposome properties and faster drying rates. Although it was possible to optimize the lyophilization cycle and increase the efficiency, the resulting processes are still rather time and energy consuming.

5. REFERENCES

-
- [1] Crowe, J.H., Crowe, L.M., Preservation of liposomes by freeze-drying, In: *Liposome Technology*, vol 1, Ed. Gregoriadis, G., CRC Press (1993).
- [2] Vanleberghe, G., Handjani, R.M., Storage stability of aqueous dispersions of spherules, GB2013609 (1979).
- [3] Crowe, J.H., Leslie, S.B., Crowe, L.M., Is vitrification sufficient to preserve liposomes during freeze-drying?, *Cryobiology*, 31: 355-366 (1994).
- [4] Gatlin, L.A., Nail, S.L., Protein Purification Process Engineering, *Freeze Drying: A Practical Overview*, *Bioprocess. Technol.*, 18: 317-367 (1994).
- [5] Jennings, T.A., *Lyophilization, Introduction and Basic Principles*, Interpharm press, (1999).
- [6] Luthera, S., Obert, J-P., Kalonia, D.S., Pikal, M.J., Investigation of drying stresses on proteins during lyophilization: Differentiation between primary and secondary-drying stresses on lactate dehydrogenase using a humidity controlled mini freeze-dryer, *J. Pharm. Sci.*, 96(1): 61-70 (2007).
- [7] Tang, X., Nail, S.L., Pikal, M.J., Evaluation of manometric temperature measurement, a process analytical technology tool for freeze-drying: part I, product temperature measurement, *AAPS PharmSciTech*, 7(1): [electronic resource] (2006).
- [8] Wisniewski, R., Principles of large-scale cryopreservation of cells, microorganisms, protein solutions, and biological products, In: *Cryopreservation, appl. in pharm. Biotech., Drug Manu. Tech. vol. 5*, (Eds) Avis, K.E., Wagner, C.M., Interpharm press (1999).
- [9] Van Winden, E.C.A., Crommelin, D.J.A., Long term stability of freeze-dried, lyoprotected doxorubicin liposomes, *Eur. J. Pharm. Biopharm.*, 43(3): 295-307 (1997).
- [10] Crowe, L.M., Reid, D.S., Crowe, J.H., Is Trehalose Special for Preserving Dry Biomaterials?, *Biophy. J.*, 71(4): 2087-2093 (1996).
- [11] Crommelin, D.J.A., van Bommel, E.M.G., Stability of Liposomes on Storage: Freeze Dried, Frozen or as an Aqueous Dispersion, *Pharm. Res.*, 4(1): 159-163 (1984).
- [12] Tang, X.C., Pikal, M.J., Design of Freeze-Drying Processes for Pharmaceuticals: Practical Advice, *Pharm. Res.*, 21(2): 191-200 (2004).
- [13] Pikal, M. J., Shah, S., Roy, M. L., Putman, R., The secondary-drying stage of freeze drying: drying kinetics as a function of temperature and chamber pressure, *Int. J. Pharma.*, 60(3): 203-217 (1990).
- [14] Liu, J., Viverette, M., Virgin, M., Anderson, M., Dalal P., A study of the impact of freezing on the lyophilization of a concentrated formulation with a high fill depth, *Pharm. Dev. Technol.*, 10(2): 261-272 (2005).
- [15] Matz, G., Possibilities for the technical execution of freeze-drying, *Vakuum-Technik*, 3: 115-123 (1955).
- [16] Chang, B.S., Randall, C.S., Use of subambient thermal analysis to optimize protein lyophilization, *Cryobiology*, 29(5): 632-656 (1992).
- [17] Rambhatla, S., Pikal, M.J., Heat and mass transfer scale-up issues during freeze-drying, I: A typical radiation and the edge vial effect, *AAPS. Pharm. Sci. Tech.*, 4(2): article no. 14 (2003).
- [18] Pikal, M.J., Roy, M.L., Shah, S., Mass and heat transfer in vial freeze-drying of pharmaceuticals: role of the vial, *J. Pharm. Sci.*, 73(9): 1224-1237 (1984).
- [19] Trappler, E., Lyophilization equipment, in *Biotechnology: Pharmaceutical Aspects, Lyophilization of Biopharmaceuticals*, 3-41, Eds. Pikal, M.J., Costantino, H.R., AAPS Press (2004).
- [20] Jennings, T.A., Role of product temperature in the lyophilization process, *Amer. Pharm. Review* 4(1): 14-22 (2001).

-
- [21] Bindschaedler, C., Lyophilization process validation, In: Freeze-drying / lyophilization of pharmaceutical and biological products, vol, 9(2), Eds. Rey, L., May, J.C., Marcel Dekker (2000).
- [22] Wisniewski, R., Large-scale cryopreservation: process development for freezing and thawing of large volumes of cell suspensions, protein solutions, and biological products, In: Cryopreservation, appl. in pharm. Biotech., Drug Manu. Tech. vol. 5., (Eds) Avis, K.E., Wagner, C.M., Interpharm press (1999).
- [23] Pikal, M.J., Rambhatla, S., Ramot, R., The impact of the freezing stage in lyophilization: effects of the ice nucleation temperature on process design and product quality, *Amer. Pharm. Rev.*, 5(3): 48-52 (2002).
- [24] Taylor, L.S., York, P., Characterization of the phase transition of trehalose dehydrate on heating and subsequent dehydration, *J. Pharm. Sci.*, 87(3): 347-355 (1998).
- [25] Pikal, M. J., Shah, S., Roy, M. L., Putman, R., The secondary-drying stage of freeze drying: drying kinetics as a function of temperature and chamber pressure, *Int. J. Pharma.*, 60(3): 203-217 (1990).
- [26] Ybema, H., Kolkman-Roodbeen, L., Te Booy, M.P.W.M, Vromans, H., Vial lyophilization: calculations on the rate of limitations during primary-drying, *Pharm. Res.*, 12(9): 1260-1263 (1995).
- [27] Pikal, M.J., Shah, S., Intravial distribution of moisture during the secondary-drying stage of freeze drying, *J. Pharm. Sci. Tech.*, 51(1): 17-24 (1997).
- [28] Tsvetkova, N.M., Phillips, B.L., Crowe, L.M., Crowe, J.H., Risbud, S.H., Effect of sugars on headgroup mobility in freeze-dried dipalmitoylphosphatidylcholine bilayers: solid-state ³¹P NMR and FTIR studies, *Biophys. J.*, 75(6): 2947-2955 (1998).
- [29] Teagarden, D.L., Baker, D.S., Practical aspects of lyophilization using non-aqueous co-solvent systems, *Eur. J. Pharm. Sci.*, 15(2): 115-133 (2002).
- [30] Van Drooge, D.J., Hinrichs, W.L.J., Frijlink, H.W., Incorporation of lipophilic drugs in sugar glasses by lyophilization using a mixture of water and tertiary butyl alcohol as solvent, *J. Pharm. Sci.*, 93(3): 713-725 (2004).
- [31] International conference of harmonization (ICH) of technical requirements for registration of pharmaceuticals for human use, Q3C (R3): Impurities: Guideline for residual solvents (2005).
- [32] Flink, J., Karel, M., Retention of organic volatiles in freeze-dried solutions of carbohydrates, *J. Agr. Food Chem.*, 18(2): 295-297 (1970).
- [33] Flink, J., Gejl-Hanse, F., Retention of organic volatiles in freeze-dried carbohydrate solutions: Microscopic observations, *J. Agr. Food Chem.*, 20(3): 691-694 (1972).
- [34] Seager, H., Taskis, C.B., Syrop, M., Lee, T.J., Structure of products prepared by freeze-drying solutions containing organic solvents, *J. Paren. Sci. Tech.*, 39(4): 161-179 (1985).
- [35] Buitink, J., Van den Dries, I.J., Hoekstra, F.A., Alberda, M., Hemminga, M.A., High critical temperature above T_g may contribute to the stability of biological systems, *Biophys. J.*, 79: 1119-1128 (2000).
- [36] Chang, B.S., Fischer, N.L., Development of an efficient single-step freeze-drying cycle for protein formulations, *Pharm. Res.*, 12(6): 831-837 (1995).
- [37] Crowe, J.H., Hoekstra, F.A., Nguyen, K.H., Crowe, L.M., Is vitrification involved in depression of the phase transition temperature in dry phospholipids?, *Biochim. Biophys. Acta*, 26(2): 187-196 (1996).

CHAPTER 3

Spray Freeze-Drying of Liposome Paclitaxel Formulations

Abstract :

Spray freeze-drying (SFD) was evaluated as a method to prepare and stabilize particles of placebo liposomal formulations with the lipids DOTAP-Cl/DOPC in a molar range of 50/50, as well as of drug loaded formulations made up from DOTAP-Cl/DOPC/Paclitaxel in the molar range 50/47/3. The SFD process consists of two separate processing steps: spray-freezing to produce the particles and a subsequent lyophilization to dry the product. With the SFD technology particle sizes between 10 and 3000 μm can be obtained. The drying speed and the physicochemical properties of such particles were comparable to conventional freeze-drying. After reconstitution of the particles the liposome size distribution was not influenced. Lipid and drug content stayed constant during the freezing and drying procedure. The main advantage of SFD is the resulting free flowable spherical product. Due to the particle formation and the drying process at low temperatures heat exposure could be circumvented.

1. INTRODUCTION

Spray freeze-drying (SFD) is a relatively new method for the preparation of particles and microparticles [1,2,3]. SFD is widely used for the production of biopharmaceuticals and different applications for protein therapeutics [4]. Nutropin Depot[®] a recombinant human growth hormone (hGH) from Genentech and Alkermes was prepared with the so called ProLease[®] process as a first product using spray freeze-drying technology [5]. An overview of studies on SFD and their applications is provided by Maa and Costantino (2004) [6]. SFD is often used because of the high porosity of the product and the controlled particle size distribution which make such a process an alternative to the conventional techniques like spray-drying [7,8].

The spray freeze-drying process can be isolated into two separate processing steps: the spray-freezing into a cryogenic liquid and the lyophilization step. As cryogenic liquids, liquid nitrogen or liquid carbon dioxide are preferred [9]. Two freezing techniques are commonly used to prepare particles, the spray-freezing directly into liquid nitrogen (SFL) and spray freeze-drying (SFD) above the cryogenic surface. The SFL process can be used if a contact of the drug solution with the atmosphere needs to be circumvented [10]. In SFL the liquid solution is sprayed directly into the liquid nitrogen through a fine orifice nozzle (capillary peak) equipped with a pressure system. Such a capillary peak nozzle generates high velocities and the droplets produced thereby are frozen instantly [11]. We used a SFD process where the solutions are sprayed above the liquid surface to obtain fine or small particles. An alternative for the formation of larger particles is to spray first into a cold vapour phase over a cryogenic liquid. Such a process was first described by Gusman and Johnson (1990) [12] for ceramic powders and by Gombotz et al. (1991) for carbohydrates and proteins. While falling through the cold vapour the formed droplets begin to freeze, but the main freezing process takes place upon contact of the prefrozen droplets with the cryogenic liquid phase [13]. Atomized droplets during SFD maintain their spherical shape and size upon freezing and the subsequent drying process [14,15]. The main advantage of the SFD method is the absence of heat exposure during the particle formation and the drying process contrary to spray-drying [16,17]. The limitations of the method are the use of expensive cryogenic fluids, which is technically impractical, and the need of the time consuming lyophilization step. A freeze-dried cake in a vial is still the typical form for currently marketed biopharmaceuticals [18,19]. However, SFD is widely used in the field of protein stabilization to achieve a particulate system. The use of this technique for the stabilization of liposomes was not yet extensively discussed in literature. One example is the manufacturing of a liposomal powder formulation containing ciprofloxacin for pulmonary drug delivery [20]. During

reconstitution of the powder, spontaneous in vitro formation of liposomes in aqueous media occurred. The main advantage of such a process is the improved mass median aerodynamic diameter.

The objective of this study was to investigate spray freeze-drying as a method to stabilize liposomal formulations as dry solid particles. With the SFD technology free flowable particles with controlled size could be achieved under gentle process conditions.

2. MATERIAL AND METHODS

2.1 LIPOSOME PREPARATION

The ethanol injection technique was used for preparing placebo and drug containing liposomes. Briefly, for the placebo formulation a lipid stock solution of 400 mM DOTAP-Cl (1,2-dioleoyl-3-trimethylammonium-propane-chloride) and DOPC (1,2-dioleoyl-*sn*-glycero-3-phosphocholine) in ethanol was prepared (Merck, Darmstadt, Germany). 25 ml of this lipid stock solution were subsequently injected under stirring into 975 ml 10.5 % [w/v] trehalose solution to result in a total final lipid concentration of 10 mM. The ethanol injection was followed by five cycles of extrusion through a 0.2 μm polycarbonate membrane. The liposomal Paclitaxel containing formulation consisted of molar concentrations 50/47/3 of DOTAP-Cl/DOPC/Paclitaxel (Natural Pharmaceuticals Inc., Beverly, MA, USA) and was prepared in the same way.

2.2 SPRAY-FREEZING METHODS

Two different technical set-ups were applied to spray-freeze small and large particles. Small particles were atomized using a two-fluid nozzle by direct spraying above the liquid nitrogen (Fig 1, (A)). The two-fluid nozzle was operated at atomizing air volumetric flow rate (v_{aa}) of 120 and 470 l/h with a liquid feed volumetric flow rate (v_{lf}) of 2.7 ml/min for all experiments. The so formed droplets freeze rapidly after contact with the cryogenic nitrogen. To generate large particles the liposome suspension was pumped through an orifice nozzle to produce a uniform stream of droplets. Depending on the liquid feed rate the droplet size could be varied in the range of 10 to 3000 μm . In this set-up the droplets begin to freeze while falling through a cold gaseous phase of vaporized nitrogen in a pre-freezing vessel (Fig 1, (B)). Due to the pre-stabilization, the large partially frozen droplets do not rupture when they immerse into the liquid nitrogen, where the major freezing step takes place. In both set-ups the liquid nitrogen was stirred during the process to avoid agglomeration of the freezing particles.

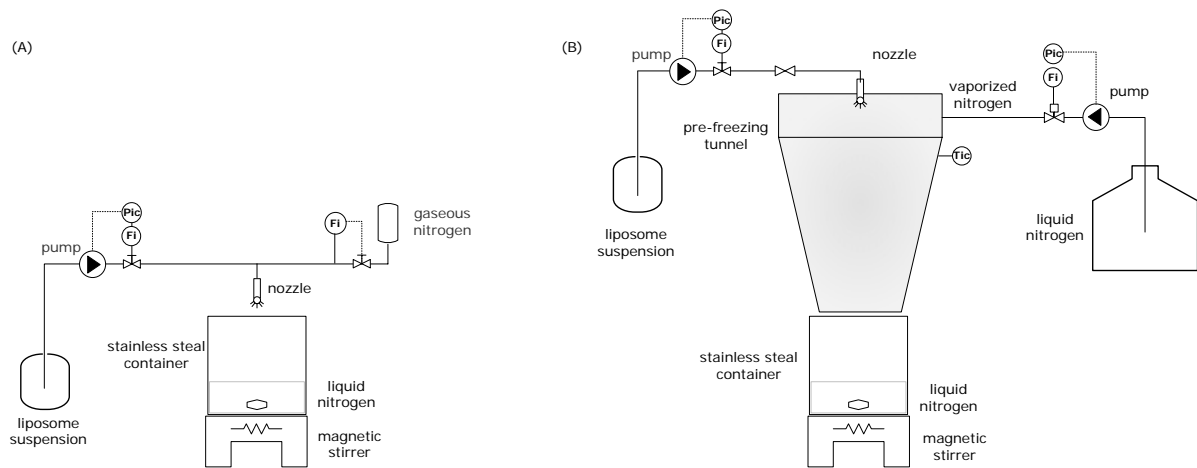


Figure 1: Schematic constructions of the SFD by direct spray-freezing in liquid nitrogen for fine and small particles (A) and the developed spray-freezing with pre-freezing vessel for large particles (B).

2.3 FREEZE-DRYING METHOD

The particles frozen in liquid nitrogen were transferred either into a lyoguard R&D container (W.L. Gore, Newark, USA) or into 10R glass vials (Schott, Mainz, Germany). The vials were stored in a -80°C freezer until the liquid nitrogen evaporated. Afterwards, the lyoguard/vial containing the frozen particles was loaded onto the pre-cooled shelves (-40°C) of the conventional freeze-dryer Epsilon 2-6D (Martin Christ, Osterrode, Germany). After loading, the vacuum was set to 0.045 mbar and the shelf temperature was increased to -16°C for primary drying and held for 36 h. For secondary drying, the shelf temperature was increased to 20°C and held for 12 h (Figure 2, left). The process used for conventional vial freeze-drying of the liposomal formulation is shown in Figure 2 (right) with a freezing step to -50°C and comparable primary- and secondary-drying steps.

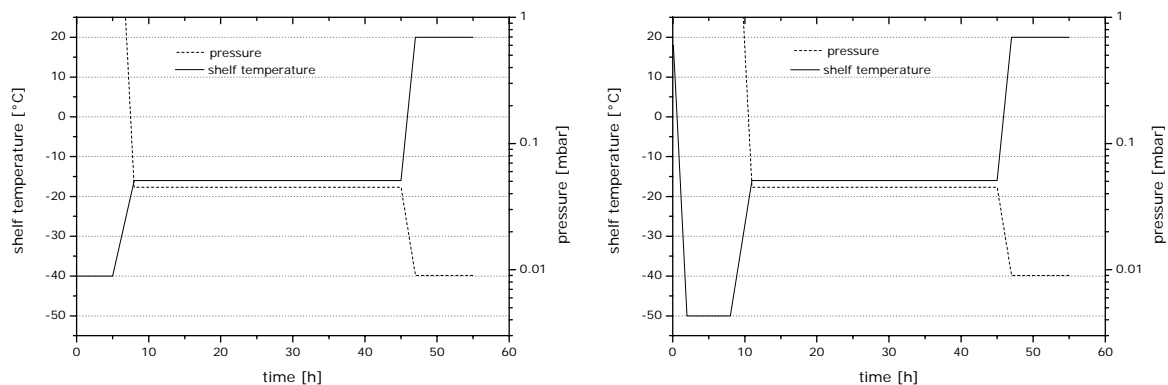


Figure 2: Freeze-drying cycle for the particles prepared by the spray-freezing method (left), and for the conventional vial freeze-drying with a process including the freezing step (right).

2.4 FREEZE-DRYING VELOCITY

Weight loss and drying rate were investigated by a microbalance (Martin Christ, Osterode, Germany). The microbalance was placed on a shelf inside the freeze-drying chamber. A single vial filled with an equal volume of liposomal suspension respectively of pre-frozen particles was placed onto the holding-arm of the microbalance. Every 3 minutes, the holding-arm moves upwards and thereby lifts the vial for weighing. The lifting and weighing step takes ~10 s. The microbalance was connected via a co-axial cable through a sealed flange in the chamber wall to a computer. Microbalance programming and data evaluation were performed using Christ's proprietary software.

2.5 ANALYSIS OF PELLET MORPHOLOGY

Images of the products were obtained by scanning electron microscopy (SEM) to study pellet morphology and size. Conductive double sided tape was used to fix the pellets onto the specimen holder before sputtering them with a thin layer of carbon under vacuum. Scanning electron microscopy images were obtained using a Philips XL-Series XL20 (Philips, Netherlands).

Pellet size distribution was determined with a He-Ne laser beam equipped laser diffraction analyzer (Mastersizer X, Malvern, Herrenberg Germany). The small-volume-presentation-unit was used to pump the powder suspension into the sample cell. About 20 mg of SFD powder were dispersed in 10 ml Migylol 812 containing 1 % Span 85. Background alignment with pure dispersion was performed before the pellet medium was added. Laser light scattering intensity was evaluated by Fraunhofer analysis using a polydisperse mode.

All further methods used in this chapter are already described before.

3. RESULTS AND DISCUSSION

3.1 PARTICLE FORMATION PROCESSES

With the spray freeze-drying methods used in this study the modifications of the freezing set-up allowed a production of small and large particles with size distributions between 10 and 3000 μm (Figure 3). At both spray freeze-drying set-ups the formed droplets maintained their spherical shape and size upon immediate freezing. In addition, the subsequent drying process did not affect the particle shape or size. Depending on the droplet size and the spraying technique the freezing time varied for small and large particles. Freezing of fine and small droplets by spraying directly above liquid nitrogen resulted in high cooling rates, although the aqueous droplets floated some seconds on the liquid nitrogen [21]. This phenomenon can be described by a boiling of the cryogen in contact with the droplets as a result of the Leidenfrost effect [22]. The larger droplets, which were pre-frozen in gaseous nitrogen by the described method (Fig 1, (B)) exhibit a much lower freezing rate due to their tenfold size and their different freezing process. Before the droplets were completely solidified in the liquid nitrogen, they floated for almost 20 seconds on the surface of the liquid nitrogen before sinking, which is indicative for a complete freezing [23]. With the pre-freezing step no fragmentation or clustering of the particles occurred. Compared to freeze-drying with a freezing step over several hours, the very high cooling rates employed in SFD inhibit ice crystal growth after nucleation, leading to small ice crystals and a large ice crystal surface area by Burke et al. (2004).

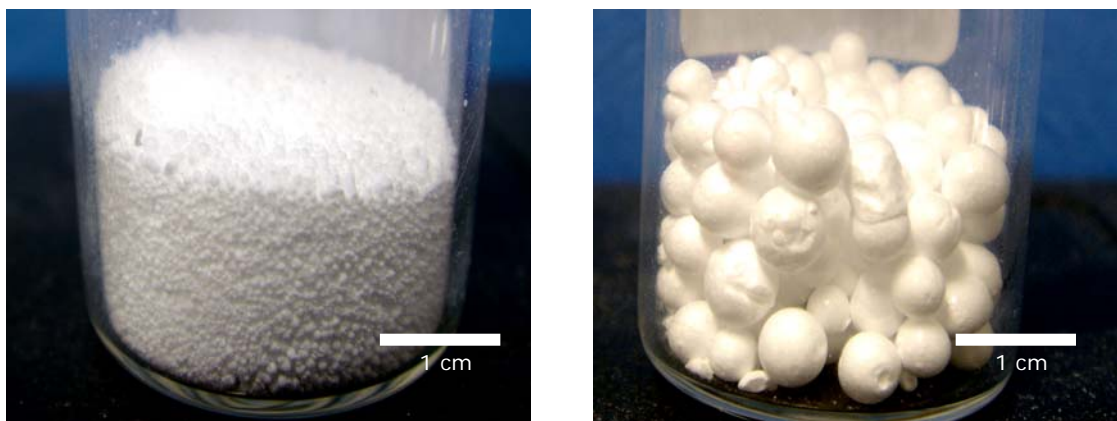


Figure 3: Spray freeze-dried small particles (left) produced by set-up A with direct spraying into liquid nitrogen, and large particles (right) produced by set-up B including a pre-freezing step.

3.2 DRYING VELOCITY

The primary drying behavior of a regular freeze-drying cake and SFD particles were compared using the microbalance to elucidate how the different freezing protocols affect the drying velocity. Although the samples were frozen with different techniques and freezing rates, the drying behavior during primary-drying was quite similar for the studied FD cake (Fig 4, left) and fine SFD particles (Fig 4, right). The initial drying rate for the freeze-dried cake was slightly higher than for the fine SFD particles. This can be assigned to the more efficient heat transfer into the cake structure [24]. However, in both cases the water loss faded out after 24 hours. With the additional surface of the porous particles the drying speed was not improved, although other authors suggested a shorter drying time of highly porous SFD particles [25]. They proposed that the short conduction and diffusion length and the resulting low heat and mass transfer resistance are responsible for the shorter drying cycle.

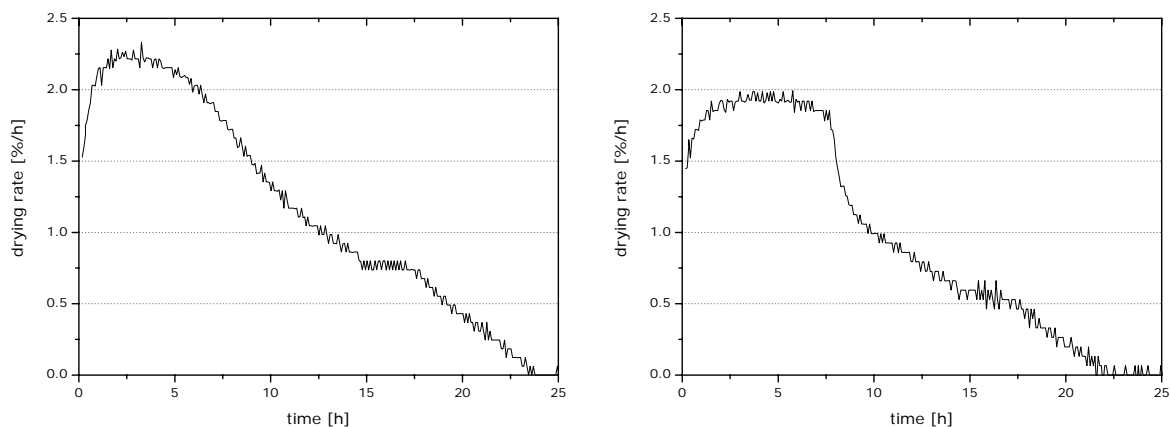


Figure 4: Drying rate during primary drying in the lyophilization process of cake structure (left) and spray freeze-dried of fine particles (right).

3.3 PARTICLE YIELD AND RESIDUAL SOLVENT CONTENT

Within vial freeze-drying no product loss occurred and a 100 % yield was achieved. For the SFD particles the yield varied between 63 % for fine and 97 % for large particles (Tab 1). The large material loss for the fine particles was assigned to the Leidenfrost effect, as the particles disappeared to the wall or out of the stainless steel container. Handling of liquid nitrogen, as well as the collection and transfer of particles into the drying chamber was more complicated for the fine particles and resulted in a greater material loss.

Table 1: Yield of particles prepared with the different set-ups and residual ethanol content in comparison to the conventional freeze-dried cake.

parameter	freeze-drying	spray freeze-drying		
	cake	fine particles	small particles	large particle
yield [%]	100.0 ± 0.0	63.0 ± 5.2	93.0 ± 2.8	97.0 ± 1.5
residual ethanol [ppm]	4120 ± 254	397 ± 85	1007 ± 128	1845 ± 104

FD cakes contained residual ethanol contents above 4000 ppm. Two possible explanations for the high residual ethanol content after lyophilization were already discussed in chapter 2: the retention of ethanol by hydrogen bonding to trehalose and the entrapment of ethanol in microregions within the freeze-dried cake. Especially for the fine particles a tremendous decrease in residual ethanol down to 397 ppm compared to the larger particles with 1845 ppm was determined (Tab 1). The fine porous structure improved the extraction of ethanol out of the particles. The formation of so called microregions could be reduced due to the very fast freezing process. Furthermore, an extraction of ethanol during the freezing step by liquid nitrogen should be considered as well and further studies are necessary to prove this assumption.

3.4 PARTICLE SIZE DISTRIBUTION

The major advantage of the SFD technique is the ability to control particle size characteristics. By varying liquid feed and with it the atomization rate and the droplet formation, the particle size can be adjusted. The SFD process rendered particles with a mean size $d[4,3]$ of 37.5 μm for the fine particles compared to 485 μm for small particles and 2915 μm for large particles (Fig 5).

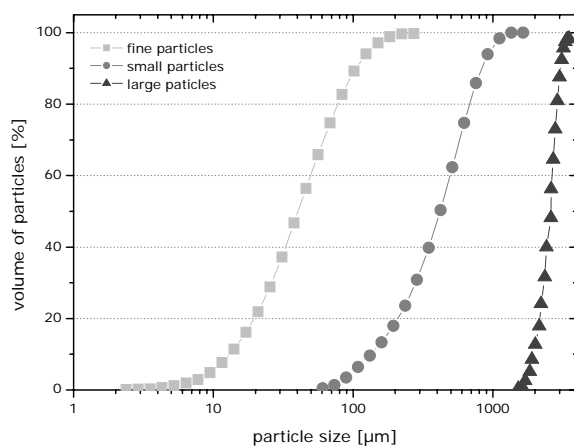


Figure 5: Volume-based size distribution of fine, small and large particles prepared with the different spray freeze-drying set-ups.

Without a pre-freezing vessel a controlled size distribution could not be achieved for large particles, due to the rupture of the droplets upon contact with the liquid nitrogen surface. However, due to the Leidenfrost effect an agglomeration of droplets occurred dependent on the size, although the liquid nitrogen bath was stirred. Such agglomeration resulted in larger agglomerated particles, especially for the small particle fraction. With direct spraying of the liquid feed into the liquid nitrogen this effect can be overcome as described by Yu et al. (2004).

A pre-freezing step, as it was described for the larger particles in set-up (B), would also avoid such coalescence effects on the liquid nitrogen surface. However, direct spraying into the used freezing vessel was not feasible in our laboratory due to technical limitations. Scanning electron microscopy revealed a more porous structure for the fine particles (Fig 6, left), as compared to the larger particles which exhibit a solid interior (Fig 6, right). The porous structure of the small particles can be explained by the very fast freezing and hence the formation of small ice crystals within the frozen droplets. A denser structure was obtained for the large particles due to the pre-freezing of the outer shell in the pre-freezing vessel followed by the complete freezing in the liquid nitrogen.

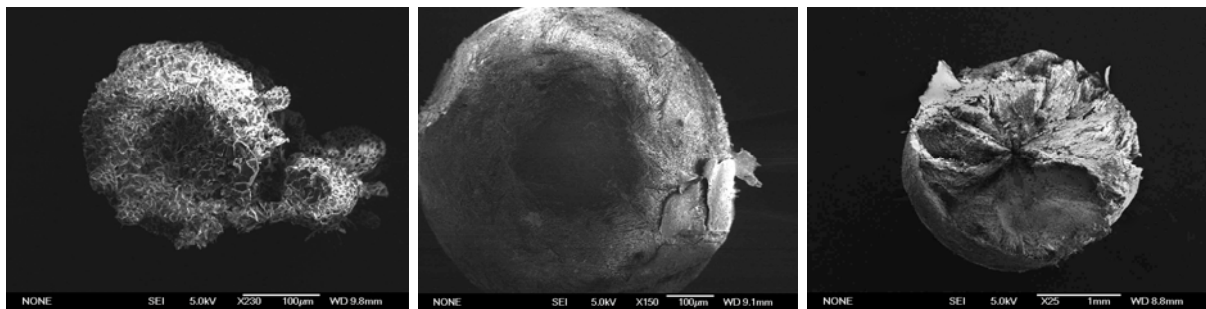


Figure 6: Scanning electron micrographs of fine porous particles (left), small spray freeze-dried particle (middle) and large compact spray freeze-dried particle (right).

3.5 RESIDUAL MOISTURE

A low residual moisture content of 1.0 % was achieved for the freeze-dried cakes. The almost similar residual moisture of SFD small particles was 1.8 and 1.5 % for fine and larger particles (Tab 2). The heat transfer into particles was reduced compared to the FD cake, due to the large convective gas layer between the particles. Although reduced residual moisture levels were expected for the greater surface to mass/volume ratio of smaller particles [26], the water evaporation was not more efficient with the increasing particle surface compared to the freeze-dried cake.

Table 2: Yield of particles prepared with the different set-ups, residual moisture and residual ethanol content in comparison to the conventional freeze-dried cake.

parameter	freeze-drying	spray freeze-drying		
	cake	fine particles	small particles	large particles
residual moisture [%]	1.0 ± 0.12	1.5 ± 0.2	1.8 ± 0.3	1.5 ± 0.4

3.6 PARTICLE MORPHOLOGY

The particle morphology of the SFD particles was analyzed by DSC and XRD and compared to regular FD cakes. A glass transition temperature at about 40°C for small and 44.5°C for the larger particles compared to 65.7°C for the freeze-dried samples was measured by DSC (Fig 7, left). The glass transition temperatures were indicative for an amorphous state of the spray freeze-dried products. The lower Tg of the SFD particles can be attributed to the higher residual moisture contents.

To confirm the amorphous state of the products X-ray powder diffraction was performed. The scattering curve of a freeze-dried sample displayed a broad maximum in the range from 17 to 25° 2-Theta with two maxima at about 20 and 24° 2-Theta, corresponding to a lattice spacings of about 4.4 and 3.7 Å, respectively (Fig 7, right). It was expected that these were due to the packing of the amorphous trehalose matrix. The spray freeze-dried samples displayed a slightly different pattern and mainly the broad halo was less pronounced. This behavior was particularly obvious for the small particles, which were directly frozen in the liquid nitrogen. The data suggested that the fundamental structure of the trehalose matrix was amorphous and similar for the large spray freeze-dried particles and the freeze-dried samples.

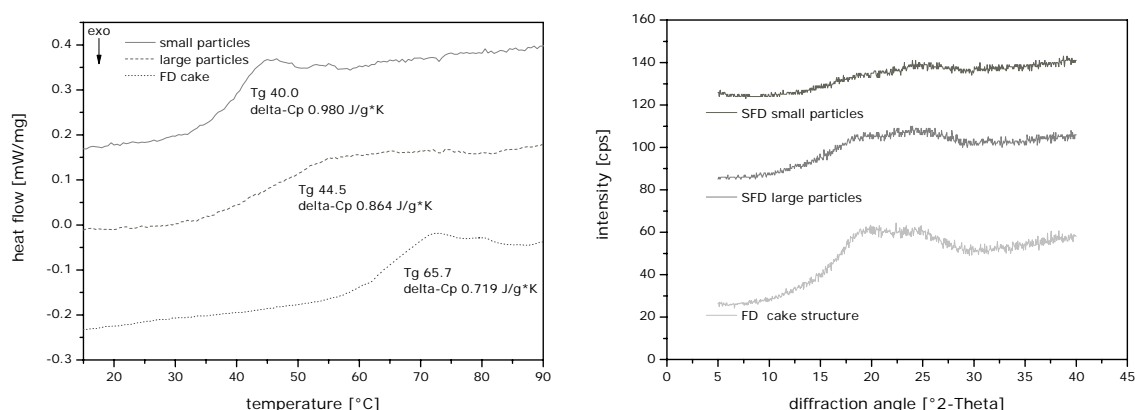


Figure 7: Glass transition temperature (Tg) of small and large SFD particles and the FD cake (left) and wide-angle X-ray diffraction pattern for SFD small and large particles and the FD cake (right).

3.7 LIPOSOME CHARACTERIZATION

Preformed placebo and drug loaded liposomal formulations were used for spray freeze-drying and the freeze-drying experiments. After SFD the dry free flowable particles exhibited excellent redispersibility characteristics in an aqueous medium, better than the FD product, due to the enlarged surface area. For the placebo formulations the liposome size decreased by 22 % for fine particles and by 17 % for large particle after SFD as compared to the initial solution before processing. The polydispersity index on the other hand increased from 0.16 to 0.20 for small particles and to 0.19 for large particles. No changes in liposomes size and polydispersity were determined for the lyophilized sample (Fig 8, left). Freeze-drying of Paclitaxel loaded liposomal formulations affected the liposomal polydispersity in all investigated cases (compare chapter 2). For the Paclitaxel formulations the liposome size and polydispersity index increased only slightly for SFD particles (Fig 8, right). For the freeze-dried Paclitaxel formulation the liposome size remained constant. However, the polydispersity index significantly increased to 0.34 after the freeze-drying process.

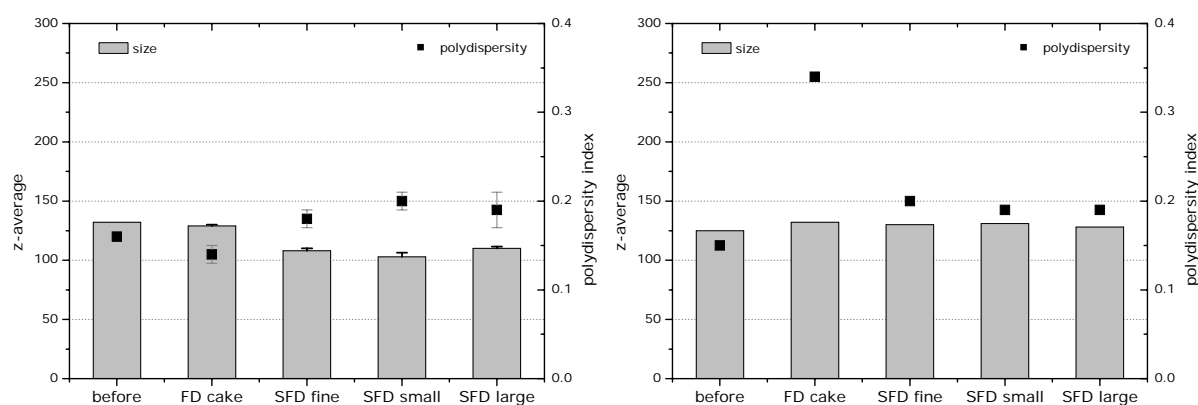


Figure 8: Liposome size before processing compared to the freeze-dried cake and the spray freeze-dried fine, small and large particles of placebo formulations (left) and Paclitaxel loaded formulations (right).

The very fast freezing in the SFD process improved the preservation of the liposomes, which was very pronounced for the Paclitaxel formulation probably due to the formation of smaller ice crystals compared to freeze-drying. Because of the fast freezing no phase separation within the droplets between the pure ice and the frozen eutectic liquid occurred [27]. The Paclitaxel remained associated to the membrane structure of the liposomes as before processing, which is a major advantage of using SFD for the stabilization of these formulations.

3.8 LIPID AND PACLITAXEL RECOVERY

The lipid recovery in placebo and Paclitaxel formulations was completely preserved for the freeze-dried cake and the larger spray freeze-dried particles (Tab 3). A significant reduction in lipid content by about 30 and 50 % for placebo and Paclitaxel formulations was determined for the fine particles. Such tremendous changes in lipid recovery can be explained by the particle loss resulting from the Leidenfrost effect during the contact of the fine aqueous droplets with the liquid nitrogen. The boiling of cryogenic liquid nitrogen caused stress to the particles, which led to decomposition and the variation in lipid content by extraction or phase separation.

Table 3: Lipid recovery of placebo and Paclitaxel loaded formulations of the lyophilized cakes and fine, small and large particle after spray freeze-drying and reconstitution.

lipid recovery [%]	DOTAP-CL	DOPC	DOTAP-CL	DOPC
	placebo		Paclitaxel loaded	
	FD cake	102.5 ± 2.5	101.8 ± 1.9	101.3 ± 2.3
SFD large particles	103.0 ± 3.7	101.0 ± 2.2	97.4 ± 5.4	96.3 ± 5.2
SFD small particles	101.0 ± 2.1	102.2 ± 2.8	93.5 ± 3.5	93.2 ± 2.4
SFD fine particles	71.0 ± 2.1	71.5 ± 2.8	44.0 ± 6.4	47.1 ± 6.1

Quantification of Paclitaxel in the formulations revealed almost 100 % recovery of the drug for the freeze-dried cake and after spray freeze-drying for small and large particles. A decrease in Paclitaxel concentration of about 10 % was observed for fine particles (Fig 9, left). During all processes the degradation product 7-Epipaclitaxel was formed, with 1.4 % for the freeze-dried cake, 1.0 % for large and small particles and 1.2 % for fine particles (Fig 9, right). The faster freezing rates during spray freeze-drying resulted in the optimized stabilization of Paclitaxel in the membranes of the liposomes, which is indicative by the slightly lower content of 7-Epipaclitaxel.

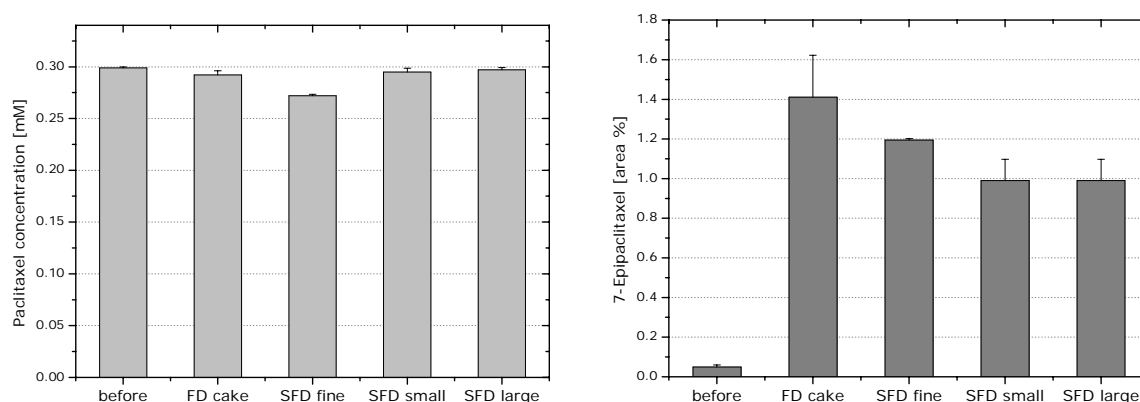


Figure 9: Paclitaxel concentration of lyophilized cake and the particles after spray freeze-drying and reconstitution (left) and the 7-Epipaclitaxel concentrations (right).

4. CONCLUSIONS

The presented study demonstrates that liposome stabilization by spray freeze-drying is a feasible alternative to the so far used freeze-drying process. An advantage of SFD is that a bulk of free-flowable particles is obtained, which can be used for flexible dosing and filling to various primary packaging. Particle size can be adjusted in a wide range between 20 μm and 3 mm by the selection of an appropriate nozzle type and the applied spraying conditions, e.g. liquid feed rate and atomization pressure. In general, higher atomizing air flow rates led to smaller particles in the final product. During spray freeze-drying the spherical shape and size of the particles was maintained for large particles upon pre-freezing in gaseous nitrogen and for small particles also by direct freezing in liquid nitrogen. For larger particles the application of the developed pre-freezing vessel was essential to obtain intact particles and to avoid disintegration. While all deployed lipid was recovered for larger particles, a loss of about 60 % occurred for fine particles which can be ascribed to the Leidenfrost effect. To avoid the Leidenfrost effect spray-freezing into liquid nitrogen could be alternatively tested.

One drawback of SFD is the complicated handling of the liquid nitrogen during the transfer from the spray-freezing equipment to the freeze-dryer. Other than expected the drying velocity of the spray-frozen particles was comparable to conventional vial freeze-drying although the surface area of the particles was larger. The residual moisture content could be reduced by decreasing the droplet size and ranged between 1.8 % and 1.5 %. Determination of liposome size and polydispersity index revealed a stabilization effect of spray freeze-drying. Most importantly, an almost complete recovery of Paclitaxel was achieved for the small and large particles after reconstitution of the dried product. Less degradation products of Paclitaxel were formed as compared to conventional vial freeze-drying.

5. REFERENCES

- [1] Gombotz, W.R., Healy, M.S., Brown, L.R., Auer, H.E., Process for producing small particles of biological active molecules, EP0432232B1 (1994).
- [2] Rogers, T.L., Hu, J., Yu, Z., Johnston, K.P., Williams, III, R.O., A novel particle engineering technology to enhance dissolution of poorly soluble drugs: spray-freezing into liquid nitrogen, *Int. J. Pharm.*, 42(3): 3-100 (2002).
- [3] Johnston, K.P., Williams, III, R.O., Chen, X., Preparation of drug particles using evaporation precipitation into aqueous solutions, U.S. Pat. WO/2002/047659 (2002).
- [4] Herbert, P., Murphy, K., Johnson, O., Dong, N., Jaworowicz, W., Tracy, M.A., Cleland, J.L., Putney, S.D., A large-scale production process to produce microencapsulated proteins, *Pharm. Res.*, 15(2): 357-361 (1998).
- [5] FDA, talk paper: FDA's REPORT ON NEW HEALTH CARE PRODUCTS APPROVED IN 1999 at <http://www.fda.gov/bbs/topics/ANSWERS/ANS00998.html> (06/05/07)
- [6] Maa, Y-F., Costantino, H.R., Spray freeze-drying of biopharmaceuticals: Applications and stability considerations, In: *Lyophilization of Biopharmaceuticals*, Ed. Costantino, H.R., Pikal, M.J., AAPS Press: 519-562 (2004).
- [7] Vaughn, J.M., Gao, X., Yacaman, M-J., Johnston, K.P., Williams, III, R.O., Comparison of powder produced by evaporative precipitation into aqueous solution (EPAS) and spray freezing into liquid (SFL) technologies using novel Z-contrast STEM and complimentary techniques, *Eur. J. Pharm. Biopharm.*, 60(1): 81-89 (2005).
- [8] Zijlstra, G.S., Hinrichs, W.L.J., De Boer, A.H., Frijlink, H.W., The role of particle engineering in relation to formulation and de-agglomeration principle in the development of a dry powder formulation for inhalation of cetorelix, *Eur. J. Pharm. Biopharm.*, 23(2): 139-149 (2004).
- [9] Baron, M.K., Young, T.J., Johnston, K.P., Williams, III, R.O., Investigation of processing parameters of spray freezing into liquid to prepare polypropylene glycol polymeric particles for drug delivery, *AAPS, Pharm. Sci. Tech.*, 4(2): 1-13 article 12 (2003).
- [10] Yu, Z., Johnston, K.P., Williams, III, R.O., Spray freezing into liquid versus spray-freeze drying: influence of atomization on protein aggregation and biological activity, *Eur. J. Pharm. Sci.*, 27(1): 9-18 (2006).
- [11] Hu, J., Rogers, T.L., Brown, J., Young, T., Johnston, K.P., Williams, III, R.O., Improvement of dissolution rates of poorly soluble APIs using the novel spray freezing into liquid technology, *Pharm. Res.*, 19(9): 1278-1284 (2002).
- [12] Gusman, M.I., Johnson, S.M., Cryochemical method of preparing ultrafine particles of high purity superconducting oxides, US4975415 (1990).
- [13] Maa, Y-F., Nguyen, P.A., Sweeney, T., Shire, S.J., Hsu, C., Protein inhalation powders: spray drying vs spray freeze drying, *Pharm. Res.*, 16(2): 249-254 (1999).
- [14] Burke, P.A., Klumb, L.A., Herberger, J.D., Nguyen, X.C., Harrell, R.A., Zordich, M., Poly(lactide-co-glycolide) microsphere formulations of darbepoetin alfa: spray drying is an alternative to encapsulation by spray-freeze drying, *Pharm. Res.*, 21(3): 500-506 (2004).
- [15] Sonner, C., Maa, Y-F., Lee, G., Spray-freeze-drying for protein powder preparation: Particle characterization and a case study with trypsinogen stability, *J. Pharm. Sci.*, 91(10): 2122-2139.
- [16] Yu, Z., Garcia, A.S., Johnston, K.P., Williams, III, R.O., Spray freezing into liquid nitrogen for highly stable protein nanostructured microparticles, *Eur. J. Pharm. Biopharm.*, 58(3): 529-537 (2004).

-
- [17] Giunchedi, P., Conte, U., Spray-drying as a preparation method of microparticulate drug delivery systems: An overview, *S.T.P. Pharma Sci.*, 5(4): 276-290 (1995).
- [18] Jiang, S., Nail, S.L., Effect of process conditions on recovery of protein activity after freezing and freeze-drying, *Eur. J. Pharm. Biopharm.*, 45(3): 249-257 (1998).
- [19] Wang, W., Lyophilization and development of solid protein pharmaceuticals, *Int. J. Pharm.*, 203(1-2): 1-60 (2000).
- [20] Sweeney, G.L., Wang, Z., Loebenberg, R., Wong J.P., Lange, C.F., Finlay, W.H., Spray-freeze-dried liposomal ciprofloxacin powder for inhaled aerosol drug delivery, *Int. J. Pharm.*, 305(1-2): 180-185 (2005).
- [21] Engstrom, J.D., Simpson, D.T., Lai, E.S., Williams, III, R.O., Johnston, K.P., Morphology of protein particles produced by spray freezing of concentrated solutions, *Eur. J. Pharm. Biopharm.*, 65(2): 149-162 (2007).
- [22] Engstrom, J.D., Simpson, D.T., Cloonan, C., Lai, E.S., Williams, III, R.O., Kitto, G.B., Johnston, K.P., Stable high surface area lactate dehydrogenase particles produced by spray freezing into liquid nitrogen, 65(2): 153-174 (2007).
- [23] Webb, S.D., Golledge, S.T., Cleland, J.L., Carpenter, J.F., Randolph, T.W., Surface adsorption of recombinant human interferon gamma in lyophilized and spray-lyophilized formulations, *J. Pharm. Sci.*, 91(6): 427-436 (2002).
- [24] Roth, C., Winter, G., Lee, G., Continuous measurement of drying rate of crystalline and amorphous systems during the freeze-drying using an in situ microbalance technique, *J. Pharm. Sci.*, 90(9): 1345-1355 (2001).
- [25] Maa, Y-F., Ameri, M., Shu, C., Payne, L., Chen, D., Influenza vaccine powder formulation development: Spray freeze-drying and stability evaluation, *J. Pharm. Sci.*, 93(7): 1912-1923 (2004).
- [26] Agbada, C.O., York, P., Dehydration of theophylline monohydrate powder-effects of particles size and sample weight, *Int. J. Pharm.*, 106(1): 33-40 (1994).
- [27] Leuenberger, H., Spray freeze-drying – the process of choice for low water soluble drugs, *J. Nanopar. Res.*, 4(1-2): 111-119 (2002).

Chapter 4

Development of a Percolative Vacuum-Drying Process

Abstract :

The newly developed percolative vacuum-drying (PVD) method combined the principles of several techniques, such as spray freeze-drying, vacuum-drying and atmospheric freeze-drying in one set-up. Due to this combination the drying of frozen particles prepared by spray-freezing was significantly accelerated. The introduction of a percolation gas enhanced the heat transfer into the particle layer and improved the sublimation rates. Dry free flowable particles were obtained with adjusted particle size by spray-freeze particle size distributions. The liposome size and loading efficiency was only affected in a minor way although a crystallization of the excipient trehalose occurred within the powder.

1. INTRODUCTION

Freeze-drying (FD) is one of the most useful techniques for drying of thermolabile compounds, which are unstable in aqueous solution. Spray freeze-drying (SFD) is a relatively new method for the preparation of particles where the particles are frozen in liquid nitrogen followed by a conventional drying process under vacuum. Both processes consist of two steps where the product is first frozen as a cake or as particles and the water is then subsequently removed as vapor from the frozen state in the dehydration step. To achieve sublimation of water/ice from the solid phase directly into the gaseous phase it is necessary to keep vapor pressure and temperature below the triple point (Fig 1). However, as already described in chapter 2 for freeze-drying and chapter 3 for spray freeze-drying the low temperature and the high vacuum only resulted in marginal driving forces for heat and mass transfer. The drying rates during SFD were very low and the process was therefore very time consuming. During SFD the drying time could not be shortened although the surface areas of SFD particles were significantly increased compared to cakes from conventional vial freeze-drying.

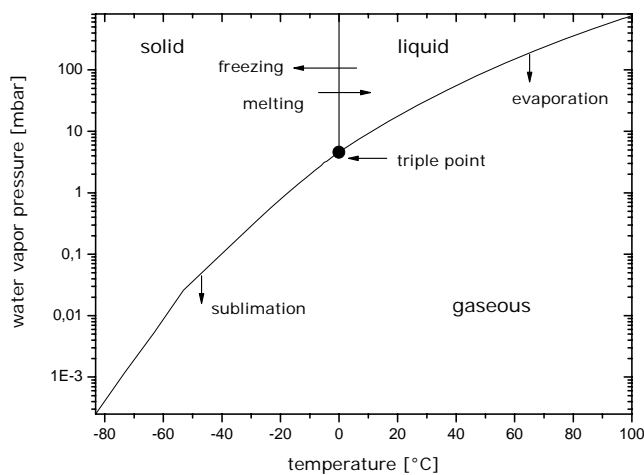


Figure 1: Phase diagram for water and the corresponding phase-transition processes.

Freeze-drying processes are generally performed by applying a vacuum to the system. However, the presence of a strong vacuum is not obligatory to induce sublimation. Only the partial pressure of water vapor in the drying medium must be kept low enough to provide a driving force for mass transfer and water vapor removal from the frozen sample. To further improve drying processes and to reduce drying time and with it the costs, technologies like atmospheric spray freeze-drying [1], fluid bed freeze-drying [2,3] or vacuum assisted drying [4] were developed. Some of these processes use cold gas to foster the water removal and as heat source to achieve sublimation close to atmospheric pressure.

Our newly developed percolative vacuum-drying (PVD) method combines several of the described approaches to improve heat and mass transfer between the circulation drying medium and the frozen sample. A vacuum was maintained during the drying process while a drying gas percolated through a cooled static particle bed [5,6]. By the application of a vacuum the thawing of the frozen particles during the drying process was inhibited. To produce particles the spray-freezing set-ups as described in chapter 3 for the production of small or large particles were used. The objective of this study was to evaluate the feasibility of the percolative vacuum-drying technique for the stabilization of liposomal formulations. The focus was set on the influence of operation variables on the quality of the dried particles and the integrity of the liposomes.

2. MATERIAL AND METHODS

2.1 LIPOSOME PREPARATION

The ethanol injection technique was used for preparing placebo and drug containing liposomes. Briefly, for the placebo formulation a lipid stock solution of 400 mM DOTAP-Cl (1,2-dioleoyl-3-trimethylammonium-propane-chloride) and DOPC (1,2-dioleoyl-*sn*-glycero-3-phosphocholine) in ethanol was prepared (Merck, Darmstadt, Germany). 25 ml of this lipid stock solution were subsequently injected under stirring into 975 ml 10.5 % [w/v] trehalose solution to result in a total final lipid concentration of 10 mM. The ethanol injection was followed by five cycles of extrusion through a 0.2 μm polycarbonate membrane. The fluorescent probe Coumarin (Sigma-Aldrich, Darmstadt, Germany) was directly dissolved within the lipid stock solution with a final lipid concentration of 10 mM in total, and a final concentration of 15.4 μM Coumarin.

2.2 FLUORESCENCE SPECTROSCOPY

Fluorescence spectroscopy was performed using a Varian Cary Eclipse (Darmstadt, Germany). 2 ml of the solutions were measured in quartz cuvettes at a constant temperature of 20°C. For the determination of the Coumarin content in the samples a standard curve with 0 to 20 mg/l Coumarin in ethanol was measured. The excitation wavelength was 410 nm and the emission intensity was recorded at 520 nm. The emission and excitation slits were set to 5 nm and the voltage of the PMT detector was set to 800 V. After PVD drying the samples were reconstituted and centrifuged using Ultrafree[®] 0.5 centrifugal filter devices (Millipore, Bedford, MA, USA) with a cut-off off at 10K to remove the free drug content.

2.3 PERCOLATIVE VACUUM-DRYING METHOD (PVD)

Preliminary experiments were carried out using the technical set-up as shown in Figure 2. Small and large particles were prepared by spray-freezing a preformed liposome suspension which contained trehalose as stabilizer. The frozen particles were loaded with liquid nitrogen into the pre-chilled drying chamber at a temperature of below -20°C . To maintain the temperature below the freezing point inside the percolation drying chamber after the evaporation of the liquid nitrogen the double walled jacket was adjusted to temperatures between -40 and 10°C during the process. The temperature was controlled by an intercooler with a cooling agent or by using a self developed liquid nitrogen supply. The percolation medium was gaseous nitrogen in an open loop system. A percolation flow rate between 15 to 30 l/h nitrogen was used. The vacuum inside the drying chamber was maintained between 1 and 4 mbar by a vacuum pump duo 10 (Pfeiffer, Assler, Germany) with a total capacity of $10\text{ m}^3/\text{h}$.

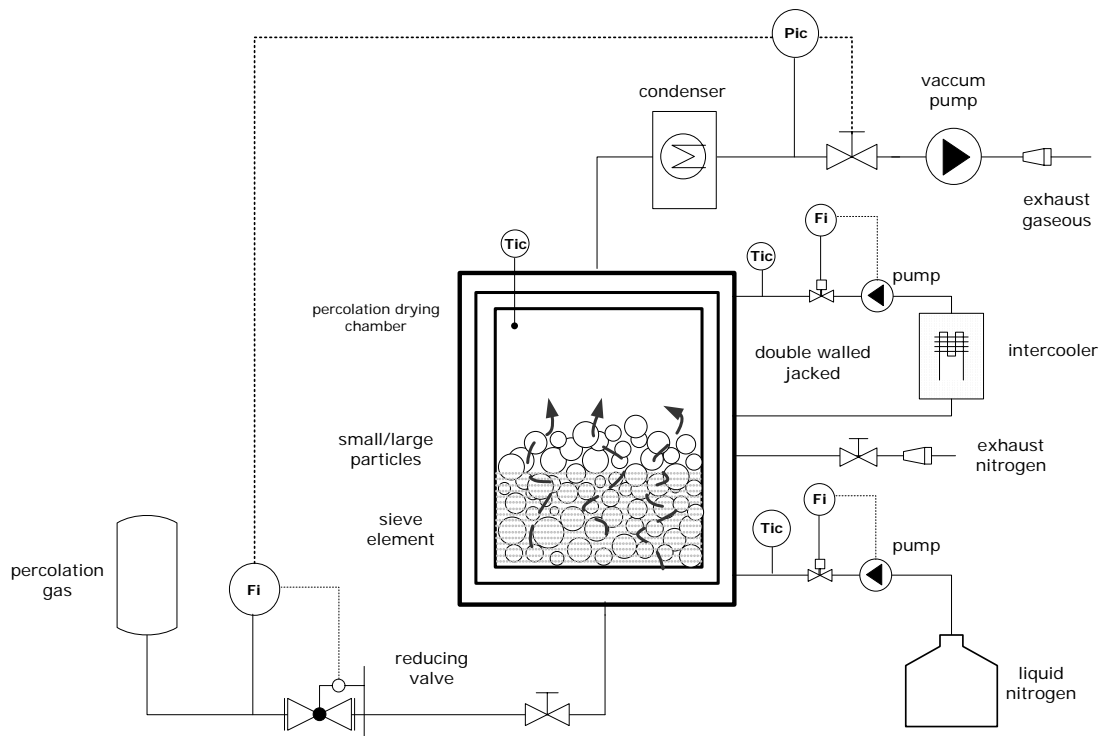


Figure 2: Schematic construction of the percolation drying apparatus to spray-freeze particles.

All further methods used in this chapter are already described before.

3. RESULTS AND DISCUSSION

3.1 THE PERCOLATIVE DRYING CONCEPT

To obtain dry PVD powders, the frozen solvents must be sublimated. Compared to freeze-drying with a freezing step over several minutes or hours, the high cooling rates in SFD inhibit ice crystal growth after nucleation, leading to small ice crystals with a large ice crystal surface area [7]. These small ice crystals produce a very fine microporous structure in the particles and affect the water vapor permeability during the drying process. However, a direct comparison of the drying rates measured during SFD and FD of a cake revealed no enhanced water sublimation rates for the SFD product.

In literature it is often referred to that liposomal fusion, aggregation and a collapse of the samples can be avoided by selecting drying conditions (product temperatures) below the glass transition temperature of the maximally freeze concentrated solution (T_g') [8,9]. However, we found a so called no collapse range (T_{nc}) above the T_g' of the formulation which was at -47°C (Fig 3).

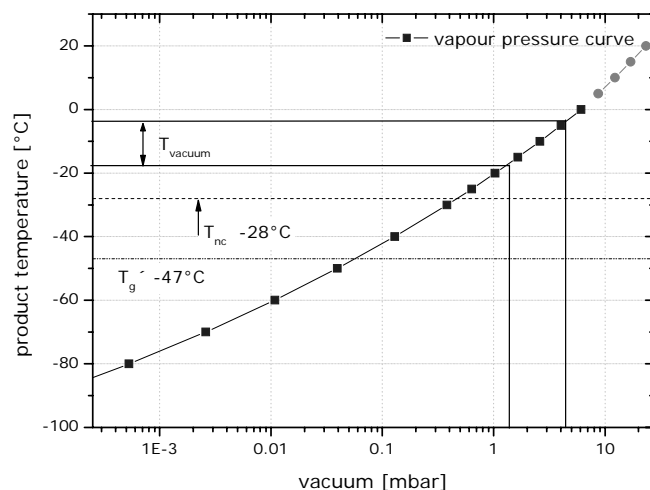


Figure 3: Product temperature of the applied vacuum [10] with the glass transition temperature of the liposomal formulation. The assumed temperature range without any collapse and the product temperature induced by the vacuum are shown.

Depending on the heat transfer and drying rate no macroscopic collapse of the cake occurred in this T_{nc} range above approximately -47°C . As upper limit of the non collapse region the T_g' of pure trehalose at -28°C was estimated. However, the non collapse region reaches probably to even higher temperature, which was not tested so far. Furthermore, only minor effects on the liposomal properties were determined. Therefore, we assumed that this T_{nc} range can be used as a working area for the PVD process. The

lowest applied vacuum was 1.5 mbar which can be assigned to a product temperature of -18°C . The applied vacuum and the great temperature difference between the product and the percolation gas resulted in a high sublimation rate. This led to an evaporative cooling effect of the product. Additionally, the heat and mass transfer were raised by a continuous increase of the chamber temperature.

The gas inlet temperature during the percolative process was about 15°C , which is clearly above the eutectic temperature and the temperature of the ice-vapor interphase of the frozen sample. Although the percolation gas temperature was relatively high the particles almost retained their structure and size during the process. The very fast sublimation rates, as well as the vacuum (T_{vacuum}) and the chamber temperature (T_{chamber}) preserved the material due to the cooling effect induced by the sublimation. The frozen particles were placed into liquid nitrogen, with a temperature of -196°C in the drying chamber and the drying process occurred ideally within the described product temperature range (T_{product}) (Fig 4).

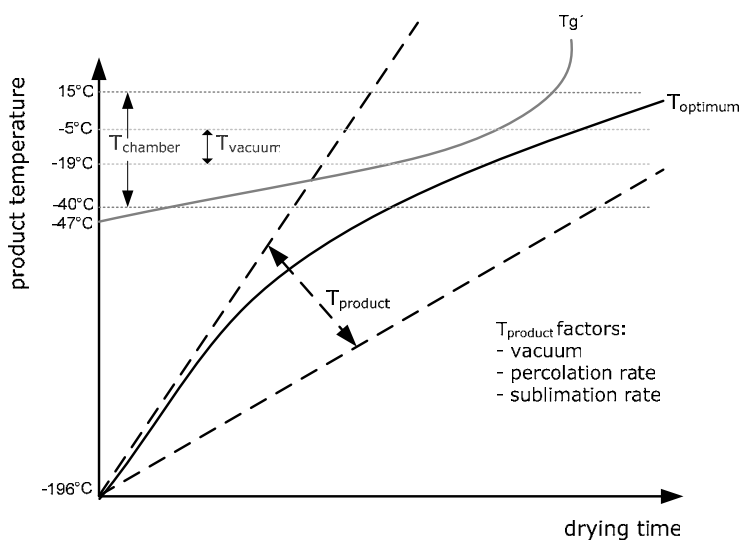


Figure 4: Schematic drying profile during percolative-drying of the spray freeze-dried particles of the liposomal formulation.

Simultaneously, the thermal treatment during the warming of the product resulted in a continuous annealing and drying process. The conventional annealing processes during lyophilization use the effect of crystal growth during the annealing step and result in faster sublimation rates during primary drying [11]. The percolative gas flow through the particle layer further enhanced the heat transfer into the product and the sublimation of ice. Furthermore, the gas temperature raised the product temperature, which should result in a balance between heat transfer and drying rate at a certain vapor pressure. The formed dry layers on the particles, which are known to increase the product

resistance, did not influence the heat transfer. The low heat conductivity of dried material and the layer resistance can be neglected in such a percolation drying processes compared to freeze-drying of a solid cake under vacuum because of the percolation of the drying gas, which further strengthens the movement of the vapor phase. The major challenge of this process is to achieve a gap where the mobile water which is present above the T_g' is removed before collapse occurs (Fig 4).

To avoid controlled collapse and/or crystallization an optimum product temperature profile defined by the percolation rate and the gas temperature is essential for the drying process. Therefore, the process parameters must be selected in the no collapse area (T_{nc}). The fact the T_g' raises with the drying status of the product support this assumption [12]. The crystallization of the powder during the process (compare 3.3) indicated that this range was not yet found sufficiently.

3.2 RESIDUAL MOISTURE

The residual moisture content varied between 4.0 % for large and 2.6 % for small particles (Tab 1). During the drying process of the particles first weak bound surface water was removed followed by the water of the large capillaries and finally the capillary water out of the particle core. With the selected drying conditions and the applied vacuum the residual absorbed water could not be removed.

During freeze-drying and spray freeze-drying ethanol could not be completely removed (compare chapter 2 and 3). After reconstitution of the particles produced by percolative drying no residual ethanol was detectable for all drying conditions (data not shown). This is a major advantage of this technique.

Table 1: Process parameters during percolative drying at varied temperature and percolation gas flows in respect of process time and residual moisture.

batch no.	particle type	chamber		percolation gas flow [l/h]	vacuum [mbar]	process time [h]	residual moisture [%]
		temperature [°C]					
		start	end				
1	large	-40	15	14.8	4.5	4	2.8
2	large	-8	10	14.8	3.5	12	4.0
3	large	-1	9	22.2	2.5	4	3.5
4	small	-1	14	22.2	3.5	4	3.5
5	small	-1	9	22.2	1.5	2	2.6
6	small	-5	5	29.6	2.0	2	3.9
7	small	-1	9	29.6	2.0	2	2.7

3.3 PARTICLE MORPHOLOGY

DSC and X-ray powder diffraction were used to characterize the morphology of the percolative dried particles. To characterize the amorphous phase the glass transition temperature was determined by DSC for percolative dried particles. The glass transition temperature was located at 49°C for the smaller particles (Fig 5, left). The X-ray diffraction pattern of percolative dried samples displayed crystalline peaks with higher intensities for the larger particles (Fig 5, right). The heat transfer and the temperature increase during the process were faster for smaller particles compared to larger particles at comparable percolation gas flow and chamber temperature. Although the small particles showed partially crystalline structure the liposome properties were preserved (compare 3.4). These data indicated that the temperature profile for the selected conditions passed the “T_g” line” and the free water was not sublimated fast enough. This resulted in glassy material with a local structure similar to that in crystals. Only a minimal rearrangement was necessary for nucleation and crystal growth [13].

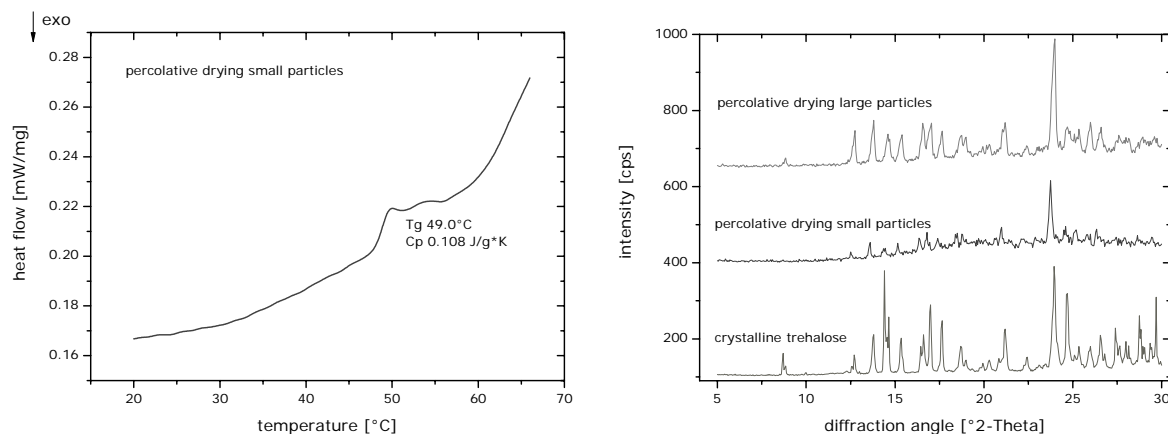


Figure 5: Glass transition temperature (T_g) of percolative dried small particles (left) and wide-angle X-ray diffraction pattern for crystalline trehalose and large and small particles of percolative dried trehalose (right).

3.4 LIPOSOME PROPERTIES AND DRUG LOADING

The percolation vacuum-drying process showed a robust and very fast drying progress for spray-freeze particles. The primary goal of the developed drying process was the preservation of the liposome size distribution and the prevention of leakage and fusion. Liposome size and polydispersity were only slightly affected by the percolative drying process (Fig 6, left) although crystallization occurred. For example the size stayed constant and only the polydispersity index increased slightly from 0.21 to a maximum of 0.22 for batch no. 6 (small particles). The drug loading studies with Coumarin as model substance did not reveal significant fusion or aggregation of the liposomes which would

result in a loss of the active compound after the percolation drying process (Fig 6, right). Only at high percolation gas flow rates the drug recovery decreased to about 90%.

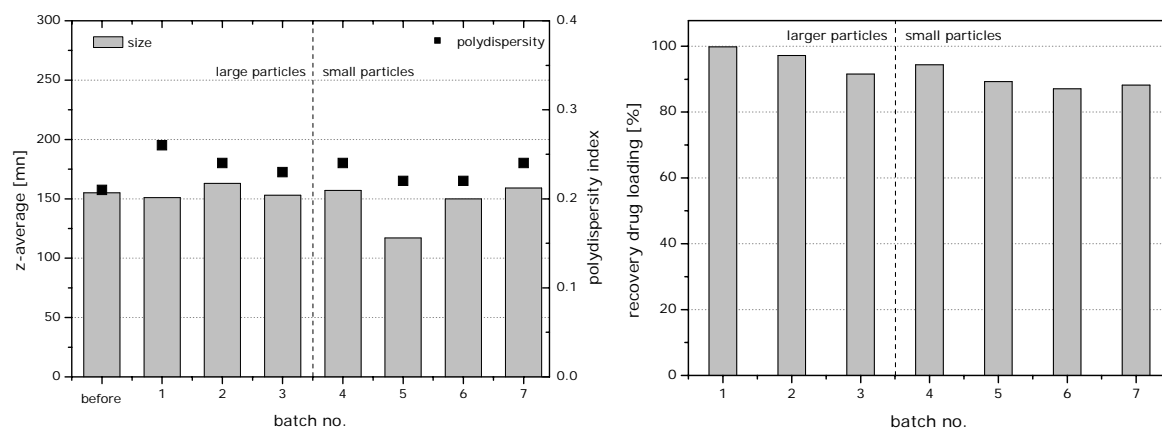


Figure 6: Liposome size and polydispersity before and after percolative drying of small and large particles (left) and drug loading recovery of Coumarin in small and large particles (right).

3.5 LIPID RECOVERY

The lipid recovery for the percolative dried products depended on the particle size (Tab 2). Larger particles showed about 100 % recovery. The smaller particles showed a lipid loss between 10 and 15 %, where it is still unclear to which process step the loss could be ascribed. During SFD a lipid loss of about 7 % was determined for the small particles although they were dried with a more gentle SFD process. Due to the preservation of the lipids within the larger particles the assumption was made that the lipid loss occurred already during the spray-freezing process. Further investigations are necessary to identify this relation. No lipid degradation products were determined for all percolative drying processes (data not shown).

Table 2: Lipid concentration of small and large particle after spray-freezing and percolative drying.

batch no.	particle type	lipid recovery [%]	
		DOTAP-CL	DOPC
1	large	101.5	102.0
2	large	99.8	100.4
3	large	-	-
4	small	87.1	87.7
5	small	85.9	86.2
6	small	90.5	90.2
7	small	-	-

4. CONCLUSIONS

The presented investigations demonstrate that liposome stabilization by percolative vacuum-drying was feasible. It can be used as a fast alternative to the time consuming freeze-drying of spray-frozen particles, which was described in chapter 3. Only 120 minutes were necessary to dry the same amount of particles compared to 24 hours with freeze-drying. Free-flowable particles were obtained, which could be handled as bulk material and used for flexible, individual filling to the desired primary packaging container. The residual moisture content was reduced to 2.6 % without any additional drying step. However, trehalose crystallization occurred during the drying process for all studied conditions. Nevertheless, a determination of liposome size and polydispersity index revealed a stabilizing effect of percolative vacuum-drying. The reduced lipid content or smaller particles most likely due to the Leidenfrost effect could not be solved in this chapter, as well.

However, the results demonstrate a first feasibility study whether drying under the described percolative vacuum-drying conditions is possible. Further investigations and process variations are necessary to optimize the drying behavior of the particles. A first approach can be the reduction of the percolation gas temperature to decelerate the thawing process of the particles. In addition, higher vacuums or different chamber temperatures should be evaluated to determine the optimum product temperature during the drying process. A full understanding of the obtained sublimation rates is essential to further optimize this process. The knowledge of the maximum cooling effect induced by a specific sublimation rate is necessary to calculate the maximum heat capacity. Overall, the use of deeply frozen particles and their behavior during thawing seems to be a promising approach for an effective drying method.

5. REFERENCES

- [1] Mumenthaler, M., Leuenberger, H., Atmospheric spray-freeze drying: a suitable alternative in freeze-drying technology, *Int. J. Pharm.*, 72(2):97-110 (1991).
- [2] Abelow, I., Wagman, J., Fluidized bed freeze drying, US 3436837 (1969).
- [3] Leuenberger, H., Pransch, A.K.T., Luy, B., Method for producing particulate goods, US 6584782 (2003).
- [4] Montgomery, S.W., Goldschmidt, V.W., Franchek, M.A., Vacuum assisted drying of hydrophilic plates: static drying experiments, *Int. J. Heat Transfer*, 41(4-5): 735-744 (1998).
- [5] Wiggenhorn, M., Haas, H., Drexler, K., Winter, G., Percolative drying for the preparation of particles, EP 06022538.0 (2006).
- [6] Mujumdar, A.S., Principles, classification and selection of dryers, in *Handbook of industrial drying*, 3rd edition, Taylor and Francis, CRC Press, 3-32 (2007).
- [7] Burke, P.A., Klumb, L.A., Herberger, J.D., Nguyen, X.C., Harrell, R.A., Zordich, M., Poly(lactide-co-glycolide) microsphere formulations of darbepoetin alfa: spray drying is an alternative to encapsulation by spray-freeze drying, *Pharm. Res.*, 21(3): 500-506 (2004).
- [8] Buitink, J., Van den Dries, I.J., Hoekstra, F.A., Alberda, M., Hemminga, M.A., High critical temperature above T_g may contribute to the stability of biological systems, *Biophys. J.*, 79(2): 119-1128 (2000).
- [9] Crowe, J.H., Hoekstra, F.A., Nguyen, K.H., Crowe, L.M., Is vitrification involved in depression of the phase transition temperature in dry phospholipids?, *Biochim. Biophys. Acta*, 26(2): 187-196 (1996).
- [10] List, R.J., *Smithsonian meteorological tables*, 6th ed. (1971)
- [11] Lechuga-Ballesteros, D., Miller, D.P., Duddu, S.P., Thermal analysis of lyophilized pharmaceutical peptide and protein formulations, in *Lyophilization of Biopharmaceuticals*, Ed. Costantino, H.R., Pikal, M.J., AAPS Press; 271-335 (2004).
- [12] Jennings, T.A., *Lyophilization, Introduction and Basic Principles*, Interpharm press, (1999).
- [13] Surana, R., Pyne, A., Suryanarayanan, R., Effect of Aging on the Physical Properties of Amorphous Trehalose, *Pharm. Res.*, 21(5): 867-874 (2004).

CHAPTER 5

Evaluation of Spray-Drying as a Stabilizing Technique for Liposomes

Abstract:

Spray-drying using a two-fluid nozzle was tested to dry liposome preparations, i.e. liposomes composed of DOTAP-Cl/DOPC with the molar ratio 50/50 at 10 mM total lipid concentration. Operating parameters such as drying air temperature and volumetric air flow were varied. Stable, flowable and dry powders with particle diameters in the range from 5 to 70 μm could be produced. Best results were obtained for an inlet air flow above 473 l/h at a temperature of about 200°C, corresponding to a product temperature (outlet temperature) of about 100°C. No indication for chemical degradation of lipids was found under these conditions. The redispersability characteristics of the dry powders were excellent. The size distribution of the liposomes after reconstitution was remarkably well maintained, with a mean size (Z_{ave}) of about 130 nm and a polydispersity index (PI) mostly below 0.2. Residual moisture was about 2 % at the best conditions.

1. INTRODUCTION

Spray-drying is an established method for the preparation of fine powders ranging from about 50 nm to several hundred μm . Its applicability for the drying of liposomal products has been demonstrated and it can also be used for regular manufacturing of dried liposomal formulations especially for the stabilization of lipophilic drugs [1,2,3,4]. However, the particular spray-dried product needs to be evaluated in respect of stabilization of the active ingredient and of liposomal integrity after the process. During spray-drying, particle formation and drying is achieved in a continuous single step. The driving force is the difference in vapor pressure between the drying air and the droplet surface. The process consists of (i) atomization of a liquid feed into a spray, (ii) the spray-air contact where the moisture evaporates and finally, (iii) the separation of the dried particles from the air [5]. A major concern in spray-drying of liposomes is the high processing temperatures, which may induce thermal degradation of the lipids and/or the active ingredient. Contrary to freeze-drying, the moisture levels should be decreased within seconds during the spray-drying process, whereby the moisture level is affected by the particle size and the used excipients. As crystallization during the process and during long term storage can be fostered by the presence of water, moisture content should be maintained at a low level.

Depending on the design of the spraying nozzle different atomization procedures are possible. The most common approaches are two-fluid atomization, pressure atomization and electrostatic or ultrasonic atomization. Droplet size and the subsequent particle size are depending on the applied nozzle. With a two-fluid nozzle the feed solution is transported to the nozzle at relatively low flow rates and mixed with a velocity gas stream. Upon mixing, the air causes the feed to break up into a spray. The droplets are principally formed at the cap-orifice of the two-fluid nozzle. The droplet size is influenced by the surface tension, the viscosity of the feed solution and most importantly, by the fluid velocity at the nozzle orifice, as well as the air/liquid mass flow ratio [6]. An increase in liquid flow rate at constant atomizing air flow rate modifies the fluid break-up and results in larger droplets and hence larger particles [7]. Lipids can reduce the surface activity as well as energy and therefore can influence the droplet formation [8,9,10]. Trehalose acts as bulking agent in the formulation and plays an important role in increasing the surface area of the lipid mixture enabling successful hydration of spray-dried products [11].

When processing heat labile materials, the spray-dryer should be operated in a co-current manner, where the spray and the drying air pass through the drying chamber in

the same direction. Thereby, droplets remain at low temperatures at high moisture evaporation rates and the particles get in contact with the coolest air after drying.

In this study the spray-drying technique (SD) using a two fluid nozzle was tested to dry cationic placebo liposomes, as well as liposomes loaded with the fluorescent dye Coumarin or the drug Paclitaxel. Two different spray-drying set-ups were tested for the spray-drying of preformed placebo and drug loaded liposomes in an aqueous-organic medium with trehalose as stabilizing excipient. Parameters like drying air temperature and atomizing air flow rate were varied. The morphology and physico-chemical properties of the spray-dried particles were analyzed after the process. After reconstituting the dried powders with water the liposomes were characterized.

2. MATERIAL AND METHODS

2.1 LIPOSOME FORMATION

The ethanol injection technique was used for preparing placebo and drug containing liposomes. Briefly, for the placebo formulation a lipid stock solution of 400 mM DOTAP-Cl (1,2-dioleoyl-3-trimethylammonium-propane-chloride) and DOPC (1,2-dioleoyl-*sn*-glycero-3-phosphocholine) in ethanol was prepared (Merck, Darmstadt, Germany). The fluorescent probe Coumarin (Sigma Aldrich, Steinheim, Germany) was used as model drug and dissolved within the lipid stock solution at a concentration of 31 μ M. 25 ml of this lipid stock solution were subsequently injected under stirring into 975 ml 10.5 % [w/v] trehalose solution to result in a total final lipid concentration of 10 mM. The ethanol injection was followed by five cycles of extrusion through a 0.2 μ m polycarbonate membrane. The liposomal Paclitaxel containing formulation consisted of molar ratio 50/47/3 of DOTAP-Cl/DOPC/Paclitaxel (Natural Pharmaceuticals Inc., Beverly, MA, USA) and was prepared in the same way.

2.2 SPRAY-DRYING METHOD WITH BÜCHI MINI SPRAY-DRYER

The liposome dispersion was spray-dried with a B-290 mini spray-dryer (Büchi, Flawil, Switzerland) combined with the dehumidifier LT mini (Much, Germany) and an improved (high resistance) cyclone. Such improved cyclone resistance results in a larger pressure drop due to a smaller radius of the cyclone chamber. A two-fluid nozzle equipped with a cap-orifice diameter of 0.7 mm was used for spray-drying. Cooling water of about 10°C circulated through the double jacket around the nozzle. After separation of the drying product the air passes a filter unit through the aspirator (Fig 1).

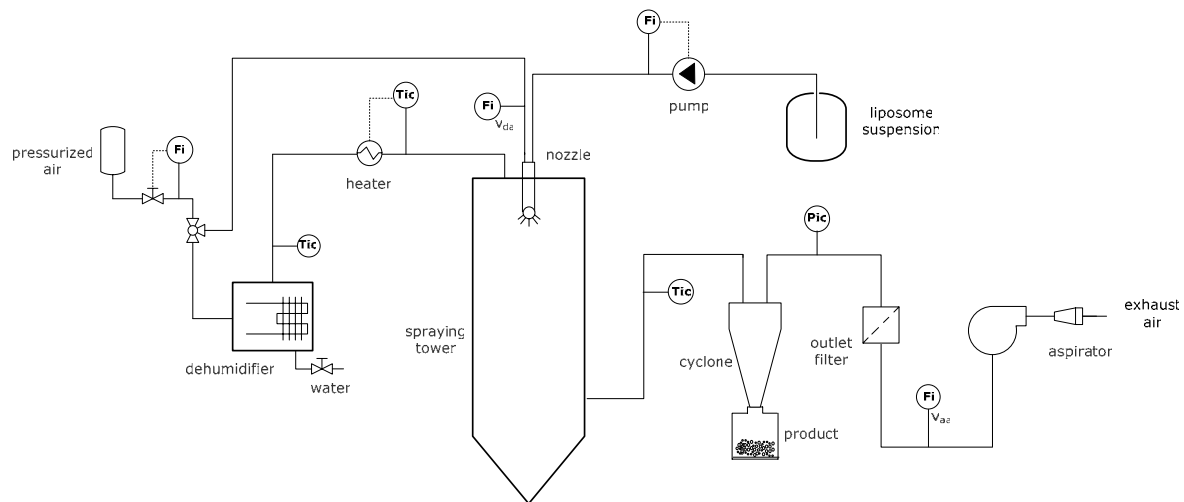


Figure 1: Schematic construction of the Büchi mini spray-dryer B-290 and the measuring points.

The following process conditions were used. The drying air with a relative humidity of 20 % and an inlet temperature (T_{inlet}) from 80 to 220°C resulted in a drying air outlet temperature (T_{outlet}) in the range from 40 to 120°C. The atomizing air volumetric flow rate (v_{aa}) ranged from 240 to 750 l/h and the drying air volumetric flow rate (v_{da}) was kept constant at a maximum of 37.8 m³/h. Finally, the liquid feed volumetric flow rate (v_{lf}) was set to 2.7 ml/min for all experiments. In some cases the mass ratio of atomizing air to liquid feed ($m_{aa/lf}$) was calculated using equation 1. These conditions were chosen to achieve a sufficiently high enthalpy throughput of the system for most process conditions [12].

Equation 1: Mass ratio of atomization air to liquid feed $m_{aa/lf}$ was calculated [7].

$$m_{aa/lf} = \frac{v_{aa} [l/h] \times 10^{-3} \times [m^3/l] \times 1.21 [kg/m^3]}{v_{lf} [ml/min] \times 60 [min/h] \times 10^{-3} [l/ml] \times 10^{-3} [m^3/l] \times 1000 [kg/m^3]} \quad (1)$$

2.3 SPRAY-DRYING METHOD WITH A NIRO SD-MICRO

Paclitaxel formulations were spray-dried using a SD-Micro (GEA-Niro, Copenhagen, Denmark) installed in an isolator safety cabinet. This scale-up apparatus allows a spray pattern comparable to full scale production units. The system was equipped with exhaust gas bag filters to increase the product recovery (Fig 3). Such filters allow the removal of fine particle fractions and to maintain the air flow rate constant. A 0.5 mm two fluid nozzle in the co-current mode with the following process conditions was used: drying air inlet temperature (T_{inlet}) from 67 to 142°C, resulting in the drying air outlet temperature

(T_{outlet}) in the range from 50 to 111°C, atomizing air volumetric flow rate (v_{aa}) 2 and 3.5 kg/h and a constant drying air volumetric flow rate (v_{da}) of 30 kg/h. The liquid feed volumetric flow rate (v_{lf}) was set from 106 to 977 g/h. An aliquot of the same batch of the spraying solution was lyophilized with conditions described in chapter 2 (drying run no.1).

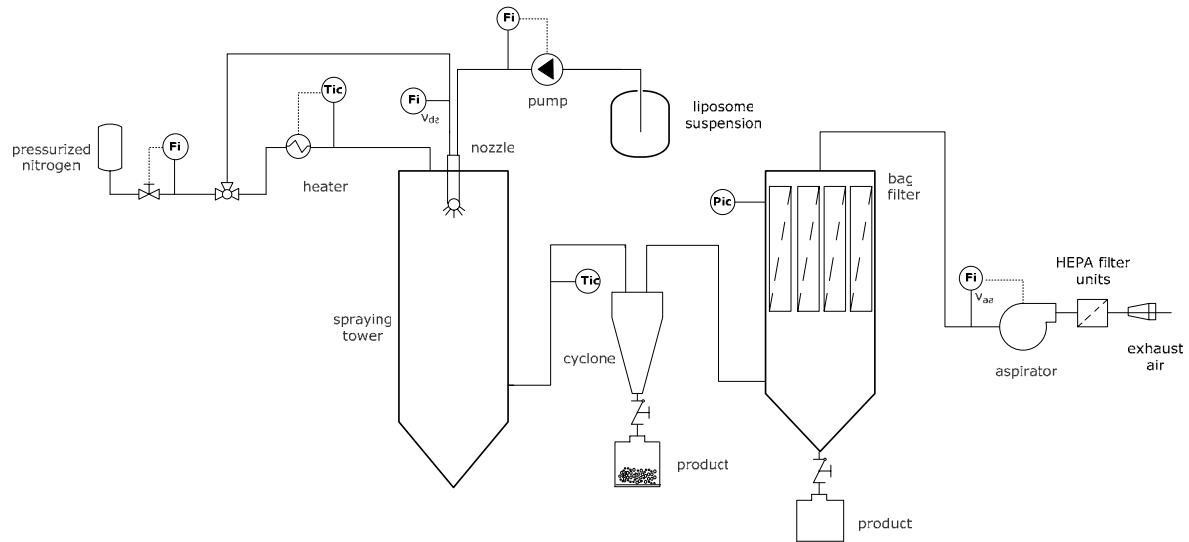


Figure 2: Schematic construction of the Niro Mobile Minor SD and the measuring points.

2.4 VACUUM-DRYING

A secondary vacuum drying (VD) step for 12 hours at 0.01 mbar and 20°C in the freeze-dryer Epsilon 2-6D (Martin Christ, Osterode, Germany) was implemented for selected experiments. This additional drying step was found to be necessary to further reduce the residual moisture below 1 %.

2.5 ANALYSIS OF PARTICLE MORPHOLOGY

The size distribution of solid particles was determined with a laser diffraction analyzer (Mastersizer X, Malvern, Germany) and the small-volume-unit, which was used to pump the powder suspension into the sample cell. About 20 mg of SD powder were dispersed in 10 ml MigyloI 812 (Sasol, Marl, Germany) containing 1 % Span 85. Background alignment with pure dispersion medium was performed prior to adding the particle medium. Laser light scattering intensity was evaluated by Fraunhofer analysis using a polydisperse mode. The data were expressed in terms of the particle size diameter at 10, 50 and 90 % of the volume distribution ($d[10]$, $d[50]$ and $d[90]$). The span of the volume distribution, a measure of the width of the volume distribution relative to the

median diameter ($d[50]$) was derived from $(d[90]-d[10])/d[50]$. In addition, the mean diameter of the volume distribution ($d[4,3]$) was reported.

2.6 VISCOSITY MEASUREMENTS

The viscosity was determined by a cone-plate rheometer MCR 100 (Paar Physica, Germany). A 75 mm plate was used for the measurement. The computer based system is equipped with a Peltier element measurement system. The measurements were conducted at a constant temperature of 25°C.

2.7 LIGHT OBSCURATION

Subvisible particle $\geq 1 \mu\text{m}$ were determined by light obscuration measurement using PAMAS-SVSS-C Sensor HCB-LD-25/25 (Partikelmess- und Analysensysteme, Rutesheim, Germany).

2.8 ZETA-POTENTIAL

The zeta-potential was determined with the Zetasizer Nano (Malvern, Herrenberg, Germany). The measurements were performed in the automatic measurement mode using disposable capillary cells (Malvern DTS 1060).

All further methods used in this chapter are already described before.

3. RESULTS AND DISCUSSION

3.1 FEASIBILITY STUDY OF LIPOSOME SPRAY-DRYING

3.1.1 Particle morphology

The feasibility studies were performed using the Büchi mini spray-dryer and liposomal formulations without drug. Within the hot dehumidified drying air, which is produced by the dehumidifier and the heater, the particles dry very rapidly in the main drying chamber with drying times shorter than 1 second for spray droplets smaller than 100 μm as described by Masters (1991) [5]. The low relative humidity of the inlet air by the dehumidifier improved the drying capacity and raised the driving force for water removal [13]. The droplet size is affected by various parameters, e.g. liquid feed rate or atomizing air flow. The drying process can be divided in two phases beginning with a constant drying rate followed by a steadily decreasing drying rate. The particle shape and size correlates with the drying rate, which is determined by the liquid feed and basically by the outlet temperature described by Maa et al. (1997) [8]. The particle morphology of the spray-dried powders for the different atomizing air flows is shown in the scanning electron microscopy (SEM) photographs (Fig 3). In general, SEM of the spray-dried powders revealed smooth spherical surfaces of the particles for all conditions. At 246 l/h larger droplets were formed and the particles tended to partly agglomerate. This can be mainly attributed to the low atomization energy and the sticky nature of trehalose during spray-drying [14]. However, no rough surface structures or particle shrinkage were observed for all studied conditions.

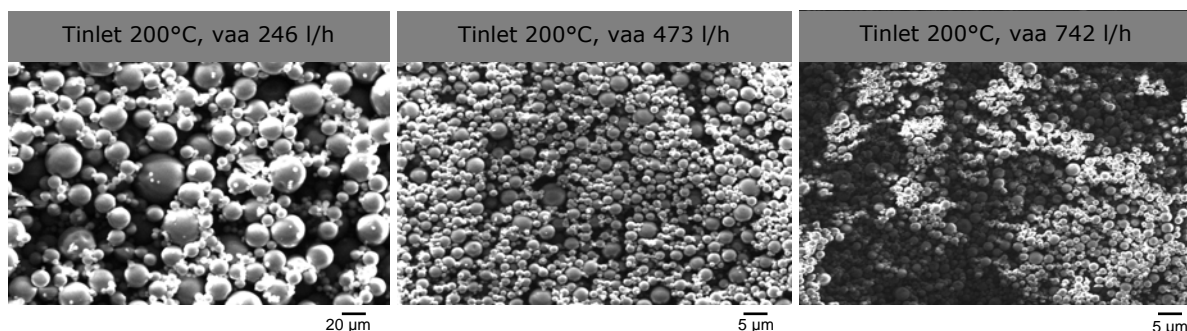


Figure 3: Scanning electron micrographs of spray-dried liposomes dried with atomizing air flows of 246 l/h, 473 l/h and 742 l/h.

3.1.2 Product temperature during the process

The correlation between the inlet air temperature and the outlet temperature depends on various parameters, in particular the liquid feed, the atomizing air flow rate and the solid content in the fluid solution. During the early stage of the drying process the surface of a

droplet remains moisture saturated with a temperature lower than T_{inlet} . This beneficial effect preserves the liposomes and the incorporated drug, as it is suggested that the majority of water is removed early on the top of the chamber. As the drying continues, the droplet temperature raises because the surface is not saturated with moisture due to reduced diffusion and convection rate. If the ratio of drying rate to diffusion of water to the particle surface is too high, a crusted surface or a viscous film forms, and the temperature increases above the so called wet bulb temperature (T_{wb}). This can result in collapsed or burst structures due to the high interior vapor pressure and in higher residual moisture content [13]. Considering this, T_{outlet} can be used as the representative temperature of the drying droplet and finally the exposed temperature during the evaporation process [15]. For the tested trehalose concentrations the outlet temperature is plotted against the inlet temperature and the mass ratio of atomizing air and liquid feed, as these parameters influence the drying rate (Fig 4).

A linear relation between outlet temperature and inlet temperature/ $m_{aa/lf}$ was found at a trehalose concentration of 5 % [w/v] for the studied conditions (Fig 4, (A)). At a trehalose content of 10.5 % [w/v] the outlet temperature increased at low mass ratio atomizing feed to liquid feed (Fig 4, (B)). A further increase in trehalose concentration led to a reduced T_{outlet} and suggested a faster evaporation of water (Fig 4, (C)). Here the viscosity and the increased mass ratio of atomized air and liquid feed resulted in different droplets sizes and finally a faster drying rate visible by the steeper decreased T_{outlet} .

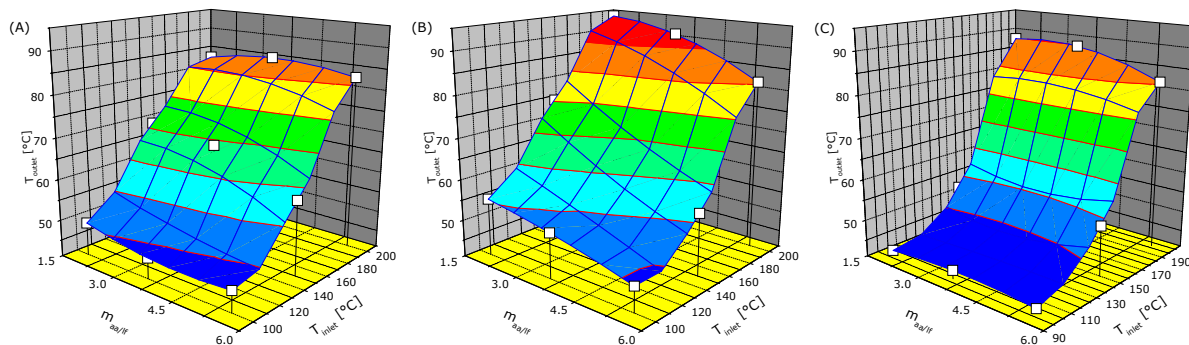


Figure 4: Outlet temperature (T_{outlet}) at increasing trehalose concentration of 5 (A), 10.5 (B) and 15 (C) % [w/v], mass ratio of atomizing air to liquid feed ($m_{aa/lf}$) at an air inlet temperature of 100, 150 and 200°C.

The high viscosity and solid content influenced the droplet formation and drying performance. More energy was required to evaporate the water and consequently the outlet temperature decreased. Already at 150°C T_{inlet} the product temperature revealed values of about 55°C and was further reduced below 40°C (Fig 4, (C)). To reduce the outlet temperature/product temperature a high mass ratio of atomized air and liquid feed or high trehalose concentrations are beneficial.

3.1.3 Particle size distribution

The liquid break-up at the two-fluid nozzle is influenced by the viscosity of the formulation, the atomizing air flow and the drying temperature. Maury et al. (2005) showed a minor influence of varying liquid feed on the droplet velocity and droplet diameter, as compared to the atomizing airflow for trehalose solutions by measuring the droplets size distribution using the phase doppler analysis (PDA) [7]. The disintegration of the jet is significantly improved by the high velocity of the atomizing air and causes sufficient turbulences, which results in small droplets [16]. The atomization appeared to be the most important parameter for the size of the particles. The viscosity of trehalose solutions increased from 1.09 mPa s at 5% [w/v], to 1.33 mPa s at 10.5% [w/v] and to 1.56 mPa s at 15% [w/v] trehalose compared to water (0.89 mPa s / 25°C). At 5 % [w/v] trehalose and T_{inlet} of 100°C the mass ratio of atomizing air to liquid feed only had a minor effect on the particle size distribution. This indicated homogenous water evaporation from the droplets during the passing through the drying chamber (Fig 5, (A)).

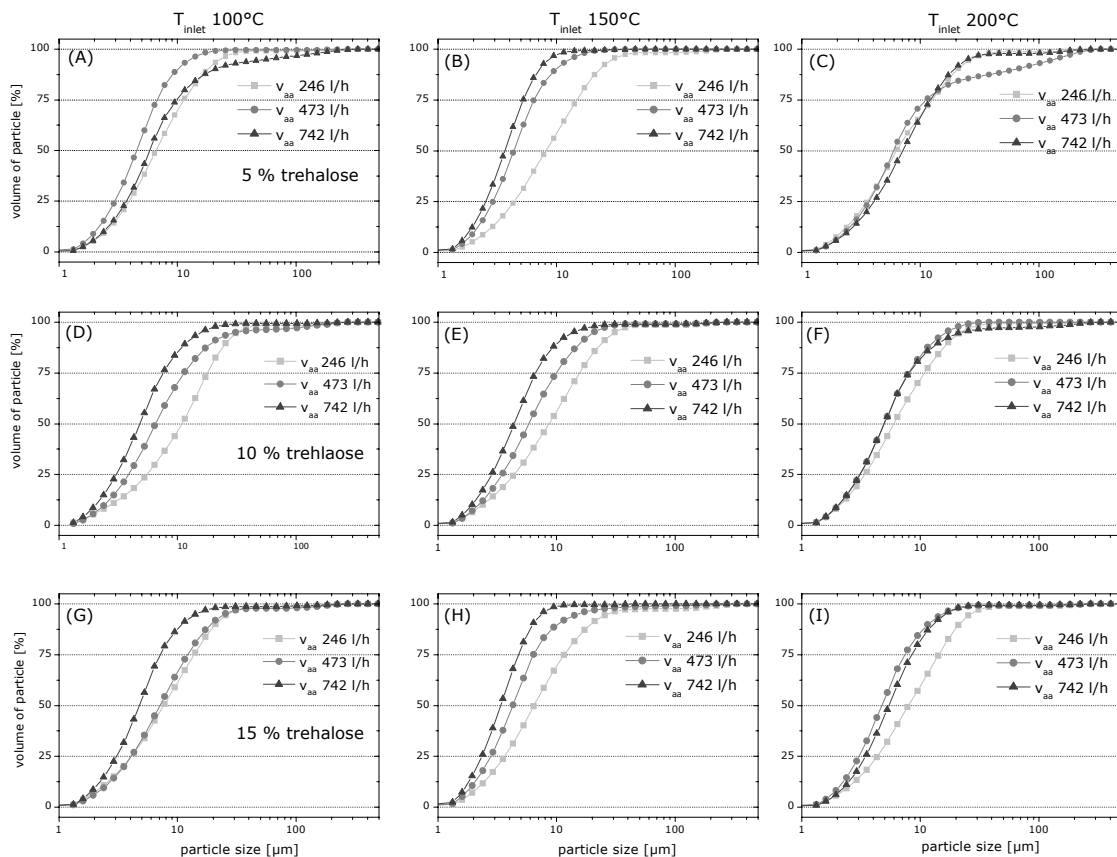


Figure 5: Volume size distribution of spray-dried particles at increasing atomizing air flow 246, 473 and 742 l/h with different trehalose concentrations of 5 % [w/v] at T_{inlet} of 100°C (A), 150°C (B) and 200°C (C) for 10.5 % [w/v] at T_{inlet} of 100°C (D), 150°C (E) and 200°C (F) and for 15% [w/v] at T_{inlet} of 100°C (G), 150°C (H) and 200°C (I).

When increasing the temperature to 150°C the drying speed rose at the high mass ratio of atomizing air to liquid feed ($m_{aa/lf}$) and resulted in smaller particles with narrow size distributions (Fig 5, (B)). However, for the studied liposomal formulations the particle size increased with temperature and drying speed (Fig 5, (C)), as well as with the viscosity (Fig 5, (D) to (E) and (G) to (J)). In literature it was already shown that the droplet size increases at higher liquid viscosities and results in larger particles shown by Adler and Lee (1999) [11] and by Bain et al. (1999) [17]. The increased mass ratio of atomizing air to liquid feed ($m_{aa/lf}$) in our study predominantly led to the smallest particles size distribution. The mass ratio of atomizing air to liquid feed at 200°C showed no significant differences in the particle size distribution. In addition, the span decreased from 2.5 to 1.5 (data not shown) with increased solid content, temperature and atomization air flow for all particle distributions.

3.1.4 Residual moisture content

The drying air volumetric flow rate (v_{da}) affected the drying efficacy of the spray-dryer and the droplet/particle residence time within the drying chamber. Although the particle size increased at higher trehalose contents, the efficient atomization and the higher enthalpy throughput resulted in moisture contents below 3 % (Fig 6). A possible explanation can be increased hydrogen bonding, which occurs between the sugar and the lipids, when more trehalose was present in the liposomal formulations [18].

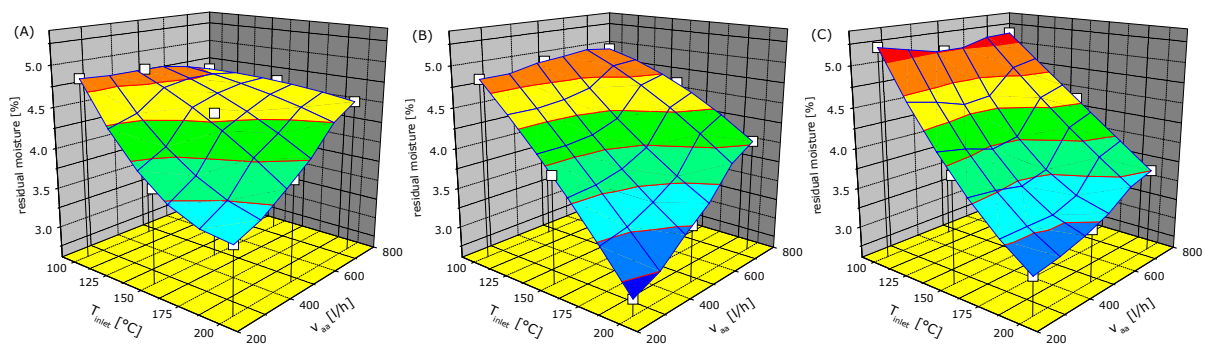


Figure 6: Residual moisture at 5 (A), 10.5 (B) and 15 % [w/v] trehalose (C), with atomizing air flow of 246, 473 and 742 l/h, determined at an air inlet temperature of 100, 150 and 200°C.

Residual moisture levels under reasonable spray-drying conditions generally range about 3 to 5 %, which can be too high for a feasible long term stabilization of the formulation [19]. Within spray-drying, inlet temperature and the mass ratio of atomizing air to liquid feed ($m_{aa/lf}$) can be varied to achieve sufficiently low moisture contents. The residual moisture content of the particles decreased from 4.5 % at 58°C to 2.2 % at outlet

temperatures above 100°C (Fig 7). Above 100°C outlet temperature the drying capacity could be not further improved. However, the manufacturing efficiency is slowed down when reducing the v_{lf} and the temperature exposure could affect the integrity of liposomes and drug.

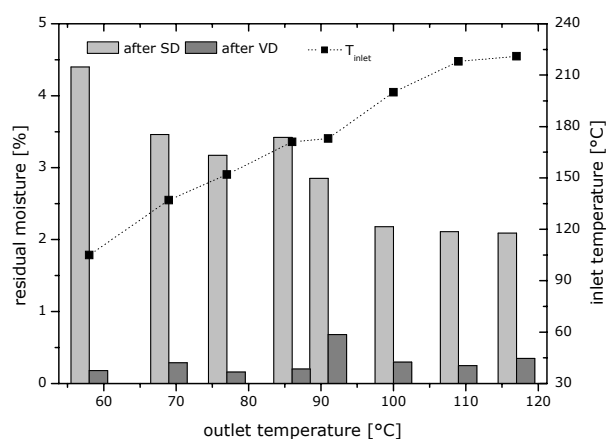


Figure 7: Residual moisture of the particles after spray-drying at 473 l/h atomizing air flow and after the additional vacuum-drying step.

Therefore, a secondary vacuum-drying process after spray-drying might be the helpful alternative to reduce the residual moisture within the spray-dried powder. With an additional vacuum-drying step of 12 hours at 0.01 mbar and 20°C (Fig 7) a level of 1 % residual moisture could be achieved for all samples. After the spray-drying process liposomal formulations furthermore contained no ethanol deriving from the ethanol injection. Using static headspace gas chromatography (HS-GC) no residual ethanol could be detected in the reconstituted spray-dried powders, indicating a complete removal during the process (data not shown).

3.1.5 Particle yield

A decline in yield during spray-drying can be induced by attachment of powder to the chamber wall and by reduced cyclone efficiency in collecting fine powders. Such fine particle fractions are retained by the back filter and cannot be calculated within this balance. However, to further reduce the material loss during spray-drying of the liposomal formulation a high resistance cyclone was used.

The effect of drying temperature and the mass ratio of atomization air to liquid feed ($m_{aa/lf}$) on the powder yield was distinct and correlated with the drying behavior of the droplets. With increasing trehalose concentrations the product yield decreased for all selected conditions (Fig 8). The highest atomizing air flow rate of 742 l/h resulted in an

ideal particle distribution for spray-drying with a reduced loss of material at the wall of as fine particle fraction. For 5 and 10.5 % [w/v] trehalose concentration a product yield above 80 % was achieved at drying conditions of 150°C, which was the optimum inlet temperature. For 15 % [w/v] trehalose the solution viscosity resulted in a broader initial droplet size distribution. The initial droplet size which is induced by the v_{aa} showed to be responsible for the product yield.

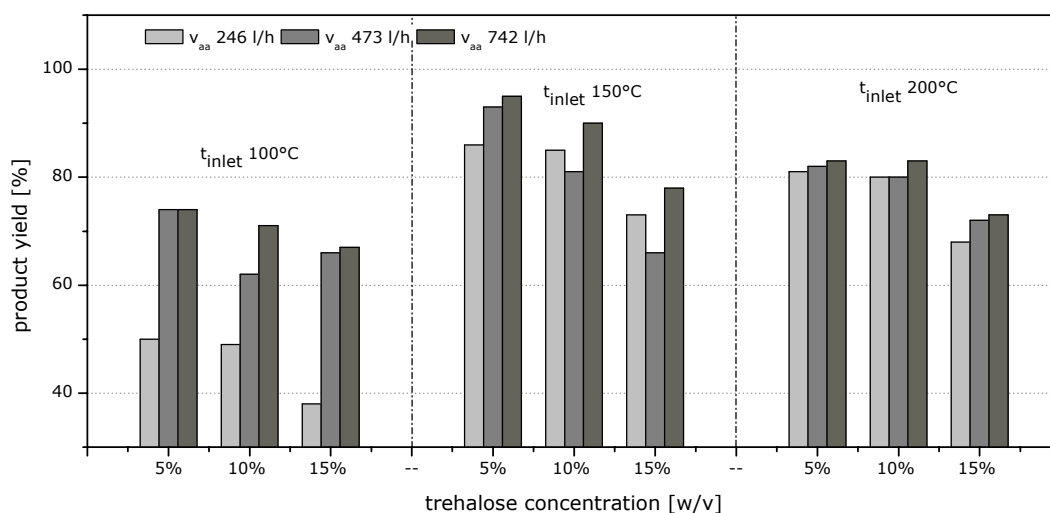


Figure 8: Product yield at 5, 10.5 and 15 % [w/v] trehalose, atomizing air flow (v_{aa}) of 246, 473 and 742 l/h determined at air inlet temperatures of 100, 150 and 200°C.

3.1.6 Liposome recovery

3.1.6.1 Liposome size and polydispersity

The liposome size was generally well retained after rehydration as measured by dynamic light scattering for all preparations. A slight decrease in liposome size by 20 nm to about 130 nm could be determined after reconstitution of the dried product (Fig 9). This tendency was more pronounced at high trehalose concentrations, which might be due to the heat exposure. Higher drying temperatures induce more stress to the lipid bilayers, resulting in increased membrane fluidity with larger permeability for the entrapped material [20]. Coumarin was used as model drug to investigate this phenomenon. For all trehalose concentrations and process conditions a drug loading of about 95 % Coumarin could be preserved after the process (data not shown), although it is known that the permeability of phospholipids increases during the spray-drying process [21]. Trehalose was capable to prevent fusion and leakage of the liposomes during the spray-drying process and the rehydration step. As described recently, two stabilizing mechanisms of trehalose on the liposomal structure are feasible. At first the sugar preserves headgroup spacing in the dried state and thereby prevents the phase transition during rehydration

[22]. Secondly, the sugar replaces the water molecules bound to lipid headgroups in the hydrate state, when the water is removed by the spray-drying process [23].

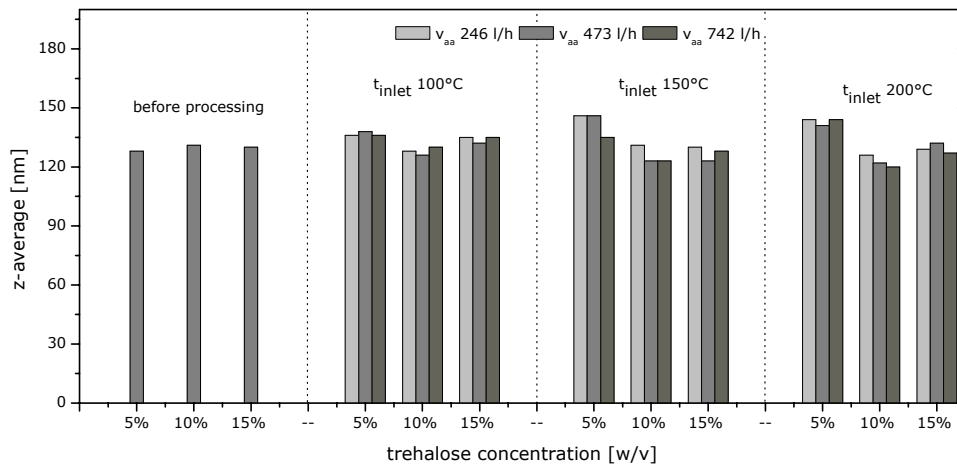


Figure 9: Liposome size at 5, 10.5 and 15 % [w/v] trehalose, atomizing air flow (v_{aa}) of 246, 473 and 742 l/h determined at an air inlet temperature of 100, 150 and 200°C.

Despite of the relatively constant liposome size, the polydispersity was affected depending on temperature and solid content (Fig 10). At higher trehalose concentrations the liposomes were preserved better because of efficient protecting properties of trehalose and the resulting lower outlet temperatures. At elevated heat exposures during our experiments the polydispersity index increased slightly. The preserving effect of trehalose depended on its concentration and finally on the droplet size. Although droplets containing only 5 % [w/v] trehalose showed a fast drying behavior, the ratio of liposomes to trehalose was not ideal. However, the polydispersity values were still in an acceptable range for all conditions and indicated preservation of the liposomal structure during the spray-drying process.

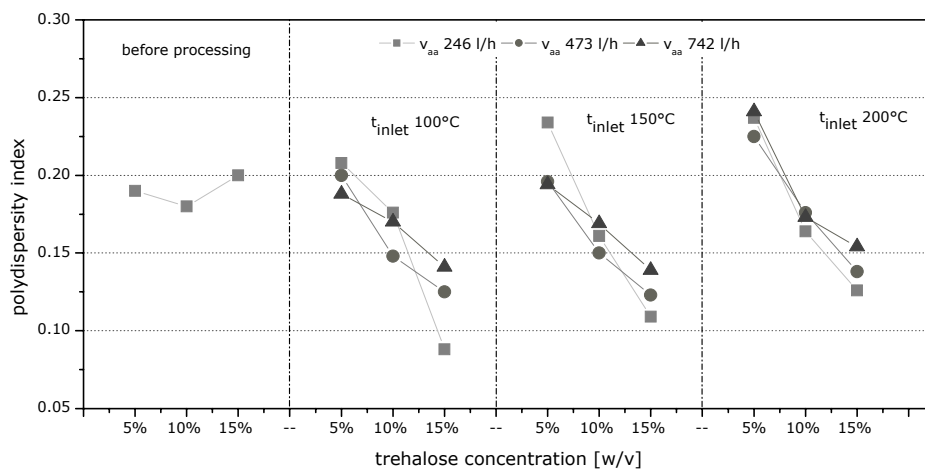


Figure 10: Polydispersity index at 5, 10.5 and 15 % [w/v] trehalose, atomizing air flow (v_{aa}) of 246, 473 and 742 l/h determined at an air inlet temperature of 100, 150 and 200°C.

To study the general impact of temperature exposure on liposome size and polydispersity DLS of the liposomal dispersion was measured during a thermal scan from 20 and 70°C using steps of 5°C (Fig 11). The liposome size decreased with increasing temperature by about 20 % down to 100 nm at 70°C. The polydispersity index was marginally affected by the induced temperature and varied between 0.13 and 0.17. After cooling back to 20°C the liposome size rose again slightly, but did not go back to the initial size before the thermal treatment.

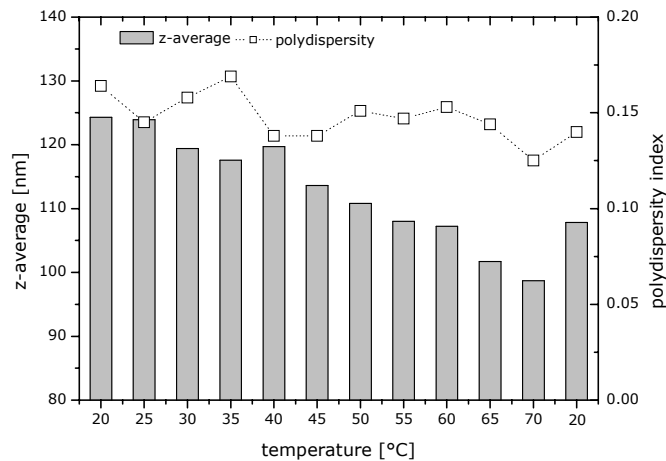


Figure 11: Liposome size distribution and polydispersity index measured at temperatures between 20 and 70°C with DLS.

No damage of the liposomes was detected during spray-drying, which indicated a stability of the liposomes to resist heat stress without any leakage. The subsequent vacuum-drying procedure showed no negative influence on liposome integrity (Fig 12). For all process conditions the liposome size and polydispersity was preserved and no fusion could be determined.

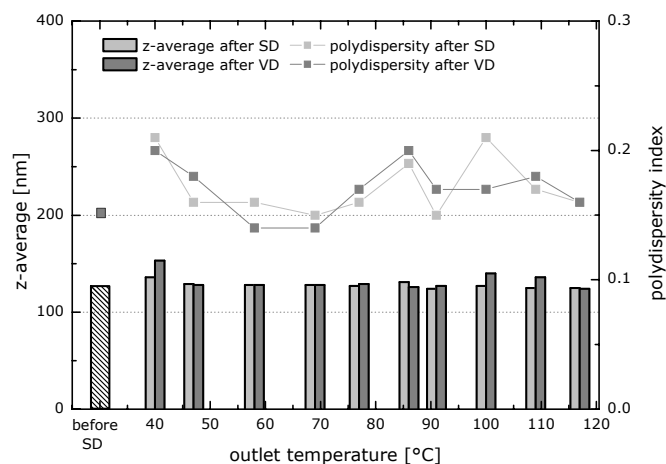


Figure 12: Liposome properties of the particles after spray-drying of 10.5 % [w/v] trehalose at 473 l/h atomizing air flow without and with the additional vacuum-drying step.

3.1.6.2 Liposome zeta-potential

Before processing, the zeta-potential was 50 mV for the liposomal formulation stabilized with 10.5 % [w/v] trehalose, which confirmed the incorporation of charged lipids [24]. Spray-drying had no significant influence on the zeta-potential, which was not substantially changed for all conditions. The values varied between 45 and 51 mV (Fig 13) and were least changed after the spray drying process in the formulations with 15 % trehalose slightly.

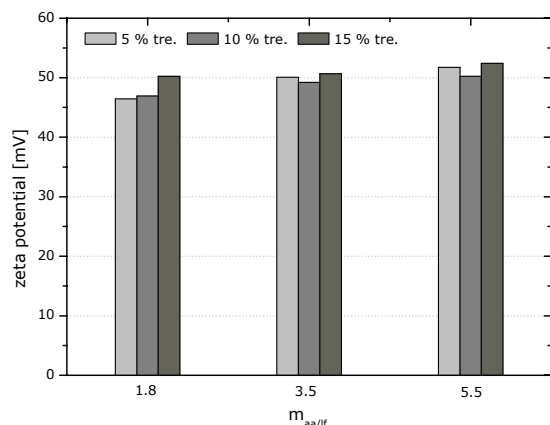


Figure 13: Zeta potential after spray-drying at varied mass ratio of atomization air to liquid feed ($m_{aa/lf}$) 150°C T_{inlet} and increased trehalose content.

The zeta-potential is an important and useful indicator to control the integrity of the liposomes. The more positive the zeta-potential the more stable is the liposomal membrane, because charged particles repel each other. High zeta potentials therefore imply more stable suspensions with less aggregation [25].

3.1.7 Physico-chemical characterization

Besides the liposome integrity, the morphology of the dried particles was analyzed, as it can affect the storage stability of the formulations. The glass transition temperature, which is characteristic for an amorphous system was determined by DSC. The interaction of trehalose and lipids, plus the formation of a glassy product have a major impact on liposome preservation [26,27]. Here, the glass transition temperature of spray-dried trehalose–liposome formulations appeared to generally increase with the drying temperature depending on trehalose concentration. At 5 % trehalose the T_g varied from 38°C at a inlet temperature of 100°C to 47.4°C at a inlet temperature of 200°C (Fig 14, (A)). For higher trehalose concentrations the effect was less pronounced, an increased T_g of 46°C at 200°C T_{inlet} was determined (Fig 14, (B-C)). The measured T_g

above 45°C is high enough to allow storage of the formulations at room temperature. Around and above T_g higher molecular mobility would facilitate fusion and leakage, which can result in increased vesicle size in the rehydrated dispersion [28]. Furthermore, a crystallization of trehalose indicated by the endothermic peak at about 100°C was distinct. The crystallization onset depended on the residual moisture content and the molecular structure [29]. The glass transition temperature rose up to 70°C when reducing the moisture content e.g by the additional vacuum-drying step (data not shown). Water is known to act as plasticizer, which decreases the T_g of formulations [30].

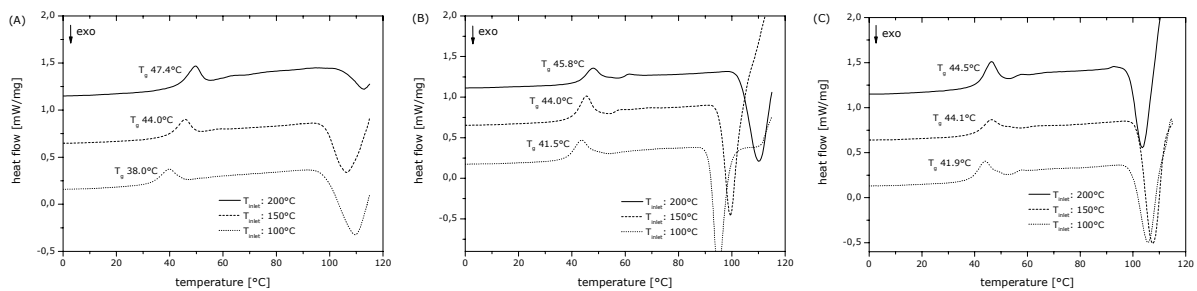


Figure 14: DSC thermograms for different trehalose concentrations for spray-dried particles with 5 % (A), 10.5 % (B) and 15 % (C) [w/w] trehalose.

While DSC is capable to give information about the existence of an amorphous fraction, X-ray diffraction can be used to determine potential crystalline fractions in the spray-dried product. The X-ray diffraction pattern of all spray-dried samples displays a broad halo in the range from 17 to 27° 2-Theta with two maxima at about 10° 2-Theta. The broad halo and thereby the packaging of trehalose was influenced by the trehalose concentration (Fig 15, (A-C)). The lack of resolved reflections in the diffraction patterns clearly indicated that no crystalline material could be detected by powder X-ray diffraction [24].

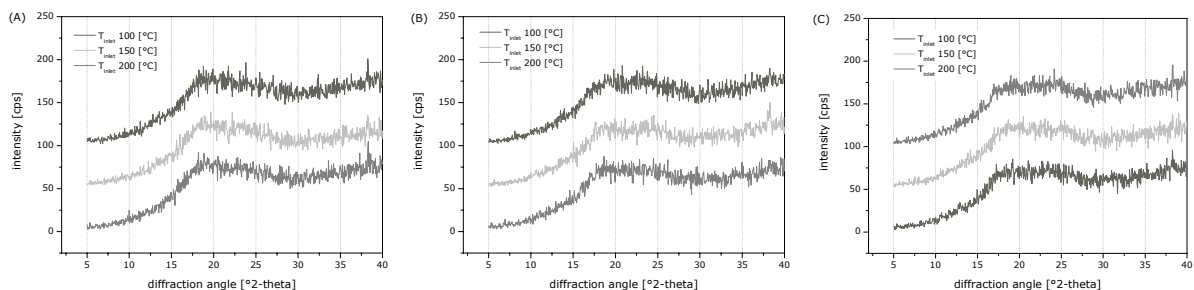


Figure 15: Wide angle X-ray diffraction pattern for spray-dried particles for different trehalose concentrations 5 % (A), 10.5 % (B) and 15 % (C) [w/w] trehalose.

The data from DSC and XRD suggested that the fundamental structure of the trehalose matrix in the spray-dried particles was amorphous. The glass transition temperature increased with inlet drying temperature and a reduction of residual moisture, which was evident by vacuum-dried particles with reduced residual moisture and higher T_g.

3.1.8 Lipid recovery

The initial lipid concentration of the liquid formulation before spray-drying was set as 100 %. A slight increase and decrease in lipid concentration between 0.5 and 3 % for DOPC and DOTAP-Cl could be determined when spray-drying was performed at higher temperatures (Fig 16, left). When varying the atomizing air flow only a slight lipid loss of approximately 1.0 % was observed for the mass ratio of atomizing air to liquid feed ($m_{aa/lf}$) 1.83 and an increase of 3 % for 5.54 ($m_{aa/lf}$) (Fig 16, right).

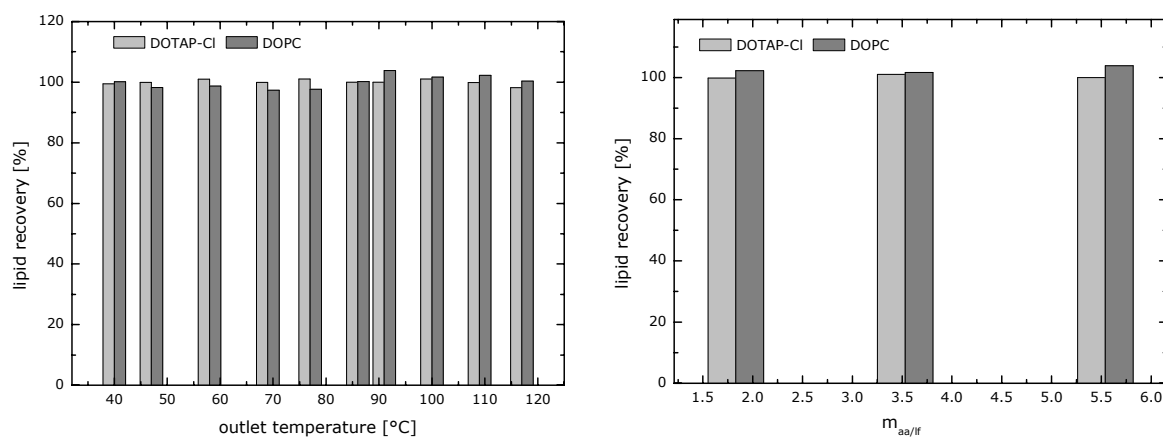


Figure 16: Lipid concentration of DOTAP-Cl and DOPC after spray-drying with an atomizing air flow of 473 l/h performed at different temperatures (left), spray-drying at T_{outlet} of 100°C with a variation of atomizing air flows (right).

However, at the low trehalose concentration of 5 % [w/v] the lipid degradation product oleic acid was determined for all studied conditions by RP-HPLC (data not shown). It can be concluded that more than 5 % [w/v] trehalose is required to prevent lipid degradation.

3.2 SPRAY-DRYING OF PACLITAXEL FORMULATIONS

Handling of cytostatic drugs always requires safety arrangements like working benches and protective clothing. Paclitaxel is a high potent anti-cancer drug candidate [31], which

makes working in a fully sealed off equipment mandatory like in the Mobile Minor system (Niro, Copenhagen, Denmark) installed in an isolator.

3.2.1 Particle properties

The scale-up equipment revealed an improved drying capacity. With such improved equipment the drying air volume behavior changed with respect to evaporation and heat transfer capacity. The process and nozzle gas rate and the maximum values of water evaporation were doubled compared to the Büchi equipment.

In detail the drying capacity with a higher constant drying air volumetric flow rate (v_{da}) of 30 kg/h and the heat capacity (kinetic energy) were more efficient. This resulted in substantial higher mass ratios of atomizing air to liquid feed ($m_{aa/lf}$) values (Fig 17, left). The residual moisture could be reduced down to 0.6 % at 111°C T_{outlet} due to the larger scale of the spray-dryer and the very low liquid feed rate. A direct comparison with a $m_{aa/lf}$ value of 3.58 to the experimental set-up used for the feasibility study with the placebo liposomes revealed comparable residual moisture levels. A linear behavior between T_{inlet} and T_{outlet} was found and the drying performance could be adjusted at an elevated mass ratio of atomizing air to liquid feed (Fig 17, right). With decreased residual moisture the glass transition temperature raised (Tab 1).

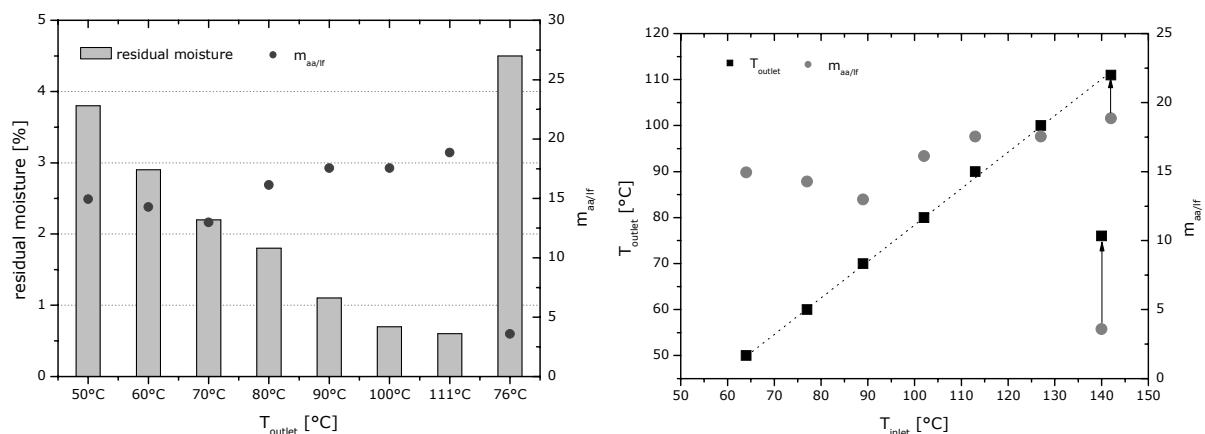


Figure 17: Residual moisture at increased outlet temperatures (left) and the relation of temperature and mass ratio of atomizing air to liquid feed ($m_{aa/lf}$) (right).

The powder yield ranged between 69 and 106 % at high mass ratios of atomizing air to liquid feed ($m_{aa/lf}$) (Tab 1). At settings comparable to those used at the Büchi spray-dryer for the placebo studies the yield decreased by about 50 %. The loss of material could be assigned to lack of drying ability and the selected ratio drying gas to liquid feed.

Table 1: Product yield at different mass ratios of atomizing air to liquid feed ($m_{aa/lf}$) and temperatures.

$m_{aa/lf}$	14.9	14.2	12.9	16.1	17.5	17.5	18.8	3.5
T_{inlet} [°C]	64	77	89	102	113	127	142	140
T_{outlet} [°C]	50	60	70	80	90	100	110	76
T_g [°C]	56	69	76	82	>90	>90	>90	50
yield [%]	73	83	69	76	84	84	106	36

3.2.2 Liposome recovery

Liposome size and polydispersity were affected by the drug loading with Paclitaxel and by the spraying pattern. For some process conditions liposomal integrity and drug loading was preserved comparable to the freeze-dried sample (Fig 18, left). Especially the low mass ratio of atomizing air to liquid feed ($m_{aa/lf}$) at a T_{inlet} temperature of 140°C resulted in liposomes with optimum polydispersity indices below 0.2. The lipid recovery of DOTAP-Cl and DOPC was assured for the studied conditions (Fig 18, right).

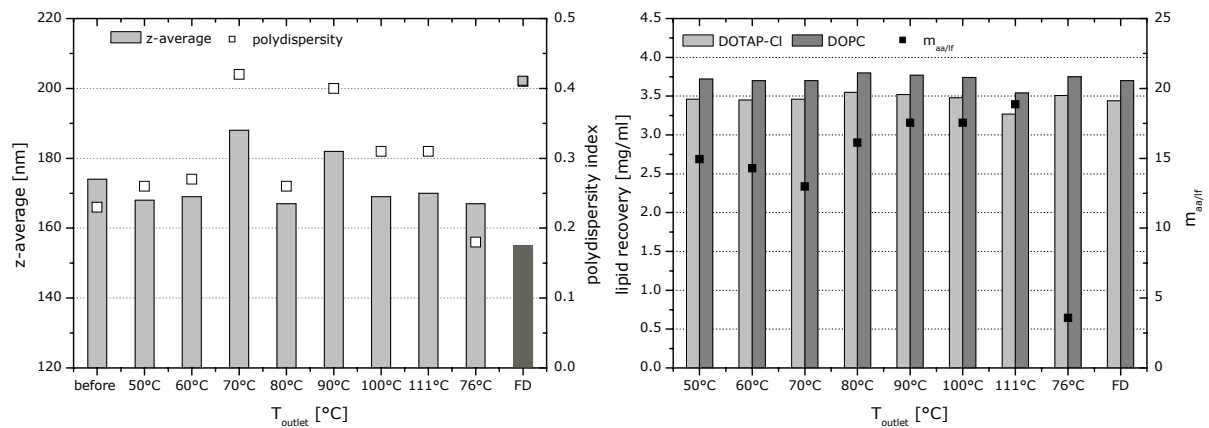


Figure 18: Liposome size and polydispersity index for spray-dried Paclitaxel formulations at increased outlet temperatures (left) lipid recovery of DOTAP-Cl and DOPC after spray-dried at increased outlet temperatures and feed rates (right) compared to the freeze-dried sample.

3.2.3 Paclitaxel recovery

As Paclitaxel stability and its loading ability in a lipid membrane are rather low in liquid formulations [32], it was of great importance for the studies to preserve the drug loading during the process. A partial crystallization of Paclitaxel was determined by light microscopy already prior the experiments. This could be attributed to the rather low storage stability and the shipping to the test station, resulting in an overall slight decrease in Paclitaxel content as compared to the freeze-drying sample. The impact of temperature exposure during the drying process on Paclitaxel was obvious by a decreased drug content (Fig 19, left). The heat sensitive anticancer drug formed

degradation products during spray-drying. Such impurities like 7-Epi-paclitaxel were determined after reconstitution of the spray-dried product (Fig 19, right). In general, the content of Paclitaxel impurities increased with higher drying temperature and ranged between 2 and 15 %. Insufficient drying capacities and the resulting high residual moisture content were the reason for the higher impurity rates of about 15 %, at the high v_{if} of 977 [g/h].

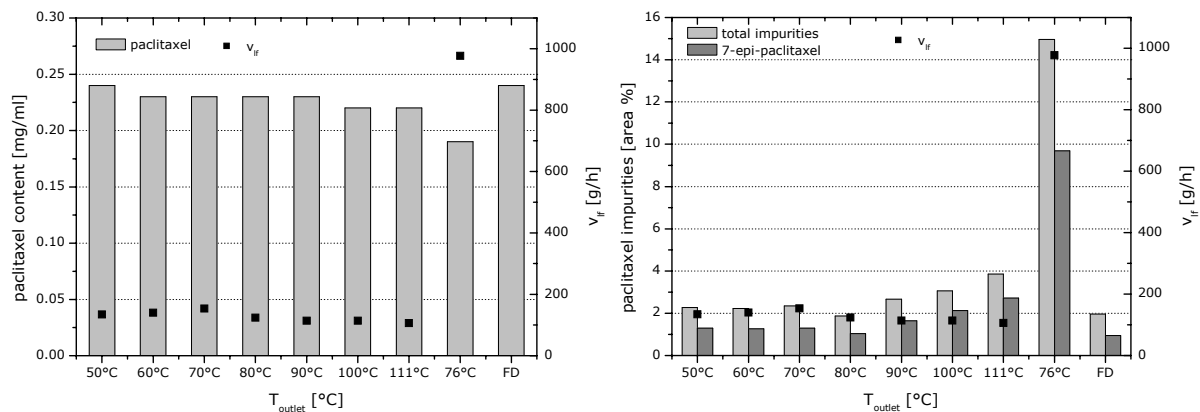


Figure 19: Paclitaxel content after spray-drying at increased outlet temperatures and feed rates (left) and the impurities at the conditions (right).

3.2.4 Particle contamination

Due to the crystallization of Paclitaxel prior to the experiments the sub-visible particle fraction was already increased before the spray-drying process. A tremendous increase in the number of small particles was found after the spray-drying (Fig 20). However, the interpretation was difficult because of the quality of starting material with respect to the Paclitaxel crystallization.

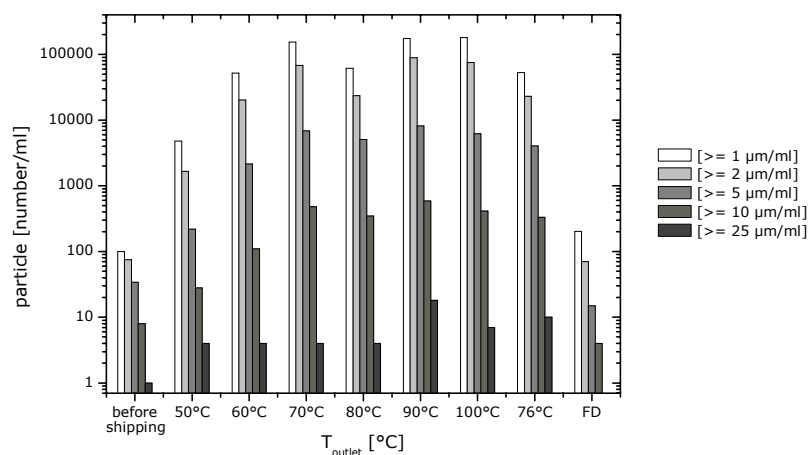


Figure 20: Sub-visible particles after spray-drying at increased outlet temperatures and feed rates

Further experiments are necessary to clarify the impact of spray-drying on the formation of sub visible and visible particles e.g. by repeating the spray-drying experiments directly after the production of the EndoTAG[®]-1 formulation.

4. CONCLUSIONS

Dry, free-flowable bulk material was obtained when spray-drying liposomal placebo formulations with the lab scale spray-drier from Büchi (B-290). The particle size ranged between 2 and 100 μm and was lowest at high atomizing airflows and low trehalose contents. At an atomizing air flow of 473 l/h and a drying temperature (outlet temperature) between 90 and 110°C yields over 80 % and residual moisture values of about 2.5 % were obtained. An additional vacuum-drying step was successfully tested to further reduce the residual moisture of the particles. The mean liposome size and polydispersity index of the starting material were remarkably well retained after spray-drying, better as with freeze-drying. The protective role of trehalose on liposomal integrity became obvious when increasing the drying inlet temperatures to 200°C. Only at the higher trehalose concentration of 10.5 % [w/v], the liposomes were sufficiently preserved and lipid degradation was impeded. Optimum process conditions for the Büchi set-up with a sufficient preservation of the liposomal integrity were found at a drying temperature of 150°C with 10.5 or 15 % [w/v] trehalose.

The Paclitaxel formulation was dried with the scale-up equipment SD Micro (Niro), operating with a higher mass ratio of atomizing air to liquid feed ($m_{\text{aa/lf}}$) and a larger drying capacity. Due to the different process conditions a direct comparison with the lab-scale placebo experiments is not possible. An optimized particle collection system with a back pressure filter after the cyclone improved the product yield up to 70 - 100 % also due to the high mass ratios of atomizing air to liquid feed. Even at a low T_{inlet} of 50°C the residual moisture could be decreased to about 4 % and below 1 % at a T_{inlet} above 90°C. For many conditions liposome size and polydispersity were well preserved compared to the formulation before processing and in some cases better than in the freeze-dried formulation. A polydispersity index below 0.2 was obtained at low mass ratios of atomizing air to liquid feed. The lipid recovery after spray-drying was comparable to the freeze-dried formulation. The main drawback of spray-drying the liposomal Paclitaxel formulation was the formation of the degradation product 7-Epi-paclitaxel. Paclitaxel degradation appeared to be triggered by elevated temperatures during the spray-drying process, especially at the highest v_{lf} of 977 [g/h]. Therefore, the focus of further investigation should be set on the optimization of the drying conditions at low inlet temperatures between 50 and 60°C.

5. REFERENCES

-
- [1] Kikuchi, H., Yamauchi, H., Hirota, S., A spray-drying method for mass-production of liposomes, *Chemical and Pharmaceutical Bulletin*, 39(6): 15-22-1527 (1991).
- [2] Goldbach, P., Borchart, H., Stamm, A., Spray-Drying of Liposomes for a Pulmonary Administration. II. Retention of Encapsulated Materials, *Drug. Dev. Ind. Pharm.*, 19(19): 2623-2636 (1993).
- [3] Lu, D., Hickey, A.J., Liposomal dry powders as aerosols for pulmonary delivery of proteins, *AAPS PharmSciTech*, 6(4): E641-648 (2005).
- [4] Lo, Y-L., Tsai, J-C., Kuo, J-H., Liposomes and disaccharides as carries in spray-dried powder formulations of superoxide dismutase, *J. Cont. Rel.*, 94: 259-272 (2004).
- [5] Master, K., *Spray drying handbook*, 5th ed., John Wiley & sons, New York, (1991).
- [6] Mui, B., Chow, L., Hope, M.J., Extrusion technique to generate liposomes of defined size, *Meth. Enzym.*, 367: 3-14 (2003).
- [7] Maury, M., Murphy, K., Kumar, S., Shi, L., Lee, G., Effects of process variables on the powder yield of spray-dried trehalose on a laboratory spray-dryer, *Eur. J. Pharm. Biopharm.*, 59(3): 565-573 (2005).
- [8] Skalko-Basnet, N., Pavelic, Z., Becirevic-Lacan, M., Liposomes Containing drug and Cyclodextrin Prepared by the One-Step Spray-Drying Method, *Drug Dev. Ind. Pharm.*, 26(12): 1279-1284 (2000).
- [9] Bosquillon, C., Lombry, C., Preat, V., Vanbever, R., Influence of formulation excipients and physical characteristics of inhalation dry powders on their aerosolization performance, *J. Cont. Release*: 70(8): 329-339 (2003).
- [10] De Boer, A.H., Gjaltema, D., Hagedoorn, P., Frijlink, H.W., Characterization of inhalation aerosols: a critical evaluation of cascade impactor analysis and laser diffraction technique, *Int. J. Pharm.*, 249(1-2): 219-231 (1990).
- [11] Adler, M., Lee, G., Stability and surface activity of lactate dehydrogenase in spray dried trehalose, *J. Pharm. Sci.*, 8(2): 199-208 (1999).
- [12] Technical data B-290, available at www.Büchi.com, Drying, Mini Spray Dryer B-290.
- [13] Maa, Y-F., Constantino, H.R., Nguyen, P-A., Hsu, C.C., The Effect of Operating and Formulation Variables on the Morphology of Spray-Dried Protein Particles, *Pharm. Dev. Technol.*, 2(3): 213-223 (1997).
- [14] Broadhead, J., Rouan, S.K., Edmond; Hau, I., Rhodes, C.T., The effect of process and formulation variables on the properties of spray-dried β -galactosidase, *J. Pharm. Pharmacol.*, 46(6): 458-467 (1994).
- [15] Maa, Y-F., Nguyen, P-A., Sit, K., Hsu, C.C., Spray-Drying Performance of a Bench-Top Spray Dryer for Protein Aerosol Powder Preparation, *Biotech. Bioeng.*, 60(3): 301-309 (1998).
- [16] Elversson, J., Millqvist-Fureby, A., Alderborn, G., Elofsson, U., Droplet and particle size relationship and shell thickness of inhalable lactose particles during spray drying, *J. Pharm. Sci.*, 92(4): 900-910 (2003).
- [17] Bain, D.F., Munday, D.L., Smith, A., Solvent influence on spray-dried biodegradable microspheres, *J. Microencap.*, 16(4): 453-474 (1999).
- [18] Tzannis, S.T., Prestrelski, S.J., Moisture effects on protein-excipient interactions in spray-dried powders. Nature of destabilizing effects of sucrose, *J. Pharm. Sci.*, 88(3): 360-370 (1999).
- [19] Taylor, L.S., York, P., Characterization of the phase transition of trehalose dihydrate on heating and subsequent dehydration, *J. Pharm. Sci.*, 87(3): 347-355 (1998).
- [20] Hansen, T., Holm, P., Schultz, K., Process characteristics and compaction of spray-dried emulsions containing a drug dissolved in lipid, *Int. J. Pharm.*, 287(1-2): 55-66 (2004).

-
- [21] Marsh, D., Watts, A., Knowles, P.F., Evidence for Phase Boundary Lipid, Permeability of Tempo-choline into Dimyristoylphosphatigycholine Vesicles at the Phase Transition, *Biochemistry*, 15(16): 3570- 3578 (1976).
- [22] Crowe, L.M., Reid, D.S., Crowe, J.H., Is trehalose special for preserving dry biomaterials?, *Biophysical J.*, 71(4): 2087-2093 (1996).
- [23] Tsvetkova, N.M., Phillips, B.L., Crowe, L.M., Crowe, J.H., Risbud, S.H., Effect of sugars on headgroup mobility in freeze-dried dipalmitoylphosphatidylcholine bilayers: solid-state ³¹P NMR and FTIR studies, *Biophysical J.*, 75(6): 2947-2955 (1998).
- [24] Kikuchi, H., Yamauchi, H., Hirota, S., A Spray-Drying Method for Mass Production of Liposomes, *Chem. Pharm. Bull.*, 39(6): 1522-1527 (1991).
- [25] Heydenreich, A.V., Westmeier, R., Pedersen, N., Poulsen, H.S., Kristensen, H.G., Preparation and purification of cationic solid lipid nanospheres-effects on particle size, physical stability and cell toxicity, *Int. J. Pharm.*, 254(1): 83-87 (2003).
- [26] Crowe, J.H., Hoekstra, F.A., Nguyen, K.H., Crowe, L.M., Is vitrification involved in depression of the phase transition temperature in dry phospholipids?, *Biochim. Biophys. Acta*, 26(2): 187-196 (1996).
- [27] Crowe, J.H., Leslie, S.B., Crowe, L.M., Is Vitrification Sufficient to Preserve Liposomes during Freeze-Drying?, *Cryobiology*, 31(4): 355-366 (1994).
- [28] Van Winden, E.C.A., Crommelin, D.J.A., Long term stability of freeze-dried, lyoprotected doxorubicin liposomes, *Eur. J. Pharm. Biopharm.*, 43(3): 295-307 (1997).
- [29] Anini, V., Byron, P.R., Phillips, E.M., Physicochemical stability of crystalline sugars and their spray-dried forms: dependence upon relative humidity and suitability for use in powder inhalers, *Drug Dev. Ind. Pharm.*, 24(10): 895-909 (1998).
- [30] Crowe, L.M., Reid, D.S., Crowe, J.H., Is trehalose special for preserving dry biomaterials?, *Biophys. J.*, 71(4): 2087-2093 (1996).
- [31] Waugh, J., Wagstaff, A.J., The Paclitaxel (TaxusTM)-Eluting Stent, *Am. J. Cardiovasc. Drugs*, 4(4): 257-268 (2004).
- [32] Gruber, F., Untersuchung zur Enkapsulierung von Paclitaxel in kationischen Liposomen, Dissertation (2004).

CHAPTER 6

New Liposome Preparation Technique by Single Pass Extrusion

Abstract:

The current preparation technique for the liposomal Paclitaxel formulation consists of several time consuming extrusion process steps. High pressure liposome preparation could be a possible method for a large scale, cost and time effective manufacturing process, which could be performed continuously. Several process conditions, e.g. nozzle size and pressure, as well as formulation composition e.g. ethanol concentration were varied to optimize the characteristics of the produced liposomes. Two different set-ups using an orifice nozzle, respectively an orifice nozzle in combination with a porous device were evaluated. The introduction of the porous device was an approach to further improve the liposome size and reduce the polydispersity index below 0.15. Higher flow rates resulted in higher pressure values and higher shear forces in the system, which could reduce the size of multi-lamellar liposome formulations. Increasing ethanol concentrations also led to smaller liposomes, even using only a nozzle. Above 30 % ethanol [w/v] a formation of liposomes was not possible, due to a dissolving of the lipids.

1. INTRODUCTION

A variety of basic procedures have been developed for the initial dispersion of lipids in an aqueous system and the subsequent preparation of liposomal suspensions. Commonly used methods are the hydratization of a dry lipid film with an aqueous medium (film method, hand shaken method) or the dispersion of an organic solvent solution of lipids into an aqueous medium (ethanol/ether-injection). The resulting multi-lamellar vesicles (MLV) usually exhibit a broad size distribution and a heterogeneous lamellarity and require additional processing steps to adjust size and uniformity. Several mechanical methods like vortexing or hand shaking of phospholipid dispersions [1], high shear homogenization [2], micro-fluidizer technique [3] or bubbling inert gas through aqueous phospholipids dispersions [4] have been employed to reduce the size of MLVs. Methods based on replacement of organic solvents by aqueous media are ethanol injection [5,6], ether vaporization [7], reversed phase evaporation [8], double emulsion or freeze thawing [9] and controlled dilution of organic solvents [10] have been applied. Other methods are based on the detergent removal, like gel exclusion chromatography [11], dialysis [12] or dilution [13]. Technical modifications of established methods based on spray-drying [14,15,16], freeze-drying of monophases [17] and the use of supercritical fluids [18,19] are described as well to reduce the size of liposomes.

In a discontinuous process, a liposomal suspension was extruded at high pressure (up to about 160 MPa) through a small orifice, for example using a so called french press-apparatus [20,21]. This process was repeated until the desired size distribution was achieved. The high pressure homogenization was also described as suitable for the preparation of liposomes from lipid/water dispersions without the use of organic solvent [22]. Here, typically small unilamellar vesicles (SUV) with quite broad and variable distribution are obtained. For the production of large unilamellar vesicles (LUV) with a defined size between about 100 and 400 nm and a narrow size distribution, methods of size-processing based on the extrusion of liposomal suspension through a uniform with defined pore size membrane have been developed [23,24]. Polycarbonate membranes with a pore size between 100 and 200 nm were employed in this method, which allowed a predetermination of the desired liposome size. To obtain liposomes of high homogeneity, they were extruded through the membrane several times [25]. For the processing of larger batch sizes, liposomal preparations were extruded through the membrane in a continuous cycling mode by a pump until the desired size and polydispersity had been achieved [26]. In general, the polydispersity of the liposomes decreased with increasing numbers of extrusion cycles.

To obtain liposomes with a narrow, well defined size distribution and to reduce the number of required extrusion steps, several variations of the extrusion membrane are known from established methods. By applying a polymer membrane with a web-like structure for the extrusion process good polydispersity indices of 0.2 were achieved for egg phosphatidylcholine (EPC) liposomes [27]. Other approaches are the use of an asymmetric membrane [28] or of a frit instead of a membrane for liposomal extrusion [29]. Different approaches to optimize the liposome formation method employed high pressure for the extrusion process with a series of staggered membranes [30]. However, no liposomal preparation procedure consisting of only one single step is available in literature up to the present. Summarizing, for the large scale production of liposomes with a suitable size and a narrow size distribution repeated processing steps either by high pressure homogenization or by membrane extrusion method are still required.

The liposome preparation technique used so far in our project consists of an ethanol injection followed by several extrusion steps through a defined polycarbonate filter. The production procedure is susceptible to interference, whereby most difficulties are related to the blocking of the extrusion membranes. There exists the need for a large scale, cost and time effective manufacturing process to produce liposomal formulations, which can meet the growing market demands. Furthermore, a process and equipment capable of continuous processing and of recycling of the non entrapped drugs, the lipids and solvents is required. A possible method to fulfill these needs is high pressure preparation of liposomes. The idea arose when using a conventional two-fluid nozzle, which was capable to reduce the size of MLVs by the shear forces at the nozzle tip. By adjusting the atomizing air flow rate, the liposome size could be reduced and the polydispersity improved (data not shown). To achieve higher shear forces a reduction of the bore diameter of the nozzle was necessary. Therefore, the preparation with high pressure using an orifice nozzle was investigated. The use of high pressure pumps has enabled a cycling through an orifice at high pressure, rendering the processing of larger batch sizes possible. Homogenization chambers or homogenization nozzles have been especially designed for the use with high pressure pumps [31,32].

Within this study a new technical approach was developed, which allows both liposome formation and the dehydration of lipid formulation in a one step process. Here, large multi-lamellar liposomes were reduced in size and homogenized by a high pressure approach.

2. MATERIAL AND METHODS

2.1 DEVELOPMENT OF THE HIGH PRESSURE LIPOSOME PREPARATION METHOD

Multi-lamellar vesicles with a total lipid content of 10 mM were prepared by ethanol injection. For the lipid stock solutions 5 mM DOTAP-Cl (1,2-dioleoyl-3-trimethylammonium-propane-chloride) and 5 mM DOPC (1,2-dioleoyl-*sn*-glycero-3-phosphocholine) (both from Avanti Polar Lipids, Alabaster) were dissolved in increasing ethanol concentrations between 10 and 60 % [w/v]. Multi-lamellar liposomes formed spontaneously upon the injection of the lipid stock solution into a 10.5 % [w/v] aqueous trehalose solution (Ferro Pfanstiehl, IL, USA). The suspension of multi-lamellar liposomes was sprayed using an ISCO E100X syringe plunger pump (Teledyne ISCO, Lincoln, NE, USA) in a pressure range between 1 and 420 bar (Fig 1).

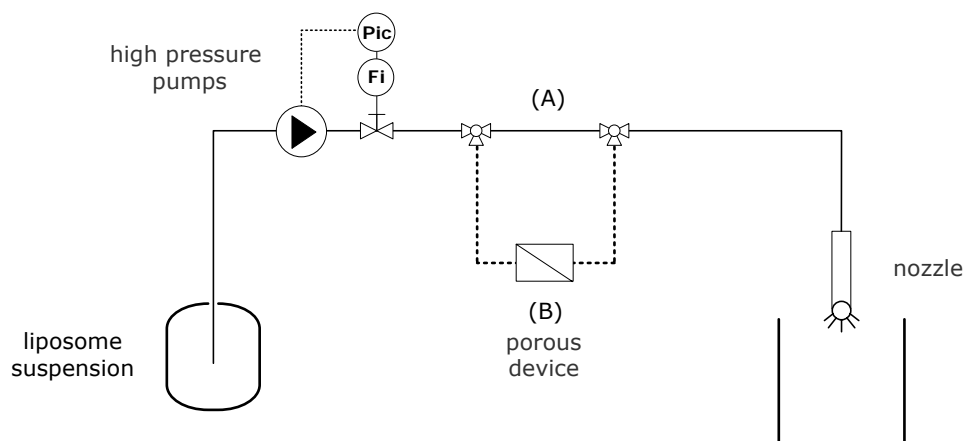


Figure 1: Experimental set-up for the spraying variations for the preparation of liposomes by direct spraying using an orifice nozzle (A) and in situ extrusion by the porous device (B) followed by nozzle atomization.

Orifice nozzles of the model 121 V G ¼ (Schlick Atomization Technologies, Untersiemau, Germany) with a diameter of 0.1, 0.2 and 0.5 mm were used. A conventional stainless steel capillary with an inner diameter of 1 mm connected the pumps, the porous device and the nozzle. Two different experimental set-ups were developed. In set-up A the suspension was pumped directly through the orifice nozzle (Fig 2, left). For set-up B an additional porous device unit was placed between the pump and the nozzle, leading to an online extrusion of the liposomes (Fig 2, right). For this purpose polycarbonate filter membranes (Osmonics Inc., MN, USA) with a pore size of 0.1 and 0.2 µm supported by two drain discs (Osmonics Inc., MN, USA) were used. A stainless steel semi prep frit (Upchurch Scientific, WA, USA) with a filtration porosity of 10 µm supported the combination of drain discs and membrane. Liposome preparation was performed at flow rates between 5 and 100 ml/min.

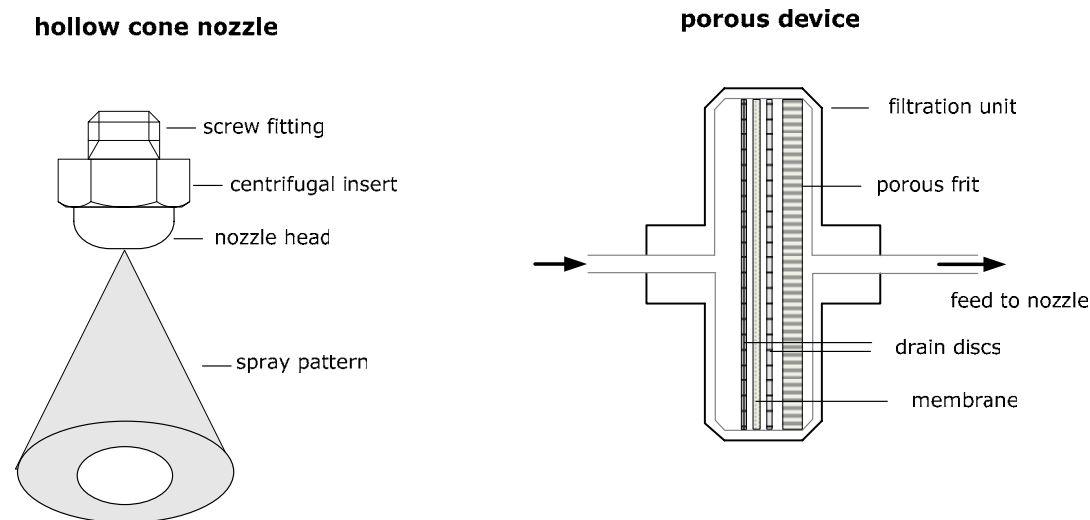


Figure 2: Experimental set-up for the spraying direct spraying using an orifice nozzle (left) and in situ extrusion by the porous device (right) followed by nozzle atomization.

2.2 DETERMINATION OF DENSITY

The density of the different solvents was determined using a 25 cm³ DIN ISO 3507 borosilicate glass pycnometer with stopper NS 10/19 (Brand GmbH & Co, Wertheim, Germany).

2.3 DETERMINATION OF SURFACE TENSION

The surface tension of the liquids was measured with a Processor Tensiometer K 100 (Krüss GmbH, Hamburg, Germany) using an abraded platinum-iridium plate (height 10 mm, width 19.9 mm and depth 0.2 mm). For the measurements a sample volume of 15 ml was employed.

All further methods used in this chapter are already described before.

3. RESULTS AND DISCUSSION

3.1 LIPOSOME FORMATION USING THE CONVENTIONAL EXTRUSION PROCESS

The conventional liposome formation process, consisting of the ethanol injection technique to provide multi-lamellar liposomes followed by the consecutive cycles of an extrusion process resulted in a continuous decrease of the liposome size. However, the polydispersity was not further improved after six extrusion cycles (Fig 3, left). The mechanism of vesicle (liposome) formation by extrusion followed the pattern of the cylindrical straight-through pores of a filter membrane. The multi-lamellar vesicles were forced through such long narrow tubes with different flow velocities depending on the size of liposomes (Fig 3, right).

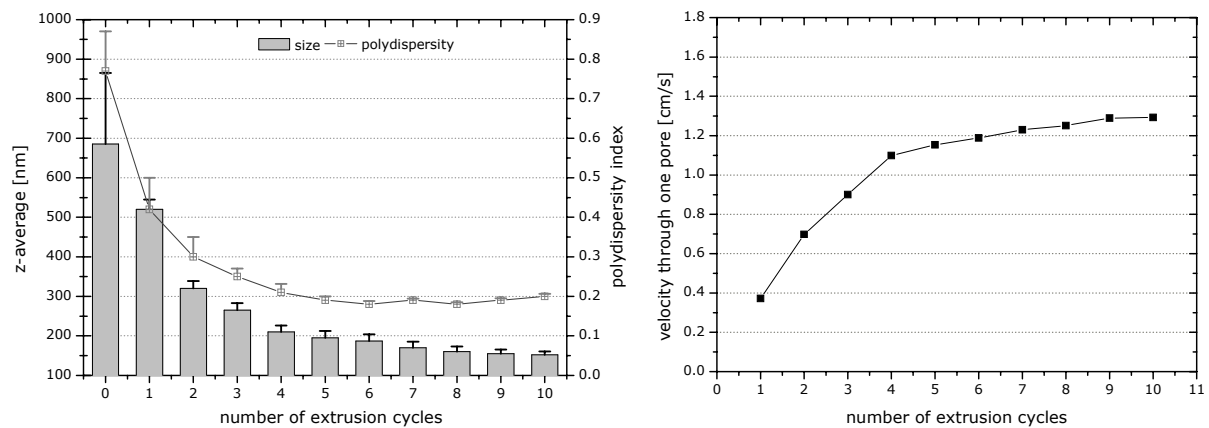


Figure 3: Liposome size and polydispersity index after several extrusion cycles using a 200 nm polycarbonate membrane at an extrusion pressure of 2.5 bar (left) and the average calculated velocity of the aqueous trehalose/lipid suspension through one pore (right).

The average linear velocity of the liposomal formulation through one pore was calculated by Equation 1 [33]. V is the total volume of the suspension, ρ the number of pores per unit area of the membrane, R the radius of the filter membrane, r the radius of the pore and t the time required to extrude the volume of liposomal suspension.

Equation 1: Average linear flow velocity [cm/s] for the liposomal suspension through one pore.

$$u = \frac{V}{\rho \pi^2 R^2 r^2 t} \quad (1)$$

Water has an average linear flow velocity of about 3 cm/s through one pore, which was calculated for a 0.1 μm membrane pore at a pressure of 3 bar. Due to the increased viscosity of the aqueous trehalose/lipid suspension the velocity through the pores was reduced. The solvent flow inside the pore can be described as a laminar flow, with a

parabolic profile. The liquid feed break-up at the nozzle results in smaller droplets and reduces the vesicle size via shear stress, whereby the size can not sufficiently be reduced within a single step [34]. The relatively low forces obtained by a laminar flow were not large enough to result in a homogenous size distribution within one passage. Therefore, several extrusion cycles were necessary and a maximum size reduction was obtained after six cycles (Fig 3, left). Once vesicles with dimensions smaller than the pore diameter were formed, further extrusion did not significantly affect their size. To further improve the homogeneity the pressure and therefore the velocity through the pores should be enhanced or the pore size radius should be decreased.

3.2 HIGH PRESSURE LIPOSOME FORMATION

3.2.1 Liposome preparation using an orifice nozzle

As starting material for high pressure liposome formation, a multi-lamellar liposome suspension produced by the standard ethanol injection with a z-average of 650 nm and a polydispersity index of 0.65 was employed. The used vaporizing nozzle type consists of three parts, the screw fitting, the centrifugal insert and the nozzle head (Fig 4, (A)). The forces inside the swirl chamber in the nozzle head are increased by the tangential slits and this energy is converted into a rotational energy. The centrifugal film of rotating liquids forms a hollow cone of fine droplets after leaving the nozzle (Fig 4, (B)).

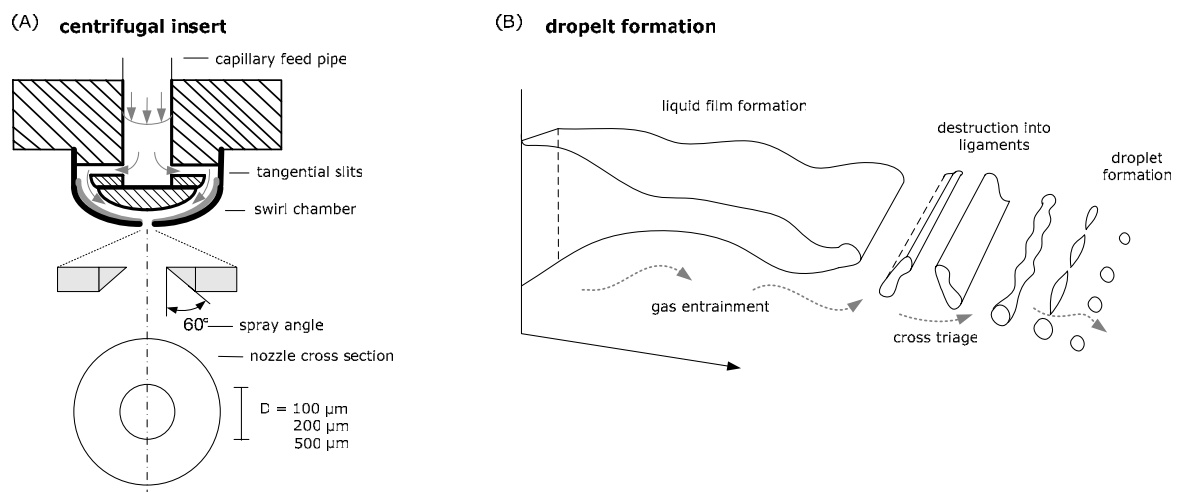


Figure 4: Liposome formation using a hollow cone nozzle and detailed description of the centrifugal insert (A) with a schematic droplet formation process (B) [35].

Gas entrainment results in destruction of the liquid film into liquid ligaments and cross triage into the final droplets. The droplet size is affected by the diameter of the orifice and pressure, as well as by density, viscosity and surface tension of the solution. Within this study the nozzle diameter and the viscosity of the solutions were varied in addition to pressure.

The liposome size distribution was affected by the bore diameter of the orifice nozzle and the induced interfacial forces between the jet and the surrounding air. When the liquid jet is discharged into air, the disturbance on the jet surface is enlarged because of the aerodynamic interaction between the jet and the surrounding ambient. Growth of these disturbances causes the liquid column to disintegrate into droplets soon after the discharge [36]. As a commonly used classification of jet disintegration the Ohnesorge number (Oh), which combines the Weber number (We) and the Reynolds number (Re) can be considered [37]. It was suggested that four different break-up regimes for waterjets depending on the Ohnesorge number are existent. The first regime is called the Rayleigh break-up regime, followed by the 1st wind-induced, the 2nd wind-induced and finally the atomization break-up regime.

The Reynolds number is the ratio between inertial forces and viscous forces and identifies the different flow regimes as laminar or turbulent flow. A turbulent stream is characterized by a random move, where the velocity of the particles has random direction compared to laminar flow. The Reynolds number is calculated by Equation 2 where ρ is the density, v the liquid velocity, D the diameter of the nozzle and η the dynamic viscosity.

Equation 2: Dimensionless Reynolds number for determination of laminar and turbulent flow.

$$\text{Re} = \frac{\rho \times v \times D}{\eta} \quad (2)$$

The dimensionless Weber number indicates whether the kinetic energy or the surface tension energy is dominant for droplet formation. The number is calculated by Equation 3 where ρ is the density, v the liquid velocity, D the diameter and σ the surface tension.

Equation 3: Dimensionless Weber number for the ratio of disruptive hydrodynamic forces to the stabilizing surface tension force.

$$\text{We} = \frac{\rho \times D \times v^2}{\sigma} \quad (3)$$

Although the viscosity of the fluid is not considered in the We number it has a considerable effect on the droplet formation process [38]. At a higher liquid viscosity the

droplet break-up is delayed. Therefore, the Ohnesorge number was calculated by Equation 4, combining the Reynolds and Weber number.

Equation 4: Dimensionless Ohnesorge number for the ratio of internal viscosity to surface tension energy.

$$Oh = \frac{\eta}{\sqrt{\rho \times D \times \sigma}} = \frac{\sqrt{We}}{Re} \quad (4)$$

Depending on nozzle bore diameter and liquid flow rate the working pressure raised up to 420 bar with high flow rates (Fig 5, left). At higher liquid flow rates the Reynolds number increased and with it the shear forces inside the nozzle. This resulted in different break-up regimes and forces at the nozzle during droplet formation (Fig 5, right). In the Rayleigh break-up mode, the droplets pinch off the nozzle with diameters greater than the jet it self. In the 1st wind-induced regime the droplets are pinched off from the end of the jet. These droplets have a diameter close to the jet diameter with droplet formation at distances far downstream of the nozzle. Water jets with higher Re numbers and a turbulent flow break-up closer to the nozzle exit and tend to produce smaller droplets [39]. In the 2nd wind-induced break-up region an unsteady break-up with droplets much smaller than the jet can be observed. The last regime is called atomization region, where the liquid jet is dispersed directly into a spray at the nozzle outlet. The so formed droplets can be dried directly using for example, the spray-drying process. Droplet size will affect also the later drying procedure and the resulting particle (compare chapter 5).

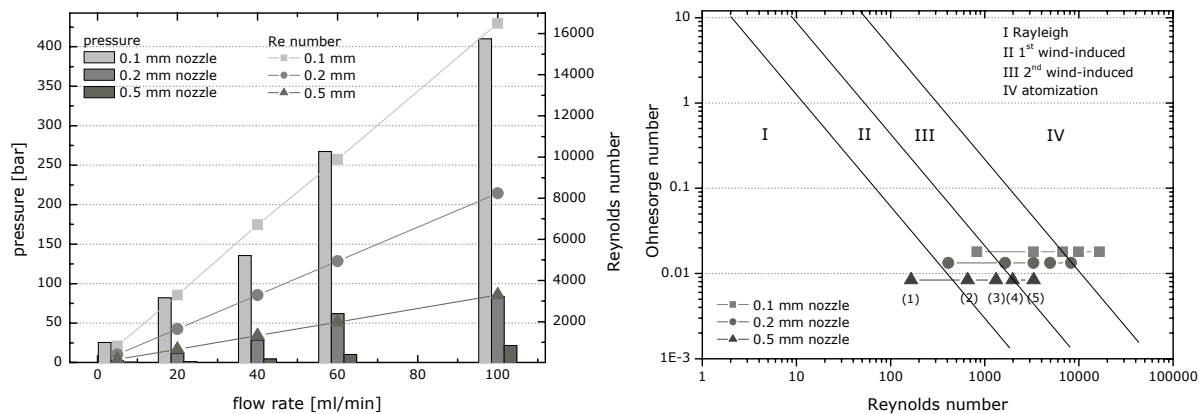


Figure 5: Liquid flow rate and the resulting pressure with the calculated Reynolds number for the used nozzles (left) and the calculated Ohnesorge number for the experiments inside the classification modes of disintegration with the different break-up regimes at flow rates 5 (1), 20 (2), 40 (3), 60 (4) and 100 (5) ml/min (right).

For the 0.1 mm nozzle pressures between 25 and 420 bar were obtained at flow rates between 5 and 100 ml/min when spraying the MLV liposomal formulations (Fig 6, left). The higher pressures at the 0.1 mm nozzle compared to the 0.2 mm nozzle led to

smaller liposome sizes and lower polydispersity indices (Fig 6, right). In the preferred working range between 60 and 100 ml/min with corresponding pressures between 260 and 420 bar liposomes with a size of about 120 nm and polydispersities of 0.28 were formed. The droplet formation and the resulting shear forces in the atomization region are responsible for the improvement in homogeneity. The droplet break-up classification with the corresponding forces can be used to describe the effect of liposome formation. With high disintegration forces in the 2nd wind-induced and atomization region the liposome size can be reduced.

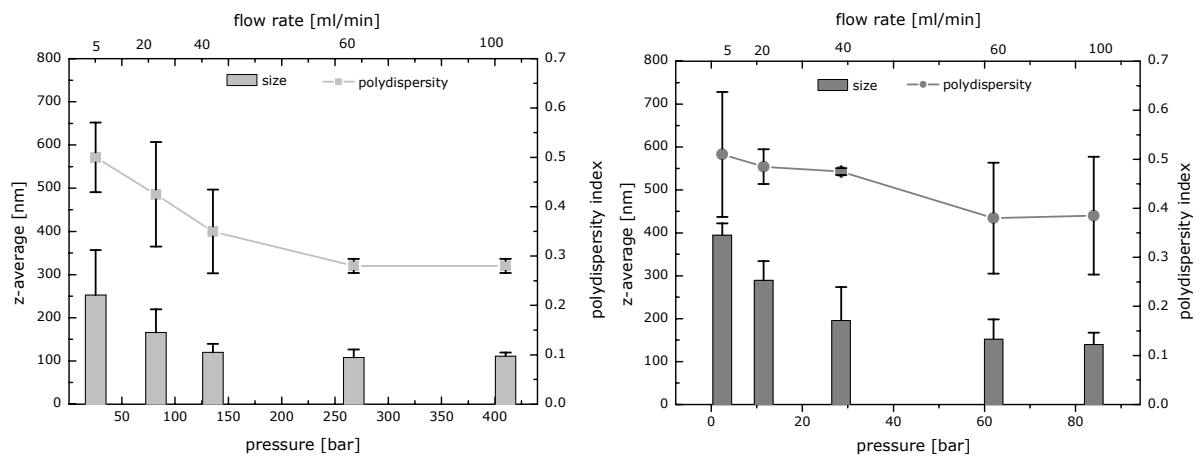


Figure 6: Size and polydispersity index of liposomes prepared by high pressure spraying with 0.1 mm nozzle (left) compared to the 0.2 mm nozzle (right)

When using the 0.2 mm nozzle at a flow rate of 5 ml/min liposome size decreased from 650 nm to 400 nm, with a polydispersity index of 0.5 (Fig 6, right). The wide standard deviation and the high polydispersity indicated an inhomogeneous size distribution of the prepared liposomes. By increasing the flow rate from 5 to 60 ml/min and with it the corresponding pressure from 2 to 62 bar, smaller liposomes with lower polydispersity indices were obtained. The obtained Re numbers for the 0.2 mm nozzle were relatively small compared to the 0.1 mm nozzle and all experiments were done in the 1st and 2nd wind-induced region. The droplet break-up changed into smaller droplets and a turbulent flow at the highest feasible liquid feed rate of 100 ml/min. However, the still high standard deviations for the polydispersity index were noticeable.

When using the 0.5 mm nozzle it was only possible to work in the Rayleigh and the 1st wind-induced region and Reynolds numbers ranged between 160 and 3302. Only above 80 ml/min turbulent flow rates (> 2500 Re number) were achieved. However, it was not feasible to obtain homogenous vesicles (data not shown).

3.2.2 Liposome Preparation using a porous device and the orifice nozzle

3.2.2.1 Liposome preparation using a porous device

Adjustment of the liposome size between 120 and 180 nm and with a polydispersity below 0.28 was not feasible using the orifice nozzle alone. To further improve the liposomal properties high pressure nozzles with bore diameters smaller than 0.1 mm and controlled parameters would be necessary. However, those nozzle qualities are not available on the market yet. Therefore, we developed a high pressure extrusion approach, the so-called porous device based on the well known extrusion concept. We combined this porous device with the orifice nozzle to further reduce the vesicle size.

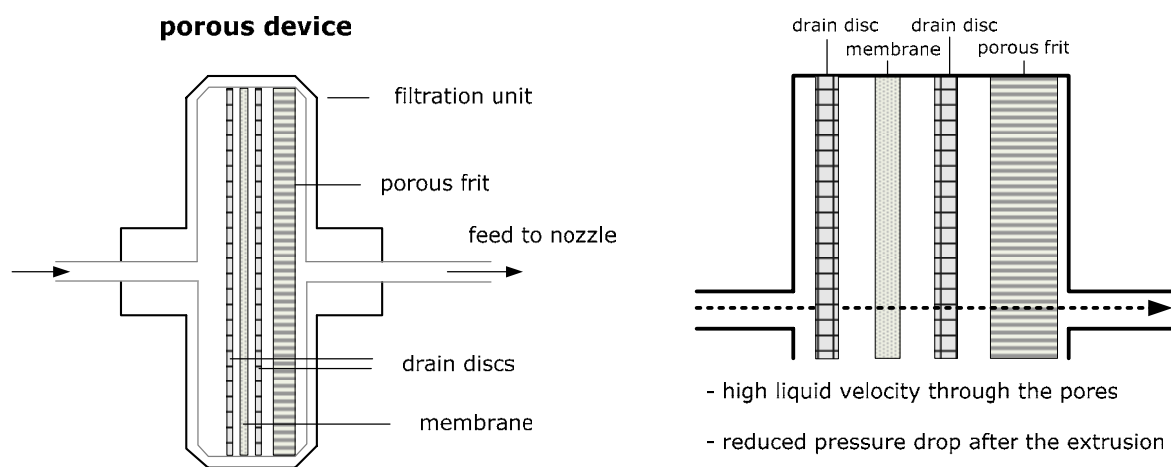


Figure 7: Liposome formation using the porous device (left) with a detailed construction (right).

The porous device unit consists of a standard polycarbonate membrane with pore sizes of 0.1 or 0.2 μm . To avoid rupture and deformation of the membrane at higher pressures, drain discs and a porous frit were necessary to stabilize the membrane (Fig 7). Furthermore, the porous device ended within the capillary pipe preventing a direct pressure drop within or after the porous device. Preformed multi-lamellar vesicle suspensions were pumped through the porous device equipped with a 0.1 and 0.2 μm membrane at a flow rate of 20 ml/min.

Table 1: Liposome formation using only the porous device and polycarbonate membranes with 0.1 and 0.2 μm pore size.

membrane [μm]	pressure [bar]	z-average [nm]	polydispersity index	velocity through one pore [cm/s]
0.1	5.5 ± 3.3	157 ± 2.1	0.24 ± 0.01	2.16
0.2	4.5 ± 6.4	166 ± 1.4	0.24 ± 0.01	0.72

At the corresponding pressures of 5.5 bar for the 0.1 μm membrane, respectively 4.5 bar for the 0.2 μm membrane liposome sizes of 157 nm, respectively 166 nm were obtained and the polydispersity index could be reduced to 0.24 for both membrane sizes (Tab 1). Different velocities through one pore were calculated for the used membranes with a three times faster velocity for the 0.1 μm membrane compared to the 0.2 μm membrane.

3.2.2.2 Considerations on liposome preparation using a porous device

The approach presented above allowed the formation of liposomes with a narrow size distribution by only one extrusion passage through the porous device. Still it is not yet clear, which mechanism leads to a break-up of large and polydisperse multi-lamellar vesicles into smaller, unilamellar and homogeneously dispersed vesicles during membrane extrusion (Fig 8, (A)). Several mechanisms are described in literature, for example a break-up of cylindrical vesicles while passing the pore described by Clerc et al. (1994) [33]. The shear forces inside the membrane result in a deformation and at the end of the pore in a rupture of the liposomal membrane.

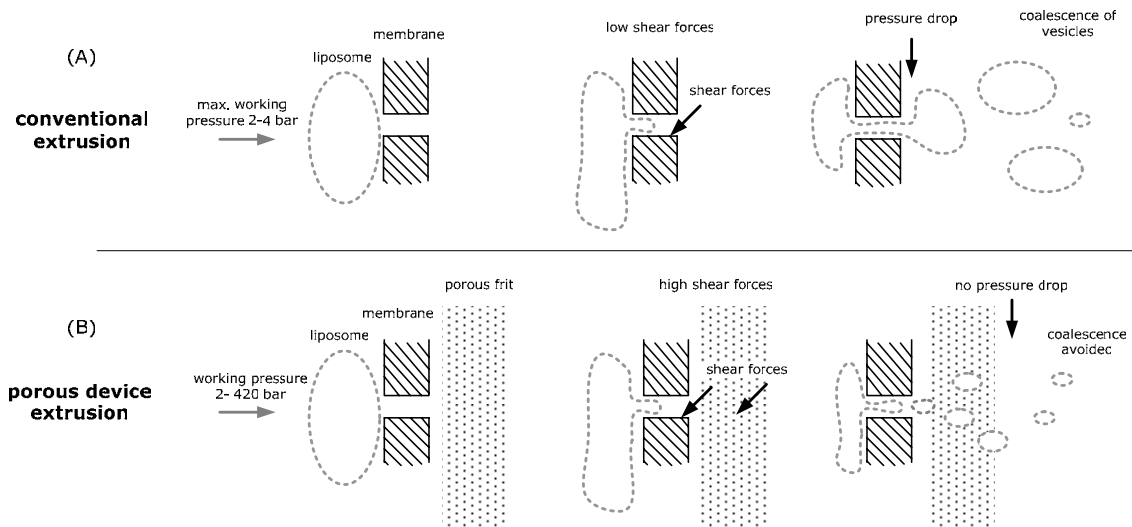


Figure 8: The models of conventional extrusion (A) and the porous device extrusion (B) with the mobility of vesicles in pores and additionally the pores frit as function of driving field.

The commonly occurring pressure drop across a moving vesicle through the membrane in the classical used extrusion equipment was found to increase linearly with the velocity of the solution [40]. This pressure drop to ambient conditions favors a coalescence of vesicles [41]. Furthermore, theoretical studies revealed vesicle formation within pores under shear stress [42]. Other studies focused on the flow of vesicles inside cylindrical

pores and the shape deformation occurring inside the pore [43]. The large size of polydisperse vesicles after ethanol injection requires energy to press the liposome into the smaller pore of the membrane. The formation of liposomes by conventional extrusion processes is limited since a further increase in shear force by an increase in pressure above 4 bar would rupture the membrane.

We adopted a model for the porous device extrusion and liposome formation in figure 8 (B). The pressure drop directly after the membrane is inhibited by the porous device and the pressure in the down stream line, which additionally improved the vesicle formation and preserved the membrane. With our porous device the possibility was given to increase the flow rate into turbulent flow and achieve higher shear forces leading to smaller liposomes. The linear velocity of such viscous suspensions through a uniform pore is described with a parabolic profile [44]. The velocity gradient for the investigated liposome suspension using the porous device passage could be described as very steep. The vesicles move through the pores with a determined velocity and are separated from the pore wall by a lubrication layer of a certain thickness. This thickness is a function of the velocity of the vesicle in the pore and the surface tension in the lipid bilayer as described by Bruinsma (1996) [43]. As the lubrication layer increases, the radius of the vesicles in the pore will decrease. This results in a size reduction of the vesicles already in the filter membrane induced by the shear forces as well as the amount of lipids and viscous solution within the pore.

3.2.2.3 Liposome preparation using a porous device and the orifice nozzle

In the next step the nozzle was introduced in line after the porous device, equipped with a polycarbonate membrane. At a pressure of 4.6 bar (flow rate of 5 ml/min) liposomes with a size of 250 nm and a polydispersity index of 0.5 were obtained using only the nozzle, while a size of 144 nm and a polydispersity index of 0.26 was obtained when combining a 0.1 μm membrane and a 0.1 mm nozzle within the system. With further increased pressure at higher flow rates the liposome size decreased (Fig 9, (A)). When using the 0.2 μm membrane the homogeneity of the formed liposomes was comparable (Fig 9, (C)). After the introduction of the porous device, lower working pressures were found in comparison to using only the nozzle, which depended on membrane pore diameter and liquid feed. For the 0.1 μm membrane high liquid velocities between 1 to 11 cm/s with a distinct gradient through the pores could be calculated (Fig 9, (B)).

The membrane reduced the working pressure up to a flow rate of 40 ml/min. This suggested different vesicle formation processes depending on the flow rate and the maximum pressure resistance of the membrane to deform the vesicles based on the

lubrication layer thickness. The maximum in the plot indicated the changed permeability of the filter at a pressure of 20 bar. Within these experiments much higher forces and flow rates were obtained leading to turbulent behavior. The different pressure drop induced by the porous device depending on the pore size could be explained by the reduced pore density of $3.0 \times 10^8 \text{ cm}^{-2}$ at the $0.2 \mu\text{m}$ membrane compared to $4.0 \times 10^8 \text{ cm}^{-2}$ at the $0.1 \mu\text{m}$ membrane. However, the speed and the resulting shear forces within the pores of the membrane were reduced in a $0.2 \mu\text{m}$ membrane and resulted in three times slower velocities (Fig 9, (D)). The lubrication layer in the larger pores was more pronounced at the $0.2 \mu\text{m}$ membrane and the ratio of lipids to viscous solution was optimized.

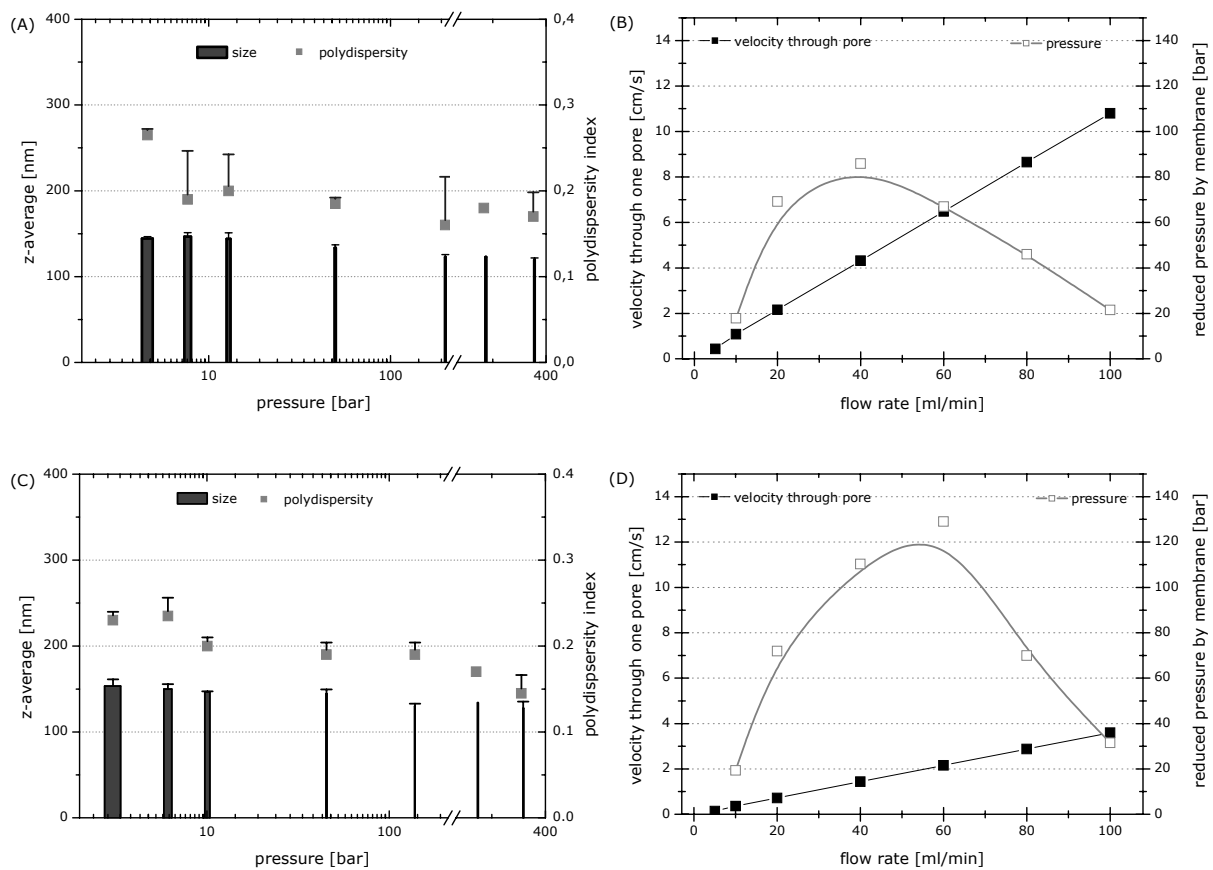


Figure 9: Liposomes prepared by high pressure preparation using a porous device at flow rates of 5, 10, 20, 40, 60, 80 and 100 ml/min with $0.1 \mu\text{m}$ polycarbonate membrane (A) and a $0.2 \mu\text{m}$ membrane (C) both adjusted with a nozzle size diameter of 0.1 mm and the related liquid velocity with the reduced pressure after the introduction of the porous device for the $0.1 \mu\text{m}$ (B) and $0.2 \mu\text{m}$ (D) membrane.

With an increased nozzle diameter the pressure generation in the system was diminished (Fig 10, (B and D)). However, the liposome size decreased slightly with increasing pressure and the polydispersity was lower for both membranes (Fig 10, (A and C)). The changed liposome size was affected by the reduced turbulences due to the lower Reynolds number at that flow rate.

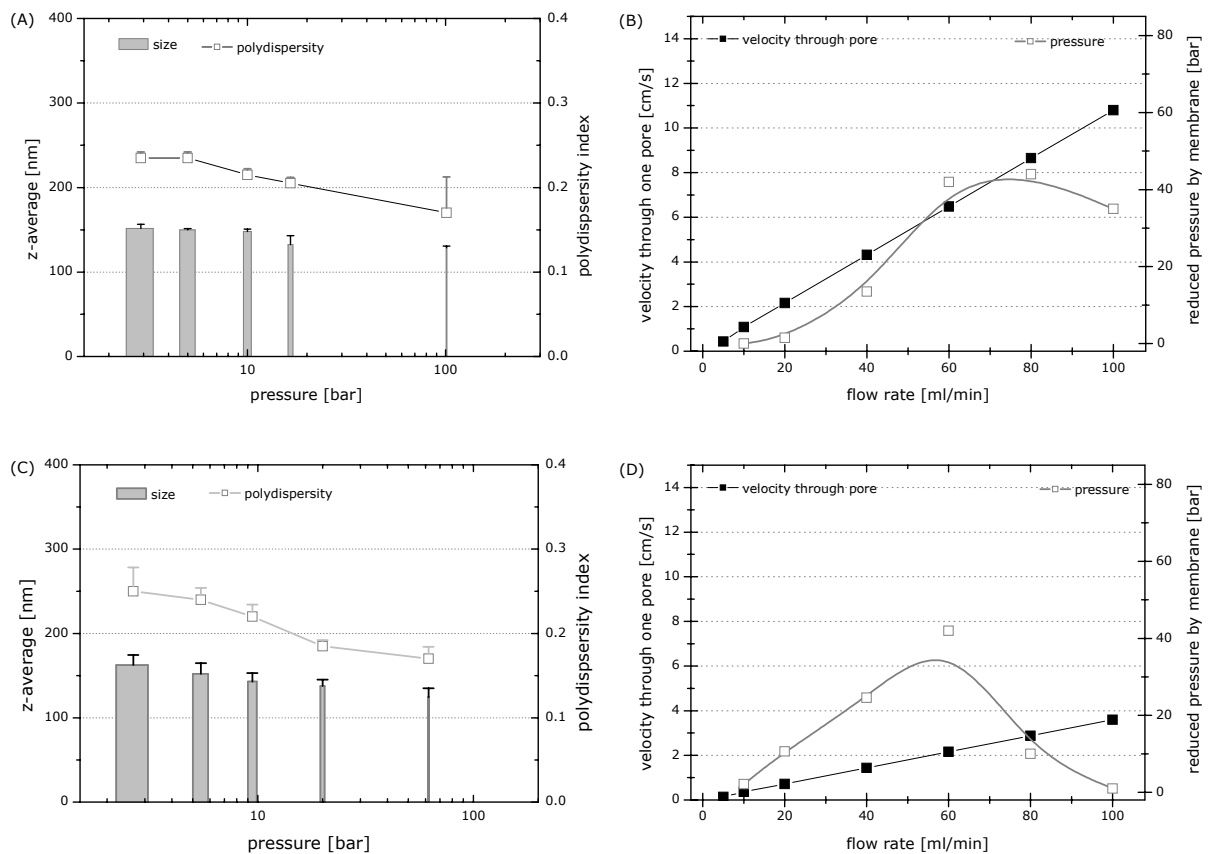


Figure 10: Liposomes prepared by high pressure preparation using a porous device at flow rates of 5, 10, 20, 40, 60, 80 and 100 ml/min with 0.1 μm polycarbonate membrane (A) and a 0.2 μm membrane (C) both adjusted with a nozzle size diameter of 0.2 mm and the related liquid velocity with the reduced pressure after introduction of the porous device for the 0.1 μm (B) and 0.2 μm (D) membrane.

In summary, it can be pointed out that the combination of a porous device and the orifice nozzle resulted in a single size adjusting step to achieve homogenous liposomes smaller than 200 nm with polydispersity indices below 0.2 for many process parameters.

3.3 HIGH PRESSURE LIPOSOME FORMATION AT HIGH ETHANOL CONCENTRATIONS

3.3.1 Liposome preparation by ethanol injection

Ethanol is one of the few organic solvents acceptable in the manufacturing process of pharmaceutical products. Due to its good miscibility with water it can be removed easily from liposomal preparations by gel filtration, dialysis or tangential flow. Within our evaluations, the removal of the aqueous-ethanol phase was investigated by a novel inert spray-drying process, which is described in chapter 8. For this purpose, evaluation studies to prepare homogenous liposomes with increasing ethanol concentrations were performed. Our goal was to investigate up to which ethanol concentrations liposomes form spontaneously. At ethanol concentrations between 2.5 and 30 % [w/v] multi-lamellar vesicles (MLV) formed spontaneously when the ethanolic lipid stock solution was injected into an aqueous trehalose solution. The size of the multi-lamellar vesicles decreased with increasing ethanol contents in the aqueous phase. At a final ethanol concentration of 30 % [w/v] a size of 338 nm and a promising polydispersity index of 0.38 were achieved (Fig 11)

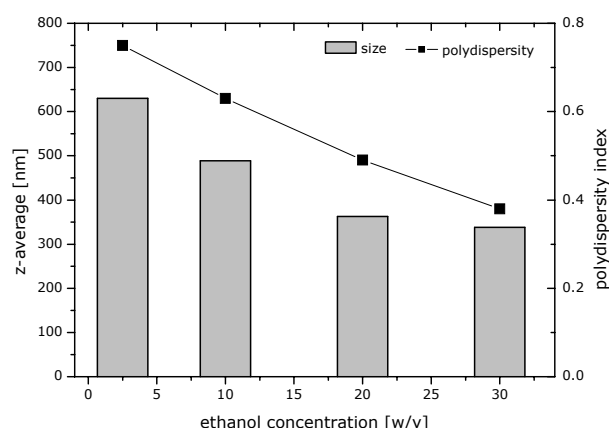


Figure 11: Liposome size after ethanol injection with varied ethanol concentrations in the final formulation.

The results could not be improved by higher stirring or injection rate. Upon the injection of lipid solution into the water/trehalose mixture smaller lipid containing droplets are formed at higher ethanol concentrations, which yield in smaller vesicles after reorientation of the lipid monomers [45]. The liposomes were solubilized at ethanol concentrations above 30 % [w/v] resulting in clear solutions (data not shown). This result indicates that the liposomes were dissolved at concentrations above 30 % [w/v] ethanol to a molecular disperse solution.

3.3.2 Liposome preparation using an orifice nozzle

In the following experiments multi-lamellar vesicles prepared by ethanol injection containing between 10 and 30 % ethanol [w/v] in the formulations were fed into the high pressure preparation process to achieve monodisperse vesicles. The shear forces inside the nozzle are affected by the diameter of the orifice, the pressure, spray-angle, as well as the density and the viscosity of the solutions (Fig 12, left). At increased ethanol concentrations the viscosity was raised, which resulted in higher shear forces at the nozzle determined by the Reynolds number. The viscosity has a considerable effect on the droplet formation process and the distribution within a droplet [38]. The different ethanol concentrations at various pressures and flow rates resulted in varied droplet break-up regions (Fig 12, right). The lower the Ohnesorge number, the weaker are the friction losses due to the viscous forces. For this reason most of the energy at the nozzle is converted into the surface tension energy

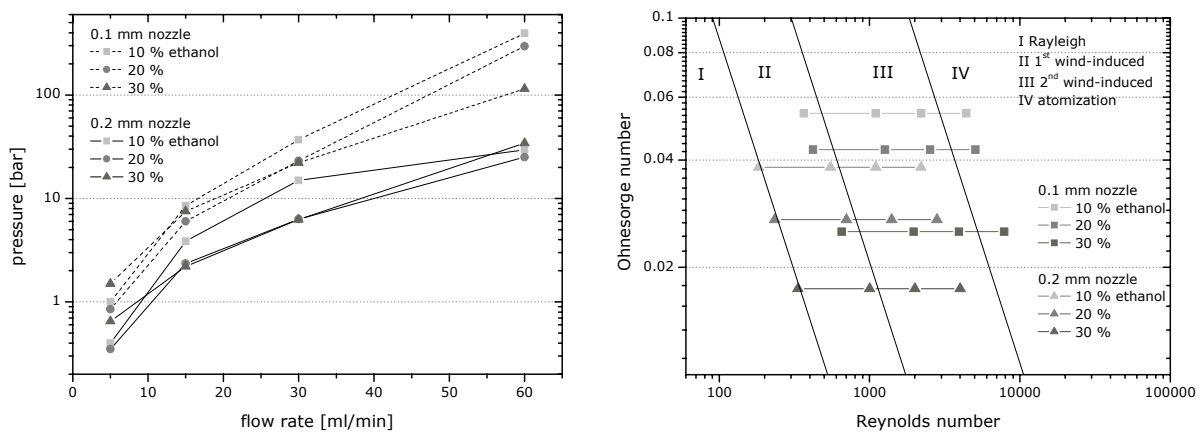


Figure 12: Pressure at the liquid flow rates 5, 15, 30 and 60 ml/min for the 0.1 and 0.2 mm nozzle at 10, 20 and 30 % [w/v] ethanol concentration (left) and the calculated Ohnesorge number vs. the Reynolds number for the same conditions (right).

Higher ethanol concentrations resulted in a higher Weber numbers (smaller Ohnesorge numbers) and a dominant kinetic energy. For this reason liposome size and polydispersity are reduced. Depending on the orifice diameter, pressure and the Re number the forces of droplet break-up changed. Small uniform vesicles were achieved at a flow rate of 60 ml/min for all ethanol concentrations using the 0.1 mm nozzle (Fig 13, (A)). At this flow rate the experiments were performed inside the atomization region. The polydispersity only decreased for the ethanol concentration of 30 % [w/v] to values below 0.1 (Fig 13, (C)), because most of the inserted energy is converted into kinetic energy. This effect was less pronounced for the larger nozzle (Fig 13, (B and D)).

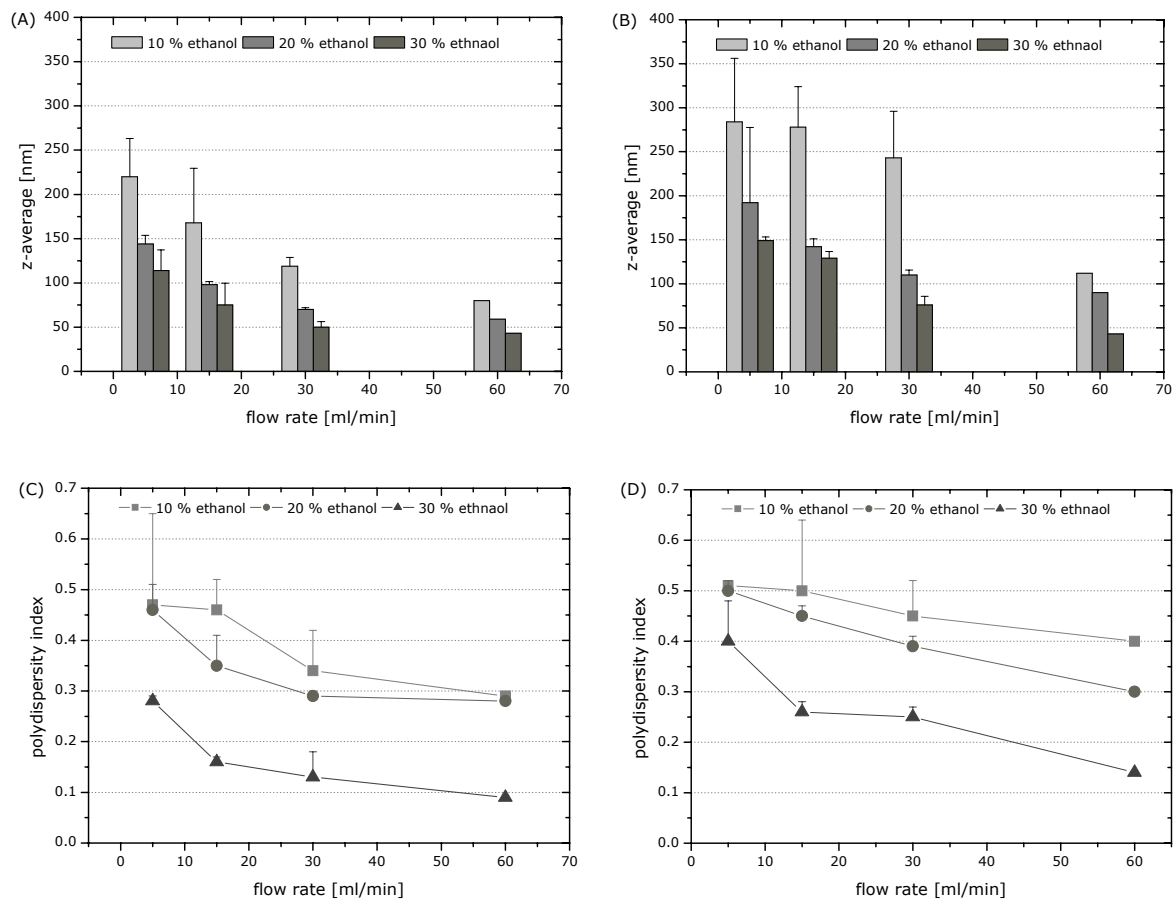


Figure 13: Liposome size and polydispersity index at ethanol concentrations between 10 and 30 % [w/v] ethanol after pressurization through the orifice diameter of 0.1 mm (A and C) and of 0.2 mm (B and D).

With the addition of ethanol the viscosity increased as well as the shear forces increased with lower Ohnesorge numbers and improved kinetic energy by higher Weber numbers. This resulted in very small liposomes with an optimized polydispersity. With the porous device very high flow rates and pressures are technically feasible and together with increasing viscosities this can be used to adjust the liposome size.

3.3.3 Liposome preparation using a porous device and the orifice nozzle

Upon the introduction of the porous device with 0.1 and 0.2 μm membranes into the system, a decrease in liposome size was observed even at lower flow rates (Fig 14). Depending on the increased viscosity of the multi-lamellar suspension at higher ethanol concentrations the liposome size decreased significantly. The 0.2 μm membrane resulted in smaller and more homogeneous liposome sizes. With increased flow rates the size decreased as described before (compare 3.3.1).

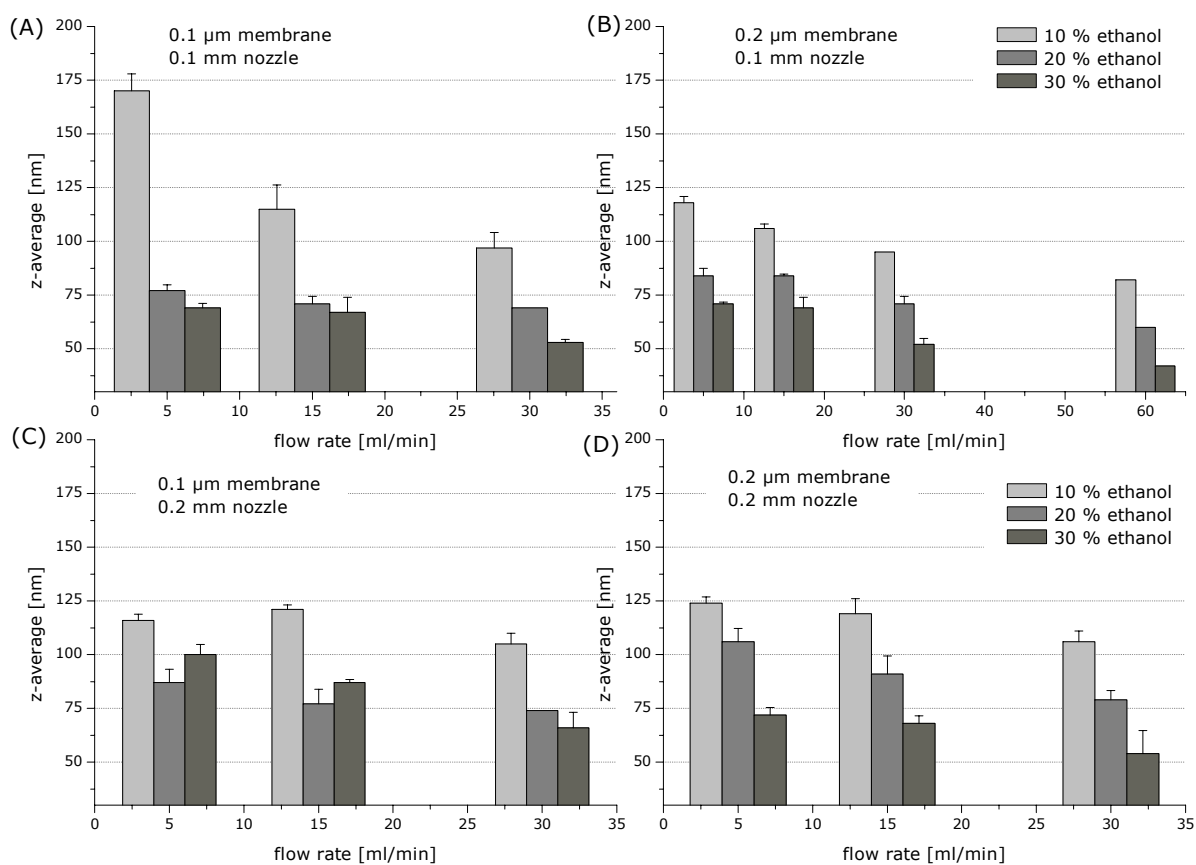


Figure 14: Liposome size using membranes with a pore size of 0.1 and 0.2 μm and nozzles of 0.1 and 0.2 mm orifice bore diameter.

The polydispersity of the liposome size distribution was dependent on the extrusion pressure and the viscosity of the suspension. Compared to the experiments without membrane, particularly the polydispersity index was positively affected by the combination of membrane and nozzle (Fig 15). For example at 30 ml/min and 10 % [w/v] ethanol the polydispersity index was 0.34 without and 0.18 with a 0.1 μm membrane for the 0.1 mm nozzle. The effect of shear stress on the structure of liposomal membranes can be assumed as a perturbation or a change in its spatial organization.

With such higher energy levels and hydrodynamic stress the short range order of the liposomes can be modified [46]. Above a certain pressure and flow velocity the vesicle structure with their binding energy was overcome and reorientation was possible resulting in very homogenous vesicles.

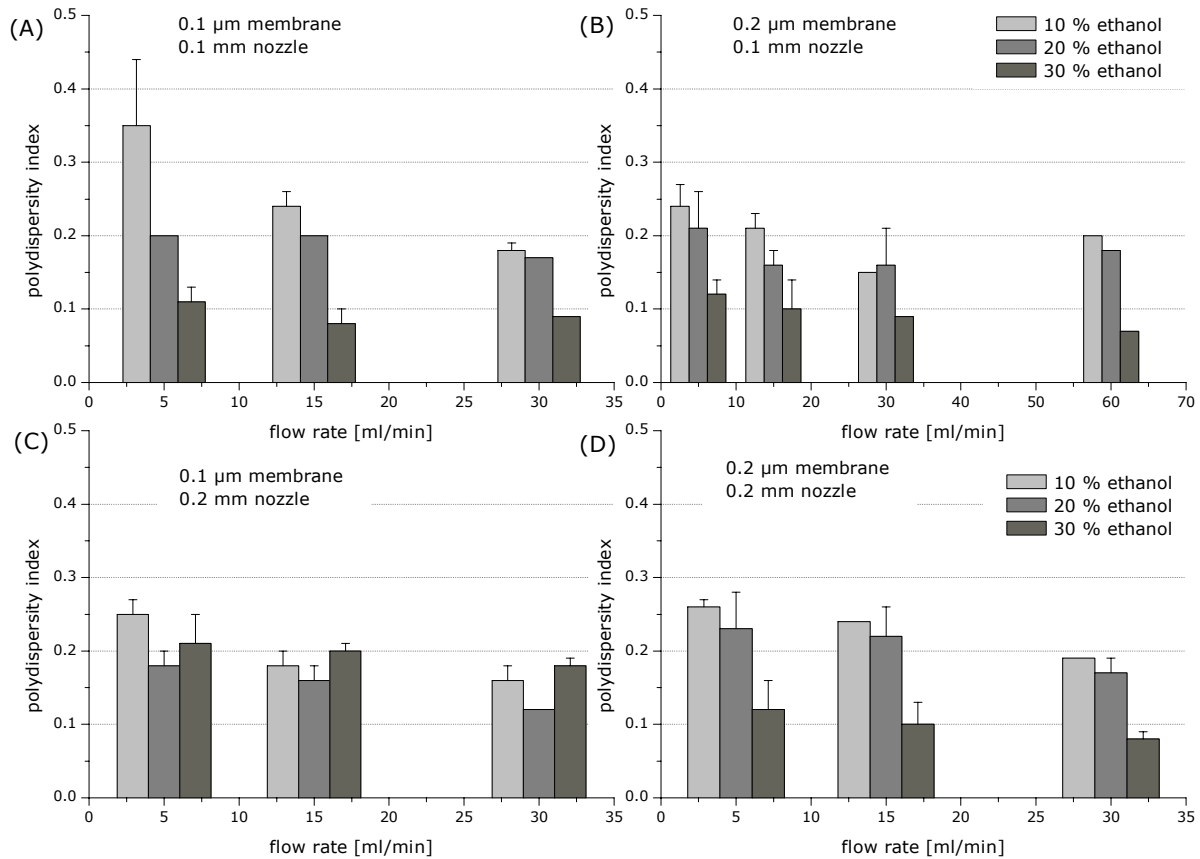


Figure 15: Polydispersity index using membranes with a pore size of 0.1 and 0.2 μm and nozzle of 0.1 and 0.2 mm orifice bore diameter.

Although the liquid feed rate and the velocity through the membrane pores were constant, the pressure in the system rose compared to the conditions used without the additional ethanol content. This effect was a result of the higher viscosity of the liposomal suspensions (Fig 16). For all membrane and nozzle combinations and liquid feed rates up to 30 ml/min a linear pressure increase was determined. The extrusion process of the ethanol containing formulations required more power of the system to maintain the feed rate and this resulted in smaller liposomes.

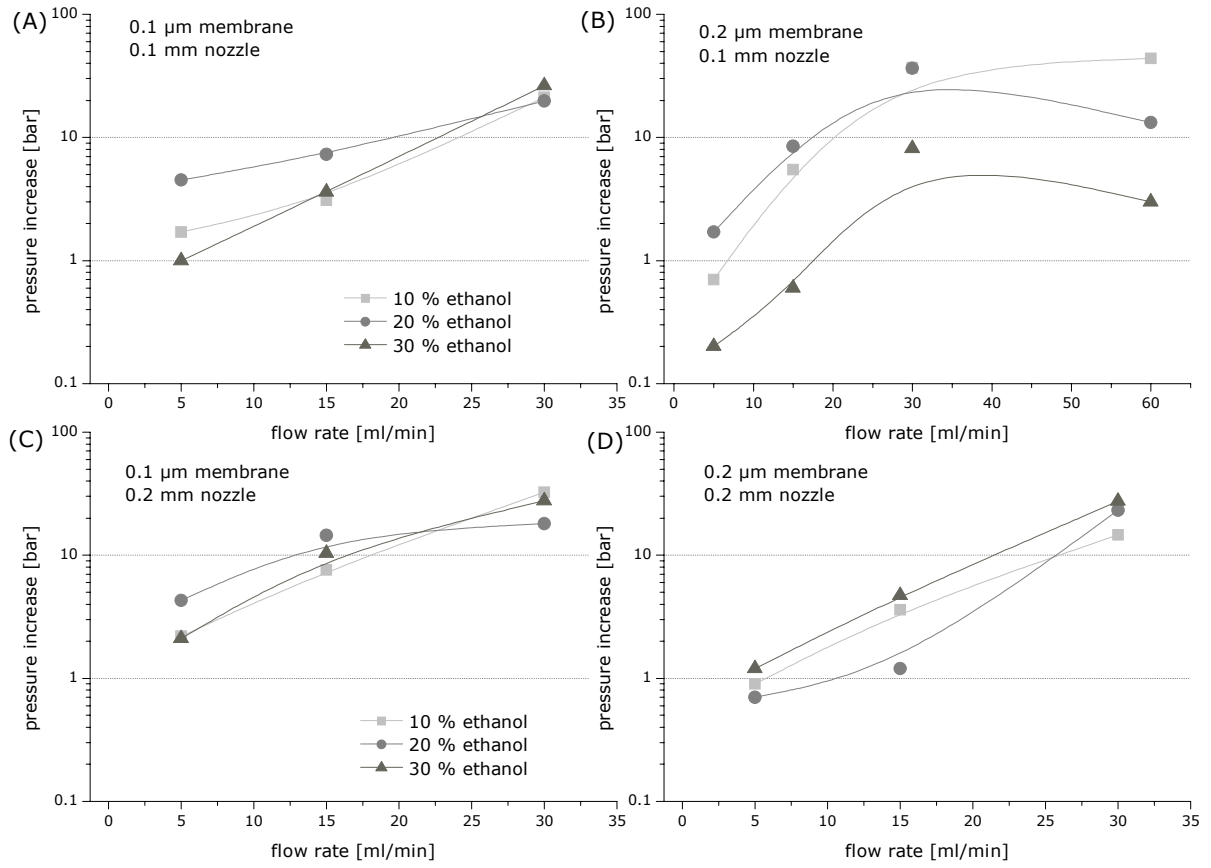


Figure 16: Additional pressure increase of ethanol containing formulations after introduction of the porous device using membrane with a pore size of 0.1 and 0.2 μm to the nozzle of 0.1 and 0.2 mm orifice bore diameter.

4. CONCLUSIONS

The newly developed porous device allowed the use of conventional polycarbonate membranes to extrude liposomes and adjust size and polydispersity in a single step. A 0.2 μm membrane together with a 0.1 mm nozzle was found as optimum combination. The advantage of the high pressure preparation is that the shear forces at the nozzle described by the Ohnesorge number and at the membrane are sufficient to generate liposomes within narrow specifications in a one-step process. The reproducibility of the so prepared liposomes was extremely good, low standard deviations for size and polydispersity. The high pressure liposome formation performed continuously and is not limited in batch size, since it can be easily up-scaled by using larger pumps, filter units and nozzle installations. Even with the used continuous working lab-scale equipment, flow rates of 100 ml/min were reached corresponding to 6 l/h or 48 l/day.

The homogeneity of the resulting liposomes was improved by varying membrane and nozzle size and thereby increasing the shear forces. The second approach to improve the homogeneity was a change of the composition of the formulation by increasing the ethanol concentrations and thereby changing kinetic energy values inside membrane and nozzle. Very small liposomes with extremely narrow size distributions were obtained at high ethanol concentrations. Such a high pressure liposome formation technique could be implemented into a spray-drying process, whereby the higher ethanol concentrations could positively influence the drying behavior and reduce the drying temperature.

5. REFERENCES

-
- [1] Bangham, A.D., Standish, M.M., Watkins, J.C., Diffusion of univalent ions across the lamellae of swollen phospholipids, *J. Molecular Bio.*, 13(1): 238-252 (1965).
- [2] Barenholz, Y., Gibbes, D., Litman, B.J., Goll, J., Thompson, T.E., Carlson, F.D., A simple method for the preparation of homogeneous phospholipid vesicles, *Biochem.* 16(12): 2806-2810 (1977).
- [3] Mayhew, E., Nikolopoulos, G., Siciliano, A., An advanced technique for the manufacture of liposomes, *Am. Biotech. Lab.*, 3(6): 36-38 (1985).
- [4] Talsma, H., van Steenberg, M.J., Borchert, J.C.H., Crommelin, D.J.A., A novel technique for the one-step preparation of liposomes and nonionic surfactant vesicles without the use of organic solvents. Liposome formation in a continuous gas stream: The 'bubble' method, *J. Pharm. Sci.*, 83(3): 276-280 (1994).
- [5] Batzri, S., Korn, E.D., Single bilayer liposomes prepared without sonication, *Biochim. Biophys. Acta Biomem.*, 298(4): 1015-1019 (1973).
- [6] Wagner, A., Platzgummer, M., Kreismyr, G., Quendler, H., Stiegler, G., Ferko, B., Vecera, G., Vorauer-Uhl, K., Katinger, H., GMP production of liposomes – a new industrial approach, *J. Lip. Res.*, 16(3): 311-319 (2006).
- [7] Deamer, D., Bangham, A.D., Large volume liposomes by an ether vaporization method, *Biochim. Biophys. Acta, Nucleic Acids and Protein Syn.*, 443(3): 629-634 (1976).
- [8] Szoka, F., Olson, F., Heath, T., Vail, W., Mayhew, E., Papahadjopoulos, D., Preparation of unilamellar liposomes of intermediate size (0.1-0.2 μ mol) by a combination of reverse phase evaporation and extrusion through polycarbonate membranes, *Biochim. Biophys. Acta*, 601(3): 559-571 (1980).
- [9] Kim, S., Martin, G.M., Preparation of cell-size unilamellar liposomes with high captured volume and defined size distribution, *Biochim. Biophys. Acta*, 646(1): 1-9 (1981).
- [10] Isele, U., van Hoogevest, P., Hilfiker, R., Capraro, H-G., Schieweck, K., Leuenberger, H., Large-Scale Production of Liposomes Containing Monomeric Zinc Phthalocyanine by Controlled Dilution of Organic Solvents, *J. Pharm. Sci.*, 83(11): 1608-1616 (1994).
- [11] Schubert, R., Liposome preparation by detergent removal, *Meth. Enzym. (Liposomes, Part A)*, 367: 46-70 (2003).
- [12] Milsmann, M.H., Schwendener, R.A., Weder, H.G., The preparation of large single bilayer liposomes by a fast and controlled dialysis, *Biochim. Biophys. Acta*, 512(1): 147-55 (1978).
- [13] Schurtenberger, P., Mazer, N., Waldvogel, S., Kaenzig, W., Preparation of monodisperse vesicles with variable size by dilution of mixed micellar solutions of bile salt and phosphatidylcholine, *Biochim. Biophys. Acta Biomem.*, 775(1): 111-114 (1984).
- [14] Hauser, H., Stabilization of liposomes during spray – drying, *Liposome Technol. (2nd Ed)* 1: 197-208 (1993).
- [15] Goldbach, P., Brochart, H., Stamm, A., Spray - drying of liposomes for a pulmonary administration, I., Chemical stability of phospholipids, *Drug Dev. Ind. Pharm.*, 19(19): 2611-2622 (1993).
- [16] Goldbach, P., Brochart, H., Stamm, A., Spray - drying of liposomes for a pulmonary administration, II., Retention of encapsulated materials, *Drug Dev. Ind. Pharm.*, 19(19): 2623-2636 (1993).
- [17] Li, C., Deng, Y., A novel method for the preparation of liposomes: Freeze drying of monophasic solutions, *J. Pharm. Sci.*, 93(6): 1403-1414 (2004).
- [18] Frederiksen, L., Anton, K., van Hoogevest, P., Keller, H-R., Leuenberger, H., Preparation of Liposomes Encapsulating Water-Soluble Compounds Using Supercritical Carbon Dioxide, *J. Pharm. Sci.*, 86(8): 921-928 (1997).

-
- [19] Magnan, C., Badens, E., Commenges, N., Charbit, G., Soy lecithin micronization by precipitation with a compressed fluid antisolvent - influence of process parameters, *J. Supercrit. Fluids*, 19(1): 69-77 (2000).
- [20] Hunt, A.C., Papahadjopoulos, D.P., Method for producing liposomes in selected size range, US4529561 (1985).
- [21] Brandl, M., Bachmann, D., Unilamellar liposomal preparations with high active substance content, WO9605808 (1996).
- [22] Brandl, M., Bachmann, M., Drechsler, D., Bauer, M., Kurt H., Liposome preparation using high - pressure homogenizers, *Liposome Technol. (2nd Ed.)* 1: 49-65 (1993).
- [23] Szoka, F.C., Jacobson, K., Papahadjopoulos, D., The use of aqueous space markers to determine the mechanism of interaction between phospholipid vesicles and cells, *Biochim. Biophys. Acta Biomemb.*, 551(2): 295-303 (1979).
- [24] Olson, F., Hunt, C.A., Szoka, F.C., Vail, W.J., Papahadjopoulos, D., Preparation of liposomes of defined size distribution by extrusion through polycarbonate membranes, *Biochim. Biophys. Acta Biomemb.* 557(1): 9-23 (1979).
- [25] Cullis, P.R., Hope, M.J., Extrusion techniques for producing liposomes, WO 8600238 (1986).
- [26] Janoff, A.S., Blocsak, L.E., A method of extruding liposomes, EP0460720 (1991).
- [27] Morano, J.K., Martin, F., Liposome extrusion method, US4927637 (1990).
- [28] Benameur, H., Moes, A., Liposome preparation method and plant, US6217899 (2001).
- [29] Suddith, R., Liposome continuous size reduction method and apparatus, US5556580 (1996).
- [30] Sachse, A., Schneider, T., Continuous high pressure extrusion process for the production of liposomes and emulsions, DE4328331 (1995).
- [31] Brunke, R.A., Apparatus for the size reduction of liposomes, DE3905254 (1990).
- [32] Klinksiak, B., Mahiout, S., Method and device for producing a parenteral medicament, US6331314 (2001).
- [33] Clerc, S.G., Thompson, T.E., A possible mechanism for vesicle formation by extrusion, *Biophys. J.*, 67(1): 475-477 (1994).
- [34] Mui, B.L-S., Cullis, P.R., Evans, E.A., Madden, T.D., Osmotic properties of large unilamellar vesicles prepared by extrusion, *Biophys. J.*, 64(2): 443-453 (1993).
- [35] Bauckhage, K., Zerstäubung von Flüssigkeiten, Suspensionen und Schmelzen, in: *Handbuch der Mechanischen Verfahrenstechnik*, vol 1: 383-431, (Ed) Schubert, H., Wiley-VCH (2003).
- [36] Lefebvre, A.H., Atomization and sprays, Hemisphere, Washington (DC), (1989).
- [37] Lin, S.P., Reitz, R.D., Drop and spray formation from a liquid jet, *Ann. Rev. Fluid Mech.*, 30: 85-105 (1998).
- [38] Thomas, G.O., The aerodynamic break-up of ligaments, *Atom. Sprays*, 13(1): 117-129 (2003).
- [39] Tafreshi, H.V., Pourdeyhimi, B., The effect of nozzle geometry on waterjet breakup at high Reynolds numbers, *Exp. Fluids*, 35: 364-371 (2003).
- [40] Suter, S.P., Seshadri, V., Croce, P.A., Hochmuth, R.M., Capillary blood flow II. Deformable model cells in tube flow, *Microvas. Res.*, 2(4): 420-433 (1970).
- [41] Berger, N., Sachse, A., Bender, J., Schubert, R., Brandl, M., Filter extrusion of liposomes using different devices: comparison of liposome size, encapsulation efficiency, and process characteristics, *Int. J. Pharm.*, 223(1-2): 55-68 (2001).
- [42] Gompper, G., Kroll, D.M., Driven transport of fluids through narrow pores, *Phys. Rev. E*, 52(4): 4198-4208 (1995).

- [43] Bruinsma, R., Rheology and shape transitions of vesicles under capillary flow, *Physica A*, 234(1-2): 249-270 (1996).
- [44] Sun, S.F., *Physical chemistry of macromolecules, Basic principles and issues*, (2nd Ed.), Hoboken (NJ) (2004).
- [45] Kremer, J.M., Esker, M.W., Pathmamanoharan, C., Wiersema, P.H., Vesicles of variable diameter prepared by a modified injection method, *Biochem.*, 16(17): 3932-3955 (1977).
- [46] Diat, O., Roux, D., Nallet, F., Effect of shear on a lyotropic lamellar phase, *J. Phys. II*, 3: 1427-1452 (1993).

CHAPTER 7

Preparation and Spray-Drying of Liposomes using a Single-Step Process

Abstract:

High pressure liposome formation out of a multi-lamellar vesicle suspension followed by subsequent spray-drying is a smart one-step process resulting in a dry free flowable powder. Hollow spherical particles were obtained, whereby the size of the used nozzle influenced the particle size distribution. By using an orifice nozzle to rupture the multi-lamellar vesicles, liposome size decreased depending on the used flow rate and pressure. The introduction of a porous device to achieve an in-situ extrusion was essential to improve the polydispersity index. Finally, liposome size and polydispersity were dependent on spray-drying conditions and pressure in the system. Within a wide temperature range the drying-step did not affect liposome integrity and lipid content of the formulations. The combination of high pressure liposome formation with spray-drying offered a promising new combination, which is capable for large-scale production of homogeneous liposomes.

1. INTRODUCTION

In the spray-drying process the drug containing feed solution is atomized into droplets that dry rapidly in a drying gas [1]. The drying time depends on the process conditions e.g. liquid feed rate, drying air temperature and aspirator capacity. The heat exposure of the droplets is considerably lower than the temperature of the drying air because of the evaporative cooling effect. The relatively fast drying process within the drying chamber reduces stress for the material. Finally, the product is removed from the air stream by the cyclone. A promising study using the spray-drying technique for liposomal formulations was already discussed in chapter 5. For large scale production of liposomes with a suitable and narrow size distribution usually several repeated sizing steps of the liposomal material either by high pressure homogenization [2] or by the membrane extrusion are required [3].

A single step extrusion method for the continuous preparation of appropriately sized liposomes was investigated [4] and described in chapter 6. Here, a single extrusion process through a porous device is followed by an atomization over the orifice nozzle. In the study presented in this chapter the high pressure liposome formation was combined with spray-drying to form and dry liposomes in a single step. A multi-lamellar vesicle (MLV) liposome suspension was pressurized by an orifice nozzle or by a combination of porous device and orifice nozzle followed by a subsequent spray-drying step. Parameters like nozzle size, flow rate and corresponding pressure, as well as drying air temperature were varied. Both, the spray-dried particles and the liposomes were characterized.

2. MATERIAL AND METHODS

2.1 LIPOSOME PREPARATION AND DRYING PROCESS

Multi-lamellar vesicles (MLV) with a total lipid content of 10 mM were prepared by ethanol injection. A lipid stock solution with 5 mM DOTAP-Cl (1,2-dioleoyl-3-trimethylammonium-propane-chloride) and 5 mM DOPC (1,2-dioleoyl-*sn*-glycero-3-phosphocholine) (both from Avanti Polar Lipids, Alabaster) dissolved in ethanol was used as lipid component for liposome preparation. Multi-lamellar liposomes formed spontaneously upon the injection of the lipid stock solution into 10.5 % [w/v] aqueous trehalose solution (Ferro Pfanstiehl, IL, USA). The suspension of multi-lamellar liposomes was sprayed using an ISCO E100X syringe plunger pump (Teledyne ISCO, Lincoln, NE, USA). Orifice nozzles of the model 121 V G ¼ (Schlick Atomization Technologies, Untersiemau, Germany) with a diameter of 0.1, 0.2 and 0.5 mm were used. Two different experimental set-ups were evaluated (Fig 1). In the first set-up the suspension

was pumped directly through the nozzle into the pilot-plant drying chamber with a height of 135 cm and a diameter of 80 cm (Mobile Minor, Niro, Copenhagen, Denmark) (Fig 1, (pathway A)). Such a pilot plant apparatus with a wide drying chamber and an enlarged drying capacity is necessary because of the liquid flow rate of 20 ml/min up to 100 ml/min and the resulting spray-angle of the orifice nozzle. This drying equipment avoided the droplets colliding with the walls and the loss of material during the spraying process. For set-up B the porous device was incorporated between the pump and the nozzle, leading to an online extrusion of the liposomes (Fig 1, (pathway B)) followed by drying process. For the extrusion polycarbonate filter membranes (Osmonics Inc., MN, USA) with a size of 0.1 and 0.2 μm supported by two drain discs (Osmonics Inc., MN, USA) were employed. Liposome preparation was performed at flow rates of 5 to 100 ml/min resulting in a pressure of 1 to 780 bar. The spray-drying process consists of atomization of the liquid feed over the nozzle into a spray, spray air contact, moisture evaporation of the spray inside the drying chamber and the separation of the dried particles from the air. Within the hot dehumidified drying air produced by the dehumidifier and air in-take-heater, particles dry very rapidly less than 1 second for spray droplets smaller than 100 μm in the main drying chamber. Powder collection occurs by a cyclone separator into the final product container. After separation of the dried product the air passes through the aspirator.

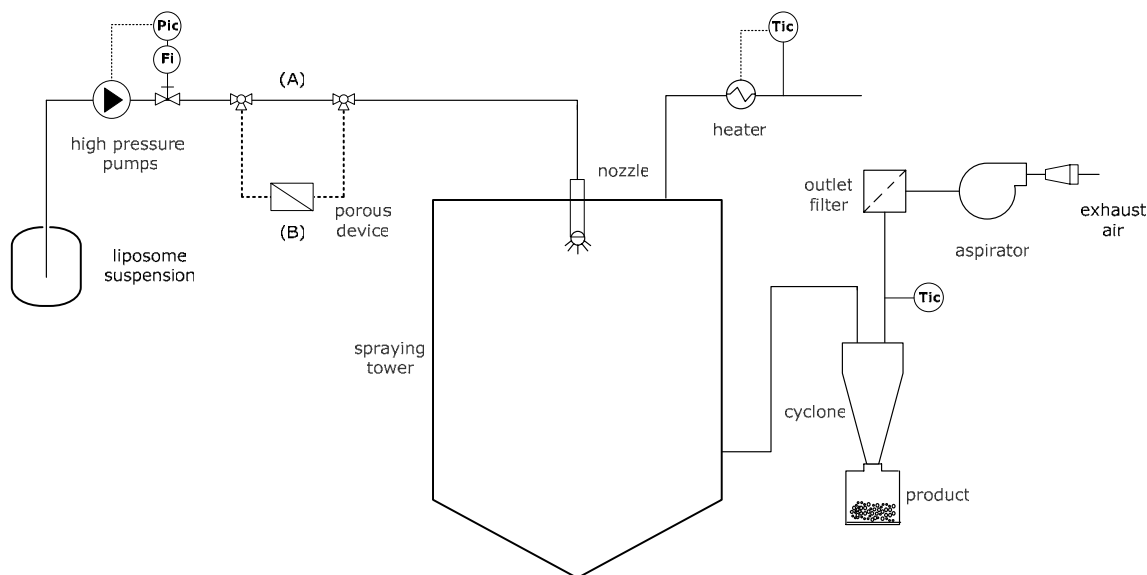


Figure 1: Schematic construction of the experimental set-up with high pressure pump and the used Mobile Minor pilot plant production spray-drying unit with the diagram of the product and air flow.

The following process conditions were employed for the high pressure liposome formation: orifice nozzle diameters were 0.1, 0.2 and 0.5 mm, membrane pore size was 0.2 μm and the liquid feed volumetric flow rate (v_{lf}) was between 20 and 100 ml/min

resulting in a corresponding pressure between 20 and 780 bar. The process conditions for the spray-drier were: drying air inlet temperature (T_{inlet}) between 100 and 240°C, drying air outlet temperature (T_{outlet}) in the range of 60 and 150°C and the drying air volumetric flow rate (v_{da}) was constant at 80 kg/h.

All further methods used in this chapter are already described before.

3. RESULTS AND DISCUSSION

3.1 PARTICLE FORMATION PROCESS

The used vaporizing nozzle consisted of three parts: a nozzle head, a centrifugal insert and a screw fitting (Fig 2, (A)). When increasing the liquid feed rate and consequently the pressure, the spray-angle changed from 76° at 20 ml/min to 127° at 100 ml/min using a 0.1 mm (Fig 2, (B)) and from 53° at 20 ml/min to 90° at 60 ml/min using a 0.2 mm (Fig 2, (C)) orifice diameter nozzle.

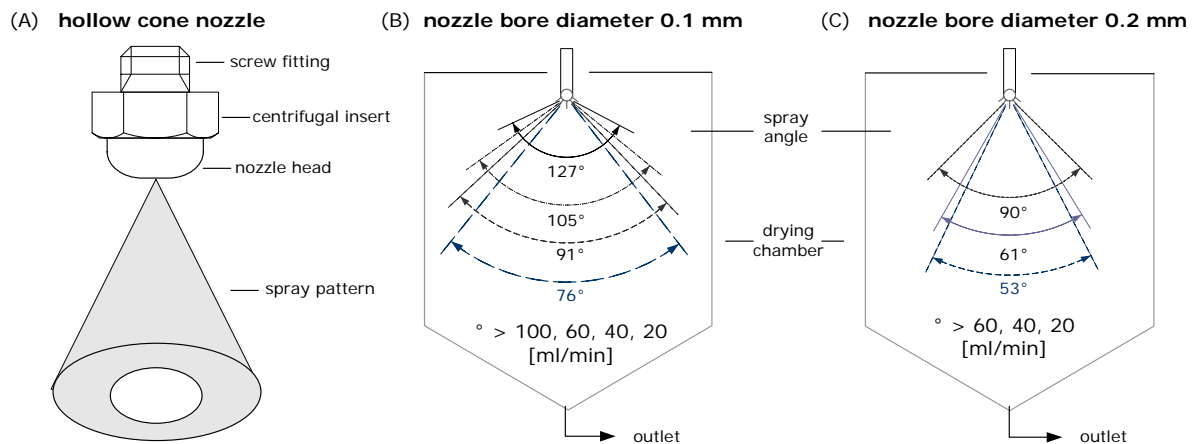


Figure 2: Schematic drawing of the hollow cone nozzle with the spray pattern (A), and spray angle related to the diameter of the orifice 0.1 mm (B) and 0.2 mm (C) in respect of the liquid feed.

First experiments within a Büchi spray-dryer with an inner diameter of the drying chamber of 16 cm were not satisfying because of the too small drying chamber size and volume. Particle preparation was not feasible with the Büchi spray-dryer because a minimum liquid feed rate of 20 ml/min was necessary to obtain a homogenous droplet pattern within the orifice nozzle of 0.1 mm diameter. The drying of the droplets and particles did not proceed sufficiently before they impacted with the wall. The still wet

droplets and particles attached to the wall, moreover the liquid rinsed from the wall already after starting the process. The technical approach to overcome this problem was to raise the drying capacity of the equipment. With a reduced flow rate the atomization of the liquid feed within the nozzle was not sufficient, which resulted in too large droplets impossible to be dried. Therefore, a pilot plant spray-dryer with a wider drying chamber of 80 cm was used to avoid the droplets colliding to the wall. With such a larger production scale unit and the higher liquid throughput the outlet temperature decreases resulting in higher residual moisture values. Therefore, to achieve the same drying levels assigned by the outlet temperature a higher air inlet temperature was inevitable.

The combination of high pressure vesicle formation with a subsequent spray-drying step was feasible in the described mobile minor system. A high pressure nozzle with wider spraying angles was successfully implemented into the spray-drying process. Free flowable powder could be collected and even high liquid feeds up to 100 ml/min were dried without any droplet deposition at the vertical wall of the drying chamber. As already described in chapter 6 the formation of liposomes was feasible using only the orifice nozzle without the drying step. The liposomes were formed out of a multi-lamellar suspension induced by the shear forces at the nozzle (pathway A) or by the second approach (pathway B) using a single extrusion step through the porous device followed by the atomization according.

3.2 PARTICLE MORPHOLOGY

Particle size and shape were influenced by the properties of the droplets formed by the orifice nozzle, as well as by the drying conditions like temperature and aspirator flow. The particles exhibited a smooth spherical surface in the SEM micrographs for the 0.1 mm and the 0.2 mm nozzle (Fig 3).

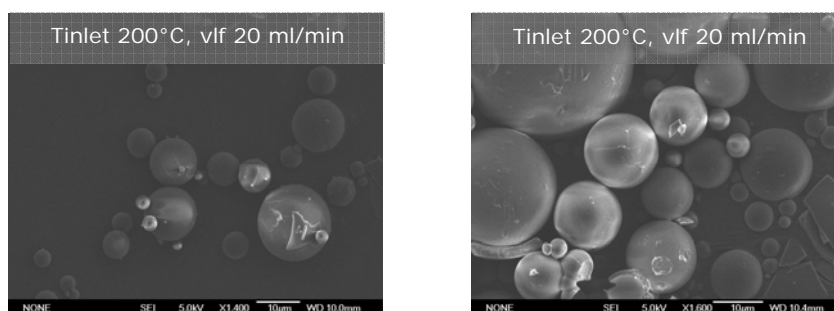


Figure 3: Scanning electron micrographs of spray-dried particles containing liposomes using a 0.1 mm nozzle (left) and 0.2 mm nozzle (right).

Particles dried at an inlet temperature of 200°C and a vlf of 40 ml/min were composed of an outer shell with a thickness of about 2.5 μm and a hollow core, which is obvious in figure 4. However, a fraction of broken particles suggested a too high drying rate compared to the rate of water diffusion to the particle surface, which resulted in a raised internal vapor pressure [5].

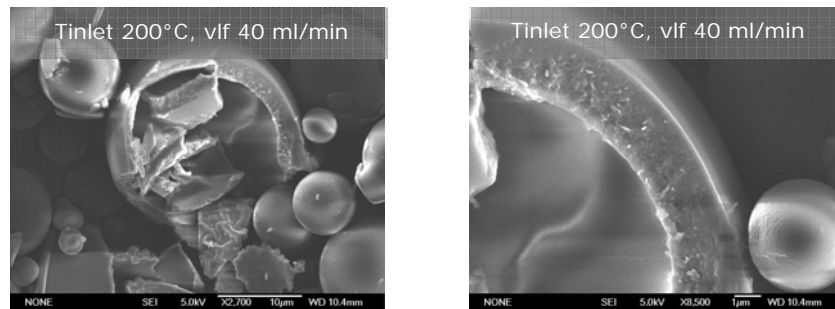


Figure 4: Scanning electron micrographs with at a magnification of 2700x (left) and 8500x (right) of spray-dried fractured particles using a 0.2 mm nozzle.

Droplet break-up within a two fluid nozzle is influenced by differences in the relative velocity of the flowing liquid and the atomizing air [6]. The dimensionless Reynolds number describes the inertial force to friction force ratio of the used orifice nozzle. The Reynolds number only depends on the nozzle size and the viscosity, and therefore different droplet break-up conditions were found for the used nozzles (compare chapter 6). When using a hollow cone nozzle the liquid feed is pressurized through the tangential slits and this energy is converted into rotational energy. The angular momentum is maintained and the peripheral velocity increases towards the orifice bore. This results in a reduced static pressure in the nozzle tip itself leading to a liquid film inside the spray orifice and a droplet break-up into radial and axial direction building a hollow cone spray pattern. Water jets with higher Reynolds number ($> 2500 \text{ Re}$) and turbulent flow break-up closer to the nozzle exit and tend to produce smaller droplets [7]. With increased nozzle diameters and reduced Reynolds number larger droplets were formed with lower spraying angles. Exemplarily shown for a flow rate of 40 ml/min the mean particle fractions were found at 32, 124 and 180 μm for the 0.1 mm, 0.2 mm and 0.5 mm nozzles (Fig 5, left). A second, larger particle fraction was obtained for the 0.2 and 0.5 mm nozzle. The lower pressure of 20 bar for the 0.2 mm nozzle compared to 83 bar for the 0.1 mm nozzle led to this bimodal distribution. The span average, which describes the width of the volume size distribution, varied significantly with maximally 2.0 for the 0.1 mm nozzle diameter compared to values above 5 for the 0.2 mm nozzle and above 10 for the largest 0.5 mm nozzle (Fig 5, right). To sufficiently improve the particle size

distributions, a higher liquid flow rate resulting in raised pressure and a higher rotational energy would be required. The so formed smaller droplets should be more homogenous.

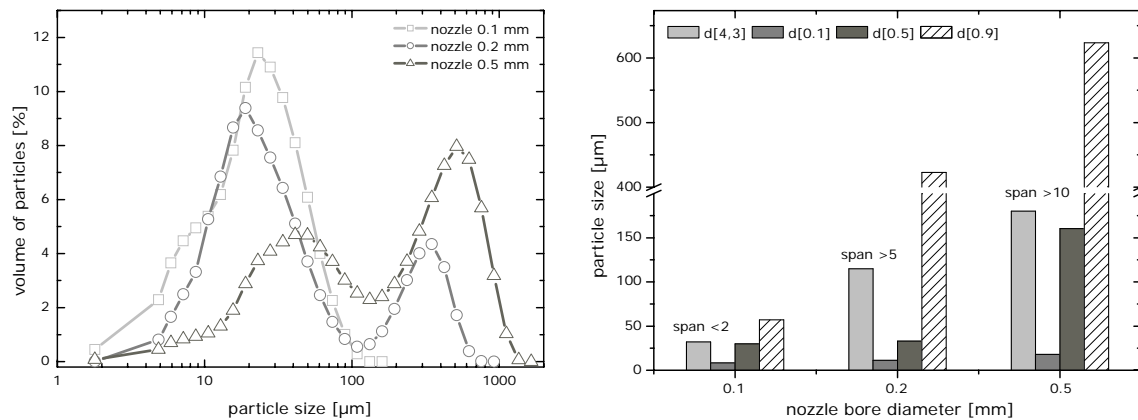


Figure 5: Particle size distribution using 0.1, 0.2 and 0.5 mm nozzle at a flow rate of 40 ml/min (left) and the average particle sizes with resulting span (right).

In respect of a more homogenous particle size distribution the 0.1 mm nozzle should be used for these experiments. The droplet break-up in the between the 2nd wind-induced and the atomization region resulted more homogeneous droplets at the selected conditions, which resulted in a span value below 2. For the 0.2 mm nozzle in between the 1st and 2nd wind-induced the droplets are more heterogeneous.

3.3 PROCESS TEMPERATURES

The relation between the inlet air temperature (T_{inlet}) and the outlet temperature (T_{outlet}) depended on the bore diameter of the applied nozzle and the so formed droplet size. For the 0.1 mm nozzle a linear relationship between the T_{inlet} and T_{outlet} was found (Fig 6, left). This is in agreement with the observations made during the spray-drying process using a two-fluid nozzle (compare chapter 5). Additionally, the spray-angle within the drying chamber impacts the T_{outlet} . With reduced liquid feed rates and the larger orifice diameter the spray-angle is smaller and therefore the drying efficiency is reduced. This influence was already evident for the 0.2 mm nozzle where the outlet temperature remained constant independent of the inlet temperature in the range of 120 to 210°C and a pressure below 100 bar (60 ml/min liquid feed rate) (Fig 6, right). This can be explained by the larger droplets formed at the 0.2 mm nozzle with a more heterogeneous size distribution due the reduced atomization forces and the low Re numbers of the 0.2 mm nozzle. The larger droplets and the small spray angles at the selected conditions affected the mass transfer and water vapor evaporation.

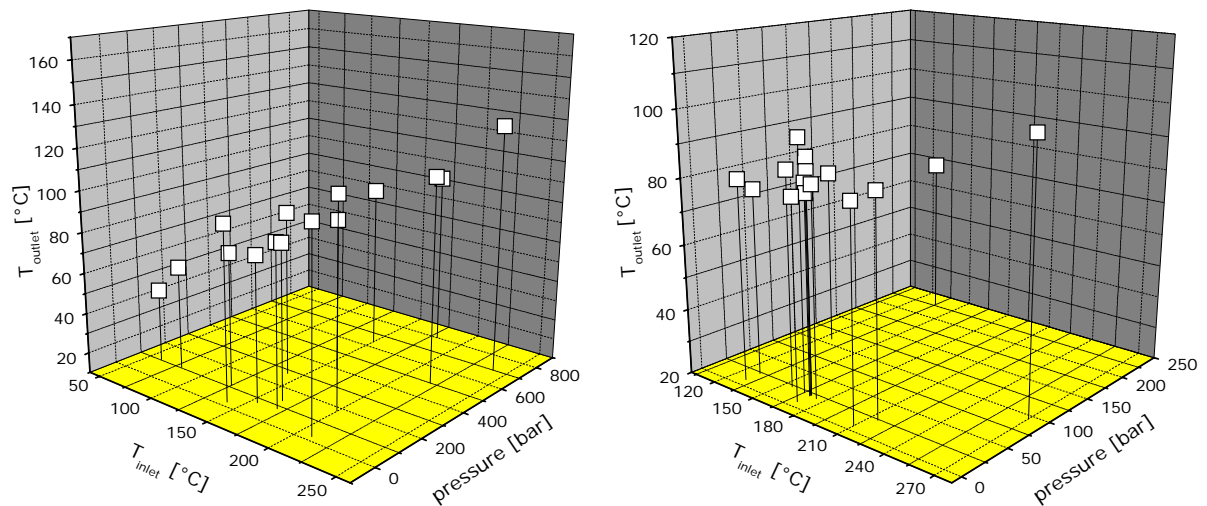


Figure 6: Outlet temperature (T_{outlet}) versus inlet temperature in respect of the pressure for the 0.1 mm (left) and 0.2 mm (right) nozzle.

To achieve optimum drying efficiencies the droplet size distribution should be as homogenous as possible and use of the 0.1 mm nozzle is more favorable compared to the 0.2 or 0.5 mm nozzles.

3.4 PARTICLE YIELD AND RESIDUAL MOISTURE

The yield at the different process conditions strongly depended on the nozzle size and the spray-drying conditions (Tab 1). Although the drying capacity of the pilot plant with a drying volumetric flow rate of 80 kg/h and a water evaporation capacity up to 6 kg/h was sufficient for all tested conditions the product yield remained low. Generally, material loss occurs mostly due to the attachment of sprayed droplets and dry powder at the wall of the drying chamber and the poor cyclone efficiency in collecting fine particles [8]. In our case a sufficient drying of the formed droplets was observed, because less than 1 % of the droplets, respectively of the dried particles were attached to the drying chamber after all drying processes. For the 0.2 mm nozzle higher yields were achieved compared to the 0.1 mm nozzle. A relatively good yield of 52.1 ± 14.9 % was obtained at a flow rate of 40 ml/min with a pressure of 26 bar and an outlet temperature of 85°C with the 0.2 mm nozzle. The larger droplets and finally larger particles were necessary to increase the yield with outlet temperatures below 85°C. The relatively low yield could be assigned to the very fine droplet sizes generated by the orifice nozzle. Therefore, the reduced particle separation might be induced due to an insufficient cyclone resistance, which was not able to collect such small powder particles. A larger pressure drop when using a cyclone with a smaller radius could improve product recovery [9].

Table 1: Yield and residual moisture achieved for the used process conditions and experimental set-ups.

flow rate [ml/min]	pressure [bar]	T _{outlet} [°C]	residual moisture [%]	yield [%]
0.1 mm nozzle				
30	23	105	2.1	44
40	75	75	2.9	44
50	162	85	2.8	65
60	500	110	3.1	10
80	690	130	4.0	18
100	800	95	4.5	38
0.1 mm nozzle and 0.2 µm membrane				
10	20	96	2.7 ± 0.6	20.0 ± 9.9
40	180	89	2.8 ± 1.2	14.5 ± 13.4
50	280	130	3.3 ± 0.2	42.0 ± 5.6
60	525	86	3.2 ± 0.3	41.0 ± 5.6
0.2 mm nozzle and 0.2 µm membrane				
40	21	90	3.2 ± 0.5	52.1 ± 14.9
60	94	110	3.5 ± 0.8	49.0 ± 10.4
0.5 mm nozzle and 0.2 µm membrane				
40	11	110	3.3	1.1

An increase in residual moisture was observed independent of the experimental set-up when higher flow rates were applied (Tab 1). With the 0.1 mm nozzle 2.1 % residual moisture was determined for a flow rate of 30 ml/min and 4.5 % for a flow rate of 100 ml/min. The drying-temperature only had a minor impact on the residual moisture of the products compared to droplet size. Residual ethanol could not be detected for any process conditions, even for relatively low inlet temperatures by HS-GC chromatography. The evaporation temperature during the drying process revealed sufficient extraction forces for ethanol.

Thus, the droplet break-up of the liquid feed in respect of the drying temperature is responsible for the drying efficiency. Optimum condition with favorable residual moisture and product yield were not yet achieved. Although the moisture content could be reduced to 2.1 % and for some conditions a product yield increased above 50 % further investigations are necessary to find appropriate working parameters.

3.5 LIPOSOME CHARACTERIZATION

3.5.1 Using the orifice nozzle

Without the porous device only the 0.1 mm nozzle resulted in relatively small and homogenous liposomes. Similar results were described for the liposome formation process in chapter 6 without the drying step. After rehydration of the spray-dried powder liposome size properties comparable to that before drying were obtained. Above a pressure of 500 bar (v_{lf} of 50 ml/min) the size decreased to 125 nm and the polydispersity was significantly lowered to values of 0.29 (Fig 7). As already shown within the spray-drying process using a two-fluid nozzle (compare chapter 5) the drying conditions in respect of outlet temperature did not affect the liposome properties.

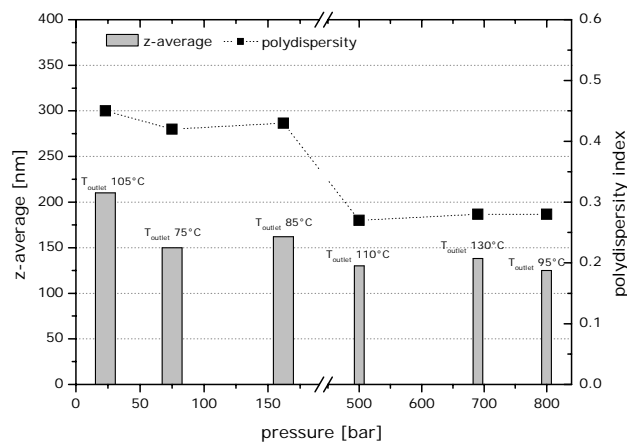


Figure 7: Size and polydispersity index of the liposomes produced by the 0.1 mm nozzle without a porous device in relation to pressure and outlet temperature.

3.5.2 Using the porous device and the orifice nozzle

During the spray-drying process the porous device equipped with a 0.2 μm membrane combined with the 0.1, 0.2 or 0.5 mm nozzle diameter was added. The optimum conditions for the 0.1 mm nozzle with a membrane were found around 270 bar with an outlet temperature of about 90°C (Fig 8, left). The 0.2 mm nozzle on the other hand resulted in pressures between 5 and 100 bar for the flow rates of 20 to 100 ml/min liquid feed rates. By the use of the larger 0.2 mm nozzle in combination with the porous device liposome size and polydispersity decreased as well with increasing the pressure in the system (Fig 8, right). At 40 ml/min flow rate at 20 bar and an outlet temperature of 83°C an optimum size of 135 nm and a polydispersity index of 0.15 was achieved. Finally, with the 0.5 mm nozzle and a 0.2 μm membrane it was possible to produce liposomes, with a

size of 152 nm and a polydispersity index of 0.23 at a pressure of 11 bar (data not shown).

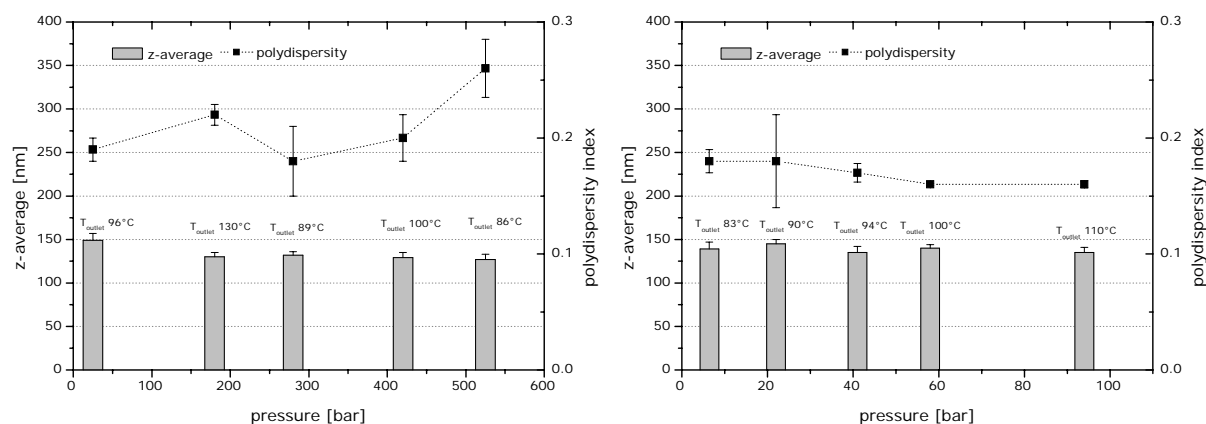


Figure 8: Size and polydispersity index of the liposomes produced by the 0.1 mm nozzle (left) and 0.2 mm nozzle (right) with a 0.2 μm membrane in relation to pressure and outlet temperature.

When calculating the Ohnesorge number and the Reynolds number for the employed set-ups differences in the jet disintegration and break-up regimes were obvious. During spray-drying the liposomal properties were not affected when working in the 1st and 2nd wind-induced droplet break-up region. For the 0.1 mm nozzle the atomization region was reached (compare chapter 6), which was reflected in a higher PI of the reconstituted liposomes. The 0.2 mm nozzle resulted in larger droplets and a favorable drying behavior, which preserved the liposomes during the drying process.

3.6 LIPID RECOVERY

RP-HPLC revealed that the stability of the lipids was assured after the drying process. A slight increase in the lipid concentration could be determined when spray-drying was performed with the 0.1 and 0.2 mm nozzle at temperatures around 100°C (Tab 2). When using the 0.5 mm nozzle a slight decrease in lipid recovery was observed. However, more important no oxidized or hydrolyzed lipids were present, indicating chemical stability of the lipids at the heat exposure during the drying process (data not shown).

Table 2: Lipid recovery after reconstitution of the spray-dried powder for the different nozzle sizes and outlet temperatures.

nozzle diameter [mm]	T _{outlet} [°C]	DOPC recovery [%]	DOTAP-Cl recovery [%]
0.1	110	104.9	104.7
0.2	100	100.6	101.3
0.5	110	97.3	96.1

Only when working with the 0.1 mm nozzle, the lipid recovery declined with increasing outlet temperatures (Fig 9, left). Above an outlet temperature of 150°C degraded and oxidated lipids were detectable, which was reflected in a decreased lipid recovery by about 13 %. The flow rate and the pressure on the other hand did not influence the lipid recovery. In the temperature range from 85 to 100 °C the recovery was constant for the 0.1 mm and 0.2 mm nozzle (Fig 9, right).

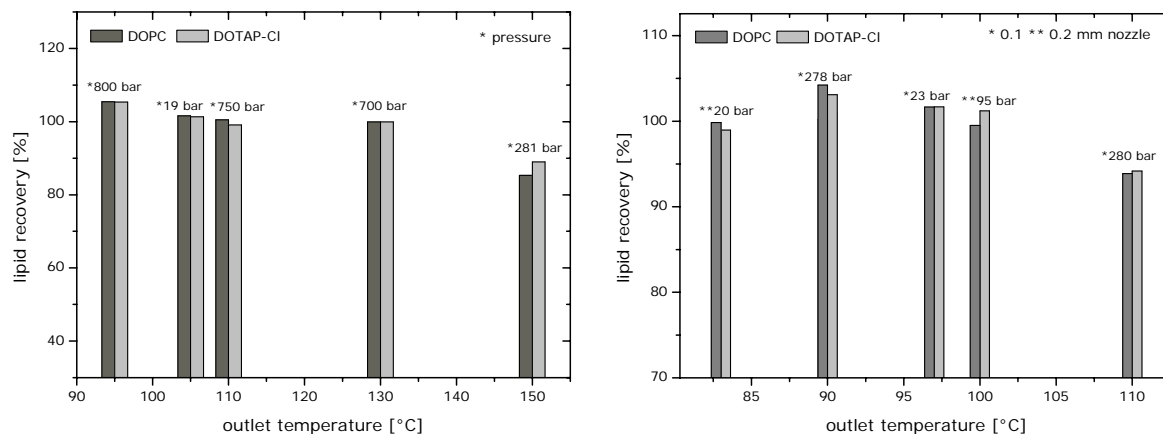


Figure 9: Lipid recovery of the spray-dried powder produced by the 0.1 mm nozzle (left) and by 0.1 mm and 0.2 mm in comparison for the different outlet temperatures and pressure ranges.

Finally, it can be stated that the lipid recovery was reduced at higher drying temperatures due to a degradation of the lipids. The applied pressure, nozzle type and the resulting droplet break-up regime had no obvious impact on the degradation of the lipids.

3.7 DRUG LOADING STUDIES

To simulate drug loading of the liposomes the fluorescent dye Nile Red was used as model compound in this study. The maximum solubility of Nile Red in water ranges below 1 µg/ml [10], which makes it a suitable model substance for poorly soluble compounds. Furthermore, the fluorescence properties of Nile Red are strongly depending on the polarity of its environment. In polar media Nile Red fluorescence exhibits a very low fluorescence intensity and the emission maximum is red shifted compared to less nonpolar solvents. The maximum is located at 657 nm in water compared to 595 nm in chloroform [10]. Furthermore, a significant increase in fluorescence intensity is measured in non-polar solvents and hydrophobic environment. This solvatochromic effect can be explained by the concept of the twisted intramolecular charge transfer (TICT) type

excited state. The TICT state, which forms upon the excitation of Nile Red is characterized by a higher polarity as compared to the ground state. Therefore, its formation is favored in more polar environments. As the TICT state is the major radiationless relaxation process of Nile Red the fluorescence intensity is declining when the TICT is favored in more polar solvents [11,12]. The very low fluorescence in water combined with the solvatochromic effect makes Nile Red a valuable marker in biological membrane research. For example the fluorescence anisotropy of Nile Red was used to gain information concerning the polarity and hydration levels [13].

An aliquot of the ethanolic Nile Red stock solution was added to the lipid stock solution followed by the subsequent ethanol injection. The resulting liposomal solution contained 0.26 $\mu\text{g/ml}$ Nile Red. The emission maximum of Nile Red in the liposomal formulation after the ethanol injection was located at 633 nm. When using the 0.1 mm nozzle for spray-drying at different temperatures a decline in fluorescence intensity was measured after the reconstitution of the spray-dried powder (Fig 10, (A)).

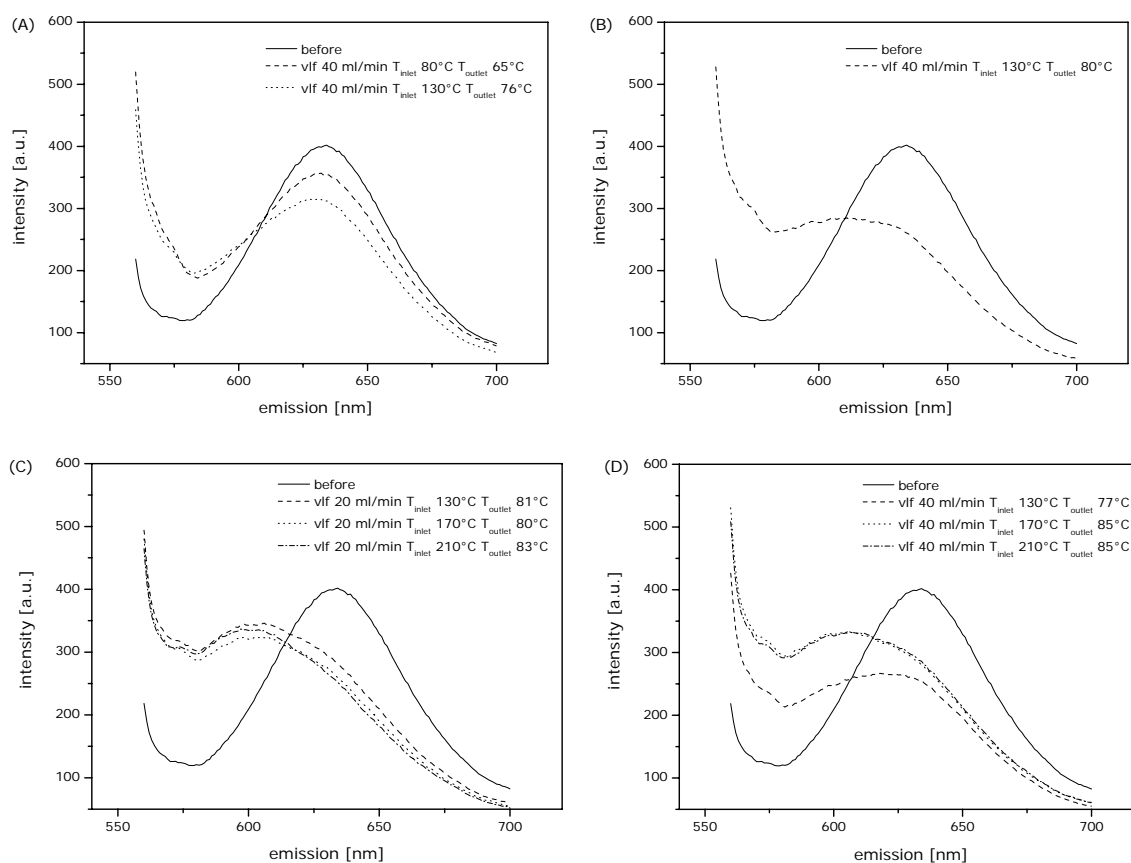


Figure 10: Fluorescence emission spectra after excitation at 550 nm of Nile Red containing liposomal formulations dried with the 0.1 mm nozzle at a liquid flow-rate of 40 ml/min (A), the 0.5 mm nozzle at a liquid flow-rate of 40 ml/min (B) and the 0.2 mm nozzle at a liquid flow-rate of 20 ml/min (C) and 40 ml/min (D).

The decline in intensity was more pronounced at T_{outlet} of 76°C compared to T_{outlet} 65°C. Furthermore a slight shift of the emission maximum to 629 nm at T_{outlet} of 76°C was observed. The decrease in intensity after rehydration could be explained by a slight change of the environment of Nile Red to a less polar environment. More pronounced changes were observed when spray drying was performed with the larger 0.2 and 0.5 mm nozzles (Fig 10, (B-D)). Besides the decline in intensity at 633 nm a clear shift of the emission maximum to about 600 nm occurred. This shift of the emission maximum indicates a reduction of the polarity of the Nile Red environment and a lower hydration level, compared to the process solution feed [14].

It can be concluded that the process using the 0.1 mm nozzle appears to be more feasible in preserving the integrity of Nile Red within the liposomes. Using the 0.1 mm nozzle smallest droplets are formed. These smaller droplets require shorter drying times. Consequently, viscosity within the droplets increases, leading to a change of the liposomal structure.

4. CONCLUSIONS

The work in this chapter demonstrated that the preparation of liposomes by combining the high pressure preparation process either with the nozzle alone or in combination with the porous device with a subsequent spray-drying is feasible. The selection of an appropriate spray-dryer with sufficient drying capacity was a prerequisite to obtain a dry product. The droplet formation and the consecutive drying process were optimized for both the 0.1 and 0.2 mm orifice nozzle. Nozzle size and liquid feed rate affected the particle properties significantly. Smaller, more homogeneous particles could be achieved by the 0.1 mm nozzle and a higher liquid feed rate and resulting higher atomization pressure. The residual moisture content was below 2 % for a flow rate of 20 ml/min, while it ranged above 4 % at a flow rate of 100 ml/min. Although the obtained yield between 1 and 65 % was low, the technical feasibility was proven. With an optimized collection of particles, e.g. by using improved cyclones or vacuum filter units it should be possible to increase the yield [9,15]. When using the 0.1 mm nozzle, the size of the spray-dried and reconstituted liposomes decreased below 150 nm due to the elevated shear forces at the smaller bore diameter. This was in good correlation with the results of the high pressure liposome preparation (compare chapter 6). The introduction of the porous device was important to further reduce the polydispersity index. However, the droplet break-up for the 0.1 mm nozzle, which was in the atomization region, negatively affected the liposomes size to a larger polydispersity although the porous device was used. The larger droplets obtained by the 0.2 mm nozzle in combination with the porous device led to more favorable liposome properties, regarding size and PI at all process conditions.

The combination of liposome formation and drying offered a promising new combination to produce and dry liposomal formulations in a one-step process. Furthermore, the up-scale of this one-step process to a larger pilot production unit, which showed already comparable drying behavior to a large scale production unit, was possible.

5. REFERENCES

- [1] Master, K., *Spray drying handbook*, (5th Ed.), John Wiley & sons, New York, (1991).
- [2] Barenholz, Y., Gibbes, D., Litman, B.J., Goll, J., Thompson, T.E., Carlson, F.D., A simple method for the preparation of homogeneous phospholipid vesicles, *Biochem.* 16(12): 2806-2810 (1977).
- [3] Szoka, F.C., Jacobson, K., Papahadjopoulos, D., The use of aqueous space markers to determine the mechanism of interaction between phospholipid vesicles and cells, *Biochim. Biophys. Acta Biomemb.*, 551(2): 295-303 (1979).
- [4] Wiggenghorn, M., Haas, H., Drexler, K., Winter, G., *Liposome Preparation by Single-Pass Process*, EP06023155.0 (2006).
- [5] Maa, Y-F., Constantino, H.R., Nguyen, P-A., Hsu, C.C., The Effect of Operating and Formulation Variables on the Morphology of Spray-Dried Protein Particles, *Pharm. Dev. Technol.*, 2(3): 213-223 (1997).
- [6] Johnson, K.A., Preparation of peptide and protein powders for inhalation, *Advanced Drug Deliv.*, 26(1): 3-15 (1997).
- [7] Tafreshi, H.V., Pourdeyhimi, B., The effect of nozzle geometry on waterjet breakup at high Reynolds numbers, *Exper. Fluids*, 35(4): 364-371 (2003).
- [8] Maa, Y-F., Nguyen, P-A., Sit, K., Hsu, C.C., Spray-Drying Performance of a Bench-Top Spray Dryer for Protein Aerosol Powder Preparation, *Biotech. Bioeng.*, 60(3): 301-309 (1998).
- [9] Maury, M., Murphy, K., Kumar, S., Shi, L., Lee, G., Effects of process variables on the powder yield of spray-dried trehalose on a laboratory spray-dryer, *Eur. J. Pharm. Biopharm.*, 59(3): 565-573 (2005).
- [10] Greenspan, P., Fowler, S.D., Spectrophotometric studies on the lipid probe, Nile red, *J. Lipid Res.*, 26(7): 781-789 (1985).
- [11] Dutta, A., Kamada, K., Ohta, K., Spectroscopic studies on Nile red in organic solvents and polymers, *J. Photochem. Photobiol. A: Chem.*, 93(1): 57-64 (1996).
- [12] Golini C.M., Williams B.W., Foresman, J.B., Further Solvatochromic, Thermochromic, and Theoretical Studies on Nile Red, *J. Fluoresc.*, 8(4): 395-404 (1998).
- [13] Coutinho, P.J.G., Castanheira, E.M.S., Ceu Rei, M., Real Oliveira, M.E.C.D., Nile red and DCM fluorescence anisotropy studies in C12E7/DPPC mixed systems, *J. Phy. Chem. B*, 106(49): 12841-12846 (2002).
- [14] Hungerford, G., Baptista, A.L.F., Coutinho, J.G. Castanheira, E.M.S., Real Oliveira, E.C.D., Interaction of DODAB with neutral phospholipids and cholesterol studied using fluorescence anisotropy, *J. Photochem. Photobiol. A: Chem.* 181(1): 99-105 (2006).
- [15] Maa, Y-F., Nguyen, P-A., Sit, K., Hsu, C.C., Spray-Drying Performance of a Bench-Top Spray Dryer for Protein Aerosol Powder Preparation, *Biotech. Bioeng.*, 60(3): 301-309 (1998).

CHAPTER 8

Inert Spray-Drying using High Organic Solvent Concentrations for the Preparation and Drying of Liposomes

Abstract :

Inert spray-drying enables the processing of formulations with high organic solvent content. It was investigated if the process temperature during spray-drying can be reduced by the addition of the organic solvents ethanol, methanol or acetone to liposomal formulations. A further goal was to analyze to which extent the liposome size distribution can be optimized by a new method using a porous device and an orifice nozzle for a size adjustment of the liposomes followed by the inert spray-drying step. Nitrogen was used as inert-drying gas and the process was performed at different temperatures and nozzle bore diameters. We demonstrated that stable, free flowable and dry powders of liposome preparations were obtained under inlet temperatures between 80 to 200°C resulting in corresponding outlet temperature between 30 and 120°C. The feed was adjusted to 20 ml/min resulting in nozzle pressures between 18 and 25 bar. Optimum conditions were found when using a 0.1 mm nozzle connected to a 200 nm membrane with 20 % [w/v] ethanol or 40 % [w/v] acetone added to the formulation. The resulting liposomes were 120 nm in size with polydispersity indices of 0.13 for both solvents. In comparison to the conventional two-fluid nozzle spray-drying, the process temperature could be reduced by at least 20°C down to about 40°C. Major advantages of this technique are the online preparation of liposomes from crude multi-lamellar suspensions, the very low drying temperatures and the high flow-rates of the liquid feed.

1. INTRODUCTION

It was shown that spray-drying is a feasible technique to dry liposomal formulations (compare chapter 3 and 7). The orifice nozzle used during spray-drying generated a cloud of very fine droplets with a tremendous air-liquid interfacial area. The liquids can evaporate rapidly from the droplets with the consequence that the drying process is completed within milliseconds up to a few seconds [1]. However, in most cases high temperatures are required to obtain a dry product with improved particle properties. With the addition of organic co-solvent like ethanol, methanol or acetone this specific drying behavior can be further enhanced. Several publications described the influence of organic solvents during spray-drying, for example of ethanol [2], acetone [3] or halothane [4].

A dehydration process was so far not often described for formulations with high organic solvent contents above 10 %. Under atmospheric spray-drying conditions only a maximum ethanol concentration of 10 to 12 % can be brought into a regular set-up, due to the risk of explosion at high temperatures [5]. To dry formulations with higher organic solvent concentrations a closed drying system must be used. Under such inert conditions the system is maintained with over-pressure using gaseous nitrogen and under exclusion of oxygen. The idea behind using higher organic solvent concentrations is the different heat capacities of solvents compared to water and their higher evaporation speed. It was assumed that the evaporation rate of e.g. ethanol could be increased in a way that phase separation or an increased concentration of lipids in water takes place, so that spontaneous liposome formation could occur during the inert spray-drying.

We tested if the size distribution of liposomes can be retained with this inert spray-drying process. Because inert spray-drying is performed using an orifice nozzle at high pressure and at a much higher flux as compared to two-nozzle spray-drying, very high shear-forces are involved. It was shown in chapter 6 that liposomes with a defined size distribution can be formed directly by making use of the shear-forces of an orifice nozzle and an extrusion membrane in the high-pressure set-up. However, due to the introduction of additional organic solvents to the formulation the drying behavior differed. The ratio water-organic solvent raised the drying capacity and the inert spray-drying process made this adjustment feasible. Formulations with different organic solvent concentrations were employed. The major aspects during this process were the product qualities, which were investigated with respect to yield, residual moisture, particle and liposome size distribution, as well as integrity of the lipids.

2. MATERIAL AND METHODS

2.1 LIPOSOME PREPARATION

The ethanol injection technique was used for preparing the liposomes. Briefly, a solution of 200 mM DOTAP-Cl (1,2-dioleoyl-3-trimethylammonium-propane-chloride) and 200 mM DOPC (1,2-dioleoyl-*sn*-glycero-3-phosphocholine) was injected under stirring into a 10.5 % [w/v] trehalose solution. The fluorescent probes Nile Red and Coumarin were directly dissolved within the lipid stock solution. 25 ml of the ethanolic lipid stock solution were injected into 975 ml of the aqueous phase to obtain a final lipid concentration of 10 mM in total, and a final concentration of 15.4 μ M Coumarin and 0.26 μ g/ml Nile Red. Afterwards, ethanol was step-wise added to the multi-lamellar liposome suspension to achieve final ethanol concentrations between 10 and 30 % [w/v]. Above 30 % [w/v] ethanol a clear solution was obtained. The homogenization of liposomes was carried out by an online extrusion through a 0.2 μ m polycarbonate membrane (Osmonics, Inc., MN, USA) and a 0.1 and 0.2 mm orifice nozzle 121 VG $\frac{1}{4}$ (Schlick Atomization Technologies, Untertsiemau, Germany).

In a second process approach the same concentrations of lipids were used and directly dissolved in 40 to 60 % [w/v] ethanol, methanol or acetone at 40 % [w/v]. Dissolving all components without any pre-formulation step like ethanol injection to prepare multi-lamellar vesicles would simplify the whole process. The lipids dissolved in organic solvent contents and water mixtures were added into the aqueous trehalose solutions to achieve a total lipid concentration of 10 mM. This approach inhibited the formation of liposomes and led to clear solutions after adding the lipid stock solution to the aqueous trehalose. The solutions were sprayed through the porous device with a 0.2 μ m polycarbonate membrane (Osmonics, Inc., MN, USA) and the 0.1 and 0.2 mm orifice nozzle 121 VG $\frac{1}{4}$ (Schlick Atomization Technologies, Untertsiemau, Germany) and subsequently dried.

2.2 INERT SPRAY-DRYING METHOD

The different formulations were spray-dried under inert conditions using nitrogen with a B-290 mini spray-dryer (Büchi, Switzerland) combined with a dehumidifier LT mini (MUCH, Germany) and an inert-loop system B-295 (Büchi, Switzerland). The high pressure pump ISCO E100x syringe plunger pump (Teledyne ISCO, Lincoln, NE, USA) was equipped with an orifice fluid nozzle, respectively a combination of orifice nozzle and porous device (compare chapter 6). The employed orifice nozzles of the model 121 VG $\frac{1}{4}$ (Schlick Atomization Technologies, Untertsiemau, Germany) had diameters of 0.1 and 0.2 mm. Two different experimental set-ups, which are shown in Figure 1, were evaluated.

Due to the absence of an atomizing gas in the orifice nozzle a relatively high liquid flow rate of 20 ml/min flow rate was necessary. Further studies with slower or even higher flow rates were not feasible, because of the minimum atomization power and the limited drying capacity of the equipment to obtain dry particles. In set-up A the liquid was pumped directly through the nozzle (Fig 1, pathway A). For set-up B an additional filtration unit, the already described porous device, was placed between the pump and the nozzle, leading to an online extrusion of the liposomes (Fig 1, pathway B). For this purpose polycarbonate filter membranes (Osmonics Inc., MN USA) with a pore size of 0.2 μm supported by two drain discs (Osmonics Inc., MN USA) were used. Liposome preparation was performed at a flow rate of 20 ml/min resulting in a pressure between 1 and 110 bar depending on nozzle size and solution viscosity.

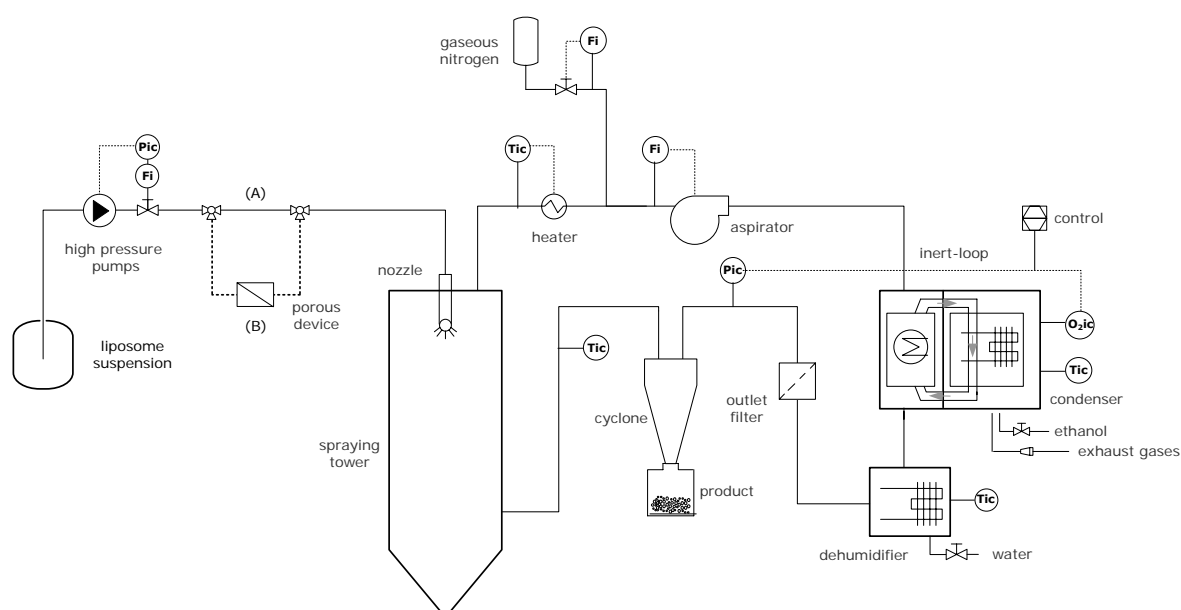


Figure 1: Schematic construction of a Büchi mini spray-dryer B-290 equipped with a dehumidifier LT Mini and an inert loop B-295 coupled with a nitrogen supply.

The inert spray-drying process consists of the atomization of the aqueous-organic feed over the nozzle into a spray, spray nitrogen contact, aqueous-organic evaporation out of the spray inside the drying chamber and the separation of the dried particles from the gaseous nitrogen. Within the hot dehumidified drying nitrogen gas produced by the dehumidifier and the gaseous in-take-heater, particles dry very rapidly for spray droplets smaller than 100 μm . Powder collection was conducted by the improved cyclone into the final product container. After separation of the dried product the nitrogen passes a filter unit through the dehumidifier into the inert-loop, where the organic phase is separated before the aspirator circulates the nitrogen back into the pressurized system at about 50 mbar. Thereby, the employed ethanol is recycled by the inert loop in the spray-drying

set-up. The following process conditions were used for the inert spray-drying process: drying nitrogen inlet temperature (T_{inlet}) between 80 and 200°C, drying nitrogen outlet temperature (T_{outlet}) in the range of 30 to 110°C, the drying air volumetric flow rate (v_{da}) was constant at 100 %, which is given as percentage of total aspirator rate.

All further methods used in this chapter are already described before.

3. RESULTS AND DISCUSSION

3.1 INERT SPRAY-DRYING OF MULTILAMELLAR SUSPENSIONS

3.1.1 Influence of ethanol concentration on powder yield

With the addition of ethanol to the formulation and the relatively dry nitrogen used as drying gas, it was again feasible to work with the lab scale equipment in combination with the orifice nozzle. Contrary to the observations made in chapter 7, no material loss was observed on the chamber wall of the lab scale equipment during the atomization of the ethanol containing suspensions, although the orifice nozzle resulted in a wider spray-angle at the liquid feed rate of 20 ml/min. As working range the 2nd wind-induced region was achieved for both nozzles (Fig 2, left). The product yield was mainly affected by the nozzle diameter and the resulting droplet size distribution. High Reynolds numbers at lower ethanol concentrations resulted in turbulent flows and agglomeration of the droplets. For the 0.2 mm nozzle the obtained droplets were even too large to be dried sufficiently. The high flow rate and the limited drying capacity of the spray-dryer resulted in high material loss (Fig 2, right).

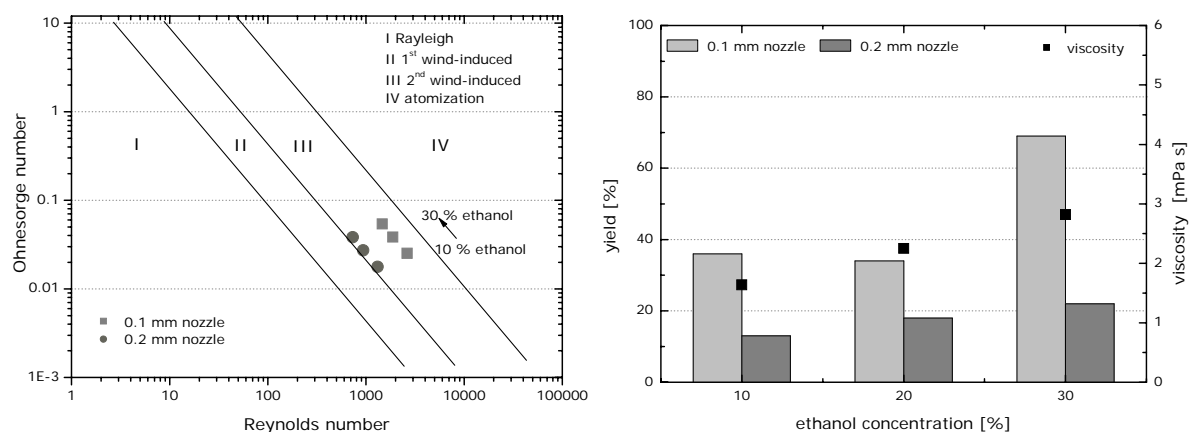


Figure 2: Calculated Ohnesorge numbers for formulations with 10 to 30 % [w/v] ethanol using the 0.1 and 0.2 mm nozzle equipped with 0.2 µm membrane (left) and product yield (right) after inert spray-drying of formulations with 10 mM lipid and 10.5% trehalose at T_{inlet} of 150°C and a 0.2 mm nozzle with a 0.2 µm membrane at T_{inlet} of 200°C.

The yield after inert spray-drying could be improved by increasing the ethanol concentrations in the formulation and the drying temperatures (Fig 3, left). Limited by the drying capacity of the spray-drier, a maximum yield of about 85 % was obtained for formulations with 30 % [w/v] ethanol dried at an inlet temperature of 200°C. Optimized droplet size distribution and evaporation favored the result. An almost linear relationship between inlet and outlet temperature could be observed. Changes can be explained by the relatively high liquid feed rate of 1.2 l/h, which exceeded the maximum drying capacity of 1.0 l/h of the used spray-dryer (Fig 3, right). Using ethanol concentration in the formulations it has to be considered that water has a much higher heat capacity than ethanol and the flow rates of drying air and liquid feed should be aligned [6].

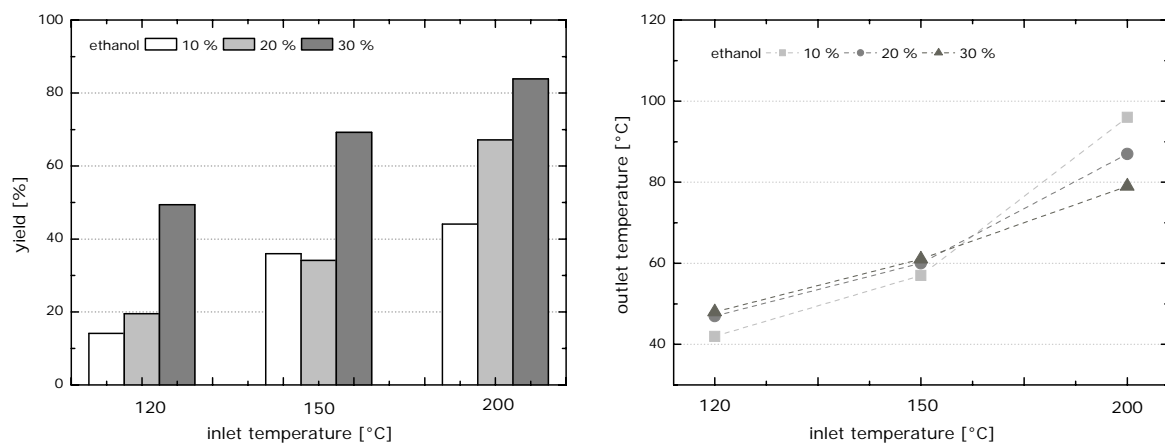


Figure 3: Yield after inert spray-drying of multi-lamellar liposome suspensions with 10 mM lipid and 10.5% trehalose with 10 to 30 % [w/v] ethanol using a 0.1 mm nozzle (left), the corresponding outlet temperatures (right) at liquid feed rate of 20 ml/min.

3.1.2 Influence of ethanol concentration on particle morphology and size

The particle morphology of the inert spray-dried powders for multi-lamellar liposomes (pathway B with porous device) and ethanol concentrations between 10 and 30 % [w/v] are shown in the scanning electron microscopy (SEM) pictures (Fig 4). For formulations with 10 and 20 % [w/v] ethanol agglomerated spherical particles were obtained. At higher ethanol concentrations the agglomeration tendency was reduced due to the faster drying process and the reduced turbulences of the droplets. However, a rupture of the particles occurred, which was evident by broken, hollow particles. The addition of ethanol resulted in a higher vapor pressure that led finally to a rupture of large particles.

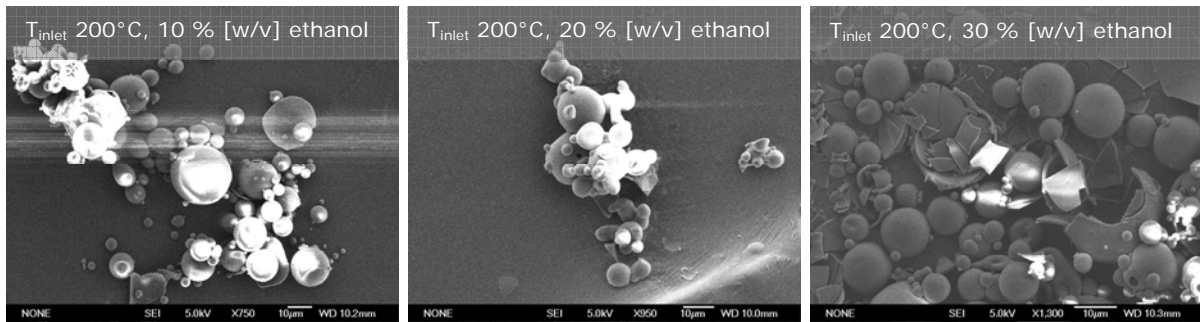


Figure 4: SEM micrographs of the dried particles for the formulations of 10.5 % trehalose, 10 mM lipid content with 10 to 30 % [w/v] ethanol using a 0.1 mm nozzle and a 0.2 μm membrane.

At increasing ethanol concentrations within the multi-lamellar suspensions using the process with the porous device (Fig 1, (pathway B)) the mean particle diameter was shifted to smaller sizes from 320 μm for 10 % [w/v] ethanol to 120 μm for 30 % [w/v] ethanol (Fig 5, left). Furthermore, the size distributions changed from bimodal to monomodal. This was also indicated by the span, which was reduced from 3.88 at 10 % [w/v] ethanol to 1.94 at 30 % [w/v] ethanol (Fig 5, right). As described before, the limited size of the drying tower further enhanced the turbulences and assisted the collision of wet particles especially at lower ethanol concentrations.

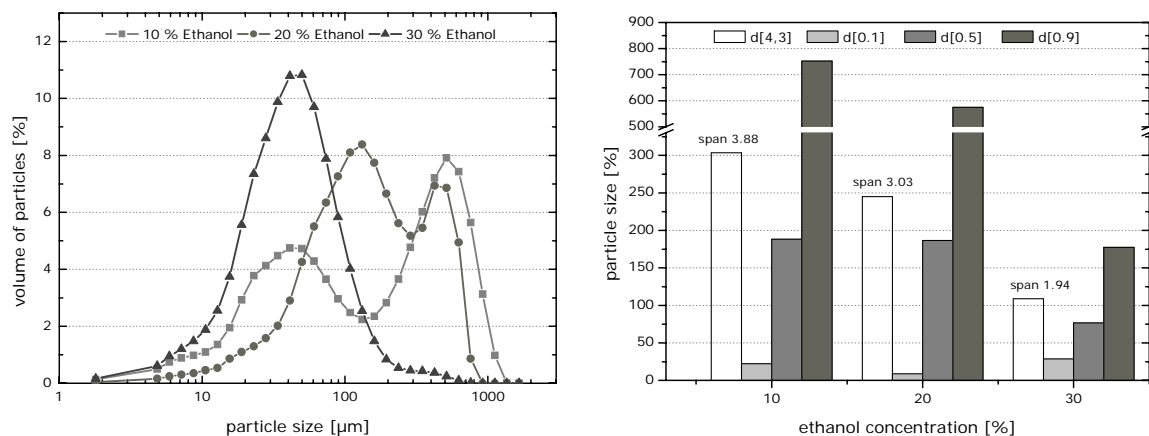


Figure 5: Particle size distribution with ethanol concentrations between 10 and 30 % [w/v] (left) and average particle size including span (right) after inert spray-drying of multi-lamellar-liposome suspensions with 10.5 % trehalose and 10 mM lipid with using a 0.1 mm nozzle and a 0.2 μm membrane with 10 to 30 % [w/v].

3.1.3 Effect of ethanol on residual moisture and residual solvent content

With increasing ethanol content the goal to reduce the drying outlet temperature was achieved. For 30 % [w/v] ethanol concentration the inlet air temperature could be reduced to 100°C, which resulted in an outlet temperature of 38°C (Fig 6, left).

Compared to the conventional spray-drying using a two-fluid nozzle the drying temperature can be reduced by at least 10°C (compare chapter 5). The residual moisture of the particles was also affected by increasing ethanol contents and drying temperature. Residual moisture varied for 10 % [w/v] ethanol between 6.5 % at a T_{inlet} of 130°C and 4.5 % at a T_{inlet} of 200°C (Fig 6, right).

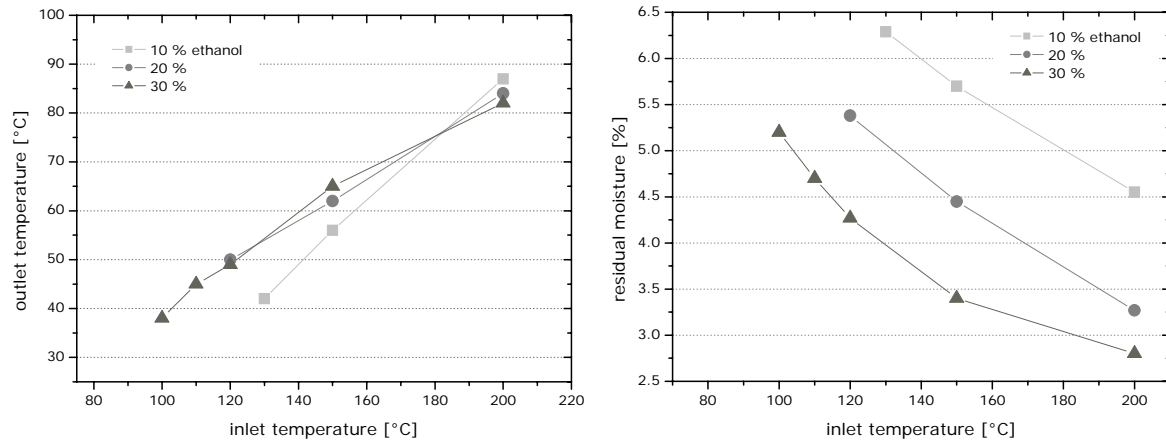


Figure 6: Outlet temperatures of multi-lamellar suspensions (left) and the residual moisture content (right) in relation to inlet temperature with 10, 20 and 30 % [w/v] ethanol in the formulation using a flow rate of 20 ml/min and a 0.1 mm nozzle.

With the addition of organic solvents to the formulation a reduction in drying temperature was achieved. Due to the relatively short drying process with high solvent concentrations the remaining residual solvent traces need to be quantified and considered with respect of their concentration limits [7,8]. After the conventional spray-drying processes (compare chapter 5 and 7) no residual ethanol content could be determined by static headspace chromatography for reconstituted powders. After inert spray-drying, the residual ethanol concentration depended on the initial ethanol content of the formulation and the drying temperature. Only about 700 ppm ethanol could be determined in the reconstituted dried product at 10 % [w/v] ethanol at a drying temperature of 120°C (Fig 7). A maximum residual ethanol content of 4500 ppm was observed for formulations with 30 % [w/v] ethanol dried at 120°C, which is similar to the concentration obtained after freeze-drying (compare chapter 2). At the highest drying temperature of 200°C the residual ethanol concentrations could be decreased below 1600 ppm for all used ethanol concentrations. An additional vacuum-drying step applied to the inert spray-dried powders (described in chapter 5) resulted in residual ethanol concentration below the detection limit for all formulations (data not shown).

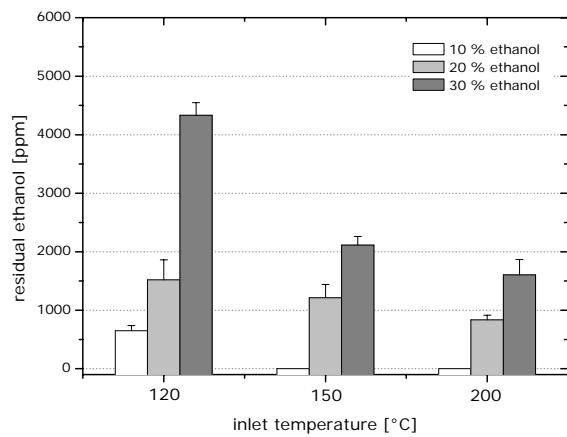


Figure 7: Residual ethanol concentration of multi-lamellar inert spray-dried liposomes with 10, 20 and 30 % [w/v] ethanol after reconstitution using a flow rate of 20 ml/min 0.1 mm nozzle.

3.1.4 Morphological characterization of the inert spray-dried products

DSC and X-ray powder diffraction were used to characterize the morphology of the inert spray-dried products. The morphology of the dried particles was analyzed, as it can affect the storage stability of the formulations regarding the liposomal integrity. The glass transition temperature, which is characteristic for amorphous systems, was determined by DSC. For the studied formulations, the glass transition temperature of inert spray-dried trehalose containing liposomal formulations increased when the drying temperature rose from 150 to 200°C (Fig 8, left).

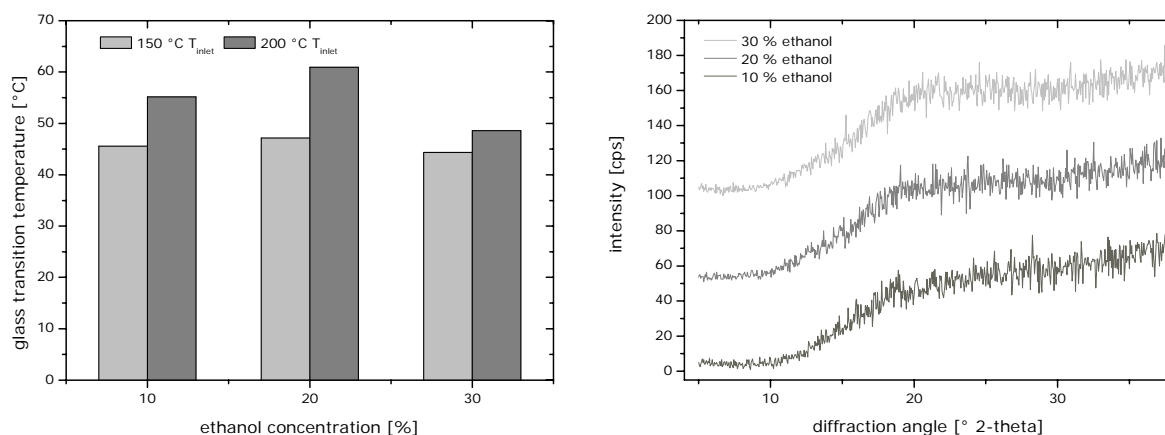


Figure 8: The glass transition temperature (left) and wide-angle X-ray diffraction pattern (right) after inert spray-drying of multi-lamellar liposome suspensions with 10.5 % trehalose and 10 mM lipid with 10 to 30 % [w/v] ethanol using a 0.1 mm nozzle and the porous device with a 0.2 μm membrane at a inlet temperature of 150°C and 200°C (DSC), respectively 200°C (XRD).

This effect was most pronounced for 20 % [w/v] ethanol where the T_g raised from 47.2°C at T_{inlet} 150°C to 61°C at T_{inlet} 200°C. The T_g of the formulations needs to be considered when selecting appropriate storage conditions for the formulations. Above T_g a higher molecular mobility would foster the fusion and leakage of the liposomes and an increased vesicle size in the rehydrated dispersion [9]. The amorphous state of the product was also assured by the X-ray powder diffraction pattern (Fig 8, right).

3.1.5 Liposome Properties

3.1.5.1 Effect of ethanol on liposome size using the orifice nozzle

In set-up (A) multi-lamellar suspensions were directly sprayed through the orifice nozzle. Size adjustment of liposomes by this set-up was successful as described in chapter 6. Ethanol concentration and nozzle size affected liposome size and polydispersity index after reconstitution of the inert spray-dried products. With the 0.1 mm nozzle liposomes of about 100 nm and a polydispersity index of 0.26 were obtained from a multi-lamellar liposome suspension with 10 and 20 % [w/v] ethanol (Fig 9, left). With 30 % [w/v] ethanol, the polydispersity index of the liposomes increased significantly to 0.35 with a larger standard deviation. For the 0.2 mm nozzle larger liposomes of 150 nm were formed while the polydispersity index remained at a constant level of 0.27 (Fig 9, right). For both nozzles, the liposome size and polydispersity were lower after the drying step as compared the data without the drying step.

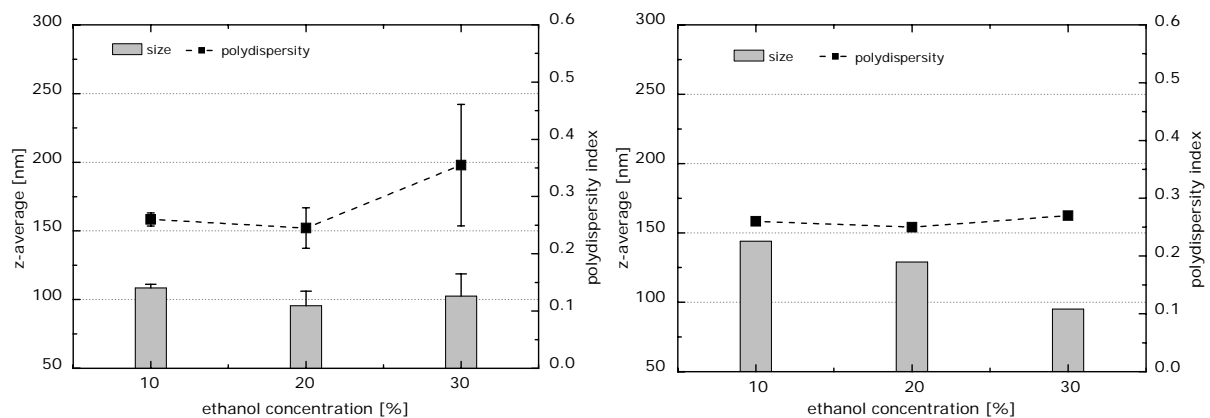


Figure 9: Liposome size and polydispersity index with increasing ethanol concentrations after inert spray-drying of multi-lamellar liposome suspension with 10 mM lipid and 10.5 % trehalose at 200°C (T_{inlet}) using a 0.1 mm (left) and 0.2 mm (right) nozzle.

3.1.5.2 Effect of ethanol on liposome size using the porous device / orifice nozzle

The ethanol concentration has a considerable effect on the droplet formation process. However, the main size adjustment of the liposomes takes place during the extrusion through the porous device (compare chapter 6). It can be assumed that the extraction of the solvents during the dehydration step influences the liposome size. High concentration of ethanol evaporated much faster, which resulted in larger polydispersity of 0.37 at 30 % [w/v] ethanol due to the partial rupture of the liposomes (Fig 10, left). Without the drying step very small and homogenous liposomes were obtained under these conditions. Only the 10 % [w/v] ethanol concentration revealed adequate liposomal properties (Fig 10, right). Although the data from chapter 6 suggested an improved polydispersity index for all formulations when using the porous device the drying step affected the liposomal properties. Too rapid drying and droplet size with higher ethanol concentrations reduced the liposomal quality after the drying process.

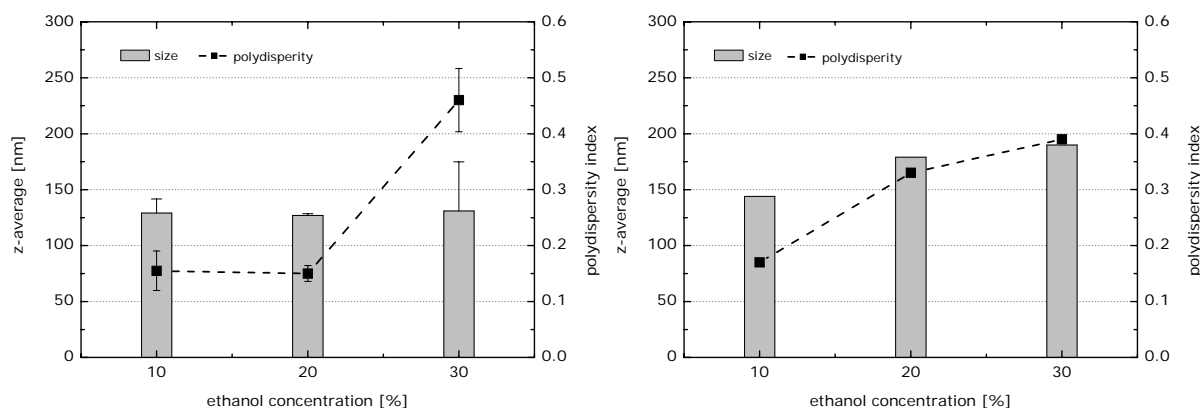


Figure 10: Liposome size and polydispersity index with increasing ethanol concentrations after inert spray-drying of multi-lamellar liposome suspension with 10 mM lipid and 10.5 % trehalose at 200°C (T_{inlet}) using a 0.1 mm (left) and 0.2 mm (right) nozzle both in combination with a 0.2 μ m membrane.

3.1.5.3 Effect of drying temperature on liposome size using the orifice nozzle

The liposome size and polydispersity were not only affected by the droplet size and ethanol concentration, but also by the drying temperature (T_{inlet}). Smaller liposomes (Fig 11, left) with improved polydispersity indices (Fig 11, right) were obtained using the 0.1 mm nozzle at higher inlet temperatures above 120°C for all evaluated ethanol concentrations. An optimum was found with 20 % [w/v] ethanol for inlet temperatures between 120 and 200°C.

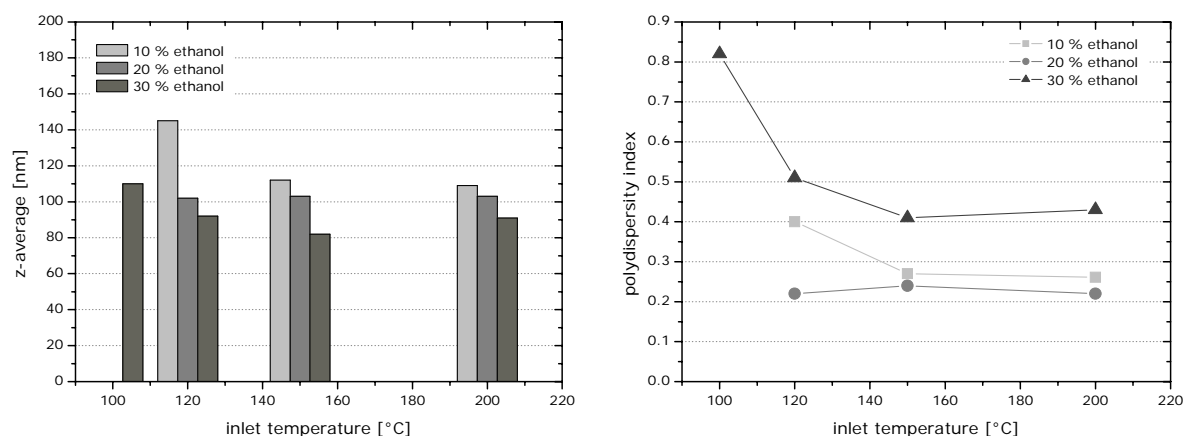


Figure 11: Liposome size (left) and polydispersity index (right) with increasing T_{inlet} and ethanol concentrations of 10, 20 and 30 % [w/v] after inert spray-drying using a 0.1 mm nozzle.

3.1.6 Lipid recovery after inert spray-drying

The lipid composition of the particles after the inert spray-drying process was analyzed by RP-HPLC. The major aspects affecting the lipid recovery are the heat exposure and a possible phase separation of the lipids within the particles at high ethanol contents. In all experiments no degradation products were determined after inert spray-drying between 10 and 30 % [w/v] ethanol up to an inlet temperature of 200°C. The homogeneity of the lipids was preserved for all conditions without any decomposition. Lipid recovery varied between 65 and 105 % depending ethanol concentration and drying conditions, when using the orifice nozzle (Tab 1). Compared to the combination of porous device and nozzle the lipids recovery varied between 120 and 148 %. Such an effect was observed neither with the two-fluid nozzle in chapter 5 nor the orifice nozzle in chapter 7.

Table 1: Lipid recovery after inert spray-drying at inlet temperatures of 120°C, 150°C and 200°C using a 0.1 mm nozzle at 10, 20 and 30 % [w/v] ethanol.

T_{inlet} [°C]	10 % ethanol [w/v]			20 % ethanol [w/v]			30 % ethanol [w/v]		
	DOTAP- CL [%]	DOPC [%]	T_{outlet} [°C]	DOTAP- CL [%]	DOPC [%]	T_{outlet} [°C]	DOTAP- CL [%]	DOPC [%]	T_{outlet} [°C]
120	-	-	-	95.2	94.7	47	96.8	95.7	48
150	65.4	66.8	57	97.1	97.3	60	99.9	98.9	61
200	86.9	87.2	87	99.9	99.2	87	104.1	102.4	79
200*	120.9	119.4	77	125.5	123.7	74	142.5	140.4	72

* data obtained using the porous device and the nozzle.

Varied ethanol concentrations within the formulation and the resulting higher Reynolds numbers induced the shear forces. The droplet formation and break-up probably resulted in a phase separation of the lipids and the solvents within a single droplet due to the mixture of ethanol and water. It is known that higher viscosity delays the onset of the droplet formation [10]. And with the different surface tension and density of ethanol and water these droplet formation process could be responsible for the reduced lipid content. Very fine droplets containing more water or ethanol with varied or even no lipid could occur. On the other hand, the porous device used in the system increased the lipid recovery. This can be explained by the homogeneity of the lipid distribution within the liquid feed. Higher residual ethanol content and lower residual moisture content with increasing the ethanol fraction indicated such a phenomenon.

The lipid recovery in the dry particles depended on the ethanol concentration and the drying behavior of the formulation. Droplet formation and distribution of the lipids were mainly affected by the nozzle bore diameter and the droplet break-up. Optimum conditions with 10 mM lipids and 10.5 % [w/v] trehalose were found at 20 % [w/v] ethanol.

3.1.7 Drug loading studies

3.1.7.1 Using Nile Red as model compound

The model compound Nile Red was dissolved together with the lipids and subsequently ethanol injection into aqueous trehalose solution was performed to produce liposomes. After ethanol injection the emission maximum Nile Red was located at 640 nm (excitation with 550 nm) for 30 % [w/v] ethanol and was slightly blue shifted to 636 nm for 10 and 20 % [w/v] ethanol with a slight increase in intensity at the same time (Fig 12, (A)). The blue shift indicated that Nile Red is present in a slightly more hydrophobic environment at lower ethanol concentrations. For a comprehensive interpretation of these findings control experiments were performed, to clarify the impact of ethanol and liposomes on the fluorescence properties of Nile Red. In a control experiment Nile Red was added to liposomes after the ethanol injection (Fig. 12, (B)). A comparable blue shift of the emission depending on the ethanol concentration occurred. Furthermore, the fluorescence intensity was significantly higher for the lower ethanol concentrations of 10 and 20% [w/v]. When measuring Nile Red in the presence of 10, 20 and 30% [w/v] ethanol the emission maximum was not affected, while the intensity was slightly higher for the less polar solutions with 30% [w/v] ethanol (Fig. 12, (C)).

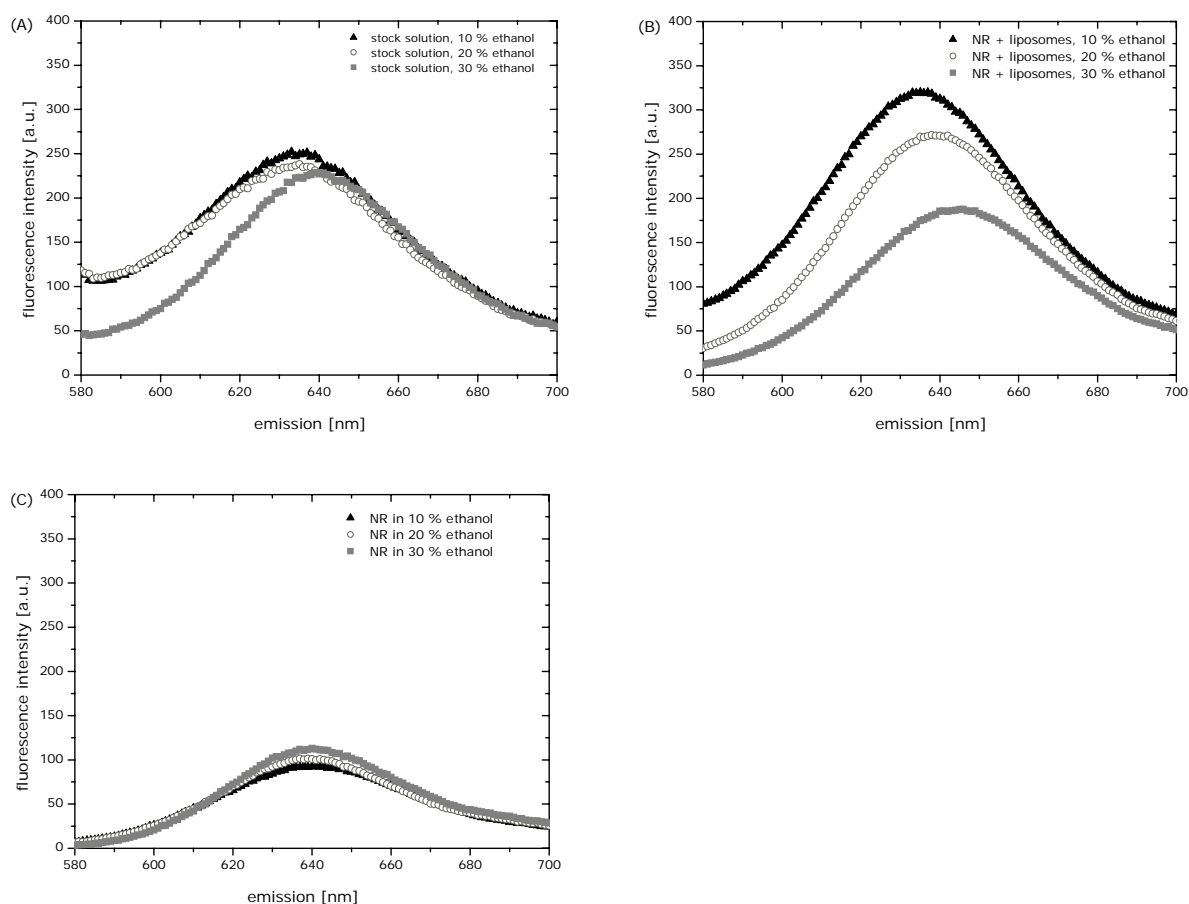


Figure 12: Fluorescence intensity when Nile Red was added to the lipid stock solution and subjected to ethanol injection (A), Nile Red added to preformed liposomes in 10, 20 and 30 % [w/v] ethanol (B) and of Nile Red in 10, 20 and 30 % [w/v] ethanol (C).

The data indicated that Nile Red is incorporated into the liposomes in a similar way for all ethanol concentrations when the compound was already present during the ethanol injection process. The tremendous increase in Nile Red fluorescence at lower ethanol concentrations when the probe was added to liposomes after the ethanol injection is indicative for changed interactions with the hydrophobic lipids. It can be assumed that the interactions between Nile Red and the lipids are more favored at lower ethanol concentrations, due to the low solubility of Nile Red in the aqueous phase.

After rehydration of the inert spray-dried particles, the fluorescence intensity of Nile Red increased for all studied conditions (Fig 13). The increased Nile Red fluorescence intensity of the reconstituted inert spray-dried products can be indicative for a stronger interacting of Nile Red with the hydrophobic liposomes. It was evident that the Nile Red fluorescence intensity after inert spray-drying depended on the ethanol content of the stock solutions, with a more pronounced intensity increase for 30 % [w/v] ethanol (Fig 13, (C)). This is in

agreement with the results from DLS, which revealed that the liposome size and PI were most affected at 30 % [w/v] ethanol. The second parameter influencing Nile Red fluorescence was the drying temperature. For 10 % and 20 % [w/v] ethanol the intensity increase of the Nile Red fluorescence was more pronounced at 200°C compared to 150°C (Fig 13, (A and B)). For 30 % [w/v] ethanol on the other hand the intensity was slightly higher after the drying process with 150°C as compared to 200°C.

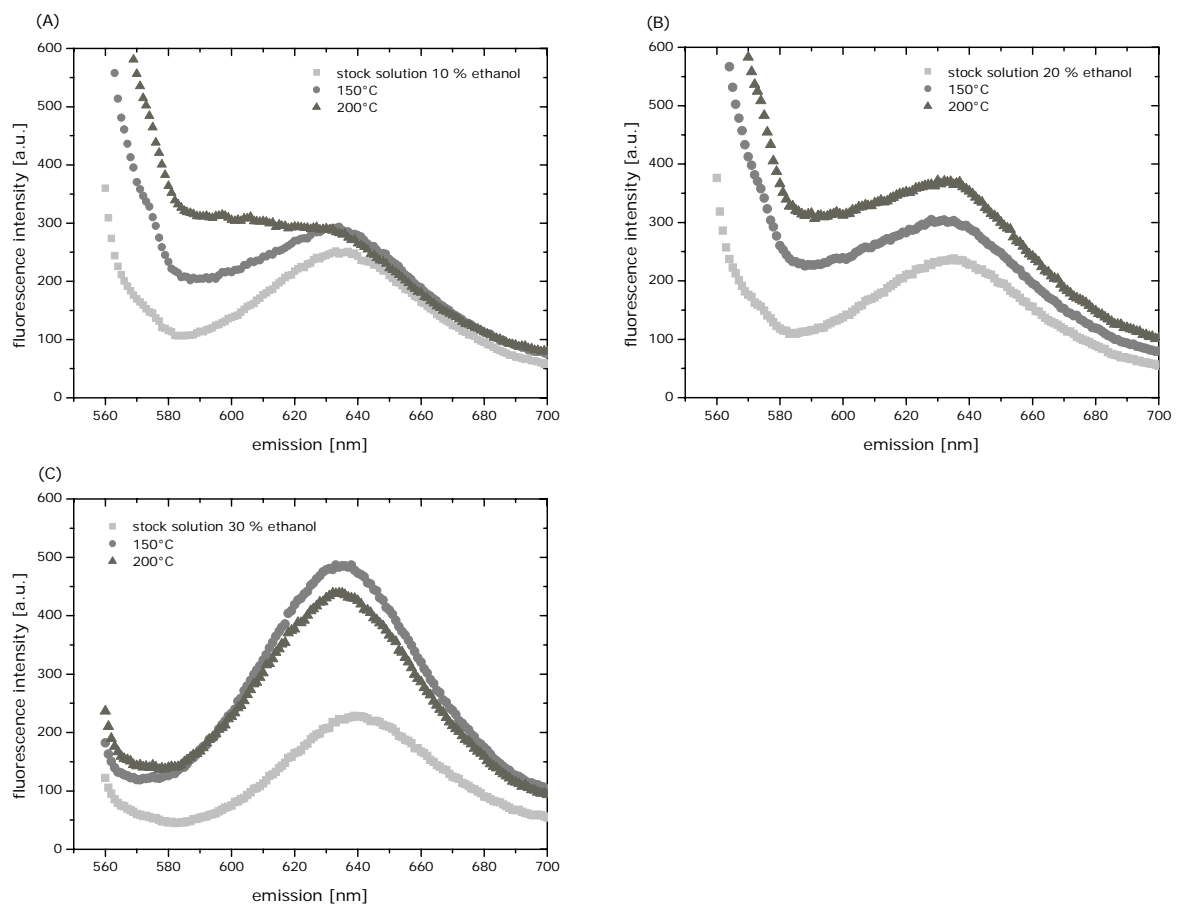


Figure 13: Fluorescence intensity of Nile Red loaded liposomes for T_{inlet} of 150 and 200°C for ethanol contents of 10 % (A), 20 % (B) and 30 % [w/v] (C).

It can be concluded that Nile Red is present in a more hydrophobic environment after drying when the initial solutions contained higher ethanol content, which could be related to the greater change in liposome size and polydispersity index of these formulations. More precisely the more hydrophobic environment could be equal to a stronger binding of Nile Red to the liposomes.

3.1.7.2 Drug loading using Coumarin

The liposomes were furthermore loaded with Coumarin. The Coumarin content after inert spray-drying was slightly reduced for 10 and 20 % [w/v] ethanol (Fig 14) at T_{inlet} 200°C. At T_{inlet} 150°C the concentration was not affected for all ethanol concentrations. With a higher ethanol content of 30 % [w/v] a stronger influence of drying temperature was determined resulting in raised Coumarin content. For the used lipids no leakage induced by inert spray-drying and rehydration occurred.

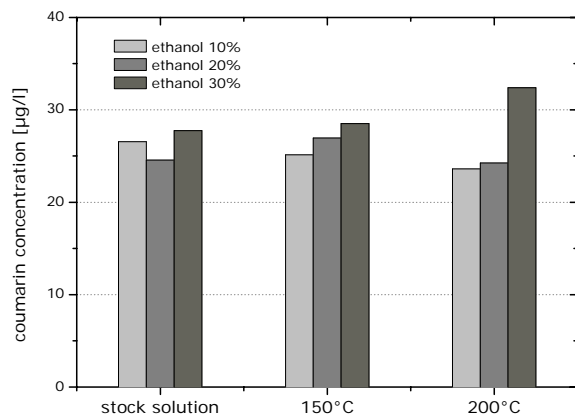


Figure 14: Coumarin concentration in relation to drying temperature T_{inlet} of 150 and 200°C and ethanol content between 10 and 30 % [w/v].

3.2 INERT SPRAY-DRYING OF CLEAR LIPID-TREHALOSE SOLUTIONS

3.2.1 Influence of initial ethanol concentration on powder yield

With higher Ohnesorge numbers the internal viscous dissipation is more dominant and most of the inserted energy is converted, which makes droplet formation difficult (Fig 15, left). In general, an increased amount of ethanol in the formulation prior to spray-drying and with it a higher Ohnesorge number increased the yield after inert spray-drying (Fig 15, right). Furthermore, the liquid feed break-up at the orifice nozzle significantly influenced the droplet size and with it the drying performance. With a 0.1 mm nozzle the yield ranged between 70 and 85 %. Lower yields of maximum 35 % at 4.5 mPas were reached with the larger 0.2 mm nozzle even at the higher inlet temperature of 200°C. Compared to the product yield obtained at ethanol contents between 10 and 30 % [w/v] the yield was doubled because of the changed droplet formation and the faster drying at higher ethanol contents.

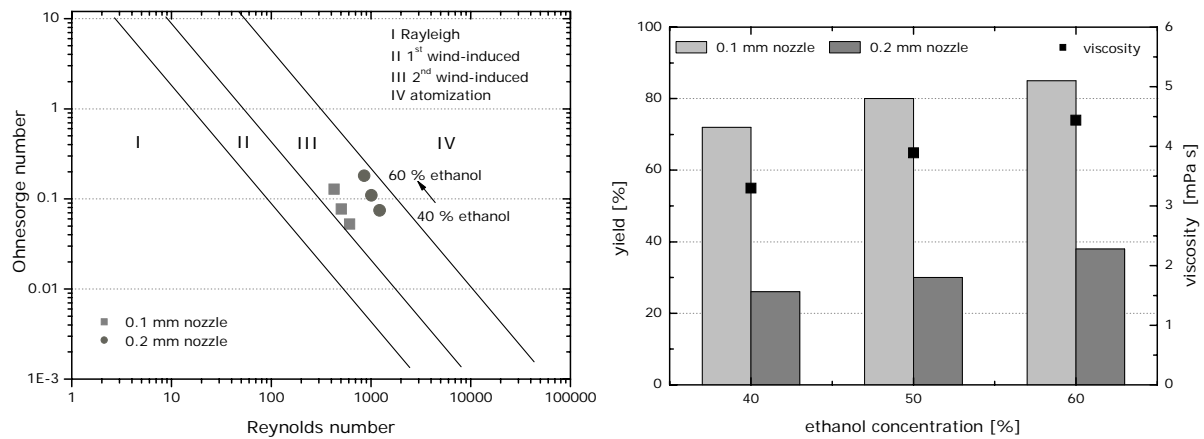


Figure 15: Calculated Ohnesorge numbers for 0.1 and 0.2 mm nozzle and increasing ethanol concentrations between 40 and 60 % (left) and product yield (right) after inert spray-drying of formulations with 10 mM lipid and 10.5% trehalose using a 0.1 mm nozzle 0.2 μ m membrane at T_{inlet} of 150°C and a 0.2 mm nozzle with a 0.2 μ m membrane at T_{inlet} of 200°C.

3.2.2 Influence of ethanol concentration on particle morphology and size

The particle rupture was more pronounced at higher ethanol concentrations between 40 and 60 % [w/v] ethanol (Fig 16) when spraying the clear solutions of lipids and trehalose containing as compared to solutions with 10 to 30 % [w/v] ethanol. Due to this effect the bulk density was significantly lowered for particles dried from higher ethanol concentrations [11]. The results indicated that an increased ethanol concentration in the formulation led to a decrease in particle diameter by optimized droplets formation and drying behavior [12,13]. However, formulation characteristics such as surface tension and the saturated vapor pressure of the inert spray-drying solutions influenced the size of the droplets generated by the orifice nozzle, and hence affected the size and the morphology of the produced particles [14]. High vapor pressure occurred during the drying process resulting in a rupture of particles.

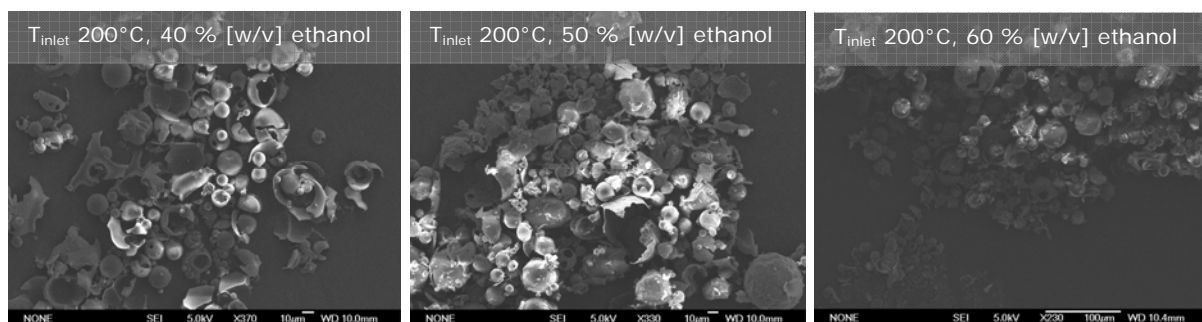


Figure 16: SEM micrographs of the dried particles for the formulations of 10.5 % trehalose, 10 mM lipid content with 40 to 60 % [w/v] ethanol using a 0.1 mm nozzle and a 0.2 μ m membrane.

Spraying of the clear solution of lipids and trehalose with ethanol concentrations between 40 and 60 % [w/v] led to more homogenous size distributions compared to lower ethanol concentration (Fig 17, left). Droplet formation due to the reduced Reynolds numbers were optimized and the evaporation resulted in smaller particles between 20 and 110 μm , which decreased slightly with raising ethanol content (Fig 17, right).

It can be concluded that the particle formation was mainly influenced by the ethanol concentration of the initial formulation. With the addition of ethanol the Ohnesorge number increased and the Reynolds number decreased, which affected the droplet formation process. The droplets consistence finally impacted the drying behavior in respect of a reduced heat capacity with raised ethanol contents.

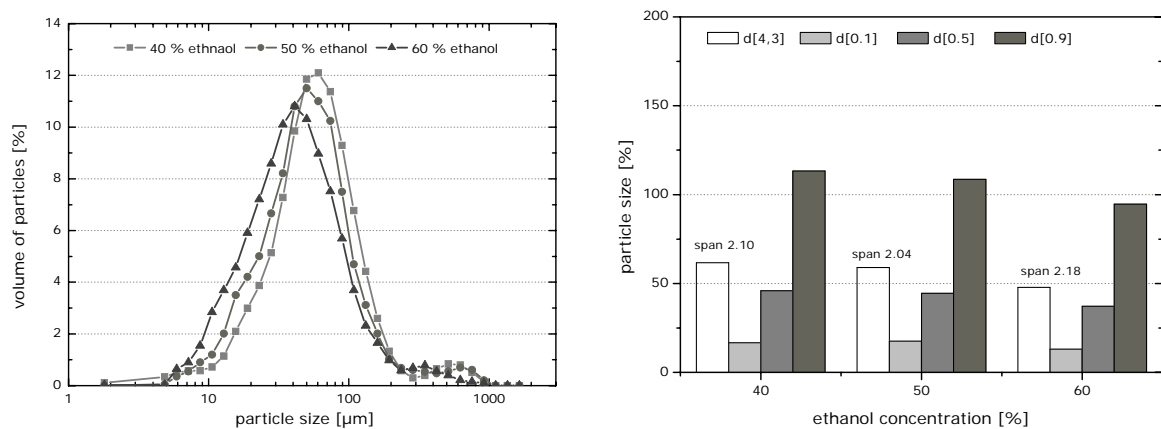


Figure 17: Particle size distribution with ethanol concentrations between and 40 to 60 % [w/v] (left) and average particle size including span (right) after inert spray-drying of multi-lamellar liposome suspensions with 10.5 % trehalose and 10 mM lipid with using a 0.1 mm nozzle and a 0.2 μm membrane.

3.2.3 Particle formation model

Based on the data a simple mechanism to illustrate the evaporation of solvents out of the droplets and finally the particle formation during the inert spray-drying of water-ethanol containing formulations was developed (Fig 18). The driving force during drying is the difference in vapor pressure between the drying gas and the droplet surface, which furthermore is affected by the varied vapor pressure of the organic solvent and water [15,16]. This driving force is responsible for the three different particle types, which were determined: spherical and smooth particles (< 30 % [w/v] ethanol), small spherical and disintegrated particles (< 50 % [w/v] ethanol) and fully disintegrated particle fragments (> 50 % [w/v] ethanol). At higher water-ethanol ratios, e.g. in the range between 30 and 50 % [w/v] ethanol, the evaporation rate was accelerated compared to the diffusion rate resulting in a hollow core. When the pressure inside the droplet reached a certain limit a

disintegration of the particle occurred. This effect was even more pronounced when using ethanol concentrations above 50 % [w/v]. Only disintegrated particles and fragments of particles were observed. The evaporation and drying rates were so high that the vapor pressure increased dramatically, resulting in cracked particles with a hollow interior. This evaporation of the solvents happens early at the top of the drying chamber [17], with a maximum droplet temperature (wet-bulb temperature) of approximately 30 to 70°C at the process conditions used here.

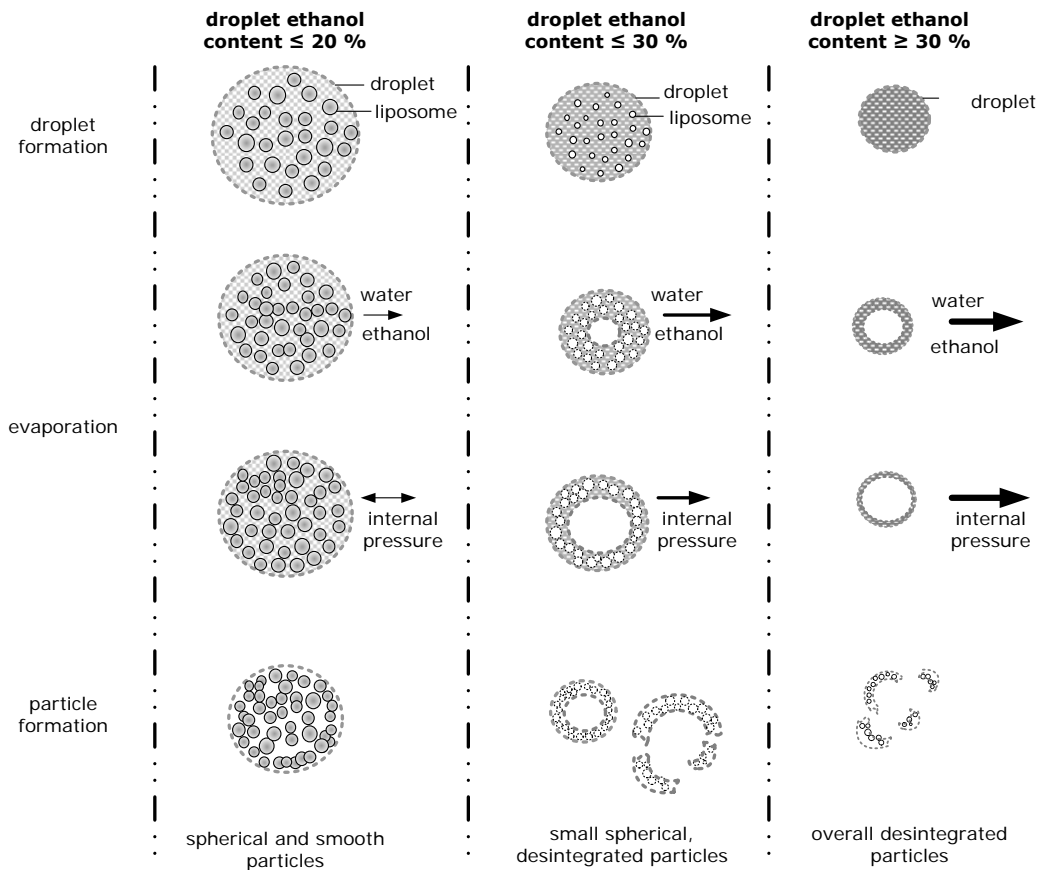


Figure 18: Schematic model of the inert spray-drying process of droplets containing vesicles or which are clear solutions with different water-ethanol ratios.

3.2.4 Effect of ethanol on residual moisture and residual solvent content

With increasing ethanol content the drying outlet temperature was reduced down to 38°C at 30 % [w/v] ethanol for multi-lamellar suspensions. For clear solutions the outlet temperature was further reduced down to 30°C at 50 and 60 % [w/v] ethanol (Fig 19, left). Compared to the conventional spray-drying process the temperature could be reduced by about 20°C for concentrations above 40 % [w/v] ethanol. For the clear

solution lower residual moisture levels between 4 % at T_{inlet} of 80°C and 3 % at T_{inlet} of 200°C (Fig 19, right) were determined.

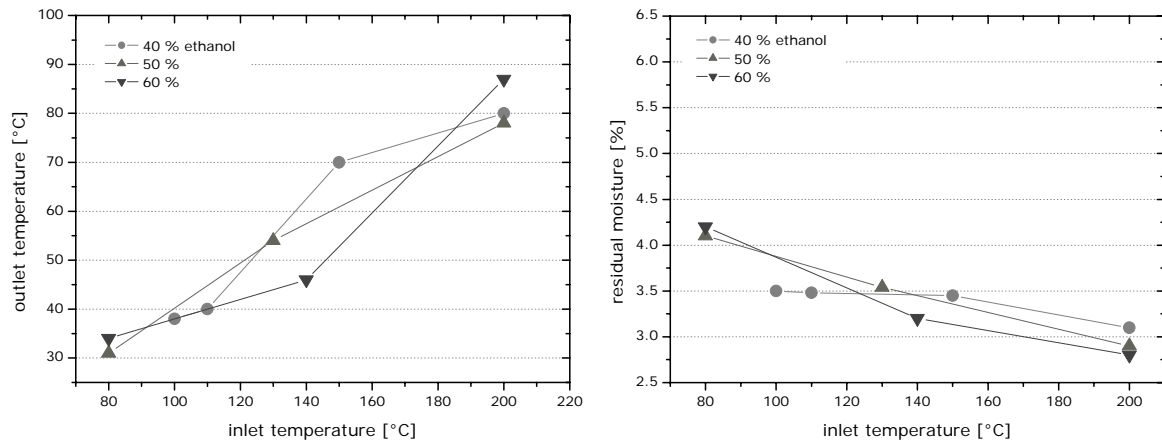


Figure 19: Outlet temperatures of multi-lamellar suspensions (left) and the residual moisture content (right) in relation to inlet temperature and ethanol content using a flow rate of 20 ml/min, a 0.1 mm nozzle with 40, 50 and 60 % [w/v] ethanol in the formulation.

When spray-drying the clear solutions with higher ethanol concentrations the residual solvent depended once more on the inlet temperature (Fig 20). High residual ethanol concentrations of about 5500 ppm were observed at 50 to 60 % [w/v] ethanol at an inlet temperature of 80°C. For the ethanol content of 40 % [w/v] the residual solvent content remained below 1200 ppm. The relation between trehalose and residual ethanol content was already discussed in chapter 2, where a linear trend was found in freeze-dried placebo formulations for different trehalose-ethanol concentrations. By increasing the inlet temperature to 200°C the residual ethanol content could be significantly decreased.

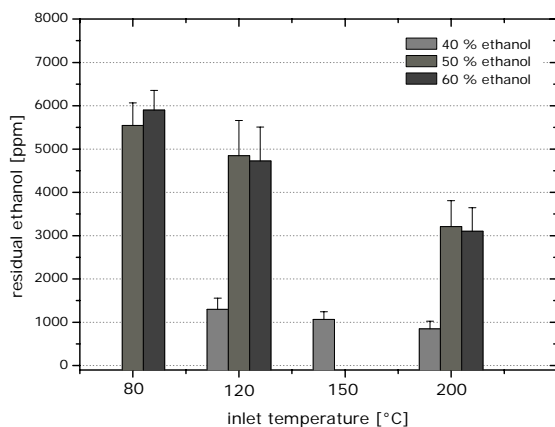


Figure 20: Residual ethanol concentration of multi-lamellar inert spray-dried clear solutions inert spray-dried with 40, 50 and 60 % [w/v] ethanol after reconstitution in respect of inlet temperature using a flow rate of 20 ml/min 0.1 mm nozzle.

3.2.5 Effect of drying temperature on liposome size using the orifice nozzle

Inert spray-drying of clear solutions using a 0.1 mm nozzle resulted in liposomes size between 100 nm at 40 % and 170 nm at 60 % [w/v] ethanol (Fig 21, left). Although the size of the liposomes varied and the polydispersity was not improved below values of 0.2, such a method offers some advantages as it can simplify the process and should therefore be further investigated (Fig 21, right). Ideally, the liposomes are formed in the water fraction when the organic-aqueous phase is removed or during rehydration. This would lead to a spontaneous formation of vesicles in the water phase.

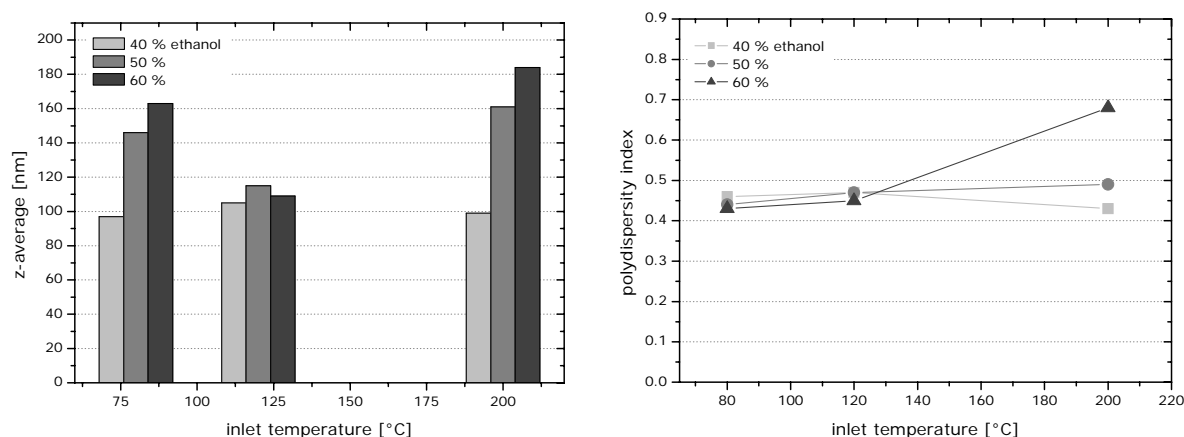


Figure 21: Liposome size (left) and polydispersity index (right) using clear solutions between 40 and 60 % [w/v] ethanol after inert spray-drying using a 0.1 mm nozzle at different T_{inlet} .

3.3 INERT SPRAY-DRYING USING OTHER CO-SOLVENTS

The influence of other co-solvents was tested on the liposome properties. Results like product yield, particle morphology and size distribution were comparable to the formulations with 40 % [w/v] ethanol content. Therefore, only the effect of residual moisture, residual methanol and acetone concentration were described, as well as the most important parameter the liposome properties.

3.3.1 Effect of solvents on residual moisture and residual solvent content

Methanol and acetone as new co-solvents were added in a concentration of 40 % [w/v] compared to ethanol. The residual solvent content of methanol and acetone decreased to lower levels, as compared to residual ethanol concentrations (Fig 22, left). Both, methanol and acetone have lower boiling points of 65 and 56.2°C compared to ethanol

with 78.5°C. With the higher vapor pressure the evaporation of the solvents during the drying process was enhanced. Especially acetone with a vapor pressure of 160 mmHg (at 20°C) compare to methanol with 87.9 mmHg and ethanol with 41.0 mmHg showed this effect most pronounced and reached the lowest level residual solvent content [18]. The residual moisture for acetone was 2.1 % and methanol about 2.9 % after inert spray-drying. Due to their higher vapor pressure and lower boiling point the drying rate could be improved. This resulted in lower residual moisture contents compared to ethanol as a co-solvent with 3.2 % at the same conditions (Fig 22, right).

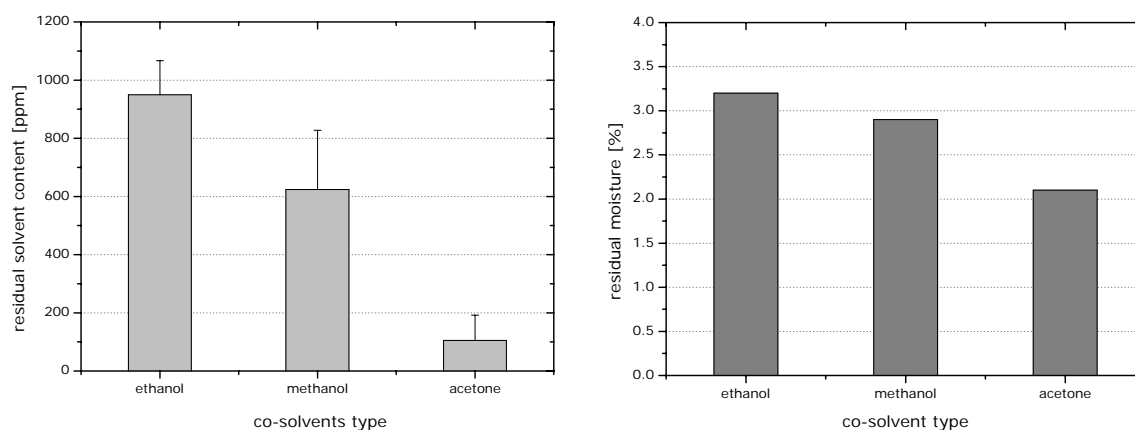


Figure 22: Residual solvent content for different co-solvents (left) and the residual moisture content (right) using a 10 mM lipid content after inert spray-drying of liposomal formulations at 200°C with a porous device equipped with a 0.2 μm membrane and a 0.1 mm nozzle.

3.3.2 Effect of other solvents on the liposome size

As already shown before (compare 3.2.5), ethanol resulted in a high polydispersity index of the liposomes as well as methanol. Only acetone preserved the liposomes size and polydispersity (Fig 23). With acetone as co-solvent liposome size remained at 125 nm and more important the polydispersity index reached a remarkable value of 0.13. A very low drying temperature of 45°C could be achieved when using acetone. The reduced solubility of the lipids in acetone with the low vapor pressure may be the reason for this positive result [19]. Further studies are necessary to clarify the effect of acetone on the preservation of liposomes at such high co-solvent concentrations.

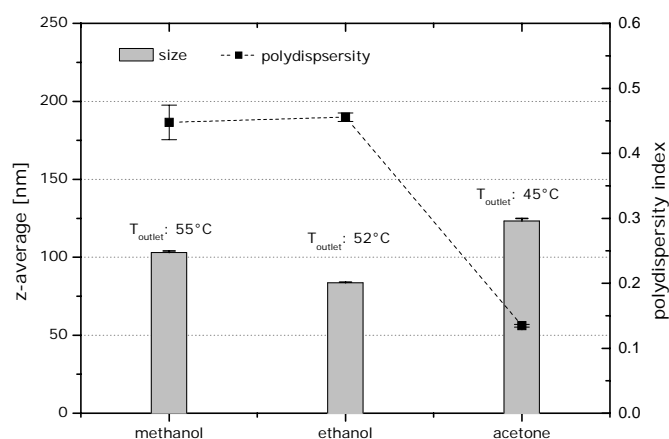


Figure 23: Liposome size and polydispersity index with 40 % [w/v] organic solvent after inert spray-drying at 120°C (T_{inlet}) using a 0.1 mm nozzle both in combination with a 0.2 μ m membrane.

4. CONCLUSIONS

An approach to reduce the heat exposure during spray-drying is the addition of organic solvents to the aqueous formulation. With the addition of such organic solvents the heat capacity and the gaseous inlet temperature can be significantly reduced. However, to prevent explosive conditions the use of inert spray-drying equipment is necessary. The presented inert spray-drying approach combined liposome formation with a porous device and an orifice nozzle as well as inert spray-drying in a single step. Organic solvents like ethanol, methanol and acetone were employed in concentrations up to 60 % [w/v].

Inert spray-drying of multilamellar liposome suspensions with ethanol concentrations up to 30 % [w/v] was feasible. Depending on ethanol content and drying temperature a product yield of up to 80 % was reached. With the addition of ethanol the outlet temperature was reduced below 40°C at a gas inlet temperature of 100°C. Comparable to the yield, the residual moisture depended on the ethanol concentration and the drying temperature, as well. With increasing inlet gas temperature the residual moisture can be reduced below 3 %. Liposomes with an optimized size of 100 nm and a polydispersity below 0.15 were obtained for ethanol concentrations up to 20 % [w/v] using the porous device in combination with the small orifice bore diameter of 0.1 mm. With higher ethanol concentrations and larger nozzle bore diameters liposome size and polydispersity were elevated. Lipid recovery and drug loading studies revealed a significant influence of the ethanol concentration on these parameters. While the lipid recovery increased with

higher ethanol contents, e.g. to 100 at 30 % [w/v], the liposomal quality decreased. The drying behavior and the droplet formations with a possible phase separation should be considered and further investigated. For a successful liposome formation and drying process optimized conditions were found, which made this technique an alternative to the conventional spray-drying approach.

At higher ethanol concentrations above 30 % [w/v] the multilamellar structure of the liposomes is destroyed resulting in a clear solution of lipids, trehalose and solvents. A study with process conditions comparable to the multilamellar liposome approach revealed higher yields and lower drying temperatures down to 30°C. The particle size was reduced to 50 µm with a homogeneous distribution compared to several 100 µm for multi lamellar solutions. Residual moisture decreased due to the reduction of water in the formulation and the lower heat capacity necessary to dry these formulations. However, homogeneous distributions could not be achieved. The resulting liposome size were between 100 and 170 nm with a polydispersity above 0.45. Only the use of 40 % [w/v] acetone resulted in small liposomes of 125 nm with excellent polydispersity of 0.13. A further reduction of the drying temperature during inert spray-drying was achieved for all studied conditions. Too high ethanol contents negatively affected the quality of the liposomal formulations, as the liposome structure was not fully formed or preserved.

Overall, the main goal of preparing liposomes and thereby reducing the drying temperature was achieved. Due to the addition of ethanol, the drying temperature could be reduced to 40°C. Drug loading studies with model compounds were done, but experiments with Paclitaxel loaded formulations are still required. Furthermore, droplet formation and break-up processes have a considerable effect on the lipid recovery. To clarify this, further studies are necessary to predict phase separation and fluctuation of lipids in the droplets.

5. REFERENCES

-
- [1] Johnston, K.A., Preparation of peptide and protein powders for inhalation, *Adv. Drug Del. Rev.*, 26(1): 3-15 (1997).
- [2] Gilani, K., Najafabadi, A.R., Barghi, M., Rafiee-Tehrani, M., The effect of water to ethanol feed ratio on physical properties and aerosolization behavior of spray dried cromolyn sodium particles, *J. Pharm. Sci.*, 94(5): 1048-1059 (2005).
- [3] Guiziou, B., Armstrong, D.J., Elliot, P.N.C., Ford, J.L., Rostron, C., Investigation of in vitro release characteristics of NSAID-loaded polylactic microspheres, *J. Microenc.*, 13(6): 701-708 (1996).
- [4] Rafler, G., Jobmann, M., Controlled release systems of biodegradable polymers, 2nd communication: Microparticle preparation by spray drying, *Drugs made in Germany*, 37(4): 115-199 (1994).
- [5] Master, K., *Spray drying handbook*, 5th ed., John Wiley & sons, New York, (1991).
- [6] Cao, X.Q., Vassen ,R., Schwartz, S., Jungen, W., Tietz, F., Stöver, D., Spray drying of ceramics for plasma spray coating, *J. Eur. Ceramic Soc.*, 20(14): 2433-2439 (2000).
- [7] International conference of harmonization (ICH) of technical requirements for registration of pharmaceuticals for human use, Q3C (R3): Impurities: Guideline for residual solvents (2005).
- [8] Camarasu, C.C., Residual solvents determination in drug products by static headspace-gas chromatography, *Chromatographia*, 56(1): 137-147 (2002).
- [9] Van Winden, E.C.A., Crommelin, D.J.A., Long term stability of freeze-dried, lyoprotected doxorubicin liposomes, *Eur. J. Pharm. Biopharm.*, 43(3): 295-307 (1997).
- [10] Thomas, G.O., The aerodynamic breakup of ligaments, *Atom. Sprays*, 13(1): 117-129 (2003).
- [11] Barron, M.K., Young, T.J., Johnston, K.P., Williams, R.O., Investigation of processing parameters of spray freezing into liquid to prepare polyethylene glycol polymeric particles for drug delivery, *AAPS PharmSciTech.*, 4(2):12 (2003).
- [12] Bain, D.F., Munday, D.L., Smith, A., Solvent influence on spray-dried biodegradable microspheres, *J. Microencapsul.*, 16(4): 453-474 (1999).
- [13] Wang, F.J., Wang, C.H., Etanidazole-loaded microspheres fabricated by spray-drying different poly (lactide/glycolide) polymers: effects on microsphere properties, *J. Biomater. Sci., Polym. Ed.*, 14(2): 157-183 (2003).
- [14] Rabbani, N.R., Seville, P.C., The influence of formulation components on the aerolisation properties of spray-dried powder, *J. Contr. Rel.*, 110(1): 130-140 (2005).
- [15] Maa, Y-F., Nguyen, P-H., Andya, J.D., Dasovich, N., Sweeney, T.D., Shire, S.J., Hsu, C.C., Effect of spray drying and subsequent processing conditions on residual moisture content and physical/biochemical stability of protein inhalation powder, *Pharm. Res.*, 15(5): 768-775 (1998).
- [16] Schiffter, H.A., Single droplet drying of proteins and protein formulations via acoustic levitation, *Dissertation* (2005).
- [17] Maa, Y-F., Constantino, H.R., Nguyen, P-A., Hsu, C.C., The Effect of Operating and Formulation Variables on the Morphology of Spray-Dried Protein Particles, *Pharm. Dev. Technol.*, 2(3): 213-223 (1997).
- [18] Teagarden, D.L., Baker, D.S., Practical aspects of lyophilization using non-aqueous co-solvent systems, *Eur. J. Pharm. Sci.*, 15(2): 115-133 (2002).
- [19] Bitz, C., Doelker, E., Influence of the preparation method on residual solvents in biodegradable microspheres, *Int. J. Pharm.*, 131(2): 171-181 (1996).

CHAPTER 9

Liposome Drying using Subcritical- and Supercritical Fluids

Abstract:

There are numerous advantages of subcritical- and supercritical fluids. The selective solvating power of supercritical fluids (SCF) makes it possible to separate a particular component from a multi-component mixture at a relatively low temperature range. Secondly, the favorable mass transfer properties and the solubility of solvents in supercritical fluids make the drying of liposomes rapid and efficient in a one-step process, using non-toxic and environmentally friendly supercritical carbon dioxide (CO₂). The particle formation and drying studies with different nozzles and process conditions were necessary to understand the thermodynamic behavior and evaluate a working area. With and without the addition of co-solvents the mutual solubility of the compounds was studied on the liposome properties. Subcritical conditions were chosen to fully avoid lipid solubility in carbon dioxide. The droplet size distribution and the mass transfer are the key parameters in the perseveration of the liposomal structure. Using acetone as a co-solvent the solubility of water was enhanced without the extraction of lipids. While using the other solvents a significant solubility of lipids was determined. Without any co-solvent and at subcritical conditions no irritation was observed, the liposome structure stay intact.

1. INTRODUCTION

Supercritical fluid (SCF) technology has been commercially used for the past 30 years as an environmentally benign, energy- and cost-saving tool in various industries. It is applied for dry cleaning, metal cleaning, as well as for preparing foods and fragrances. Also for several pharmaceutical operations in industrial scale supercritical fluids are employed, e.g. for crystallization, particle size reduction, solvent extraction, coating and product sterilization [1]. SCF technology is furthermore a feasible option to stabilize particulate drug delivery systems, such as microparticles, nanoparticles, liposomes and inclusion complexes [2]. Supercritical fluids have many attractive properties such as providing mild conditions for pharmaceutical processing, which is advantageous for labile drugs. Besides this, the use of organic solvent can be minimized and the production of particles with controllable morphology, narrow size distribution, and low static charge can be achieved [3]. A substance whose temperature and pressure are above the critical temperature (T_c) and the critical pressure (P_c) is referred to as a supercritical fluid [4]. Above this critical point the liquid and vapor phase of the substance is indistinguishable (Fig 1).

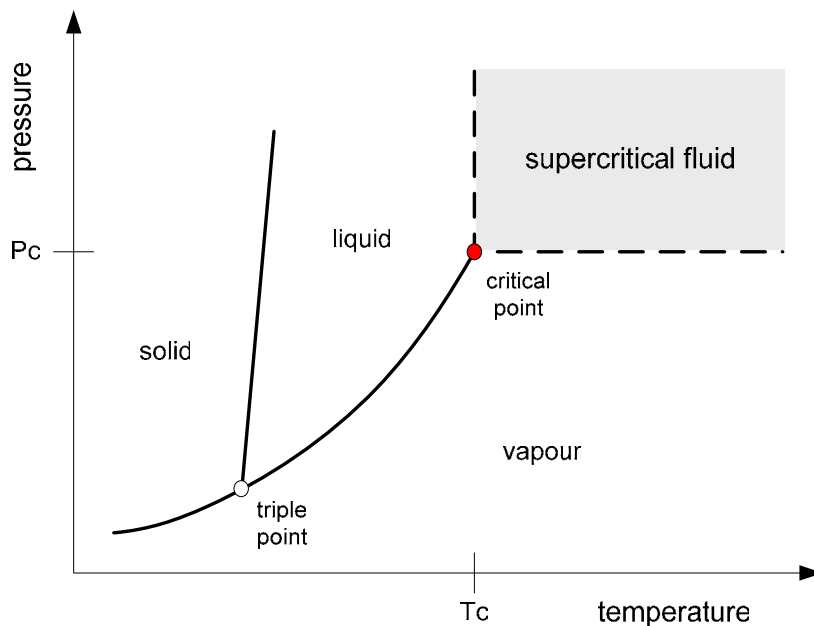


Figure 1: Pressure-temperature phase diagram of a pure substance, with different region and the supercritical fluid region.

Supercritical fluids have unique thermophysical properties [5], which are between those of the pure liquid and the pure gas. The properties of supercritical fluids, such as polarity, viscosity and diffusivity can be altered several-fold by varying the operating temperature

and/or pressure during the process. Supercritical fluids offer liquid-like densities, gas-like viscosities, gas-like compressibility properties and ten times higher diffusivities than liquids, which gives them good mixing properties. For particle formation, however, the combination of liquid-like density and the large compressibility is of interest.

Carbon dioxide (CO₂) is the most commonly used supercritical fluid in pharmaceutical processing due to its unique properties, such as an oxygen-free environment and working conditions at relatively low temperature and pressure. Furthermore, it is non-toxic, non-flammable, relatively inexpensive, recyclable and removable from the system. It has a critical temperature (T_c) of 31.1 °C and a critical pressure (P_c) of 73.8 bar. Other solvents used in supercritical fluid technology are for example ethylene, nitrous oxide, propylene, ethanol and water (Tab 1).

Table 1: Critical temperature T_c in [°C], pressure P_c in [bar] and density at critical condition D_c in [g/ml] of commonly used supercritical fluids [6,7].

solvent	T_c [°C]	P_c [bar]	D_c [g/ml]
ethylene (C ₂ H ₄)	9.0	49.7	0.220
carbon dioxide (CO ₂)	31.3	73.8	0.468
nitrous oxide (N ₂ O)	36.0	71.5	0.450
propylene (C ₃ H ₇)	91.8	46.0	0.232
ethanol (C ₂ H ₅ OH)	240.8	61.4	0.276
water (H ₂ O)	374.1	221.2	0.315

Around the critical point, density and hence solvating power of supercritical fluids can be varied widely when applying small temperature and/or pressure changes to the system. This enables the operator to use supercritical fluids as solvents or anti-solvents during particle formation [1].

Rapid expansion of supercritical solutions (RESS) and gas anti-solvent precipitation (GAS) are the two basic processes employed for the precipitation of particles (Fig 2). During RESS, the solute is first solubilized in the supercritical fluid and the mixture is then expanded across a capillary at supersonic velocities, leading to a super-saturation of the solution and a subsequent precipitation. Co-solvents, such as methanol or acetone, can be mixed with supercritical fluids to increase the solvating power of supercritical fluids during RESS. The use of RESS as a comminution alternative to for the production of ultra-fine pharmaceutical powders is very promising. The chief limitation of RESS is the very low solvent power of the commonly used supercritical solvents for potentially useful solutes, such as proteins. The GAS method overcomes this limitation by using the supercritical fluid as an anti-solvent. For GAS precipitation one or more solutes, which are immiscible with the supercritical fluid, are dissolved in a conventional pharmaceutical

solvent, which is miscible with the supercritical fluid. Within supercritical fluids, the solution is subsequently expanded, which results in the decrease of the liquids cohesive energy causing the solute to precipitate [8,9]. The solute must be insoluble in the supercritical fluid, which will then immediately be an anti-solvent. The solvent on the other hand has to be at least partially miscible with the supercritical fluid. The GAS method is typically use in a way that a supercritical fluid is introduced into a volume of solution in a pressure chamber or by spraying solution through a nozzle into a supercritical fluid-filled chamber. This technique has many acronyms, with further variation in the process: such as aerosol extraction system (ASES), precipitation with compressed anti-solvent technique (PCA), solution enhanced dispersion by supercritical fluids (SEDS) and supercritical anti-solvent method (SAS) [10,11].

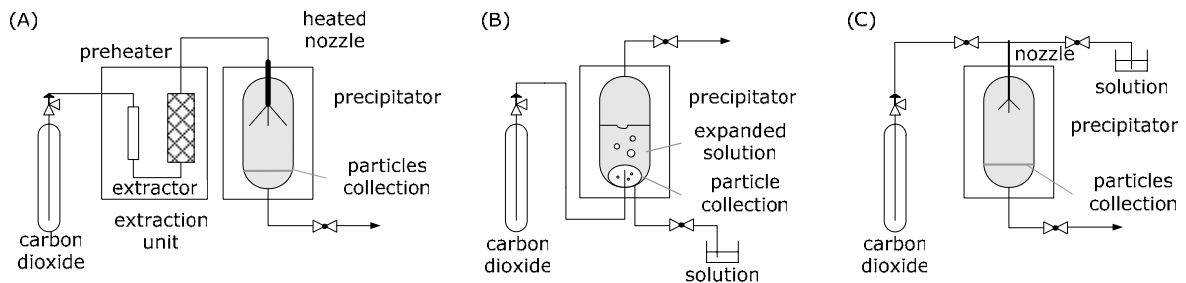


Figure 2: Schematics of the rapid expansion of supercritical solution (RESS) (A), the gas anti-solvent precipitation (GAS) (B) and the supercritical anti-solvent (SAS) process (C).

The supercritical anti-solvent method (SAS) utilized the low solvent power of supercritical fluids with moderate critical temperatures e.g., CO_2 for polymers, proteins and many biological molecules for drying [12]. The solutes of interest are dissolved either in a suitable organic or aqueous phase (Fig 2, (C)). This technique has been applied for the drying of polymeric systems [13,14]. It offers diverse advantages with respect to particle morphology, size range and reduction of heat induced stress.

1.1 THERMODYNAMIC BEHAVIOR OF SUPERCRITICAL FLUIDS (SCF)

Explanations for the infinite compressibility and other unique properties are given in a schematic diagram showing the variation of density with pressure (Fig 3). Small changes in pressure and temperature around the critical point have a deep impact on the thermodynamic behavior of the system. This diagram includes the coexistence of vapor and liquid phase, the critical point (CP) and the supercritical region. The critical isotherm ($T_R = T/T_C = 1$; used by correlation of carbon dioxide viscosity [15]) has a vertical slope at the critical point, which means that the rate of density change with respect to pressure is

infinite. In contrast, the parts of the isotherms corresponding to liquid states have almost horizontal slopes, because liquids have a very small compressibility. In the vicinity of the supercritical point fluids are almost freely compressible: the fluid density changes drastically with the pressure. Above the critical temperature the density of the vapor increases more gradually with pressure. Therefore, supercritical fluids are typically hundreds of times denser than gases at ambient conditions, but they are much more compressible than liquids. So the physical properties are intermediate between that of liquids and that of a gas.

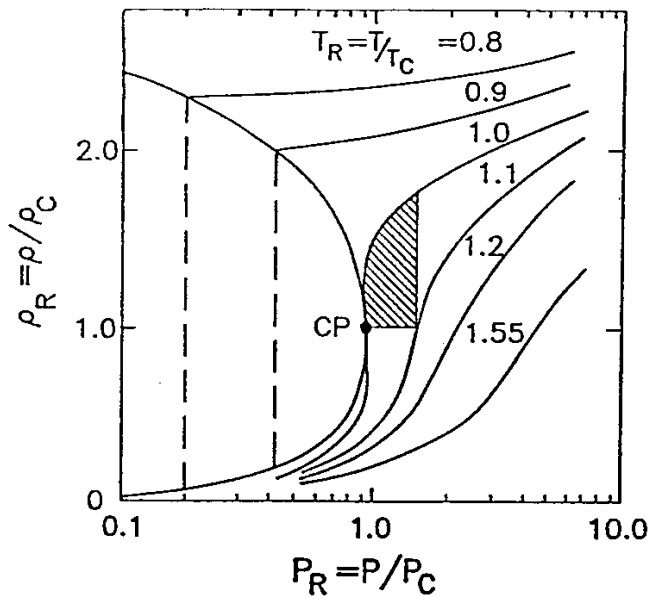


Figure 3: Schematic density-pressure phase diagram of a pure fluid in the relative vicinity of the critical point (adopted from McHugh et al. [16]). T_R = reduced temperature, T = temperature and T_C = critical temperature; ρ_R = reduced density, ρ = density and ρ_C = critical density; P_R = reduced pressure, P = pressure and P_C = critical pressure.

Based on this, the physical properties of supercritical fluids such as high density, low viscosity and high diffusivity can be adjusted to obtain optimal product characteristics by changing pressure and temperature. For particle formation, the combination of liquid-like density and large compressibility is relevant. Large density means that supercritical fluids have a solvent power that is comparable with the one of the same substance in the liquid state [17]. High compressibility implies that this solvent power is continuously adjustable between gas- and liquid-like extremes, with small changes in pressure.

1.2 TERNARY SYSTEM CARBON DIOXIDE / ETHANOL / WATER

The solubility of water in supercritical carbon dioxide is low. It is expressed as weight fraction very similar to that of water in typical natural oil [18]. Two methods can be used for drying of aqueous systems under supercritical conditions: the evaporation and the anti-solvent technique, which was described before. With the addition of co-solvents like ethanol, methanol, isopropanol or acetone to the supercritical carbon dioxide the polarity of the extraction medium is increased and the solubility of water in carbon dioxide becomes higher [19,20]. Thereby, they increase the solubility of compounds to be extracted in the supercritical carbon dioxide / organic mixture. Thus, they are used as co-solvents for extractions [21]. When using the anti-solvent process, the addition of co-solvents results in improved extraction forces for water out of the obtained particles. For particle formation processes the mass transfer and the saturation levels of the compounds are important. The solubility of the compounds in supercritical fluid affect the extent of saturation and thereby the particle properties [22].

By the introduction of an organic solvent to the supercritical phase the number and the size of co-existing phases above the critical point can be changed. At a pressure above the critical point of a binary mixture of organic solvent and supercritical CO₂ one phase exists. However, it is still possible that additional phases occur in the region of the critical point for CO₂-ethanol which is described by Durling et al. (2007) [23]. The phase equilibrium data for the CO₂-C₂H₅OH-H₂O system at 40°C and at 100 and 200 bar are shown in Figure 4. As the pressure increases at a constant temperature, the size of the single phase region in the ternary diagram is increased.

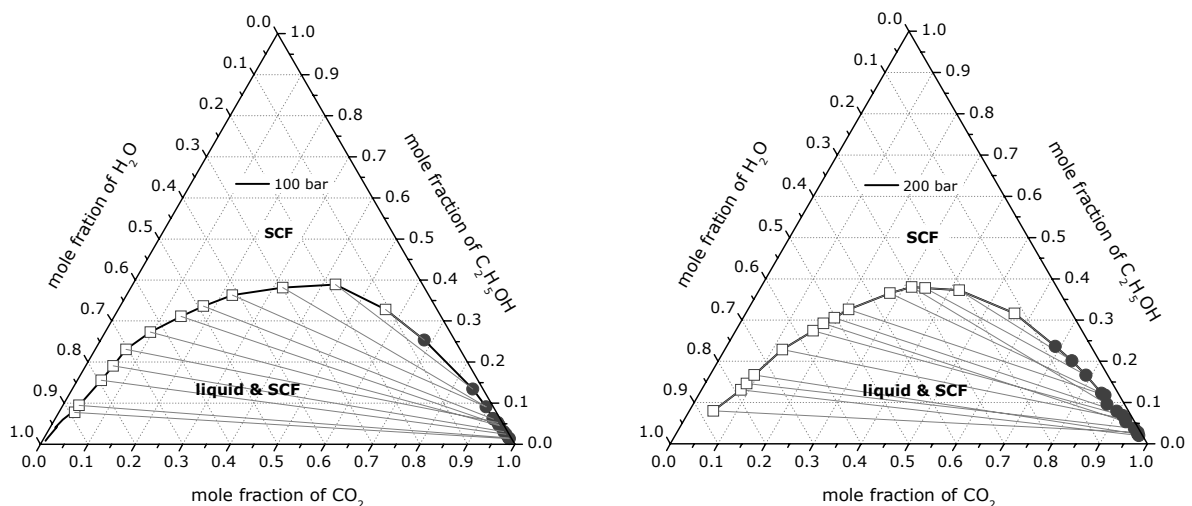


Figure 4: Ternary diagram for the CO₂, C₂H₅OH and H₂O system at 40°C at 100 bar (left) and 200 bar (right) using the light squares as SCF and the dark circles as liquid molar fraction [23,24].

The main advantage of CO₂ in particle formation by precipitation is that the solubility of solids in the supercritical phase is very low compared to that of the solids in commonly used solvents. Thus, CO₂ can function as an anti-solvent and the solid can precipitate out of the supercritical solution. At the end of the process, the pressure is reduced to atmospheric pressure and carbon dioxide becomes a gas and evaporates easily from the dry particles. Density values enable appreciable solvating power, optimized mass transfer properties and high compressibility and solvating power [25]. To optimize the precipitation process and to obtain a product with specific properties, it is necessary to study the behavior in the ternary system and the type of phase separation that occurs. A system composed of water-ethanol-carbon dioxide is not fully miscible resulting in several phases (Fig 4). Consequently, the experiments can be performed either in the one-fluid region (SFC) or in the two-fluid phase, where liquid and SFC are coexisting. The solvent power towards a particular compound can be changed significantly by the addition of a small amount of volatile co-solvent, e.g. methanol, ethanol, isopropanol and acetone, which can facilitate the extraction of water into the supercritical fluid [26,27]. Particle formation and drying are then governed by two fundamental processes, at first due to the evaporation of the organic solvent and partially the diffusion of carbon dioxide into the aqueous droplet and secondly because of the evaporation of the water into the anti-solvent phase. During the evaporation the droplets start swelling due to the condensation of the organic solvent into the droplet. This is followed by a decrease in droplet radius after saturation of the droplet with the organic solvent and carbon dioxide by the extraction of the fluids [28,29].

The drying time is reduced by the addition of ethanol and the mass transfer follows with water evaporating out of the droplets and solvent and carbon dioxide diffusing into the droplet [30]. The initial solvent concentrations, the atomization and other process parameters like pressure and types of solvents can influence the particle formation process. With the expansion of the organic solvent, the solubility of the precipitate decreases causing a better nucleation of the solute [31]. Residues of the organic solvent can be partially removed from the precipitate by flushing with the pure supercritical fluid. This is possible, because of the low surface tension of supercritical fluids, which can penetrate even in the smallest pores of the prepared particles. The formation of liposomes using supercritical fluids was already described but an aqueous based drying process was not yet tested [32,33].

The aim of this work was to identify optimum set-ups and working conditions for the drying of aqueous liposomal formulations. Therefore, numerous process development experiments were necessary to gain knowledge of such a new drying approach. Technical

requirements like atomization with varied nozzles and mass transport by carbon dioxide flow rates were tested to obtain dry powders. The limited solubility of water in supercritical carbon dioxide and the complicated phase behavior were the major concerns. The mass transfer should be selected in a way that the co-solvents evaporate first into the droplets and that carbon dioxide can diffuse into the droplets before the extraction forces induces an inverse flux and destroy the liposomes. The properties of carbon dioxide changed after the addition of co-solvents and therefore, an adapted working set-up and conditions had to be found.

1.3 PARTICLE FORMATION AND DRYING PROCESS UNDER SUBCRITICAL CONDITIONS

Using a carbon dioxide at subcritical conditions for drying of aqueous formulations is a rather new approach and was investigated especially in the field of silica aerogel formation and drying [34,35]. Only few data on solubility of carbon dioxide in water and its phase behavior are available below the supercritical point [36]. The following model approach derived from literature and from the basics of the drying experiments should help to understand the drying capability of subcritical carbon dioxide (Fig 5). The high solubility of water in CO₂ at low pressure decreased above 20 bar. The discontinuity in water solubility at subcritical conditions coincides with the phase change from a gaseous to a liquid CO₂-rich phase. The pressure interval in which three phases are coexisting (H₂O-rich liquid, CO₂-rich gas and CO₂-rich liquid) is very small. Above this saturation pressure or more precisely, above this three-phase coexisting line the water solubility in the CO₂-rich phase increases with slight changes in pressure.

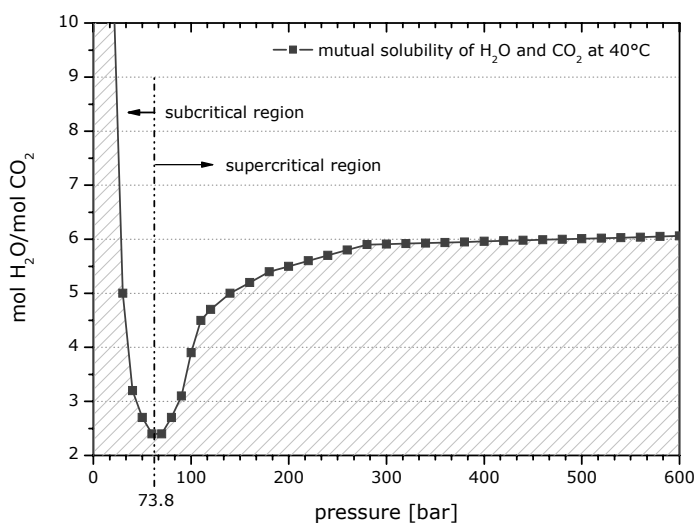


Figure 5: Mutual solubility of water and carbon dioxide at 40°C and pressures up to 600 bar based on lit. [39].

1.4 EXPERIMENTAL OUTLINE

We studied the use of sub- or supercritical fluids for the preparation of dry and free flowable powders containing liposomes in a one step process. Comparable to spray-drying (compare chapter 5) the unique feature of such a method lies in the ability to combine both particle formation and drying in one continuous process. However, the main advantage of such a technique is the very fast production and drying of liposomes at gentle temperature conditions of about 40°C. Compared to other drying techniques where the driving force are heat exposure or vacuum applied for a longer time, which lacks efficacy the mass transfer is important force [37].

Parameters like set-up configuration, nozzle type, pressure, solvent type and concentration as well as trehalose concentrations were varied. The liposome formation using the porous device described in chapter 6 was used for some experiments. Another drying approach was tested using subcritical drying conditions, which could be described as drying at ambient pressure with CO₂ as drying gas [38]. The main difference between subcritical and supercritical drying is the phase behavior of carbon dioxide. The solvent anti-solvent mixture is situated within the two-phase region with an interface between the droplet and the anti-solvent phase passing the two-phase region. The droplet diameter increases due to condensation of carbon dioxide followed by the evaporation of water once the saturation is reached, which results in dry particles [29]. The evaporation strength and solubility are changed by pressure reduction below the critical point. However, recently published phase diagrams indicate a miscibility of water within the fluidized carbon dioxide [39]. The major advantage compared to the supercritical phases could be assigned to the significantly low solubility of compounds within the subcritical phase [40].

2. MATERIAL AND METHODS

2.1 MATERIAL

The lipids DOTAP-Cl (1,2-dioleoyl-3-trimethylammonium-propane-chloride), DOPC (1,2-dioleoyl-*sn*-glycero-3-phosphocholine) from Avanti Polar Lipids (Alabaster, AL, USA) were used. Trehalose dihydrate from Ferro Pfanstiehl (IL, USA) was used as the stabilizing agent. 99 % ethanol (Merck, Darmstadt, Germany) was used for dissolving the lipids. Water for injection was used for dissolving trehalose. The 99.9 % solvents acetone, methanol, ethanol and isopropanol (Sigma-Aldrich, Zwijndrecht, The Netherlands) were

used as co-solvents within the carbon dioxide. The carbon dioxide (grade 3.5) was purchased from Hoek Loos (Schiedam, The Netherlands).

2.2 METHODS

2.2.1 Liposome preparation

Three different approaches for liposome preparation were evaluated. First the supercritical drying of preformed liposomes, secondly the preparation and drying of liposomes out of multi-lamellar suspensions and finally the preparation of liposomes using a solvent-lipid-trehalose mixture in the anti-solvent approach.

The ethanol injection technique was used for preparing multi-lamellar liposomes. A solution of 5 mM DOTAP-Cl (1,2-dioleoyl-3-trimethylammonium-propane-chloride) and 5 mM DOPC (1,2-dioleoyl-*sn*-glycero-3-phosphocholine) was injected under stirring into a 10.5 % [w/v] trehalose solution. To achieve preformed liposomes the ethanol injection was followed by five extrusion cycles through a 0.2 μm polycarbonate membrane and a sterile filtration. The fluorescent probes Coumarin and Nile Red were used as model drugs. They were dissolved within the lipid stock solution at a concentration of 31 μM .

Multi-lamellar vesicles (MLV) with a total lipid content of 10 mM were prepared by the already described ethanol injection and extruded through the porous device. Both suspensions of preformed- and multi-lamellar liposomes were sprayed into the supercritical fluid using the syringe plunger pump.

2.2.2 Particle formation methods

2.2.2.1 Supercritical spray-drying methods

By using the experimental set-ups shown in figure 6, the solution was supplied to the particular particle formation set-ups, which differed mainly in nozzle configurations. The first experimental set-up was constructed using a long residence-tube to increase the degree of supersaturation while the formed droplets are flowing through the tube (Fig 6, (A)). As a nozzle, a capillary tip with an inner diameter of 0.1 mm was centered in the residence-tube prior to the connection of the tube with the particle drying cylinder. An orifice nozzle (Fig 6, (B)) with an inner diameter of 0.08 mm was used in the second set up. Furthermore, a gravity fed spray nozzle (SS 1650 fluid cap and a 64 air cap) with external mixing was employed (Fig 6, (C)) (Spraying systems, IL, USA). For round sprays an angle of about 18° was maintained, beyond that point the spray becomes turbulent. The fourth nozzle (Fig 6, (D)) was a concentric coaxial two-fluid nozzle (HSS 600

Sonimist, Misonix, NY, USA) with inner and outer diameter 0.15 mm and 1.1 mm. A sonic field was created at the throat of the nozzle as the compressed gas accelerates and reaches the velocity of sound. High frequency waves created by the resonator cavity produce a chopping effect that breaks the liquid stream into a fine, evenly dispersed cloud of extremely small droplets.

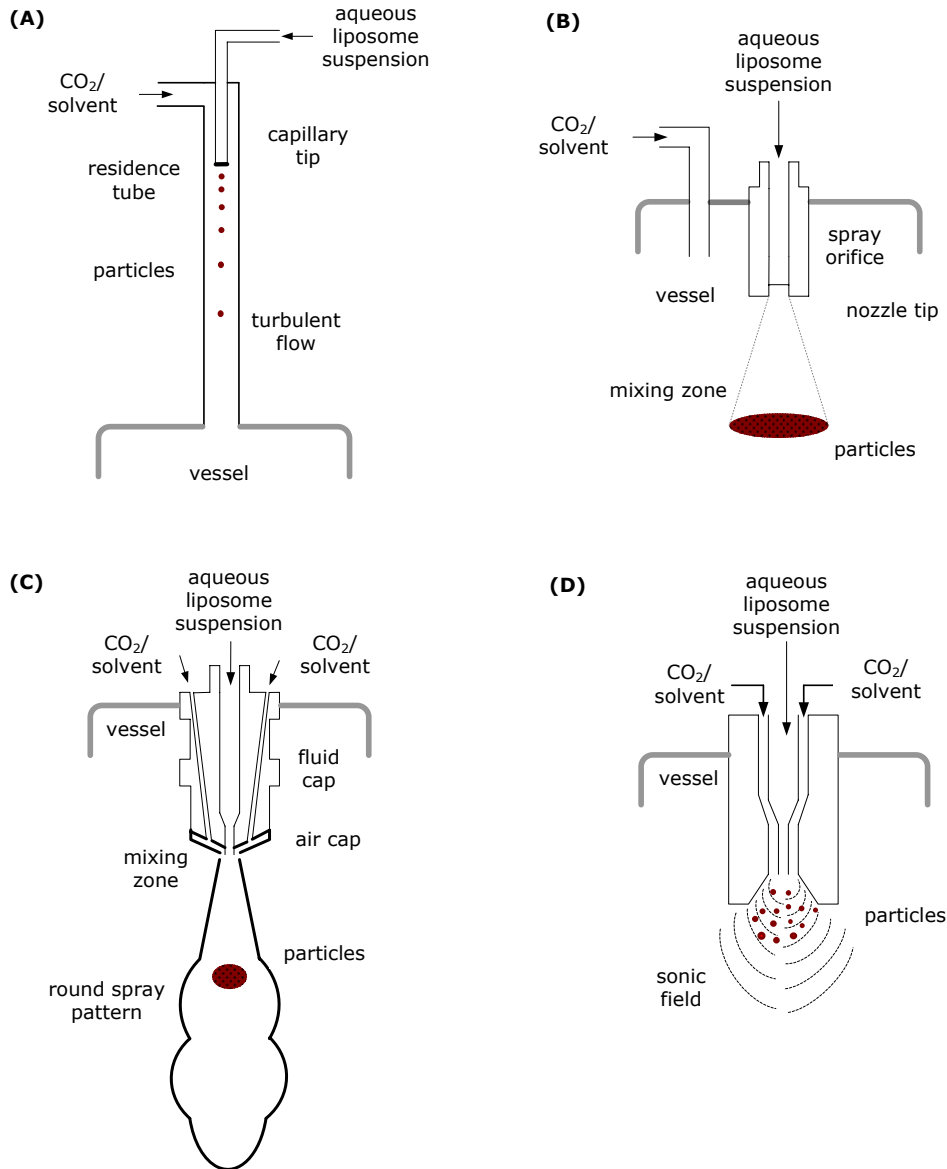


Figure 6: Scheme of the used nozzle set-ups. The residence tube (A), the orifice nozzle (B), the gravity coaxial two-fluid nozzles (C) and the concentric coaxial sonic field nozzle (D) were used in the supercritical fluid set-up.

Figure 7 shows the experimental set-up for the spraying procedure with supercritical anti-solvent. With all nozzles the ISCO DM 260 syringes pump (Teledyne ISCO, Lincoln, NE, USA) (1) was applied for spraying at a required constant volumetric flow rate between 0.11 and 1.0 ml/min for the preformed and multi-lamellar liposomal suspension.

Prior to the spraying the systems were adjusted to equilibrium with the selected pressure and temperature. The carbon dioxide was taken from the carbon dioxide tank with a dip-pipe and cooled to -5°C in a heat exchanger (6) before it entered a positive displacement pump (7). The capacity of the pump could be varied between 20 and 600 g/min. A buffer vessel (9), which was heated to 66°C , was installed after the pump. The mass flow of carbon dioxide was measured with a coriolis type mass flow meter (11).

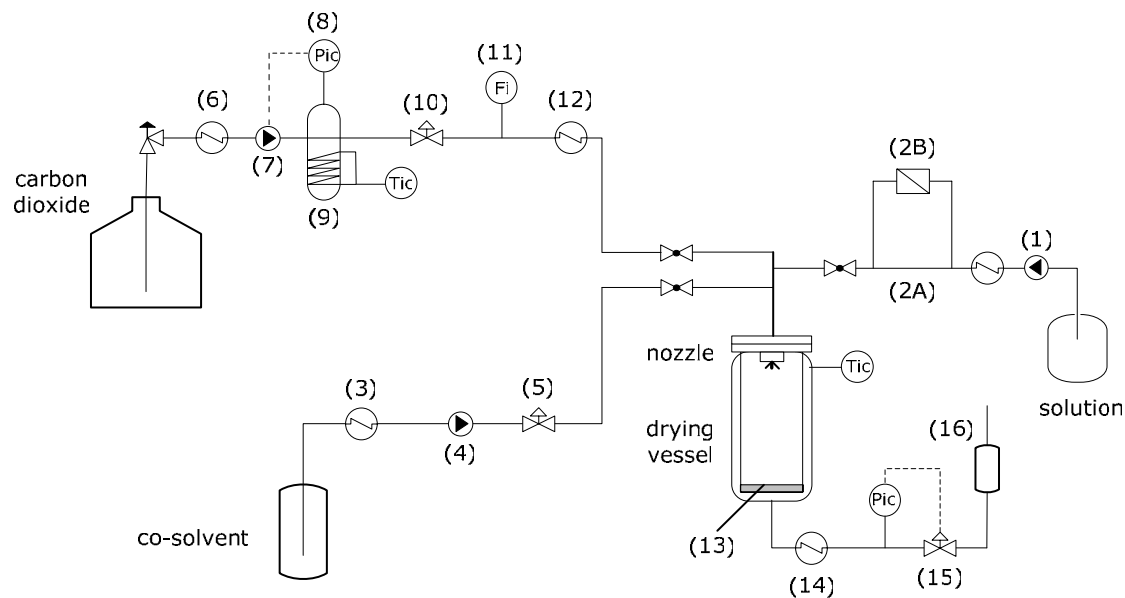


Figure 7: Schematic experimental set-up used for the spray procedure with supercritical anti-solvent.

The pressure in the buffer vessel between 18 and 170 bar was limited by a control loop (8), by which the pump also could be turned off. From the buffer vessel the carbon dioxide was supplied to the drying vessel at a constant flow rate of between 250 and 650 g/min, by opening a valve (10). Before it entered the reaction vessel the CO_2 was thermostated in a heat exchanger (12). For experiments with co-solvents, this was reheated (3) and added to the carbon dioxide flow by a syringe pump (4) before entering the drying vessel. The drying vessel had an inner diameter of 10 cm and a volume of 4 liters. A mesh size filter (13) was fitted at the bottom to retain the particles. The drying vessel was heated by a water jacket to a temperature between 37 to 41°C . To prevent condensation of the vapor at the top of the vessel the lid was isolated with expanded material. The solvent was discharged through the bottom of the vessel to a separation vessel to collect the residual solvents dissolved in CO_2 (16). Before depressurization, the solvent was heated to approximately 76°C by a heat exchanger (14) to prevent plugging of the flash valve (15) that controlled the pressure by an electronic system.

After the spraying procedure the co-solvent flow was stopped and the vessel was flushed with an additional amount of carbon dioxide (6 kg) to remove residual moisture and solvent traces. The pressure was slowly released from the system to avoid liquefaction of eventually remaining solvents. The particles were collected from the filter and the wall of the drying vessel and separately stored.

2.2.2.2 Subcritical spray-drying method

Subcritical spray-drying was performed with the described experimental set-up in Figure 7 as well. The gravity fed spray nozzle (SS 1650 fluid cap and a 64 air cap) and the concentric coaxial two-fluid nozzle (HSS 600 Sonimist, Misonix, NY, USA) described in figure 6 (C) and (D) were used. For the subcritical mode the pressure of carbon dioxide was between 17 and 24 bar with relatively high flow rates between 500 and 620 g/min. The temperature was adjusted to 40°C and the solution flow rate was set to 0.11 ml/min. After the spraying procedure, the vessel was flushed with an additional amount of carbon dioxide (10 kg) to remove residual solvent traces.

All further methods used in this chapter are already described before.

3. RESULTS AND DISCUSSION

The first studies were conducted to gain knowledge about the set-ups and parameters required for a feasible drying and particle formation process using supercritical carbon dioxide. Several technical changes of the set-up and the nozzle were necessary to find appropriate working conditions, which allow the preparation of dry particles and the preservation of the liposomal structure.

3.1 PARTICLE FORMATION AND DRYING STUDIES

A modified precipitation with compressed anti-solvent (PCA) process in the residence tube (see Fig 6, (A)) with the addition of ethanol as a co-solvent was used to study the particle formation out of preformed aqueous liposomal formulation. So far, this process was only used for the precipitation of organic compounds containing less than 5 % [w/v] water [41,42,43]. The drying of aqueous systems was not feasible, because the miscibility of carbon dioxide with water, as well as its solubility in water was too low [44,45]. Therefore, we investigated the addition of ethanol to the anti-solvent flow to enhance the solubility of water in supercritical CO₂. This addition furthermore reduced the

interfacial tension within the system (CO_2 -water) and increased the evaporation capacity and eventually the degree of saturation, finally resulting in particle formation. To further illustrate the correlation, which was prevalent in this experimental set-up the water uptake capacity was plotted against the fraction ethanol in the extractant (Fig 8). The operating pressure, temperature, droplet size and mass transfer rates between the droplet and the carbon dioxide / co-solvent controlled the particle size and morphology as described by Baldyga et al. (2004) [4].

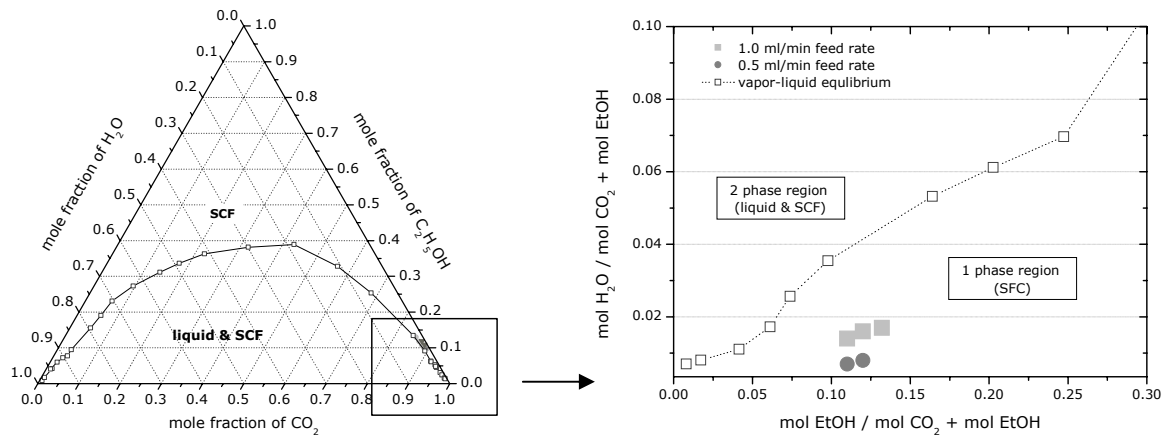


Figure 8: Phase equilibrium ternary diagram for CO_2 - $\text{C}_2\text{H}_5\text{OH}$ - H_2O including the experimental conditions (left), and converted into a drying capacity diagram using the residence tube of the CO_2 - $\text{C}_2\text{H}_5\text{OH}$ - H_2O system (right).

If the miscibility of a fluid in the supercritical phase, in our case water, is low mass transfer requires special attention and can be optimized with an improved atomization approach [46]. To improve the particle formation in the supercritical fluid process an orifice-spray-nozzle (Fig 6, (B)) was introduced to atomize the liquid feed into fine droplets directly in the drying vessel at 100 bar and 40°C . Such an enhanced particle formation process could further induce the drying behavior with optimized droplet break-up, induced mass transfer and saturation levels. This optimized spraying approach and the selection of the set-up conditions shown in figure 9 (A) could help to overcome the limitation of using the residence tube. However, the improved atomization device using an orifice nozzle did not lead to sophisticated particle morphologies and process properties. Due to the very low miscibility of water with carbon dioxide a further improvement with respect to mass transfer between these components was desired using the solution enhanced dispersion by supercritical fluids (SEDS) configuration. The advantage of the SEDS was the incorporation of a coaxial nozzle (Fig 6, (C)), with a mixing chamber to increase the relative velocity of the dispersing supercritical fluid [47]. Higher velocities of the supercritical carbon dioxide assist the droplet formation by improved jet break-up and fine droplet formation. Furthermore, the mixing properties

within the drying vessel and the saturation levels of the actively combined anti-solvent / co-solvent and solution feed could be improved [31].

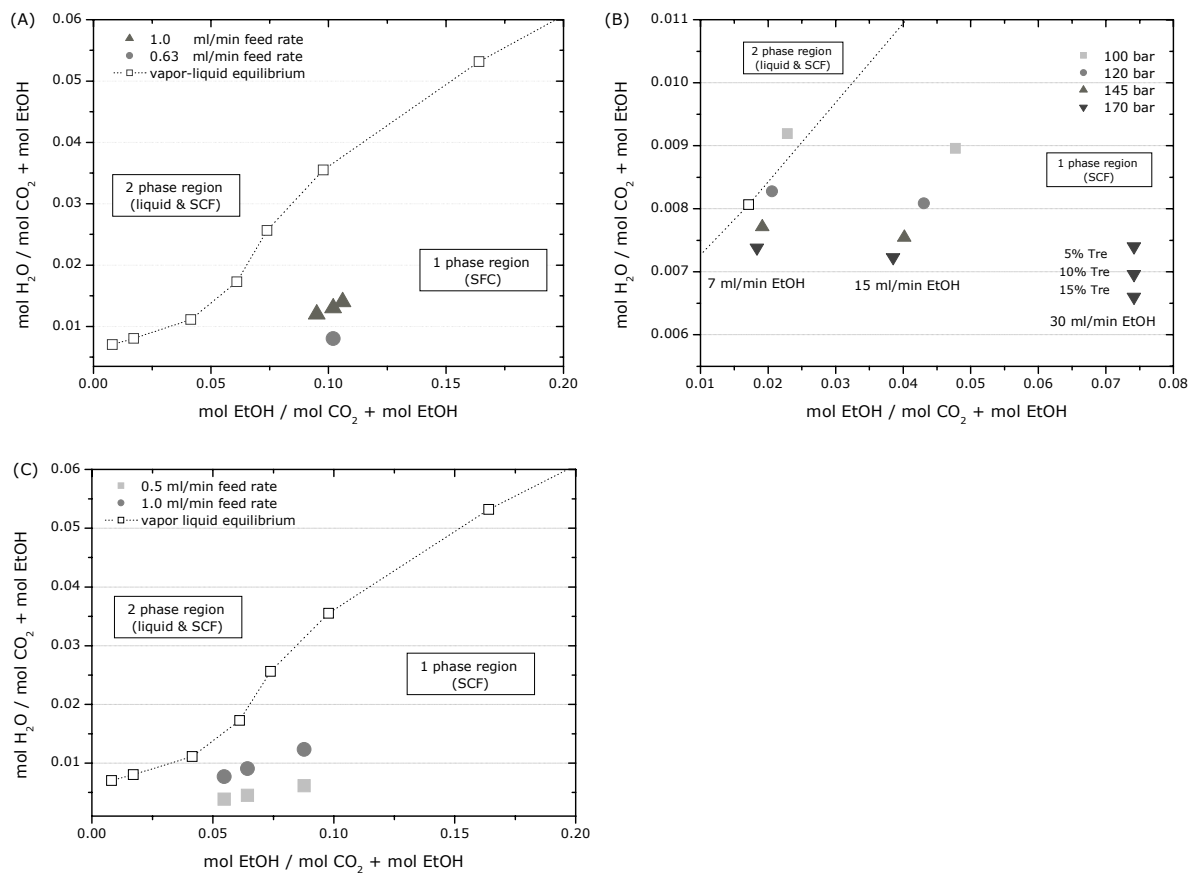


Figure 9: Drying capacity diagram using of the CO_2 - $\text{C}_2\text{H}_5\text{OH}$ - H_2O system including the experimental conditions using the orifice nozzle (A), the gravity coaxial two-fluid nozzles (B) and the concentric coaxial sonic field nozzle (C).

The liquid was dispersed through a coaxial gravity feed nozzle and the droplet formation was induced by the anti-solvent/co-solvent stream. The carbon dioxide / ethanol ratio and the relative velocity between aqueous solution and CO_2 -ethanol was increased using higher carbon dioxide flow rate and varied ethanol feed rates between 7 and 30 ml/min (Fig 9, (B)). To further improve the droplet formation process a concentric coaxial nozzle (Fig 6, (D)) was used in which the supercritical fluid flow induces ultrasounds and causing a turbulent flow mixing of the phases resulting in an improved mass transfer. The reduced liquid feed rates of 0.5 ml/min and carbon dioxide flow rates of 250, 350 and 416 g/min were investigated (Fig 9, (C)).

3.1.1 Particle morphology

3.1.1.1 Residence tube

The first studies to evaluate the experimental set-up and spraying parameters were performed at constant pressure conditions. The solution and the amount of carbon dioxide/ethanol mixture was pumped through the annular gap surrounding the capillary tip (Fig 6, (A)). Higher mass transfer of the supercritical phase into the particles directly affected the saturation levels and the morphology of dry particles (Fig 10), obvious by rough particle surface structures.

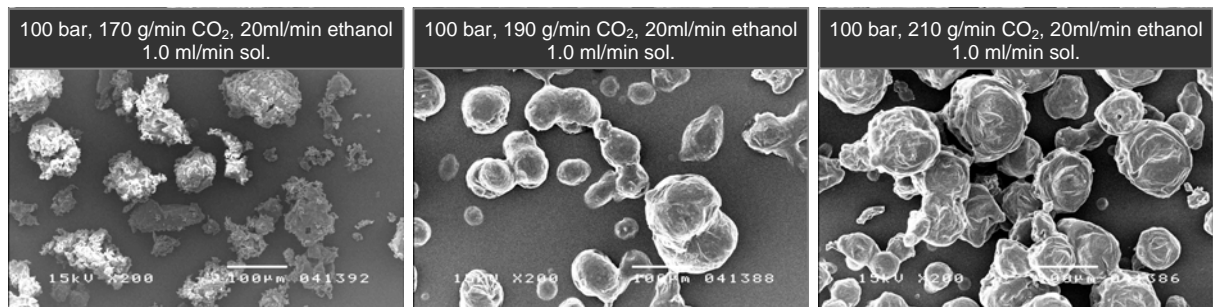


Figure 10: Scanning electron micrographs of particles obtained by supercritical-drying using the residence tube described in figure 2 (A) with 170, 190 and 210 g/min CO₂ with a solution flow rate of 1.0 ml/min.

3.1.1.2 Orifice atomization nozzle

The morphology of the particles prepared by the atomization nozzle indicated no homogenous droplet formation, as only fragments without a distinct shape were obtained (Fig 11). The mixture's critical pressure, which is required to create spherical particles, was not achieved for the main droplet fraction. This was obvious by a thin viscous film of lipids and trehalose on the inner surface of the drying vessel.

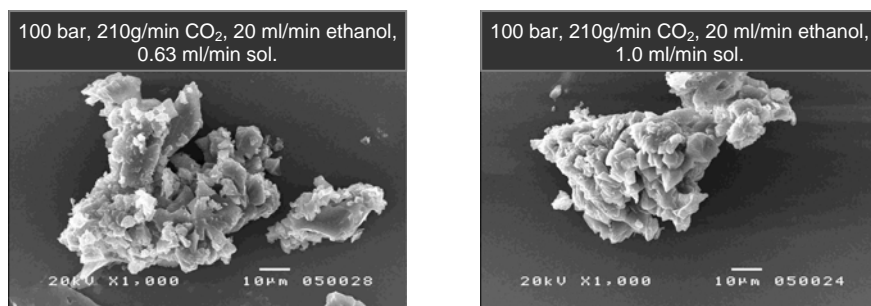


Figure 11: Scanning electron micrographs of particles obtained by supercritical-drying using the improved anti-solvent precipitation with atomization described in Figure 2 (B) with 210 g/min CO₂ and a solution flow rate of 0.63 and 1.0 ml/min.

Only fine droplets could be dried, whereby most of the liquid feed was retained and spread at the wall of the vessel. Neither a variation of the liquid feed rate and corresponding mass transfer and evaporation, nor of the droplet size itself resulted in a sufficient and homogenous particle formation process.

3.1.1.3 Gravity feed nozzle

In the coaxial two-fluid nozzle the diffusion of the CO₂/ethanol solvent stream into the liquid solvent depended on anti-solvent feed rate, pressure and co-solvent addition. This nozzle was included in the study to elucidate the influence and quality improvement of micronized jet break-up, reduction of particle agglomeration, as well as controlling the extent of mixing and solute-solvent interaction on the resulting particles. Pressure and ethanol concentration were responsible for particle shape and morphology. When produced at 100 and 120 bar the particles had an irregular shape, which changed to more spherical shapes with raising pressure (Fig 12).

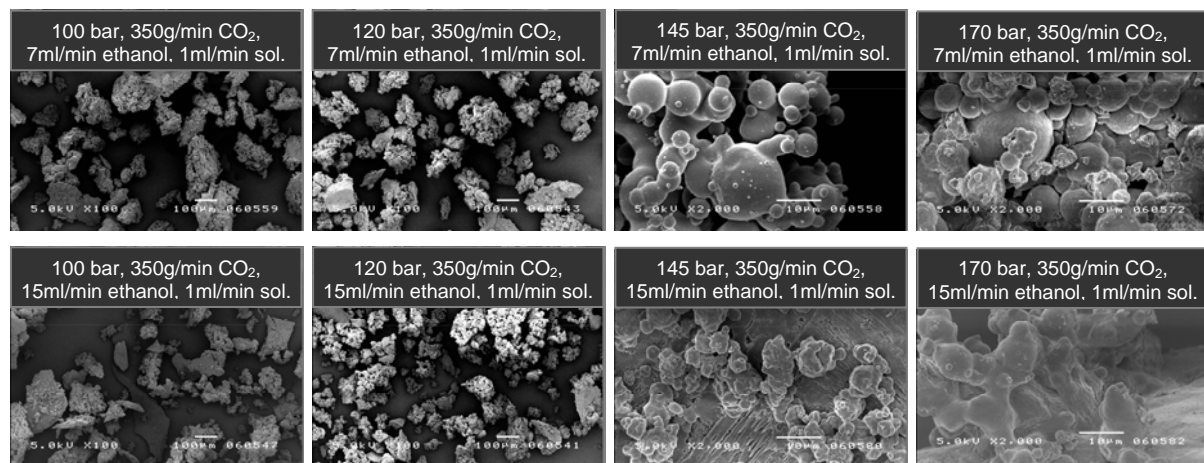


Figure 12: SEM pictures of supercritically spray-dried powders at 100, 120, 145 and 170 bar with an ethanol flow rate of 7 and 15 ml/min using the coaxial nozzle.

The low mole-fraction of ethanol within the carbon dioxide resulted in less agglomerated and spherical particles from above 145 bar (Fig 12). Thereby, the ethanol concentration was below the maximum mole fraction of ethanol (< 0.34 for 100 bar and 36.5°C), which could be loaded into a droplet [50]. Doubled ethanol mole fraction resulted in a high saturation of ethanol in the gas phase and therefore in enhanced evaporation. The droplet formation process and the jet length of the liquid feed can provide an explanation for the more spherical particles at 170 bar. At constant temperature the jet length decreases when the pressure is increased, which results in different droplet diameters and enhanced mass transfer [48]. The saturation concentration of ethanol and carbon

dioxide in droplets and droplets radius were described to decrease with increased pressure [29]. This favored two particle formation processes, the evaporation of water and the precipitation considered by supersaturation. Particle morphology was affected by this phenomenon, which was described by the reduction of convective flow [29].

Different trehalose concentrations of 5, 10.5 and 15 % [w/v] were dried at 170 bar and at a further increased ethanol rate of 30 ml/min. Two separate particle fractions were present within the drying vessel. One fraction was collected from the wall, while a larger fraction of about 60 % was retained at the filter plate. The particles adhering at the wall had no distinct shape. Needle like structures were observed for particles collected from the filter plate (Fig 13).

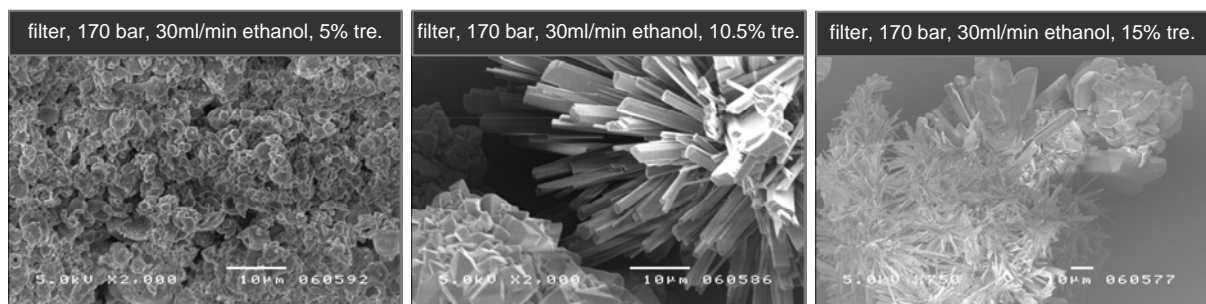


Figure 13: SEM pictures of supercritically spray-dried powders collected from filter plate at 170 bar with an ethanol flow rate of 30 ml/min and a solution flow rate of 1.0 ml/min using the coaxial nozzle and different trehalose concentrations.

3.1.1.4 Concentric coaxial nozzle

The different velocities of the CO₂-ethanol stream and the jet velocity were reduced to enhance the evaporation forces for the concentric coaxial nozzle (Fig 6, (D)). After mixing, the two streams leave the nozzle tip at a velocity equal to a two-phase flow and end up in a so called hydrodynamic relaxation zone. This zone is mainly influenced by the mass flow ratio and represents the key control parameter for mass transfer.

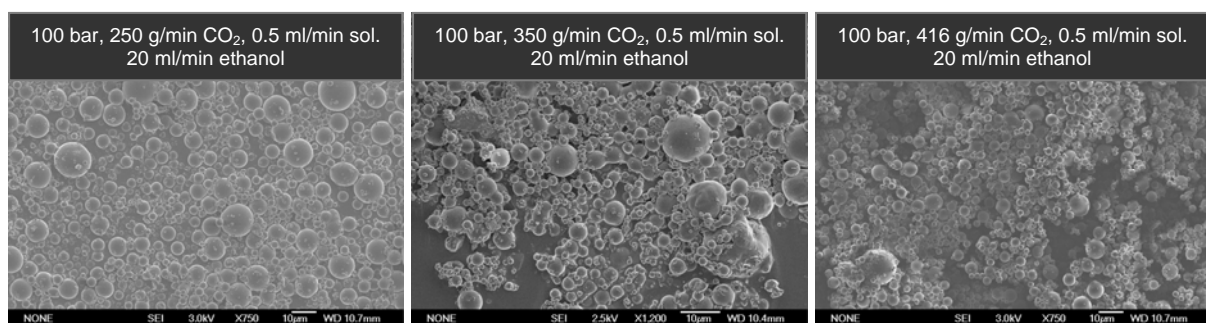


Figure 14: SEM pictures of supercritically spray-dried powders at 100 bar with an ethanol flow rate of 20 ml/min using the concentric coaxial nozzle and different carbon dioxide flow rate and solution flow rates.

If this mass transfer factor and the equilibrium phase are optimized, the subsequent mass transfer zone leads into a uniform saturation and drying zone [49]. With a solution feed rate of 0.5 ml/min a phase change of the vapor-liquid equilibrium occurred. However, scanning electron microscope images indicated predominantly spherical and smooth particles. As water required a large amount of carbon dioxide to become fully evaporated the liquid feed rate should be reduced or the carbon dioxide flow increased.

3.1.2 Particle size distribution

3.1.2.1 Residence tube

The mean particle size obtained with the residence tube ranged from 160 to 320 μm at a solution feed rate of 1.0 ml/min (Tab 2). At a carbon dioxide feed rate of 190 g/min, mixed with 20 ml/min ethanol the mean particle size was 141 μm . These large particles indicate an insufficient drying resulting in agglomeration of moist particles at the filter plate. Further increases in carbon dioxide flow and hence a lower molar fraction of ethanol in the mixture resulted in a decreased particle size, reaching a mean size of 75 μm at 210 g/min CO_2 . However, the data pointed at a phase separation of carbon dioxide and ethanol occurring at low ethanol concentration due to the broad particle size distribution. The mass transfer rates were not sufficient to reach saturation of solids in all formed droplets [50]. The particle size at 0.5 ml/min solution feed rate was reduced for both investigated experimental conditions (Tab 2). Decreasing the molar fraction of water by reducing the solution feed compared to the evaporation mixture resulted in smaller, but still agglomerated particles.

Table 2: Particle size diameter, residual moisture and product yield using the residence tube at a pressure of 100 bar with 170, 190 and 210 ml/min carbon dioxide flow and solution rates of 0.5 and 1.0 ml/min.

nozzle type	pressure [bar]	CO_2 [g/min]	ethanol [ml/min]	solution [ml/min]	d[10] [μm]	d[50] [μm]	d[90] [μm]	d[4,3] [μm]	span
res. tube	100	170	20	1.0	42.1	141.0	320.6	165.4	1.9
res. tube	100	190	20	1.0	35.1	102.6	299.6	150.3	2.5
res. tube	100	210	20	1.0	30.5	75.9	165.8	94.1	1.7
res. tube	100	190	20	0.5	15.6	47.5	116.3	54.8	2.1
res. tube	100	210	20	0.5	12.9	37.1	76.0	42.7	1.7

3.1.2.2 Orifice atomization nozzle

The additional atomization of the liquid feed directly into the compressed larger volume of carbon dioxide / ethanol resulted in smaller droplet sizes. The swelling process of the droplets due to the condensation of ethanol and CO₂ was on the other hand favored. But for both, 1.0 and 0.63 ml/min liquid feed particle fractions with sizes around 15 μm were obtained (Tab 3). The molar fractions of the ethanol / carbon dioxide and the smaller droplets were sufficient to improve evaporation of water and to finally achieve the optimized particle morphology and size. Furthermore, the agglomeration tendency was reduced because of a more homogenous evaporation

Table 3: Particle size diameter using the improved anti-solvent precipitation with atomization of 100 bar with 210 g/min CO₂ and a solution flow rate of 0.63 and 1.0 ml/min.

nozzle type	pressure [bar]	CO ₂ [g/min]	ethanol [ml/min]	solution [ml/min]	d[10] [μm]	d[50] [μm]	d[90] [μm]	d[4,3] [μm]	span
orifice	100	210	20	0.63	6.1	15.7	31.2	31.2	2.2
orifice	100	210	20	1.0	7.5	17.4	34.0	34.0	2.4

3.1.2.3 Gravity feed nozzle

An effect of pressure and ethanol concentration on particle size was visible (Tab 4). Higher operating pressures and ethanol concentration resulted in a slight decrease of particle size. Small particles with a mean diameter of 27 μm were obtained at a pressure of 170 bar and the higher ethanol content. However, the width of the volume distribution indicated by the span value remained relatively large for all conditions. A certain amount of ethanol was expected to condense into the droplet and increase the solvent extraction [51]. This effect depended on pressure and density of the system [52].

Table 4: Particle size diameter using the coaxial gravity feed nozzle at a pressure of 100, 120, 145 and 170 bar with 350 ml/min carbon dioxide flow, ethanol flow rates of 7 and 15 ml/min and a solution rate of 1.0 ml/min.

nozzle type	pressure [bar]	CO ₂ [g/min]	ethanol [ml/min]	solution [ml/min]	d[10] [μm]	d[50] [μm]	d[90] [μm]	d[4,3] [μm]	span
gravity	100	350	7	1.0	3.9	23.1	119.4	45.6	5.0
gravity	100	350	15	1.0	4.1	16.3	72.1	30.1	4.1
gravity	120	350	7	1.0	5.4	49.1	154.2	67.2	3.0
gravity	120	350	15	1.0	4.2	20.8	128.0	46.7	5.9
gravity	145	350	7	1.0	3.0	10.8	73.1	27.8	6.4
gravity	145	350	15	1.0	4.8	17.4	121.7	42.8	6.7
gravity	170	350	7	1.0	5.6	24.7	78.1	37.5	2.9
gravity	170	350	15	1.0	3.7	12.0	65.9	26.9	5.1

Due to the improved mixing of aqueous solution with carbon dioxide and ethanol already in the air-cap (Fig 6, (C)) the saturation in smaller droplets became already earlier sufficiently large, with the result of faster water evaporation. The kinetic of the saturation onset depended on the time of ethanol expansion and the so-called diffusion time, which was influenced by the radius of the droplets and the diffusivity in the solvent carbon dioxide mixture [53]. At a high ethanol concentration of 15 ml/min an anti-solvent approach within the particles could become feasible. As already described, two particle fractions were obtained when using the coaxial gravity feed nozzle. The particles collected from the wall were generally larger than the particles from the filter plate (Tab 5). Moreover, the size distribution was more homogenous for the particles from the filter plate with span values around 2.0, which could be explained by the smaller droplets formed at the nozzle.

Table 5: Particle size diameter using the coaxial gravity feed nozzle with different trehalose concentrations at a pressure of 170 bar with 350 ml/min carbon dioxide flow with an ethanol flow rate of 30 ml/min and a solution rate of 1.0 ml/min.

trehalose % [w/v]	particle collection	pressure [bar]	CO₂ [g/min]	ethanol [ml/min]	d[10] [μm]	d[50] [μm]	d[90] [μm]	d[4,3] [μm]	span
5.0	wall	170	350	30	5.5	28.0	69.5	35.0	2.2
5.0	filter	170	350	30	3.5	9.6	20.4	11.2	1.7
10.5	wall	170	350	30	4.3	13.1	40.4	21.2	2.7
10.5	filter	170	350	30	3.5	11.0	34.9	16.6	2.8
15.0	wall	170	350	30	6.5	17.8	97.5	35.2	5.1
15.0	filter	170	350	30	4.5	16.6	49.7	26.2	2.6

3.1.2.4 Concentric coaxial nozzle

The particle size measurement indicated a homogenous drying resulting in a product with a narrow particle distribution with a span of around 1.0 for the liquid feed rate of 0.5 ml/min. The mixing rate between carbon dioxide / ethanol and the solution feed influenced the particle size. When using 250 g/min CO₂ a mean size of 2.0 μm was reached. Increasing the carbon dioxide flow rate up to 350 and 416 g/min raised the particle size to 10 μm (Fig 15, left). The initial swelling stage induced by the supercritical phase influenced the particle size by the condensation of ethanol and carbon dioxide into the droplet. The different solubilities of CO₂ and ethanol in water affected this swelling. Because of the higher ethanol concentration and at the same time lower carbon dioxide flow this evaporation level was improved. The opposite was achieved with 1.0 ml/min solution feed rate, which was characterized by the insufficient diffusion of both CO₂ and ethanol into droplets in the hydrodynamic relaxation zone (Fig 15, right). If the ethanol

content and therefore the solubility of water in the supercritical phase were high enough, the drying procedure was independent from the atomization force. The mass transport process became the key control particle formation parameter.

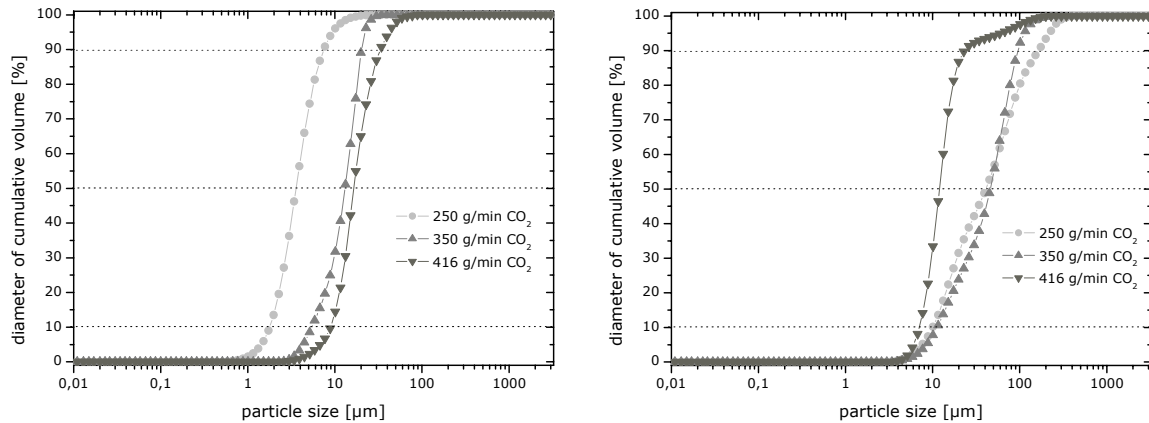


Figure 15: Cumulative volume-based size distribution curves of supercritically spray-dried particles at a solution flow rate of 0.5 ml/min (left) and 1.0 ml/min (right) with a pressure of 100 bar and carbon dioxide flow rates of 250, 350 and 416 g/min.

3.1.3 Yield and residual moisture

3.1.3.1 Residence tube

The particle formation process resulted in very low yields below 40 % for this set-up (Tab 6). The most common sources of product loss were insufficient drying and leakage of powder between filter plate and the vessel wall. The fine particle fraction also vanished through the filter itself. The mixing energy was not high enough when using the residence tube due to the restricted nozzle geometry and the large droplets.

Table 6: Residual moisture and powder yield of particles obtained within the residence tube.

nozzle type	pressure [bar]	CO ₂ [g/min]	ethanol [ml/min]	solution [ml/min]	residual moisture [%]	yield [%]
res. tube	100	170	20	1.0	6.0	30
res. tube	100	190	20	1.0	4.8	24
res. tube	100	210	20	1.0	1.4	15
res. tube	100	190	20	0.5	2.1	41
res. tube	100	210	20	0.5	2.4	37

Evaporation during the relatively short time inside the precipitation pipe followed by movement of the droplets through the drying vessel distance influenced the yield. They were floating through the drying vessel and adhered at wall or filter plate before they

reached sufficient drying levels. An additional amount of particles was retained inside the precipitation tube. The overall inhomogeneous drying procedure resulted in particles with residual moisture contents below 6.0 %.

3.1.3.2 Gravity feed nozzle

A similar residual moisture content of about 4.5 % and relatively low product yields of 40 % were found for the atomization nozzle. Therefore, further investigations were necessary to identify optimum working conditions for drying of aqueous formulations in respect of jet break-up of the liquid feed at the nozzle tip, mass transfer and nucleation. When using the concentric co-axial nozzle the residual moisture content was mainly affected by the ethanol concentration in the CO₂-ethanol mixture. The solubility of ethanol in carbon dioxide increased sharply with the pressure. High ethanol contents of 15 ml/min in the anti-solvent led to relatively low moisture values between 4 and 5 % in comparison to the lower ethanol concentration with values between 6 and 7.5 % (Fig 16, left). Ethanol concentration in the gaseous phase has large impact on the mass transfer. The droplet drying time could be significantly reduced because of the higher solubility of water when the carbon dioxide was richer in ethanol as described by Martin et al. (2007) [30]. This working region above the mixture's critical point was not fully achieved. However, the increased ethanol content at high pressure resulted in a phase behavior with increased miscibility of water resulting in higher product yield (Fig 16, right).

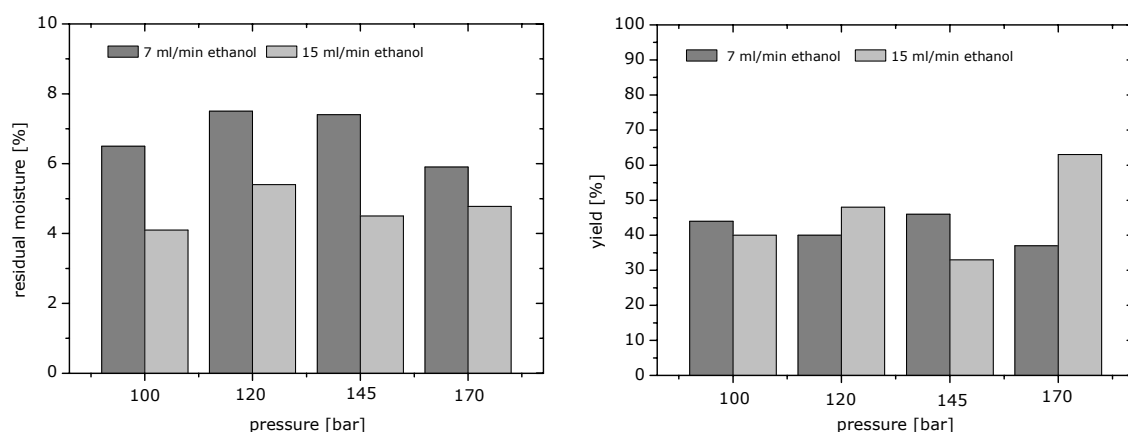


Figure 16: Residual moisture (left) and powder yield (right) after supercritical spray-drying of liposome suspensions with 10 mM lipid and 10.5 % trehalose using 7 and 15 ml/min ethanol flow rate within in the supercritical carbon dioxide flow of 350 g/min and a pressure between 100 and 170 bar using the gravity feed nozzle.

For all studied trehalose concentrations the particles from the wall had a residual moisture of about 3 % and the particles from the filter of about 4 % when using the gravity feed nozzle (Tab 7). The particle yield could be increased to almost 100 % (wall and filter combined) by these settings. High ethanol concentrations led to a favorable phase behavior. Most common sources of product loss were reduced and the filters stayed intact. However, the allocation of particle in a mass ratio of 1:3 at wall to filter pointed at two decisive factors important for aqueous formulation drying at high ethanol concentrations: the phase behavior and the choice of co-solvent concentration with the additional atomization properties.

Table 7: Residual moisture and powder yield of particles obtained with 5, 10.5 and 15 % trehalose.

trehalose % [w/v]	nozzle type	particle collection	pressure [bar]	CO₂ [g/min]	ethanol [ml/min]	solution [ml/min]	residual moisture [%]	yield [%]
5.0	gravity	wall	170	350	30	1.0	2.9	33
5.0	gravity	filter	170	350	30	1.0	4.2	64
10.5	gravity	wall	170	350	30	1.0	3.4	35
10.5	gravity	filter	170	350	30	1.0	4.3	62
15.0	gravity	wall	170	350	30	1.0	3.1	39
15.0	gravity	filter	170	350	30	1.0	4.0	59

At high ethanol concentrations in the CO₂ the formation of a second liquid phase can be suppressed and the working conditions were closer to the even critical point of the ternary mixture [50].

3.1.3.3 Concentric coaxial nozzle

When using the concentric coaxial nozzle low residual moisture contents could be achieved by increasing the molar fraction of ethanol to the carbon dioxide while reducing the solution feed rate (Tab 8).

Table 8: Residual moisture and powder yield of particles obtained at 100 bar with an ethanol flow rate of 20 ml/min using different carbon dioxide flow rates and solution flow rates.

nozzle type	pressure [bar]	CO₂ [g/min]	solvent [ml/min]	solution [ml/min]	residual moisture [%]	yield [%]
concen.	100	250	20	0.5	1.9	95
concen.	100	250	20	1.0	8.0	52
concen.	100	350	20	0.5	1.9	95
concen.	100	350	20	1.0	5.9	60
concen.	100	416	20	0.5	1.6	90
concen.	100	416	20	1.0	6.4	61

The rapid evaporation resulted in faster saturation and extraction levels of water. A water mole fraction of 0.07 within the carbon dioxide / ethanol phase should not be exceeded due to the limited solubility. The loading of ethanol into supercritical phases could not be further optimized. Leaving all other parameters constant an increased solution feed rate doubled the mole fraction of water in the system. However, this led to an insufficient drying of the formed droplets which resulted in residual moisture content above 6 % and a decline in yield to 50 to 60 %.

3.1.4 Residual solvents

For the application of the dried product as therapeutic agent it is a pre-requisite to keep the residual solvent level low [54]. No residual ethanol was detected in particles prepared with the residence tube and additional atomization using the static headspace gas chromatography (HS-GC).

3.1.4.1 Gravity feed nozzle

When using the gravity nozzle for the atomization of the liquid feed at pressures between 100 and 170 bar, the remaining residual ethanol content increased with pressure and the amount of ethanol added as a co-solvent. At higher densities and a solvent flow rate of 15 ml/min, ethanol diffusion into the particles was improved, which resulted in a residual ethanol concentration of 2500 ppm (Fig 17, left). After precipitation and particle formation the ethanol was bound via hydrogen bonds to the trehalose and could not be totally removed by the additional carbon dioxide washing step. With increasing trehalose concentrations the residual ethanol content increased, which is further indicative for the retaining effect of trehalose on ethanol (Fig 17, right).

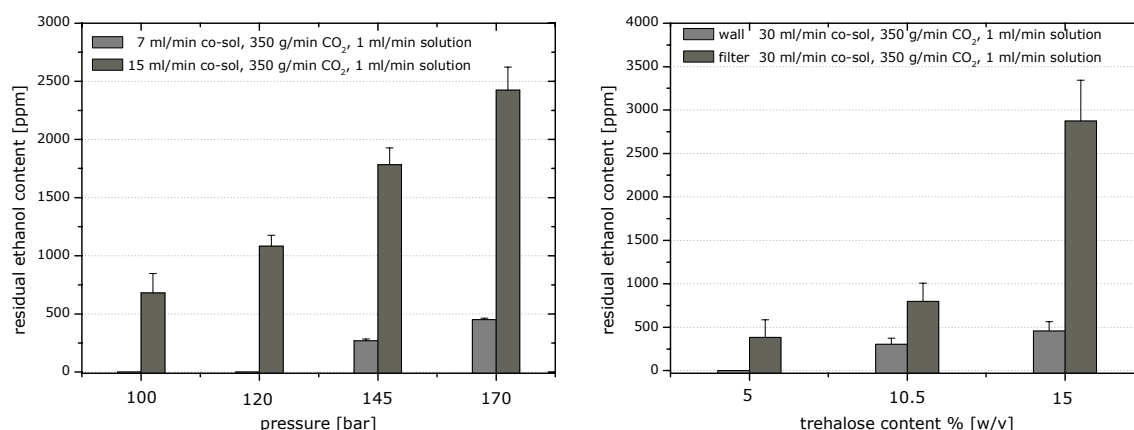


Figure 17: Residual ethanol concentration of supercritically spray-dried particles at increasing pressure with 7 and 15 ml/min co-solvent feed (left) at increasing trehalose concentration in the formulation from 5, 10.5 and 15 % [w/v] with 30 ml/min co-solvent feed and 170 bar (right).

The particles from the wall contained less residual ethanol compared to the particles from the filter. Depending on trehalose concentration, the swelling and diffusion time of ethanol into the particles rose over the time of flight in the drying vessel. The higher residual ethanol content of the particles from the filter could directly be correlated with the particle formation and drying process, due to the initial swelling of carbon dioxide and ethanol into the droplet. After reaching saturation inside the droplets the evaporation of the solvents began, which result in a decreased particle size.

3.1.4.2 Concentric coaxial nozzle

The diffusion of ethanol into the droplets and the evaporation of water was more pronounced for the concentric coaxial nozzle, resulting in very homogenous particle formation. At reduced aqueous feed the residual moisture levels were significantly reduced below 2 %. Additionally, the particle size was lowered, which was achieved by the forced diffusion of ethanol into the atomized droplet and the resulting homogenous water evaporation due to the tremendous levels of saturation. The consequence was the extraction of both, water and ethanol into the supercritical phase. The inverse flux of carbon dioxide into the droplets led to the expansion of the organic phase creating local saturation and finally precipitation of the solute. The precipitation levels of solutes were much higher because of the smaller droplet size and the larger surface area resulting in the high remaining residual ethanol content between 5000 and 7000 ppm (Fig 18). The liquid feed rate of 1.0 ml/min resulted in residual ethanol contents below 2000 ppm. However, the broader particle size distribution, the lower yield of about 60 % and particularly the high residual moisture content up to 8 % recommend the lack of drying performance and mass transfer.

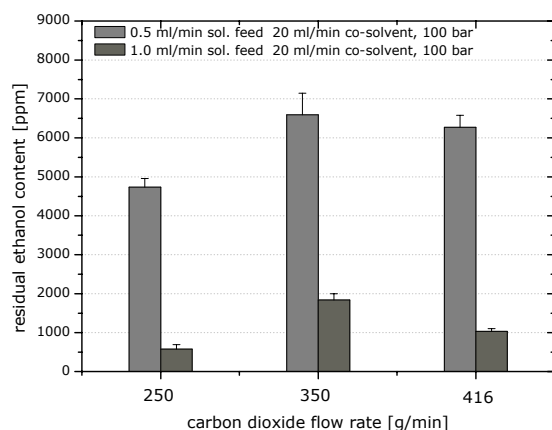


Figure 18: Residual ethanol concentration of supercritically spray-dried solution with a feed of 0.5 and 1.0 ml/min and increasing carbon dioxide flow rates 250, 350 and 416 g/min using the concentric coaxial nozzle at 100 bar with a co-solvent flow of 20 ml/min.

3.1.5 X-ray powder diffraction

When using the gravity feed nozzle at a pressure of 100 bar with additional ethanol flow of 7 ml/min the process resulted in crystalline powders, because of the longer drying time and the reduced water solubility in the supercritical phase (Fig 19, left). The XRD diffraction pattern indicated the presence of crystalline trehalose dihydrate by the peaks at 8.8 and 23.3° 2-Theta [55]. Particle morphology and size already had indicated insufficient evaporation of the carbon dioxide into the particle. Drying time increased due to the reduced water solubility in CO₂, the liberated water was not removed quickly enough out of the particles and crystallization occurred. The residual water acts as a plasticizer reducing the T_g and favoring the crystallization of the trehalose either during process or storage. After drying at higher pressure and with a higher density of the carbon dioxide a broad halo pattern, typical for amorphous material was visible in the XRD patterns. The high pressure of 170 bar enhanced the mole fraction ethanol in the carbon dioxide and increased the water solubility with the consequence of having different particle fractions at the wall and the filter plate. The fractions from wall and filter exhibited different physical properties. Particles from the wall were amorphous, whereas the fraction collected from the filter showed crystalline structures (Fig 19, right). The high residual moisture content between 4 to 5 % and the very small size of the particles from the filter resulted in a crystalline morphology.

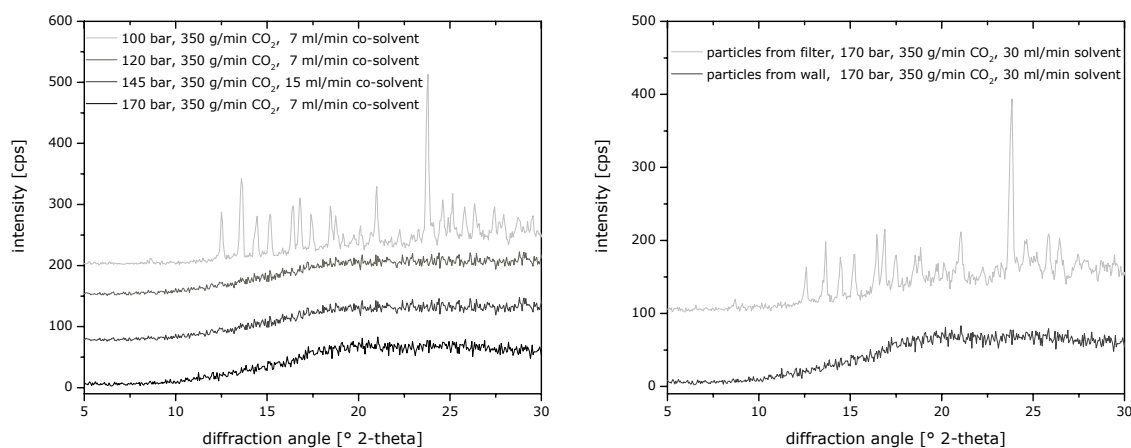


Figure 19: Wide angle X-ray diffraction pattern after supercritically spray-drying of liposomes at pressures between 100 and 170 bar with 3, 7 and 15 ml/min ethanol flow (left) and 30 ml/min (right) to the carbon dioxide flow of 350 g/min at a solution feed of 1.0 ml/min.

3.2 LIPOSOME SIZE AND LIPID SOLUBILITY

3.2.1 Liposomes dried by the residence tube

Liposome size was determined after the reconstitution of the supercritically dried powders. For the preformed liposomes dried within the residence tube the carbon dioxide flow of 210 g/min positively influenced the liposome size resulting in a size of 200 nm and a low polydispersity index (PI) of 0.21. Increasing the molar fraction CO₂-water by decreasing the solution feed rate did not further improve the PI (Tab 9). The size distribution of liposomes prepared by the atomization nozzle was not further improved compared to the residence tube (data not shown). More efficient atomization and distribution of the liquid feed rate with the carbon dioxide flow rate is necessary to reduce the influence of lipid solubility in the supercritical fluid. This will be further described in section 3.4.5.

Table 9: Liposome size and polydispersity index of supercritically dried particles obtained within the residence tube.

nozzle type	pressure [bar]	CO₂ [g/min]	ethanol [ml/min]	solution [ml/min]	z-average [nm]	polydispersity index
before					170	0.20
res. tube	100	170	20	1.0	220	0.43
res. tube	100	190	20	1.0	190	0.48
res. tube	100	210	20	1.0	201	0.21
res. tube	100	190	20	0.5	140	0.31
res. tube	100	210	20	0.5	220	0.30

3.2.2 Liposomes dried by the gravity feed nozzle

3.2.2.1 Liposomes size at varied pressure

Size and PI of liposomes dried by supercritical fluids and the co-axial nozzle were affected by pressure and ethanol concentrations. At pressures between 100 and 145 bar and high ethanol mole fraction of 0.257 mol/min liposomes with a z-average of 140 to 120 nm, but an increased PI were obtained. This could be attributed to the swelling process induced by carbon dioxide and the co-solvent. The configuration pathway 2 B (Fig 7) to form liposomes in combination with a porous device from a multi-lamellar vesicles suspension was successfully tested at 170 bar. The size of the liposomes was reduced to 130 and 115 nm with polydispersity indices of 0.25 and 0.22, respectively (Tab 10). This approach allowed the direct formation of liposomes and drying within a single process step.

Table 10: Liposome size and polydispersity index using the coaxial gravity feed nozzle at a pressure of 100, 120, 145 and 170 bar with 350 ml/min carbon dioxide flow with ethanol flow rates of 7 and 15 ml/min and a solution rate of 1.0 ml/min.

nozzle type	pressure [bar]	CO ₂ [g/min]	ethanol [ml/min]	solution [ml/min]	z-average [nm]	polydispersity index
before					165	0.21
gravity	100	350	7	1.0	225	0.51
gravity	100	350	15	1.0	143	0.45
gravity	120	350	7	1.0	200	0.48
gravity	120	350	15	1.0	127	0.47
gravity	145	350	7	1.0	181	0.44
gravity	145	350	15	1.0	120	0.42
gravity	170	350	7	1.0	130	*0.25
gravity	170	350	15	1.0	115	*0.22

* Liposomes prepared with the modification described in set-up (2B) the porous device.

3.2.2.2 Lipid recovery at varied pressure

The use of supercritical fluids is always based on the different solubility of compounds in CO₂ and/or co-solvents. The extraction of the lipids and the ethanol content in the gaseous phase was determined as the key factor on lipid solubility [56]. The solvent selectivity of ethanol for the liquid and the gaseous phase can be obtained by the ratio of the partition coefficients of ethanol and water in CO₂ [57] and calculated using the mole fraction of ethanol in the gaseous and liquid phases, respectively [35].

Figure 20 shows the solvent selectivity in comparison with the lipid recovery of DOTAP-Cl (left) and of DOPC (right). Data from literature at 100 bar and 200 bar showed that the solvent selectivity decreases with increasing pressure and ethanol concentrations in the liquid phase (symbols with dotted line). The used lipids DOTAP-Cl and DOPC revealed different solubility behavior in the experiments depending on the ethanol mole fraction in the liquid phase and the pressure in the system. For DOTAP-Cl (Fig 20, left) the high selectivity and the low ethanol mole fraction in the liquid phase resulted in lipid extraction of 30, 45, 50 and 60 % depending on pressure 170, 145, 120 and 100 bar. With reduced selectivity and a lower mole fraction ethanol in the liquid phase the extraction of lipids could be reduced to 12, 32, 45 and 47 % in the same pressure range. The solubility of DOPC at the conditions with higher selectivity differed from those of DOTAP-Cl (Fig 20, right). For DOPC almost 100 % recovery was measured at a drying pressure of 170 bar. Within the used systems the addition of the co-solvents at increased pressure reduced the solubility of the lipids due to the enhanced drying performance by the raised miscibility of water in the system.

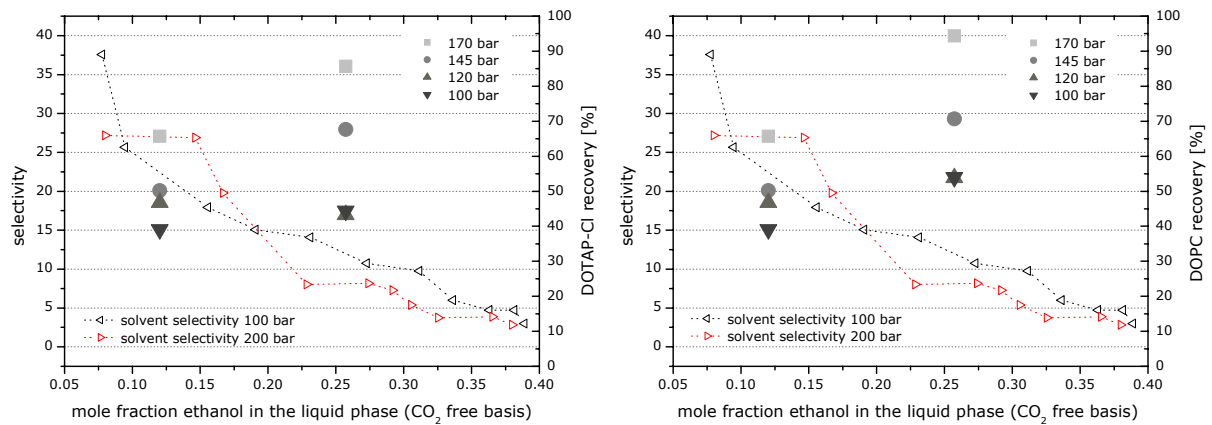


Figure 20: Solvent selectivity for the $\text{CO}_2\text{-C}_2\text{H}_5\text{OH-H}_2\text{O}$ ternary system for 100 and 200 bar at 40°C [23] compared to the lipid recovery at the pressure 100, 120, 145 and 170 bar and different lipids DOTAP-Cl (left) and DOPC (right).

The viscosity of the fluid increases with its density due to the increased intramolecular forces, when the molecules in the fluid become more closely packed as described by Durling et al. (2007) [23]. The addition of the co-solvents to the supercritical carbon dioxide increases the viscosity and the selectivity resulting in reduced lipid solubility. However, the determined lipid recoveries were not in agreement with recent publications where the solubility raised for the studied triglycerides and pure lipids at increased pressure [58]. This effect was obtained by increased density and solubility of carbon dioxide in combination with the co-solvent addition. Further studies revealed that the lipid solubility depended on the molecular weight of the lipids and on the pressure increase up to maximum saturation [59]. This level of maximum saturation depended again the molecular weight of the substance [60].

3.2.2.3 Liposomes size and lipid recovery at varied trehalose concentration

Liposome properties at a high pressure of 170 bar and varied trehalose content with additional co-solvent concentration of 30 ml/min were affected by the high ethanol content in the supercritical phase. Although particle size and product recovery were optimized, the liposome size and especially the polydispersity index for 5 and 15 % [w/v] trehalose was too high in both, particles from the wall and the filter plate (Tab 11). The internal structure of the liposomes was disordered by the different solubility of the lipids in the gaseous phase. The solubility of DOTAP-Cl compared to DOPC in ethanol was enhanced. Within the mixture of the carbon dioxide-ethanol DOTAP-Cl was extracted to a greater extent.

Table 11: Liposome size, polydispersity index and lipid recovery of DOTAP-Cl and DOPC using the coaxial gravity feed nozzle with different trehalose concentrations 5, 10.5 and 15 % [w/v] at a pressure of 170 bar with 350 ml/min carbon dioxide flow with an ethanol flow rate of 30 ml/min and a solution rate of 1.0 ml/min.

trehalose [w/v]	nozzle type	particle collection	pressure [bar]	z-average [nm]	polydispersity index	DOTAP-Cl [%]	DOPC [%]
5.0	gravity	wall	170	135	0.54	38.7	55.0
5.0	gravity	filter	170	127	0.48	58.7	63.9
10.5	gravity	wall	170	129	0.37	33.2	43.7
10.5	gravity	filter	170	120	0.30	40.3	58.9
15.0	gravity	wall	170	141	0.60	39.3	51.6
15.0	gravity	filter	170	120	0.54	43.1	75.0

3.2.2 Liposomes dried by the concentric coaxial nozzle

3.2.3.1 Liposomes size at varied co-solvent flow rate

Liposome size and the polydispersity index after supercritical drying using the concentric co-axial nozzle resulted in a broad size distribution. A reduced liquid feed resulted in a doubled carbon dioxide flow rate, which influenced the polydispersity index of the liposomes. However, the size distribution and the high polydispersity are still insufficient compared to the liposome properties before processing.

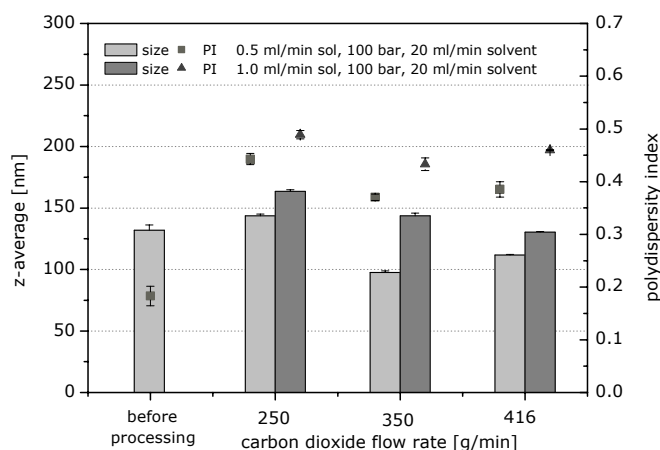


Figure 21: Liposome size and polydispersity index after supercritical spray-drying of liposomes suspensions at 100 bar, 20 ml/min ethanol flow rate using 0.5 and 1.0 ml/min solution flow rate and different carbon dioxide flow rates (250, 350, and 416 g/min).

3.2.3.2 Lipid recovery at varied co-solvent flow rate

The effect of an increased carbon dioxide flow rate on lipid recovery is also reflected in the solubility and selectivity of the lipid in the supercritical phase. With a high mole fraction of water, the lipid recovery was in relation to the carbon dioxide flow rate, as high CO₂ flow rates resulted in a reduced ethanol mole fraction and therefore in a higher

lipid recovery. The lipid recovery determined at low mole fraction of water was low. Moreover, the lipid recovery for DOTAP-Cl was enhanced under these conditions as well (Fig 22, left). DOPC solubility on the other hand was less affected by the variation of the mole fraction water and ethanol within the CO₂. At a CO₂ flow of 250 g/min the lipid recovery was 100 % and decreased slightly with increased CO₂ flow (Fig 22, right). Important for the selection of process parameters are the initial ratio of water and the mixture of carbon dioxide/co-solvent in respect to their solubility in the liquid phase.

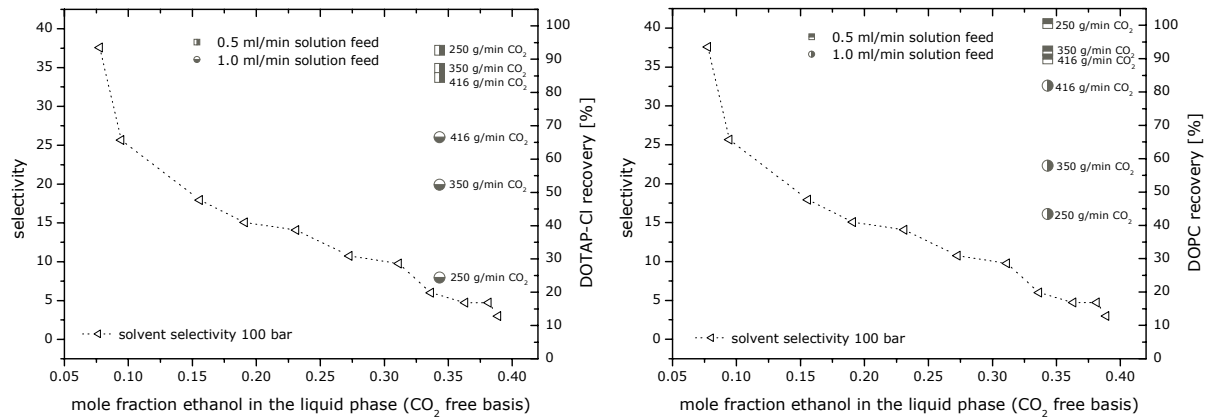


Figure 22: Solvent selectivity for the CO₂-C₂H₅OH-H₂O ternary system for 100 bar at 40°C [23] compared to the lipid recovery at different carbon dioxide flow rates of 250, 350 and 416 g/min and different lipids DOTAP-Cl (left) and DOPC (right).

3.3 PHASE DIAGRAMS FOR METHANOL, ETHANOL, ISOPROPANOL AND ACETONE

The choice of co-solvent for the supercritical fluid drying of an aqueous solution was a key parameter controlling solute solubility, particle morphology and size. The used systems were not fully miscible with water and selected process conditions were used to modify the working regions (Fig 23). The expanded solvents have potential to further increase the solubility of water, as well as that of the components in the supercritical phase and thereby enhance the mass transfer [61]. Extended ternary phase equilibrium data of the carbon dioxide / water mixtures and the used solvents ethanol and acetone are shown in Figure 23 (A) and (C). For methanol only limited data are available (Fig 23, (B)). For isopropanol only the phase equilibrium data were plotted because of the complicated unclear phase behavior (Fig 23, (D)) [62]. However, it can be assumed that the experiments were done under supercritical conditions in a one phase region. The different phase behaviors resulted in varied solubilities of co-solvent/carbon-dioxide within the aqueous droplets and therefore influenced the particle size distribution. The

working region was selected with respect to the critical point of the mixture, so that the experiments were done under ideal drying properties.

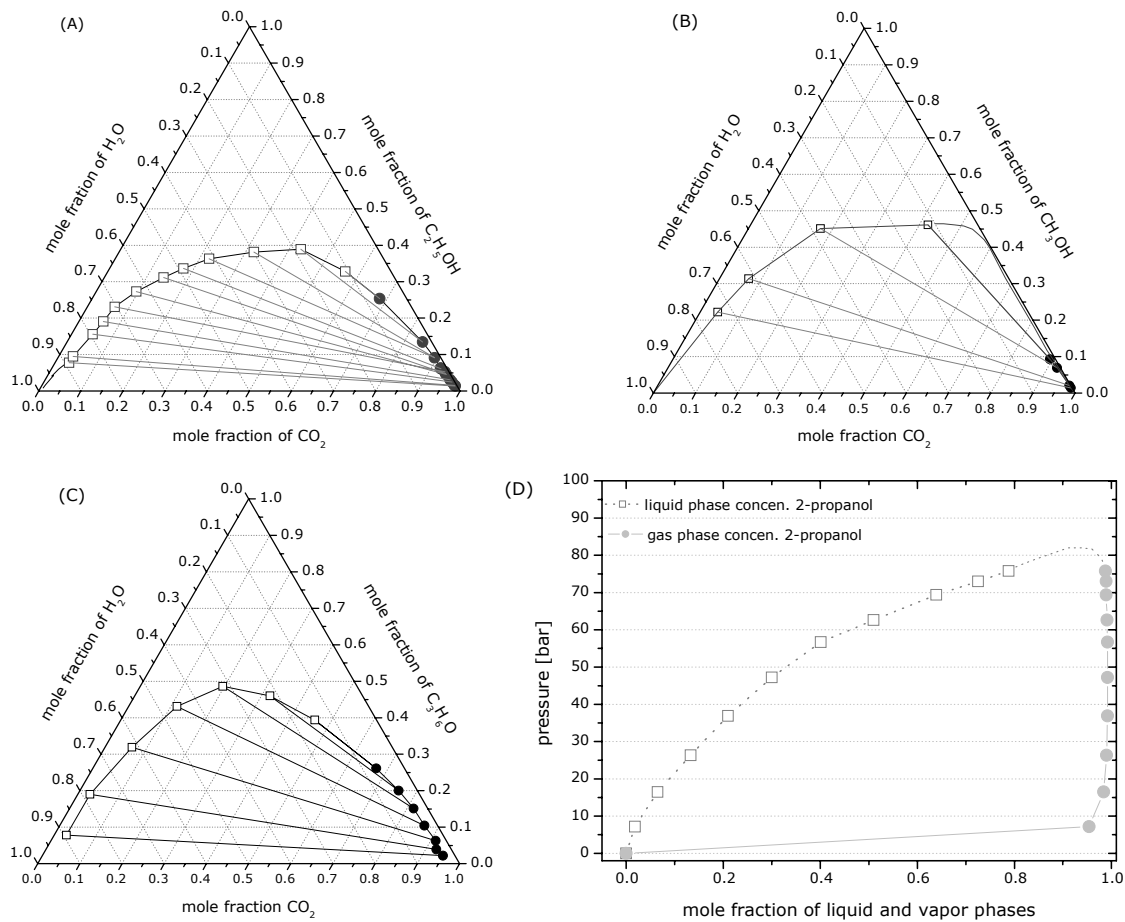


Figure 23: Ternary diagram at 40°C at 100 bar for the CO₂, ethanol (A) [50], methanol (B) [63], acetone (C) [64] and H₂O system using the light square as SCF and the dark circle as liquid molar fraction, respectively. Vapor-liquid equilibria of CO₂-isopropanol at 40°C (D) [65].

3.3.1 Particle morphology

The different co-solvent carbon dioxide mixtures were examined using the concentric coaxial nozzle (Tab 12). The impact on solvent polarity, dielectric constant and vapor pressure on the particle properties was studied.

Table 12: Summarizing the drying capacity diagram of the CO₂-solvent-water system at 100 bar using methanol, acetone or isopropanol at a 0.5 ml/min solution feed rate and CO₂ mass flow rates of 250 g/min.

nozzle type	solvent type	mol solvent		dielectric constant (ϵ)	dipole moment
		mol solvent + mol CO ₂	mol H ₂ O + mol CO ₂		
concen	methanol	0.12100	0.00595	33.0	1.70
concen	ethanol	0.08775	0.00618	25.3	1.69
concen	acetone	0.06822	0.00631	21.0	2.88
concen	isopropanol	0.07083	0.00629	18.1	1.66

All obtained particles were spherical with a porous structure (Fig 24). The surface of particles dried with methanol was rougher compared to the others. The diffusion of CO₂ and solvent into the droplet depended on the expansion of polar organic solvents and processing pressure. Polar organic solvents and solvents possessing low vapor pressure usually do not expand rapidly and/or completely in supercritical carbon dioxide at high pressure [66].

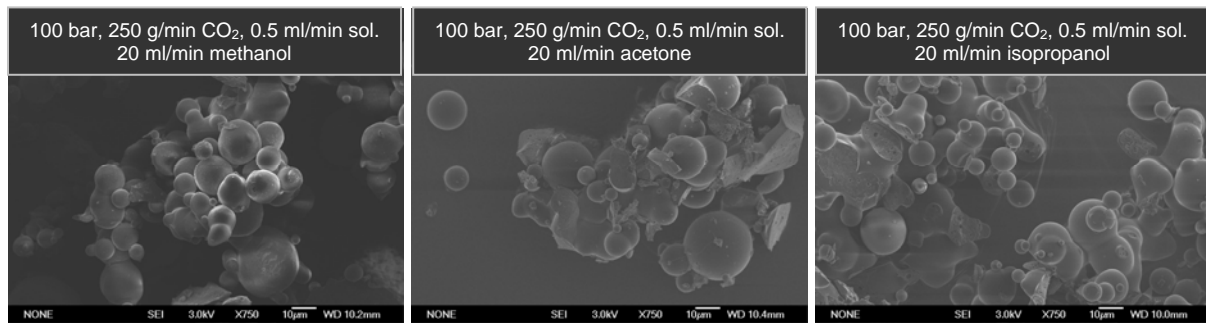


Figure 24: SEM pictures of supercritically spray-dried powders at 100 bar with methanol, acetone and isopropanol at a solvent flow rate of 20 ml/min using the concentric coaxial nozzle and 250 g/min carbon dioxide flow rates and a solvent flow rate of 0.5 ml/min.

3.3.2 Particle size distribution

The experiments revealed that incomplete expansion of the solvents influenced the saturation level of the solutions in the droplets and led to precipitates with larger particle size (Tab 13). When using methanol or ethanol as a co-solvent very small particles ($d[4,3] = 20.9 \mu\text{m}$ and $16.9 \mu\text{m}$) with the widest and the most narrow size distribution (span 4.2 and 1.9) were obtained. Both were fully soluble into water, which can help to enhance the extraction forces.

Table 13: Particle size using the concentric coaxial nozzle with methanol, ethanol, acetone and isopropanol at a pressure as co-solvents dried at a pressure of 100 bar with 250 g/min carbon dioxide flow with a solvent flow rate of 20 ml/min and a solution rate of 0.5 ml/min.

nozzle type	CO ₂ [g/min]	solvent type	solvent [ml/min]	solution [ml/min]	d[10] [µm]	d[50] [µm]	d[90] [µm]	d[4,3] [µm]	span
concen.	250	methanol	20	0.5	3.3	12.1	54.5	20.9	4.2
concen.	250	ethanol	20	0.5	4.5	12.2	27.7	16.2	1.9
concen.	250	acetone	20	0.5	6.0	30.4	85.3	38.8	2.6
concen.	250	isopropanol	20	0.5	6.2	43.5	120.8	54.1	2.6

Methanol has the highest dielectric constant value (ϵ) of 33.0 and raised the solubility of water and lipids within CO₂. Ethanol, with a dielectric constant value of 25.3, appeared to be most effective in reducing the particle size ($d[4,3] = 16.2$). Acetone also has a high

dielectric constant value of 21.0 comparable to isopropanol with 18.1. The medium size rose to 38.8 and 54.1 μm . From the results it can be concluded that the particle size increased with decreasing dielectric constant value. The higher the dielectric constant of the co-solvent the more improved was the capacity to form hydrogen bonds and the better was the miscibility with water. This favored the anti-solvent effect during swelling, and led to smaller particles.

3.3.3 Yield and residual moisture

With decreasing particle sizes the residual moisture was reduced (Tab 14). In correspondence with the evaporation rate of the co-solvents also the high methanol mole fraction-water ratio did not reduce the moisture content below 4.1 %. Isopropanol was also not able to enhance the evaporation forces compared to ethanol resulting in a residual moisture of 4.3 %. Acetone resulted in a moisture content of 3.4 % with the lowest mole fraction ratio solvent-water. The miscibility (phase equilibrium) of water in carbon dioxide was enhanced when using acetone compared to isopropanol. The resulting yield was increased by the efficient drying process (Tab 14). For the optimized ethanol conditions a residual moisture content of 1.9 with a yield of 95 % could be obtained.

Table 14: Residual moisture and powder yield of particles obtained with different co-solvents.

nozzle type	pressure [bar]	CO₂ [g/min]	solvent type	solvent [ml/min]	solution [ml/min]	residual moisture [%]	yield [%]
concen.	100	250	methanol	20	0.5	4.1	72
concen.	100	250	ethanol	20	0.5	1.9	95
concen.	100	250	acetone	20	0.5	3.4	84
concen.	100	250	isopropanol	20	0.5	4.3	73

3.3.4 Residual solvents

Two factors mainly influenced the particle formation using the solvents methanol, ethanol, isopropanol and acetone, namely the dielectric constant value and the vapor pressure. After the addition of a polar co-solvent the zero net dipole moment of carbon dioxide changed and the solubility of water increased. This becomes obvious when comparing its solubility in methanol and acetone versus its solubility in isopropanol and ethanol (Fig 25, left). Methanol as co-solvent evaporates to a higher extent into the droplets and remains associated to the trehalose. This resulted in a high residual methanol content of 6500 ppm even higher compared to the concentration of ethanol (Fig 25, right).

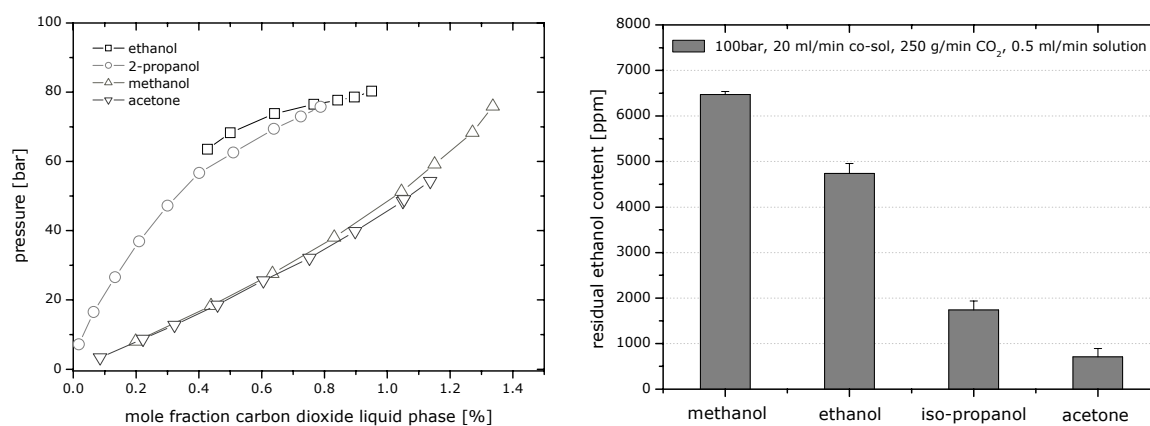


Figure 25: The solubility of carbon dioxide in the mixtures of water and co-solvent (ethanol [50], isopropanol [50], methanol* [67], acetone* [68], (*mole fraction of the co-solvent within the CO₂)) (left), and the residual solvent concentration of supercritically spray-dried particles using the concentric coaxial nozzle (right).

This could be explained by the high mole fraction ratio of solvent-water (0.121 to 0.005) and the excellent solubility of methanol in carbon dioxide and water. The acetone-water ratio was lower (0.068 to 0.006) and resulted in residual acetone contents below 1000 ppm. Drying with isopropanol-water at a ratio between 0.071 and 0.006 resulted in residual isopropanol concentrations below 2000 ppm. The solubility of the co-solvents and the carbon dioxide in the droplets were responsible for the residual solvent contents. The extraction of solvents via the final washing step could directly be correlated to the solubility of the co-solvents in the gaseous phase. The solubility behavior of the co-solvents influences the mass transfer and reached the gaseous phase earlier with the consequence of having less residual solvent in the product. One should consider to select a co-solvent which exhibits an optimized solubility in supercritical carbon dioxide and at the same time provides a reduced solubility for the compounds. For the tested co-solvents acetone was most appropriate.

3.3.5 DSC and X-ray powder diffraction

The particles dried with the co-solvents acetone, isopropanol and methanol were amorphous, although the residual moisture of about 4 % was relatively high. The local structure in the amorphous phase obvious by differences in the broad halo was affected by the selected solvent and indicated differences in swelling and evaporation behavior (Fig 26, left). DSC measurements reflected the influence of the co-solvent and the residual moisture content (Fig 26, right). Methanol as a co-solvent led to a residual moisture above 4 % and a T_g of 34.1°C for the dried particles. Using acetone and

isopropanol as co-solvent led to low moisture content around 3 % and resulted in a T_g of 46.8 and 54.3°C.

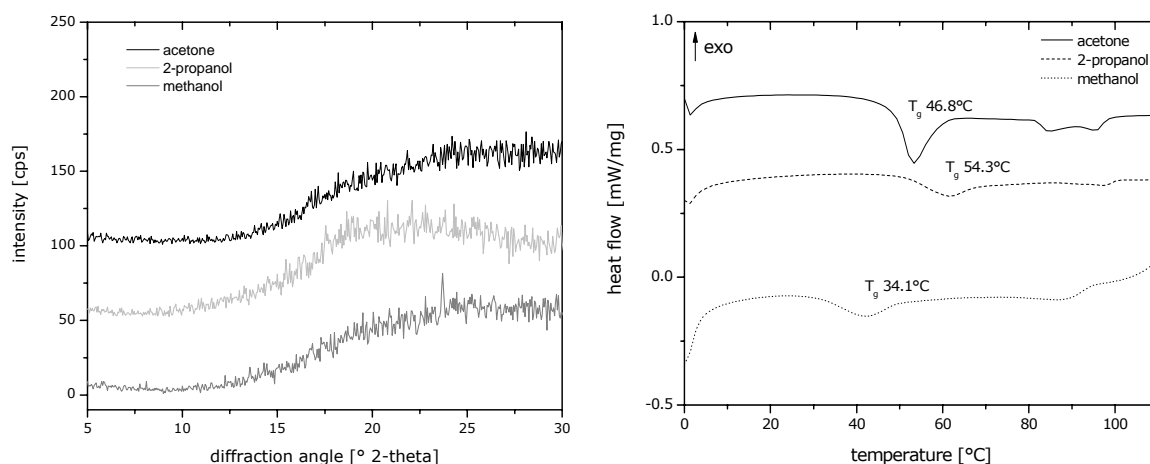


Figure 26: Wide-angle X-ray diffraction pattern after supercritical spray-drying of liposomes using co-solvents at 100 bar and 250 g/min carbon dioxide (left), and DSC thermograms (right).

3.3.6 Liposome size and lipid recovery

The effect of the solubility of the co-solvents methanol, ethanol, isopropanol and acetone in CO_2 on the liposome properties was tested. The liposome size was retained with a polydispersity of 0.1 when using acetone as co-solvent. The other co-solvents negatively affected the liposomal size distribution (Fig 27, left). Almost all lipids were extracted when using methanol as co-solvent. Methanol exhibits the highest dielectric constant, which makes it a good solvent also for the lipids, resulting in the low lipid recovery. When using ethanol the lipid recovery of DOTAP-Cl and DOPC differed because of the different solubility of the lipids within ethanol, as discussed before. For isopropanol a higher solubility of DOTAP compared to DOPC was observed, too. Furthermore, the declined lipid recovery of about 60 % pointed at a selective solubility of the lipids in isopropanol. The phase behavior and the potential ability of isopropanol to form four phases within supercritical carbon dioxide made any interpretation difficult. Only acetone exhibited no differences in lipid solubility for both liposome components with a high recovery (Fig 27, right).

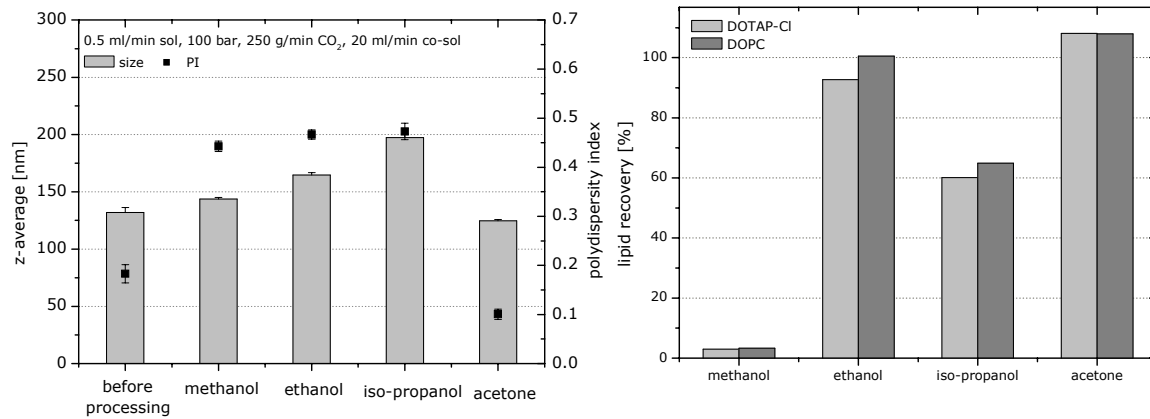


Figure 27: Liposome size and polydispersity index (left) and lipid recovery (right) after supercritical spray-drying of liposomes suspensions at 100 bar using different co-solvents with a flow rate of 20 ml/min and 0.5 ml/min solution flow rate at a carbon dioxide flow-rate of 250 g/min.

The further improved ratio between supercritical fluid and liquid feed rate, as well the solubility of carbon dioxide in the liquid phase is responsible for the results. The viscosity and thereby the solvating power of CO_2 changed by the addition of co-solvents [69]. With increasing molecular mass of the co-solvent the attraction forces and their solubility in the supercritical fluid increases via hydrogen bonds [70].

3.4 PARTICLE FORMATION WITHOUT A CO-SOLVENT

The mixing behavior of water in the compressed carbon dioxide phase is highly non-ideal [71]. The mutual solubility of water in the carbon dioxide rich phase is very low with 4.280×10^{-3} mol % as described by Spycher et al. (2003) [39]. Based on the data obtained during the process development higher ratios of carbon dioxide to the liquid feed the phase behavior and limited solubility was adjusted. The influence of CO_2 on the solubility of the compounds in the supercritical phase was further determined. By using the different carbon dioxide flow rates of 250, 350 and 416 g/min and a constant liquid feed of 0.25 ml/min the mole fractions of water in supercritical carbon dioxide were 3.386×10^{-3} , 2.418×10^{-3} and 2.035×10^{-3} mol %, respectively, which are below the critical mutual solubility of water in CO_2 . Based on this calculation a drying of the aqueous formulation was investigated.

3.4.1 Particle morphology

The concentric coaxial nozzle, which has already shown optimized saturation levels by the addition of co-solvents to the carbon dioxide, was applied. For the chosen experimental conditions spherical, hollow and smooth particles were obtained for all water mole fractions in CO₂ (Fig 28). Due to the selected mutual water solubility a supercritical drying was feasible without further co-solvents.

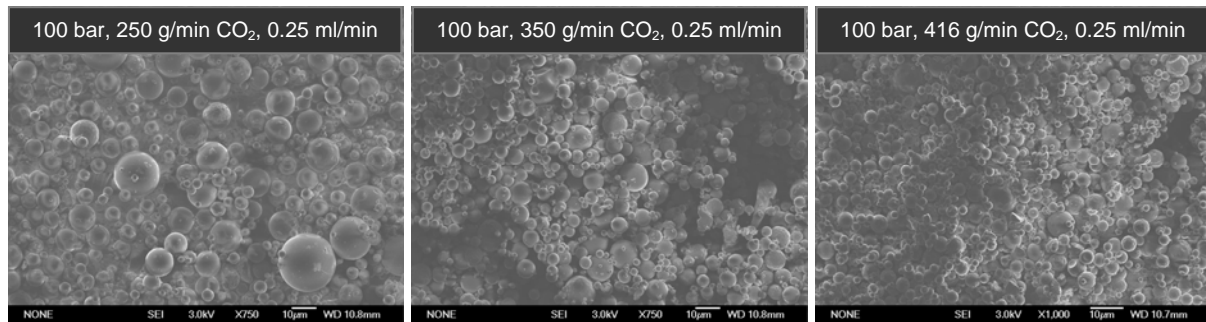


Figure 28: SEM pictures of supercritically spray-dried powders without the addition of a co-solvent at 100 bar using the concentric coaxial nozzle and different carbon dioxide flow rates of 250, 350 and 416 g/min with a solution flow rates of 0.25 ml/min.

3.4.2 Particle size distribution

At a low mixing energy and a reduced allocated carbon dioxide concentration, in our case 250 g/min CO₂, the direct consequence of the mole fraction water was agglomeration, leading to increased particle sizes (Tab 15). At a carbon dioxide flow of 350 and 416 g/min very small particles of about 6 µm with a narrow size distribution (span of 1.4 and 1.3) were collected. Only slight swelling occurred due to the lack of co-solvents and the low solubility of carbon dioxide in water. The particle size distribution was mainly influenced by the initial droplet size, which is a result of the high atomizing energy of the larger CO₂ flow rate compared to the reduced liquid feed rate.

Table 15: Particle size diameter using the concentric coaxial nozzle without any co-solvent at a pressure of 100 bar with 250, 350 and 416 g/min carbon dioxide flow with a solution rate of 0.25 ml/min.

nozzle type	pressure [bar]	CO ₂ [g/min]	solution [ml/min]	d[10] [µm]	d[50] [µm]	d[90] [µm]	d[4,3] [µm]	span
concen.	100	250	0.25	3.3	12.6	46.2	20.1	3.3
concen.	100	350	0.25	2.6	5.5	10.6	6.2	1.4
concen.	100	416	0.25	2.7	5.2	10.2	6.3	1.3

3.4.3 Yield and residual moisture

The moisture content was dependent on the mole fraction of carbon dioxide. With an increasing mole fraction of CO₂ the droplet size was reduced and correspondingly the residual moisture decreased from 3.6 % at 250 g/min CO₂ to 1.7 % at 416 g/min CO₂ (Tab 16). The particle yield above 80 % was indicative for a feasible drying procedure.

Table 16: Residual moisture and powder yield of particles obtained at different carbon dioxide flow rates without any co-solvents.

nozzle type	pressure [bar]	CO ₂ [g/min]	solution [ml/min]	residual moisture [%]	yield [%]
concen.	100	250	0.25	3.6	81
concen.	100	350	0.25	2.5	80
concen.	100	416	0.25	1.7	84

3.4.4 DSC and X-ray powder diffraction

As a reference the X-ray diffractogram pattern of crystalline dihydrate trehalose is shown in figure 29 together with the particles dried at 100 bar. The additional ethanol flow rate of 20 ml/min, which was used at the 1.0 ml/min solution feed, resulted in few low intensity peaks in the XRD diffraction pattern indicating a partially crystalline state. DSC revealed a T_g at 48.8°C followed by an exothermic crystallization peak at about 70°C and an endothermic peak around 100°C, which is indicative for the presence of amorphous trehalose in the sample. Without co-solvent and a higher mole fraction of carbon dioxide the drying process was feasible resulted in amorphous structure determined by XRD (Fig 29, left). These findings were supported by DSC measurements with a T_g of 51.9°C (Fig 29, right).

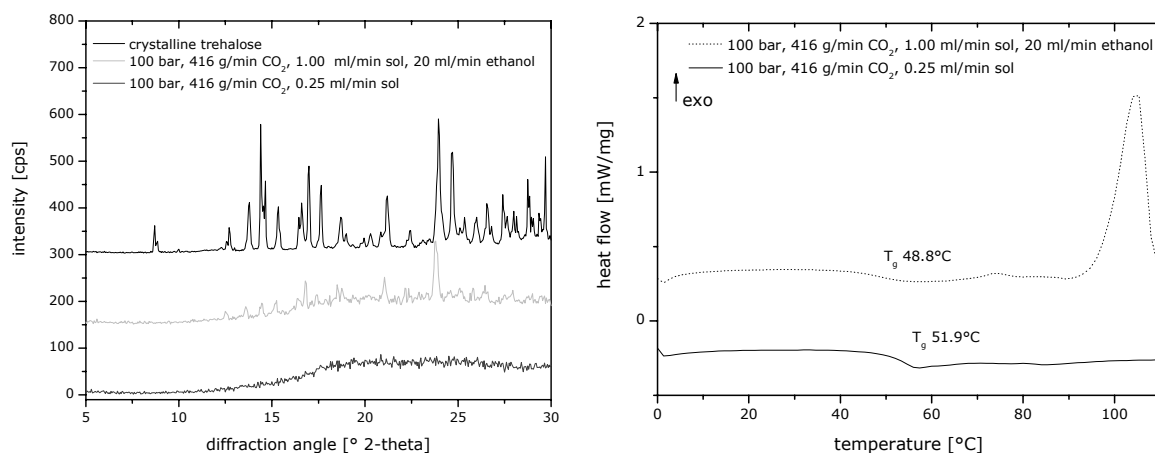


Figure 29: Wide-angle X-ray diffraction pattern after supercritical spray-drying of liposomes at 100 bar using 416 g/min carbon dioxide (left) and the corresponding DSC thermograms (right).

3.4.5 Liposomes size and lipid recovery

Without co-solvent in the supercritical carbon dioxide phase the drying procedure was feasible at reduced aqueous feed rate. A dry product was obtained and the liposome properties were preserved at different carbon dioxide flow rates. The polydispersity indices were comparable to those before processing (Fig 30, left). For low carbon dioxide flow rates they even could be improved to 0.12 with lipid recoveries of above 100 % for all investigated process conditions (Fig 30, right). At the low density and pressure of 100 bar the evaporation forces of carbon dioxide were further improved by the reduction of the liquid feed to 0.25 ml/min. The ratio CO₂-water must be increased because of the mutual solubility within CO₂-water without addition of a co-solvent. Without a co-solvent the solubility of the lipids in carbon dioxide could be neglected.

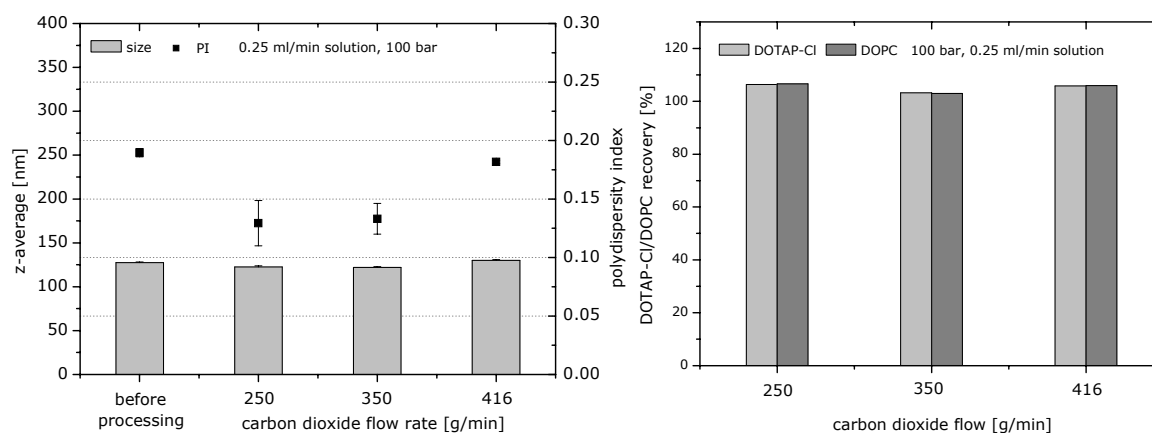


Figure 30: Liposome size and polydispersity index (left) and lipid recovery (right) after supercritical-spray-drying of liposome suspensions at 100 bar without co-solvents with a solution flow rate of 0.25 ml/min solution at different carbon dioxide flow-rates.

3.5 PARTICLE FORMATION WITHOUT A CO-SOLVENT UNDER DIFFERENT PRESSURES

The successful particle formation process without the addition of an organic co-solvent to the carbon dioxide was further investigated at different pressure. Previous studies revealed no significant differences in particle morphology and size distribution over a wide temperature range of 31 to 40°C as shown by Werling and Debenedetti (1999) [29]. Pressure has a more pronounced impact on particle morphology than temperature. By varying the pressure, the phase behavior of the supercritical fluid was changed. The mole fraction of water was predetermined and the water solubility in the carbon dioxide increased with density (Tab 17).

Table 17: Density and mole fraction water in CO₂ used at different pressure and anti-solvent flow rates.

nozzle type	pressure [bar]	CO ₂ [g/min]	solution [ml/min]	density CO ₂ [g/ml]	mol fraction water in CO ₂	solubility of water in CO ₂ [mol %] [36]
concen.	80	250	0.25	0.278	7.649×10^{-3}	-
concen.	100	250	0.25	0.628	3.384×10^{-3}	4.28×10^{-3}
concen.	150	250	0.25	0.781	2.723×10^{-3}	5.07×10^{-3}
concen.	100	416	0.25	0.628	2.035×10^{-3}	-
concen.	150	416	0.25	0.781	1.636×10^{-3}	-
concen.	170	416	0.25	0.808	1.581×10^{-3}	5.80×10^{-3}

3.5.1 Particle morphology

Figure 31 shows the influence of pressure on particle morphology. At a constant temperature the coexisting phases were reduced when the pressure increased. The solvent strength (miscibility and solubility) of carbon dioxide was raised when increasing the density of the supercritical fluid with pressure, which resulted in a wider working range. With increasing pressure the mutual solubility of water in the CO₂ rich phase changed from 4.28×10^{-3} mol % at 100 bar to 5.07×10^{-3} mol % at 150 bar and to 5.43×10^{-3} mol % at 170 bar, respectively.

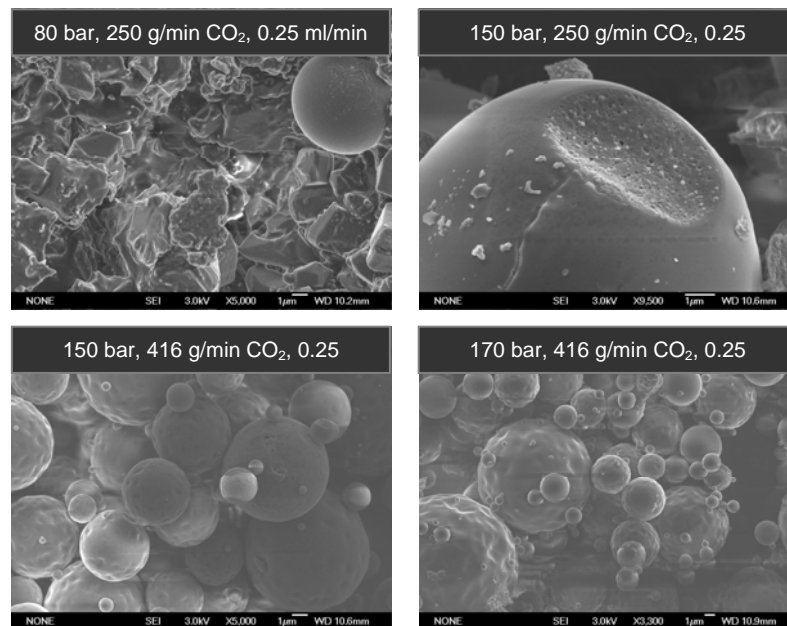


Figure 31: SEM pictures of supercritically spray-dried powders without the addition of a co-solvent at different pressure using the concentric coaxial nozzle and carbon dioxide flow rates of 250 and 416 g/min with a solution flow rates of 0.25 ml/min.

At 80 bar just above the saturation pressure the particle formation process was depressed. The mole fraction of water (7.649×10^{-3}) in the experiments was too high for sufficient evaporation and saturation levels of carbon dioxide in the droplets. The

probably existing two phase scenario with partial phase boundary between the carbon dioxide and the solution resulted in droplets and a mass transfer through the interface. After adjusting the pressure below the solubility level spherical and porous particles were obtained at 250 g/min CO₂ flow rate at 150 bar. With increasing carbon dioxide flow rate and pressure particle morphology changed to golf ball-like structures. This might be induced by a high mass transfer rate of CO₂ into the particles and by a faster water extraction out of the particles. Thereby, larger pores formed and after final extraction the capillary tension induced slight shrinkage resulting in this surface structure.

3.5.2 Particle size distribution

At a low mixing energy, in our case 250 g/min CO₂ at 80 bar, no direct particle formation occurred. Fragments of particles and droplets dried partially and agglomerated at the filter plate. The low feed rate of carbon dioxide mainly condensed onto the droplet surfaces and their size increased (Tab 18). At higher pressure and the related density change, the spherical size of the particles was retained, but agglomeration could be observed as well. The carbon dioxide / water ratio was still too low, although the density change reduced the water mole fraction below the mutual solubility. At the higher pressure the improved mixing energies at CO₂ flow rates of 350 and 416 g/min very small particles of about 11 µm with a narrow size distribution were collected. The evaporation ratio of the solvent became more important and the size of the droplets decreased.

Table 18: Particle size diameter using the concentric coaxial nozzle without any co-solvent at pressures of 80, and 150 bar with 250 g/min carbon dioxide flow and at pressures of 150 and 170 bar with 416 g/min carbon dioxide flow with a solution rate of 0.25 ml/min.

nozzle type	pressure [bar]	CO₂ [g/min]	solution [ml/min]	d[10] [µm]	d[50] [µm]	d[90] [µm]	d[4,3] [µm]	span
concen.	80	250	0.25	3.1	13.8	63.3	24.3	4.4
concen.	150	250	0.25	4.8	24.2	115.1	44.8	4.5
concen.	150	416	0.25	2.9	8.6	19.3	11.5	1.9
concen.	170	416	0.25	2.8	7.8	17.1	10.5	1.8

3.5.3 Yield and residual moisture

Evaporation of water was affected by the pressure and the mixing energy of the fluids assigned by the mole fraction value. At a low pressure, especially close to the supercritical point of carbon dioxide, drying of the droplets resulted in high moisture contents of 9.8 % (Tab 19). An increased pressure on the other hand enhanced the evaporation of water. Higher mole fraction CO₂ of 416 g/min and the reduced liquid feed rate favored the miscibility of water, because of higher atomization forces and smaller droplets. The product yield showed values around 60 % and could not be improved compared to lower pressures.

Table 19: Residual moisture and powder yield of particles obtained at different pressure without any co-solvent.

nozzle type	pressure [bar]	CO ₂ [g/min]	solution [ml/min]	residual moisture [%]	yield [%]
concen.	80	250	0.25	9.8	49
concen.	150	250	0.25	5.8	70
concen.	150	416	0.25	2.8	59
concen.	170	416	0.25	3.7	61

3.5.4 Liposome size and lipid recovery

With increased pressure the mutual water solubility in CO₂ and the evaporation raised. Experiments were conducted by varying pressure between 80 and 170 bar. The liposome size and polydispersity were negatively affected at a low pressure of 80 bar. Just above the critical point the water solubility and drying performance were insufficient. However, at 150 and 170 bar the liposome properties and the lipid recovery were preserved at the tested conditions (Tab 20). A raised solubility of the lipids with increasing pressure and density, which was observed when adding organic co-solvents, could not be confirmed in pure carbon dioxide.

Table 20: Liposome properties and lipid recovery obtained at different pressure without any co-solvents.

nozzle type	pressure [bar]	CO ₂ [g/min]	z-average [nm]	polydispersity index	DOTAP-Cl [%]	DOPC [%]
concen.	80	250	176 +/- 1.5	0.44 +/- 0.03	63.3	64.9
concen.	150	250	118 +/- 1.1	0.13 +/- 0.01	100.1	100.0
concen.	150	416	117 +/- 1.5	0.10 +/- 0.01	108.0	107.7
concen.	170	416	116 +/- 0.5	0.13 +/- 0.01	105.1	105.0

3.6 PARTICLE FORMATION USING SUBCRITICAL CONDITIONS

3.6.1 Particle morphology

It has been proposed that the hydrodynamic effect, the mixing of two miscible fluids, was generally the dominant factor for precipitation under subcritical conditions. Particles were generated by diffusion of CO₂ into the droplets and jet break-up, followed by extraction of the solvent from the droplet resulting in dry powder formation [46]. In consideration of the phase behavior, the settings were adjusted to achieve sufficient nucleation by reducing the liquid feed rate to 0.11 ml/min and increasing the CO₂ flow rate to 500 g/min CO₂. Spherical and hollow particles were obtained for the gravity nozzle and the concentric nozzle (Fig 32).

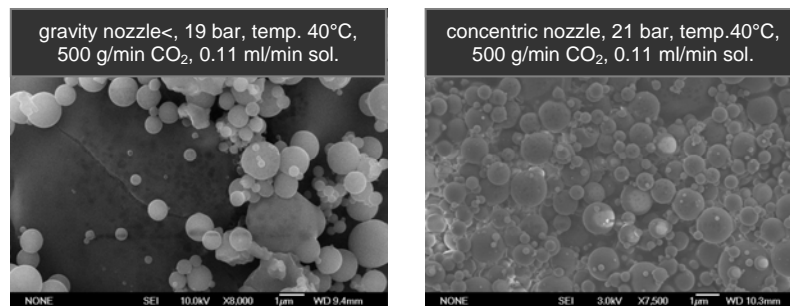


Figure 32: SEM pictures of subcritically spray-dried powders without the addition of a co-solvent using the gravity and concentric coaxial nozzle at a carbon dioxide flow rate of 500 g/min with a solution flow rates of 0.11 ml/min.

3.6.2 Particle size distribution

The concentric coaxial nozzle resulted in smaller particles with a medium size of 31.5 μm compared to 52.1 μm for the gravity coaxial nozzle (Tab 21). No strong agglomeration effects were detected, which was indicated by the low span value. An initially increased droplet diameter due the condensation of CO₂ should be considered during subcritical drying [30]. The different atomization of CO₂ and the liquid feed affected first of all the droplet size and finally the drying behavior of the droplets.

Table 21: Particle size diameter using the gravity and concentric coaxial nozzle at subcritical conditions of 19 and 20 bar with 500 g/min carbon dioxide flow and a solution rate of 0.11 ml/min.

nozzle type	pressure [bar]	temp. [°C]	CO ₂ [g/min]	solution [ml/min]	d[10] [μm]	d[50] [μm]	d[90] [μm]	d[4,3] [μm]	span
gravity	19	40	500	0.11	11.4	45.4	79.4	52.1	2.0
concen.	21	40	500	0.11	5.0	25.6	66.5	31.5	2.4

3.6.3 Yield and residual moisture

The nozzle configuration and therefore the droplet size distribution and the mass transfer properties resulted in different moisture contents. Higher mass transfer of water in the subcritical region due to optimized droplet distributions resulted in an evaporation strength high enough to reduce the moisture to 3 % (Tab 22). Particles produced with the concentric coaxial nozzle had a moisture content of 4.3 %. A further reduction is feasible by reducing the droplet size at higher atomization forces of carbon dioxide and reduced liquid feed rates. Both strategies consider the solubility of water in the gaseous phase. A sufficient yield between 77 and 80 % was found as the pressure drop between filter plate and outlet valve was prevented. Furthermore, small particles were not pressed through the filter. Also no residual ethanol was detectable.

Table 22: Residual moisture and powder yield of particles obtained at subcritical conditions.

nozzle type	pressure [bar]	CO ₂ [g/min]	solution [ml/min]	residual moisture [%]	yield [%]
gravity	19	500	0.11	3.1	80
concen.	21	500	0.11	4.3	77

3.6.4 DSC and X-ray powder diffraction

Under subcritical conditions at around 20 bar with relatively low water mole fractions and high carbon dioxide flows the amorphous structure of the powder was preserved (Fig 33, left). Drying levels were reached with residual moisture of about 3 to 4 % for particles produced by the concentric co-axial nozzle, which affected the glass transition temperature (Fig 33, right).

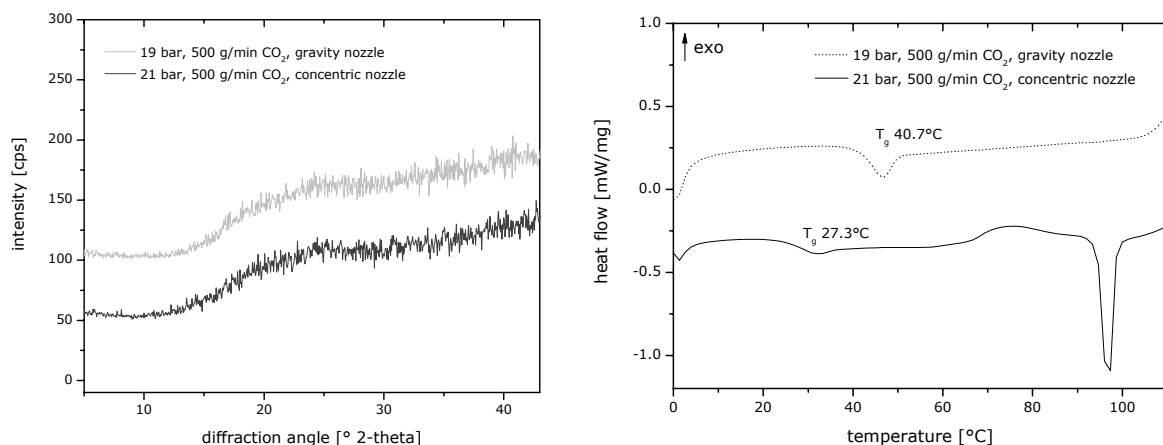


Figure 33: Wide angle X-ray diffraction pattern (left) and DSC thermograms (right) after subcritical spray-drying of liposomes at 19 and 20 bar using 500 g/min carbon dioxide and the gravity and concentric coaxial nozzle.

3.6.5 Liposome size and lipid recovery

At subcritical conditions at a pressure below the critical point the collection of dry particles with favorable liposome properties and lipid recoveries was feasible (Tab 23). The major advantages of drying with a subcritical gaseous phase were the low pressure and the reduced extraction forces of lipids. However, at such conditions the water-CO₂ ratio should be selected very low to overcome the mutual solubility.

Table 23: Liposome properties and lipid recovery of particles obtained at subcritical conditions using a CO₂ flow rate of 500 g/min with a solution feed of 0.11 ml/min.

nozzle type	pressure [bar]	z-average [nm]	polydispersity index	DOTAP-Cl [%]	DOPC [%]
gravity	19	120 +/- 1.5	0.15 +/- 0.01	104.9	103.8
concen.	21	118 +/- 0.1	0.15 +/- 0.02	101.6	101.3

3.7 DRUG LOADING STUDIES

The drug loading studies of liposomes were carried out with the model compounds Coumarin and Nile Red. According to literature solubility of Coumarin is depended on pressure and temperature (Fig 34, left) [72]. No solubility data are so far available for Nile Red. Due to the relatively low solubility of Coumarin within the supercritical carbon dioxide and due to the substantial hydrophobicity of Nile Red these two fluorescent dyes were chosen as model substances. These two model compounds were used as model substances for Paclitaxel, for which the solubility at our temperature and pressure conditions were significantly lower as compared to Coumarin (Fig 34, right) [73].

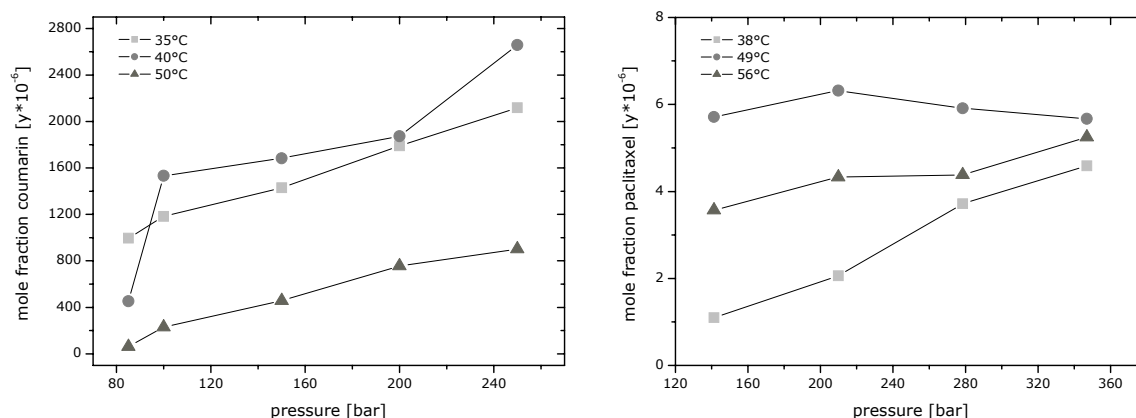


Figure 34: Coumarin [72] and Paclitaxel [73] solubility in supercritical carbon dioxide at different temperatures.

3.7.1 Drug loading gravity feed nozzle

After reconstitution of the particles produced by the coaxial feed nozzle the Coumarin recovery was 100 % for particles collected from the filter plate, while a slight reduction was measured for particles from the wall. Although the lipid extraction was pronounced at these conditions the Coumarin recovery was nearly completed (Tab 24).

Table 24: Coumarin recovery for supercritically spray-dried particles using the coaxial gravity feed nozzle with different trehalose concentrations 5, 10.5 and 15 % [w/v] at a pressure of 170 bar with 350 ml/min carbon dioxide flow with an ethanol flow rate of 30 ml/min and a solution rate of 1.0 ml/min.

trehalose [w/v]	nozzle type	particle collection	pressure [bar]	CO ₂ [g/min]	ethanol [ml/min]	solution [ml/min]	Coumarin recovery [%]
5.0	gravity	wall	170	350	30	1.0	94.0
5.0	gravity	filter	170	350	30	1.0	100.4
10.5	gravity	wall	170	350	30	1.0	97.0
10.5	gravity	filter	170	350	30	1.0	100.8
15.0	gravity	wall	170	350	30	1.0	97.9
15.0	gravity	filter	170	350	30	1.0	100.2

3.7.2 Drug loading without co-solvents

Without the addition of a co-solvent a significantly reduced Coumarin recovery of about 60 % was found at 100 bar (Fig 35, left), although the lipid recovery revealed no distinct solubility of the lipids in the subcritical phase. Without co-solvent addition the extraction of Coumarin was raised due to changed evaporation mechanisms of the water. The drying procedure and saturation within the droplets was decelerated and extraction forces dissolved the fluorescent dye.

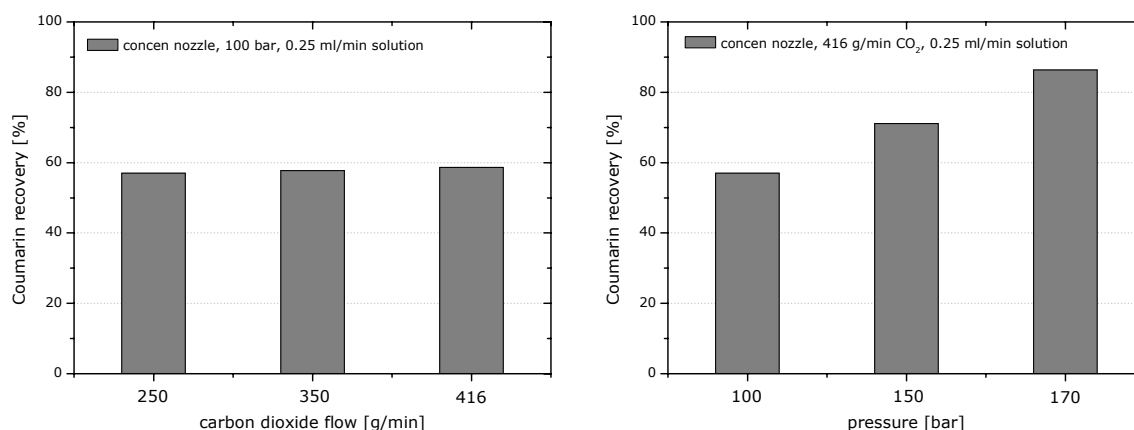


Figure 35: Coumarin recovery in supercritically spray-dried particles without any co-solvent at different carbon dioxide flow rates (left) and varied pressure (right).

However, with increased pressure the Coumarin content increased again and at 170 bar almost 90 % recovery was reached (Fig 35, right). At higher pressure the drying strength was reduced, because of an enlarged miscibility of water in the supercritical phase.

The fluorescence intensity of Nile Red depends on the polarity of the environment, with a higher intensity measured in more hydrophobic environments [74,75,76]. Therefore, the fluorescence intensity of Nile Red is increased when it is interacting with the apolar lipids of the liposomes [77]. In the presence of a co-solvent and carbon dioxide mixture Nile Red was dissolved completely out of the liposomes for all investigated processes conditions. This was indicated by a decrease in the spectral intensity as compared to the intensity before the drying process (Fig 36, left). Nile Red was soluble in pure carbon dioxide and in polar mixtures of supercritical fluids and co-solvents [78]. When using acetone as co-solvent slight Nile Red fluorescence intensity after supercritical drying was measured (Fig 36, right). Only acetone preserved the lipids during supercritical drying, due to the weak interactions between the lipid molecules and the solvent. The same effect can be used to describe this effect here.

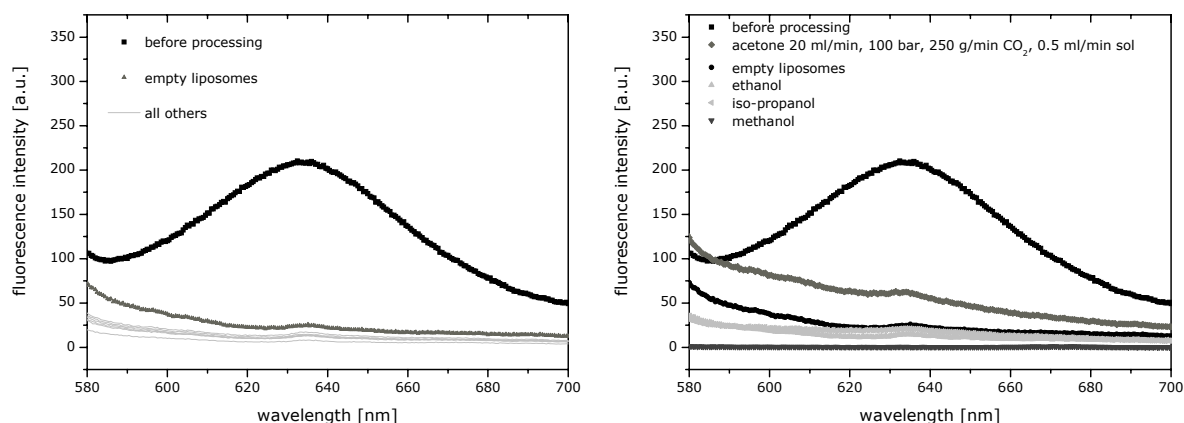


Figure 36: Fluorescence intensity of Nile Red loaded and empty liposomes after supercritical spray-drying at 100 bar, 20ml/min ethanol flow rate using 0.5 and 1.0 ml/min solution flow rate and different carbon dioxide flow rates of 250, 350 and 416 g/min (left) and at 100 bar using different co-solvents (right).

3.7.3 Drug loading at subcritical conditions

As the lipid solubility decreased under supercritical drying without any co-solvent, Nile Red was partially preserved as well (Fig 37, left). The evaporation of the carbon dioxide and hence the saturation was influenced by the droplet size induced by atomization force of the carbon dioxide. Without any additional co-solvent to the carbon dioxide the solubility was affected by the former described process. 350 g/min CO₂ showed optimum process conditions with respect to particle size distribution, liposome size and lipid

recovery. The particle formation process was fast enough and the extraction forces were reduced with minor miscibility of Nile Red. At subcritical conditions, the fluorescence intensity of Nile Red was preserved for both tested nozzles (Fig 37, right). The solubility of the fluorescent dye in the fluidized CO₂ could therefore be assigned as very low.

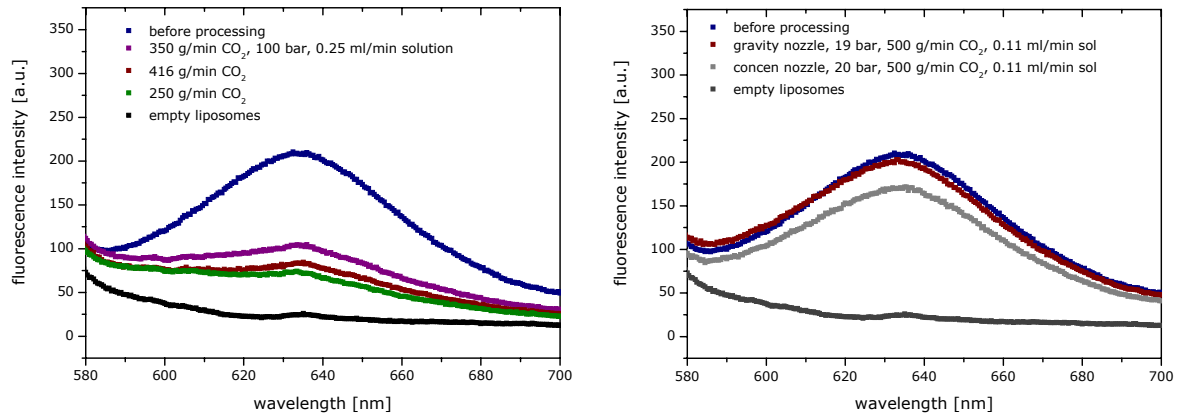


Figure 37: Fluorescence intensity of Nile Red loaded and empty liposomes after supercritical spray-drying at 100 bar without any co-solvent (left) and after subcritical spray-drying at 19 and 20 bar (right).

4. CONCLUSIONS

In the presented study different technical modifications using subcritical and supercritical carbon dioxide (CO₂), with and without co-solvents were carried out. The use of supercritical fluids to dry aqueous formulations containing liposomes was investigated because of the very gentle drying temperature around the critical point at 31°C and a pressure of 74 bar. The major limitation of this technique is the very low water solubility in supercritical CO₂. With a comprehensive particle formation and drying study, working conditions should be identified where the preservation of the liposomes was given. The major consideration was to increase the water solubility in the supercritical phase without affecting lipid recovery and liposome integrity. To overcome these limitations several factors, such as mass transfer of carbon dioxide and its thermodynamical behavior had to be optimized by selecting different flow rates, pressure and co-solvents. The addition of co-solvents to the supercritical CO₂ enhanced the solubility of water and allowed a more efficient drying process, but in contrast directly affected the liposomes due to the solubility of the lipids in the co-solvents. The comprehensive particle formation study was necessary, because of the difficult prediction for working regions suitable for aqueous suspensions. Only experimental drying studies based on the knowledge using organic solvents were available so far. Therefore, the addition of organic solvents to CO₂ was studied first, followed by the change and the omitting of co-solvents at supercritical and subcritical conditions.

To investigate the optimum mass transfer and spraying conditions from the various tested nozzle types and set-ups, only the concentric coaxial nozzle offered a sufficient high mass transfer of CO₂ into the liquid feed. The other nozzle types, co-solvent flow rates and pressures revealed either unsatisfactory particle formation properties or high lipid extraction capacities. This resulted always in a reduction of liposome quality, loss of material and high residual moisture content of the particles. For all further experiments only the concentric coaxial nozzle was used.

With the addition of the co-solvents methanol, ethanol, isopropanol and acetone the drying capacity increased, but only for acetone optimized liposome properties were obtained. The reduced solubility of lipids in acetone made this co-solvent a feasible alternative for working at higher liquid feed rates. On the other hand, without co-solvent the mass transfer of carbon dioxide must be enhanced by the reduction of liquid feed rate. Without co-solvent particle formation and liposome properties were exceptional whereby the lipid solubility in CO₂ can be completely neglected. The expected variation of lipid solubility at higher pressures was not present without co-solvent.

A new approach of subcritical drying at pressures around 20 bar, resulted in very homogenous liposomes and a narrow particle size distribution. Contrary to supercritical gases the subcritical condition allowed drug loading and full recovery of lipophilic model compounds. The drawback of such a technology is the very high carbon dioxide feed rate compared to a relatively low liquid flow rate, which is at least factor 2 slower than during supercritical drying.

Overall, the use of subcritical and supercritical CO₂ is an alternative drying approach at very gentle conditions method. As soon as appropriate working conditions are identified the process is a robust and consistent. Although Paclitaxel solubility data indicated a reduced solubility in CO₂ we were not able to confirm this data due to technical limitations. The loading of Paclitaxel followed by an economical assessment should be the next steps to finally evaluate this technique.

5. REFERENCES

-
- [1] Jung, J., Perrut, M., Particle design using supercritical fluids: literature and patent survey, *J. Supercrit. Fluids*, 20(3): 179-219, (2001).
- [2] Ribeiro Dos Santos, I., Richard, J., Pech, B., Thies, C., Benoit, J.P., Microencapsulation of protein particles within lipids using a novel supercritical fluid process, *Int. J. Pharm.*, 242(1-2): 69-78, (2002).
- [3] Bristow, S., Shekunov T., Shekunov, B.Y., York, P., Analysis of the supercritical and precipitation process with supercritical CO₂, *J. Supercrit. Fluids*, 21(3): 257-271, (2001).
- [4] Baldyga, J., Henczka, M., Shekunov, B.Y., Fluid dynamics, mass transfer, and particle formation, in supercritical fluids, in *Supercritical Fluid Technology for Drug Product Development*, (Eds, York. P., Kompella, U.B., Shekunov, B.Y.), vol 138: 91-158 (Marcel Dekker) (2004).
- [5] Debenedetti, P.G., Reid, R.C., Diffusion and mass transfer in supercritical fluids, *Amer. Inst. Chem. Eng. J.*, 32(12): 2034-2046 (1984).
- [6] Bustami, R.T., Chan, H-K., Dehghani, F., Foster, N.R., Recent applications of supercritical fluid technology to pharmaceutical powder systems, *Kona*, 19:57-69 (2001).
- [7] Clavier, J-Y., Perrut, M., Scale-up issues for supercritical fluid processing in compliance with GMP, in supercritical fluids, in *Supercritical Fluid Technology for Drug Product Development*, (Eds, York. P., Kompella, U.B., Shekunov, B.Y.), vol 138: 615-651 (Marcel Dekker) 2004.
- [8] Dixon, D.J., Johnston, K.P., Molecular thermodynamics of solubilities in gas antisolvent crystallization, *Amer. Inst. Chem. Eng. J.*, 37(10): 1441-1440 (1991).
- [9] Yeo, S.D., Lim, G.B., Debenedetti, P.G., Bernstein, H., Formation of microparticulate protein powders using a supercritical fluid antisolvent, *Biotechnol. Bioeng.*, 41(3): 341-346 (1993).
- [10] Kompella, U.B., Koushik, K., Preparation of drug delivery systems using supercritical fluid technology, *Crit. Rev. Ther. Drug Carrier System*, 18(2): 173-199, (2001).
- [11] Shekunov, B.Y., Chattopadhyay P., Seitzinger, J., Huff, R., Nanoparticle of poorly soluble drugs prepared by supercritical fluid extraction of emulsions, *Pharm. Res.*, 23(1): 196-204 (2005).
- [12] Randolph, T.W., Randolph, A.D., Mebes, M., Yeung, S., Sub-micrometersized biodegradable particles of poly(L-lactic acid) via the gas antisolvent spray precipitation process, *Biotechnol. Prog.*, 9(4): 429-435 (1993).
- [13] Dixon, D.J., Johnston, K.P., Bodmeier, R.A., Polymeric materials formed from precipitation with a compressed fluid antisolvent, *Amer. Inst. Chem. Eng. J.*, 39(1): 127-139 (1993).
- [14] Gallagher, P.M., Coffey, M.P., Krukonis, V.J., Hillstrom, W.N., Gas antisolvent recrystallization of RDX: Formation of ultra-fine particles of a difficult-to-comminute explosive, *J. Supercrit. Fluids*, 5(2): 130-142 (1992).
- [15] Altunin, V., Sakhabetdinov, M., Viscosity of liquid and gaseous carbon dioxide at temperatures 220-1300 K and pressures up to 1200 bar, *Teploenergetika*, 8: 85-89 (1972).
- [16] McHugh, M.A., Kurkonis, V.J., *Supercritical fluid extraction: principles and practice*, 2nd edition, Newton, Butterworth-Heinemann, (1994).
- [17] Palakodaty, S., York, P., Pritchard, J., *Supercritical Fluid Processing of Materials from Aqueous Solutions: The Application of SEDS to Lactose as a Model Substance*, *Pharm. Res.*, 15(12): 1835-1843, (1998).
- [18] King, M.B., Mubarak, A., Kim, J.D., Bott, T.R., The mutual solubilities of water in supercritical and liquid carbon dioxide, *J. Supercrit. Fluids*, 5(4): 296-302 (1992).
- [19] Bouchard, A., Jovanovic, N., Jiskoot, W., Mendes, E., Witkamp, G-J., Crommelin, D.J.A., Hofland, G.W., Lysozyme particle formation during supercritical fluid drying: Particle morphology and molecular integrity, *J. Supercrit. Fluids*, 40(2): 293-307 (2007).

-
- [20] Ting, S.S.T., Tomasko, D.L., Foster, N.R., Macnaughton, S.J., Solubility of naproxen in supercritical carbon dioxide with and without cosolvents, *Ind. Eng. Chem. Res.*, 32(7): 1471-1481 (1993).
- [21] Krukonis, V.J., Kurnik, R.T., Solubility of solid aromatic isomers in carbon dioxide, *J. Chem. Eng. Data*, 30(3): 247-249 (1985).
- [22] Sacha, G.A., Schmitt, W.J., Nail, S.L., Identification of Physical-Chemical Variable Affecting Particle Size Following Precipitation using a Supercritical Fluid, *Pharm. Dev. Tech.*, 11(2): 195-205 (2006).
- [23] Durling, N.E., Catchpole, O.J., Tallon, S.J., Grey, J.B., Measurement and modelling of the ternary phase equilibria for high pressure carbon dioxide-ethanol-water mixtures, *Fluid Phase Equilibria*, 252(1-2): 103-113 (2007).
- [24] Yao, S., Guan, Y., Zhu, Z., Investigation of phase equilibrium for ternary systems containing ethanol, water and carbon dioxide at elevated pressures, *Fluid Phase Equilibria*, 99(1-2): 249-259 (1994).
- [25] Shoyele, S.A., Cawthorne, S., Particle engineering techniques for inhaled biopharmaceuticals, *Adv. Drug Delivery Rev.*, 58(9-10): 1009-1029 (2006).
- [26] Eckert, C.A., Knutson, B.L., Debenedetti, P.G., Supercritical fluids as solvents for chemical and materials processing, *Nature*, 383(6598): 313-318 (1996).
- [27] Moshashae, S., Bisrat, M., Forbes, R.T., Quinn, E.A., Nyqvist, H., York, P., Supercritical fluid processing of proteins: lysozyme precipitation from aqueous solution, *J. Pharm. Pharmacol.*, 55(2): 185-192 (2003).
- [28] Fages, J., Lochard, H., Letourneau, J.-J., Sauceau, M., Rodier, E., Particle generation for pharmaceutical applications using supercritical fluid technology, *Powder Tech.*, 141(3): 219-226, (2004).
- [29] Werling, J.O., Debenedetti, P.G., Numerical modelling of mass transfer in the supercritical anti-solvent process, *J. Supercrit. Fluids*, 16(1):167-181 (1999).
- [30] Martin, A, Bouchard, A., Hofland, G.W., Witkamp, G.-J., Cocero, M.J., Mathematical modelling of the mass transfer from aqueous solutions in a supercritical fluid during particle formation, *J. Supercrit. Fluids*, 41(1): 68-73 (2007).
- [31] Subramaniam, B., Rajewski, R.A., Snavely, K., Pharmaceutical Processing with Supercritical Carbon Dioxide, *J. Pharm. Sci.*, 86(8): 885-890, (1997).
- [32] Frederiksen, L., Anton, K., van Hoogvest, P., Keller, H.R., Leuenberger, H., Preparation of liposomes encapsulating water-soluble compounds using supercritical carbon dioxide, *J. Pharm. Sci.*, 86(8): 921-928 (1997).
- [33] Walde, P., Preparation of Vesicles (Liposomes), *Encycl. Nanosci. Nanotech.*, 9: 43-79 (2004).
- [34] Brandt, R., Fricke, J., Acetic-acid-catalyzed and subcritically dried carbon aerogels with a nanometer-sized structure and a wide density range, *J. of Non-Crystalline Solids*, 350: 131-135 (2004).
- [35] Haereid, S., Nilsen, E., Einarsrud, M.-A., Subcritical drying of silica gels, *J. of Porous Materials*, 2(4): 315-324 (1996).
- [36] Aravind, P.R., Mukundan, P., Krishna Pillai, P., Warriar, K.G.K., Mesoporous silica-alumina aerogels with high thermal pore stability through hybrid sol-gel route followed by subcritical drying, *Microporous Mesoporous Mat.*, 96(1): 14-20 (2006).
- [37] Winters, M. A., Knutson, B. L., Debenedetti P.G., Sparks, H.G., Przybycien, T.M., Stevenson, C.L., Prestrelski, S.J, Precipitation of proteins in supercritical carbon Dioxide. *J. Pharm. Sci.* 85(6):586-594 (1996).
- [38] Heinrich, T., Kleit, U., Fricke, J., Aerogels-Nanoporous Materials Part I: Sol-Gel Process and Drying of Gels, *J. Porous Mat.*, 1(1): 7-17 (1995).

-
- [39] Spycher, N., Pruess, K., Ennis-King, J., CO₂-H₂O mixtures in the geological sequestration of CO₂. I. Assessment and calculation of mutual solubilities from 12 to 100°C and up to 600 bar. *Geochim. et Cosmochim. Acta*, 67(16): 3015-3031 (2003).
- [40] Sabirzyanov, A.N., Shagiakhmetov, R.A., Gabitov, F.R., Tarzimanov, A.A., Gumerov, F.M., Water Solubility of Carbon Dioxide under Supercritical and Subcritical Conditions, *Theoretical Foundations of Chem. Eng.*, 37(1): 51-53 (2003).
- [41] Wubbolts, F.E., Bruinsma, O.S.L., van Rosmalen, G.M., Dry - spraying of ascorbic acid or acetaminophen solutions with supercritical carbon dioxide, *J. of Crystal Growth* 198/199 (Pt. 1): 767-772 (1999).
- [42] Perez de Diego, Y., Pellikaan, H.C., Wubbolts, F.E., Witkamp, G.J., Jansens, P.J., Operating regimes and mechanism of particle formation during the precipitation of polymers using the PCA process, *J. of Supercritical Fluids*, 35(2): 147-156 (2005).
- [43] Perez de Diego, Y., Wubbolts, F.E., Witkamp, G.J., Jansens, P.J., Improved PCA Process for the Production of Nano- and Micro particles of Polymers, *AIChE Journal*, 50(19): 2408-2417 (2004).
- [44] Hofland, G.W.; Van Es, M., Van der Wielen, L.A.M., Witkamp, G.-J., Isoelectric Precipitation of Casein Using High - Pressure CO₂, *Industrial & Engineering Chemistry Res.*, 38(12): 4919-4927 (1999).
- [45] Jackson, M., Mantsch, H.H., Beware of proteins in DMSO. *Biochimica et Biophysica Acta, Protein Structure and Molecular Enzymology*, 1078(2), 231-235 (1991).
- [46] Palakodaty, S., York, P., Phase behavioral effects on particle formation processes using supercritical fluids. *Pharm. Res.*, 16(7): 976-985 (1999).
- [47] Hanna, M., York, P., Method and apparatus for the formation of particles, WO9401426 (1998).
- [48] Lengsfeld, C.S., Delplanque, J.P., Barocas, V.S., Randolph, T.W., Mechanism Governing Microparticle Morphology during Precipitation by a Compressed Antisolvent: Atomization vs. Nucleation and Growth, *J. Phys. Chem. B*, 104(12): 2725-2735 (2000).
- [49] Duhkin, S.S., Shen, Y., Pfeffer, D.R., Droplet mass transfer, intradroplet nucleation and submicron particle production in two-phase flow of solvent-supercritical anti-solvent emulsion, *Coll. Surf. A*, 261(1-3): 163-176 (2005).
- [50] Lim, J.S., Lee, Y.Y, Phase equilibria for carbon dioxide-ethanol-water system at elevated pressures, *J. Supercritical Fluids*, 7(4): 219-230 (1994).
- [51] Jovanovic, N., Bouchard, B., Hofland, G.W., Witkamp, G.-J., Crommelin, D.J.A., Jiskoot, W., Stabilization of proteins in dry powder formulations using supercritical fluid technology, *Pharm. Res.*, 21(11): 1955-1969 (2004).
- [52] Thiering, R., Dehghani, F., Dillow, A., Foster, N.R., The influence of operating conditions on the dense gas precipitation of model proteins, *J. Chem. Technol. Biotech.*, 75(1): 29-41 (2000).
- [53] Chavez, F., Debenedetti, P.G., Luo, J.J., Dave, R.N., Pfeffer, R., Estimation of the Characteristic Time Scales in the Supercritical Antisolvent Process, *Ind. Eng. Chem. Res.*, 42(13): 3156-3162 (2003).
- [54] European Medicines Agency, Impurities: Residual Solvents, CPM/ICH/283/95 (1998).
- [55] Taylor, L.S., York, P., Characterization of the phase transitions of trehalose dihydrate on heating and subsequent dehydration, *J. Pharm. Sci.*, 87(3): 347-355 (1998).
- [56] Castor, T.R., Phospholipid Nanosomes, *Current Drug Delivery*, 2(4): 329-340 (2005).
- [57] Adrian, T., Wendland, M., Hasse, H., Maurer, G., High-pressure multiphase behavior of ternary systems carbon dioxide-water-polar solvent: Review and modelling with the Peng-Robinson equation of state, *J. Supercrit. Fluids*, 12(3): 185-221 (1998).
- [58] Chrastil, J., Solubility of solids and liquids in supercritical gases, *J. Phys. Chem.*, 86(15): 3016-3021 (1982).

-
- [59] Bamberger, T., Erickson, J.C., Cooney, C.L., Kumar, S.K., Measurement and model prediction of solubilities of pure fatty acids, pure triglycerides, and mixtures of triglycerides in supercritical carbon dioxide, *J. Chem. Eng. Data* 33(3): 327-333 (1988).
- [60] Hamman, H., Solubilities of pure lipids in supercritical carbon dioxide, *J. Supercrit. Fluids*, 5(2): 101-106 (1992).
- [61] Reverchon, E., Caputo, G., De Marco, I., Role of Phase Behavior and Atomization in the Supercritical Antisolvent Precipitation, *Ind. Eng. Chem. Res.*, 42(25): 6406-6414 (2003).
- [62] Adrian, T., Wendland, M., Hasse, H., Maurer, High-pressure multiphase behavior of ternary systems carbon dioxide-water-polar solvent: Review and modeling with the Peng-Robinson equation of state, *J. Supercrit. Fluids*, 12(3): 185-221 (1998).
- [63] Xia, J., Joedecke, M., Perez-Salado Kamps, A., Maurer, G., Solubility of CO₂ in (CH₃OH + H₂O), *J. Chem. Eng. Data*, 49(6): 1756-1759 (2004).
- [64] Lazzaroni, M.J., Bush, D., Brown, J.S., Eckert, C.A., High - pressure vapor -liquid equilibria of some carbon dioxide + organic binary systems, *J. Chem. Eng. Data*, 50(1): 60-65 (2005).
- [65] Bamberger, A., Mauer, G., High-pressure (vapour + liquid) equilibria in (carbon dioxide + acetone or 2-propanol) at temperatures from 293 K to 333 K, *J. Chem. Thermodyn.*, 32(5): 685-700 (2000).
- [66] Reverchon, E., Della Porta, G., Di Trolio, A., Pace, S., Supercritical antisolvent precipitation of nanoparticles of superconductor precursors, *Ind. Eng. Chem. Res.*, 37(3): 952-958 (1998).
- [67] Xia, J., Joedecke, M., Perez-Salado Kamps, A., Maurer, G., Solubility of CO₂ in (CH₃OH + H₂O), *J. Chem. Eng. Data*, 49(6): 1756-1759 (2004).
- [68] Jödecke, M., Perez-Salado Kamps, A., Maurer, G., Experimental Investigation of the Solubility of CO₂ in (Acetone and Water), *J. Chem. Eng. Data*, 52(3): 1003-1009 (2007).
- [69] Zhang, X., Zhand, X., Han, B., Shi, L., Li, H., Yang, G., Determination of constant volume heat capacity of mixed supercritical fluids and study on the intermolecular interaction, *J. Supercrit. Fluids*, 24(3): 193-291 (2002).
- [70] Fulton, J.L., Yee, G.G., Smith, R.D., Hydrogen bonding of simple alcohols in supercritical fluids. An FTIR study, *ACS Symposium Series*, 514 (Supercritical Fluid Engineering Science): 175-187 (1993).
- [71] Yao, S., Guan, Y., Zhu, Z., Investigation of phase equilibrium for ternary systems containing ethanol, water and carbon dioxide at elevated pressures, *Fluid Phase Equilibria*, 99(1-2): 249-259 (1994).
- [72] Choi, Y.H., Kim, J., Noh, M.J., Choi, E.S., Yoo, K.P., Effect of functional groups on the solubilities of coumarin derivatives in supercritical carbon dioxide, *Chromatographia*, 47(1/2): 93-97 (1998).
- [73] Gupta, R.B., *Solubility in Supercritical Carbon Dioxide*, p: 735, CRC Press (1996).
- [74] Sackett, D.A., Wolff, J., Nile Red as A Polarity-Sensitive Fluorescence Probe of Hydrophobic Protein Surfaces, *Anal. Biochem.*, 167(2): 228-234 (1987).
- [75] Krishnamoorthy, I., Krishnamoorthy, G., Probing the link between proton transport and water content in lipid membranes, *J. of Phys. Chem. B*, 105(7): 1484-1488 (2001).
- [76] Hungerford, G., Castanheira, E.M.S., Baptista, A.L.F., Coutinho, P.J.G., Real Oliveira, E.C.D., Domain Formation in DODAB-Cholesterol Mixed Systems Monitored via Nile Red Anisotropy, *J. of Fluorescence*, 15(6): 835-840 (2005).
- [77] Hungerford, G., Ferreira, J.A., The effect of the nature of retained solvent on the fluorescence of Nile Red incorporated in sol-gel-derived matrices, *J. of Luminescence*, 93(2): 155-165 (2001).
- [78] Berger, T.A., Deye, J.F., Anderson, A.G., Nile Red as A Solvatochromic Dye for Measuring Solvent Strength in Normal Liquids and Mixtures of Normal Liquids with Supercritical and Near Critical Fluids, *Anal. Chem.*, 63(6): 615-622 (1990).

Chapter 10

Summary of the Evaluated Drying Technologies

Abstract:

Formulation research always has to focus on the stability of the active compound within a new formulation. For market approval a product ideally has to be stable for at least two years at the selected storage conditions. If the stability of a liquid formulation is not sufficient numerous pharmaceutical drying processes are available each with advantages and disadvantages. In this thesis several technologies were evaluated for drying the liposomal product EndoTAG[®]-1. This chapter provides an overview and a comparison of the evaluated techniques.

1. NEW LIPOSOME FORMATION TECHNIQUE

The currently used liposome formation techniques are considered as time consuming, as they are composed of several complex production steps. In this thesis various techniques for liposome preparation were compared. We investigated a new single pass extrusion technique (Chapter 6), to adjust large polydisperse vesicles in a single step to liposomes with a smaller size and a narrow homogenous size distribution. The idea of using the shear forces within the nozzle for the preparation of homogenous liposomes out of multi-lamellar vesicles (MLV) without a consecutive extrusion process originated during the spray-drying experiments. Based on this assumption we developed a new liposomal preparation technique to obtain small liposomes with homogenous size distribution in a single step by an inline extrusion at high pressure followed by an atomization step. The technique was implemented into a spray-drying (Chapter 7), inert spray-drying (Chapter 8) or supercritical fluid-drying (chapter 9) set-up.

2. SCALABILITY AND INDUSTRIAL USE OF THE EVALUATED DRYING TECHNIQUES

Figure 1 provides a classification of the techniques evaluated in the context of the thesis to dry liposomal placebo formulations and the Paclitaxel containing EndoTAG[®]-1 formulation according to their employment for industrial production and scalability. Freeze-drying, spray-drying and spray freeze-drying are already approved by regulatory authorities and there are products on the market available stabilized by these techniques. In this context, freeze-drying and spray-drying are the prevalent and most advanced techniques for industrial production.

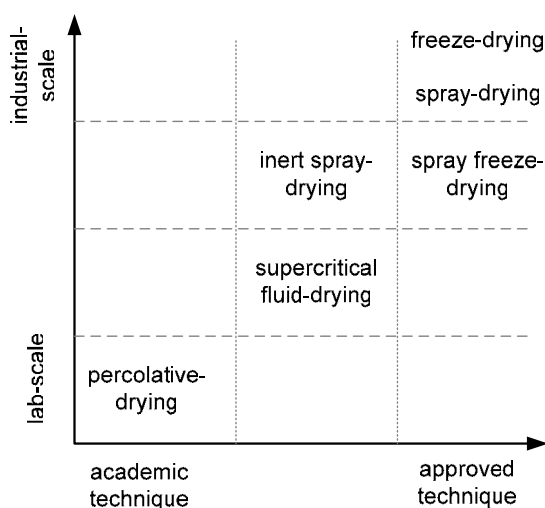


Figure 1: Classification of drying techniques for liposomal formulations in respect of scalability and employment for industrial production.

The scale-up is thereby less problematic and easier to perform for the continuous spray-drying as compared to freeze-drying, which is typically run in the batch mode. The spray freeze-dried products exhibit several advantages e.g. the liposomal integrity after the process and the properties of the freely flowable bulk material, but the scalability as an industrial process is more complex as compared to spray-drying. The handling of liquid nitrogen and transfer of particles into the drying chamber is complicated and requires special technical equipment. Inert spray-drying and supercritical fluid-drying can be classified between academic interest and approved techniques. Up to now, no pharmaceutical product is prepared by these methods and the technical requirements are, especially for the supercritical fluid-drying, more complex as compared to freeze-drying or spray-drying. Although the supercritical fluid technique is frequently used for extraction processes in food industry, like decaffeination, the acceptance in pharmaceutical production is still very low. The limited number of available commercial plants, the compliance of good manufacturing processes (GMP) and sterility impeded a faster development. The newly developed percolative vacuum-drying, which is on the basis of the vacuum fluidized bed drying proposed by the group of Leuenberger, is just at the beginning and needs further investigations.

3. COMPARISON OF THE EVALUATED DRYING TECHNOLOGIES

Table 1 provides a comparison of the used drying technologies concerning product and process parameters.

3.1 FREEZE-DRYING

Although freeze-drying is the appropriate stabilization technique for many products several drawbacks are evident. The time consuming process, limited batch sizes and the difficulties related to each drying step make this technology rather complicated for the EndoTAG[®]-1 formulation. The cake structure and the lack to obtain bulk material like particles make freeze-drying inconvenient for the production of bulk material for flexible dosing. However, the preservation of liposomes and the drug loading are the major advantages of freeze-drying. An optimization of the so far used freeze-drying process for the production of the EndoTAG[®]-1 formulation resulted in a reduction of the primary drying time of at least 20 %. For this optimization, the freezing temperature was reduced from -40 to -50°C. A further approach to increase the productivity lyophilization was an increase of the filling volume from 25 to 50 ml.

Table 1: Comparison of the drying technologies evaluated in the context of the thesis.

technique	one step process	optimum size/PI	used drugs	freezing stress	min heat exposure	process time/liter
freeze-drying	not possible	110 nm 0.25	PXL	-50°C	-	120 h 60* h
spray-drying (two-fluid nozzle)	not possible	168 nm 0.17	PXL	-	50°C	6 h
spray-drying (orifice nozzle)	possible	140 nm 0.16	C NR	-	45°C	10 min
inert spray-drying (orifice nozzle)	possible	130 nm 0.15	C NR	-	40°C	50 min
subcritical fluid-drying	possible	118 nm 0.15	NR	-	35°C	151 h
supercritical fluid-drying	possible	121 nm 0.13	C NR	-	35°C	66 h
supercritical fluid-drying (co-solvent)	possible	125 nm 0.10	NR	-	35°C	33 h
spray freeze-drying	not possible	125 nm 0.18	PXL	-196°C	-	60 h
percolative drying	not possible	150 nm 0.22	C	-196°C	-	4 h

NR: Nile Red, C: Coumarin, PXL: Paclitaxel

* increased filling volume of 50 ml

3.2 SPRAY FREEZE-DRYING

Spray freeze-drying combines the spraying approach to form particles by freezing in liquid nitrogen with a conventional freeze-drying process. Although the spray freeze-drying process revealed no faster drying performance, the advantage of this technique is the obtained particle structure and the very gentle conditions. The liposomal properties and the Paclitaxel recovery were preserved for small and large particles. The product can be handled as bulk material and a broad range of particles sizes can be produced by varying the nozzle type and the freezing conditions.

3.3 PERCOLATIVE VACUUM-DRYING

The newly developed percolative vacuum-drying step, which combines several aspects of spray freeze-drying, vacuum-drying and atmospheric freeze-drying allowed reducing the drying time of spray-frozen particles. To increase the driving force for heat and mass transfer a percolation gas was streamed through the particle layer during PVD resulting in drying times below four hours. Trehalose crystallization during the process is a disadvantage of the method, although the liposomal integrity was preserved. For the

percolative vacuum-drying process further investigations on the control of the process parameters and the impact on the product are necessary.

3.4 SPRAY-DRYING USING A TWO-FLUID NOZZLE

During the spray-drying process with a two-fluid nozzle the liposomal formulations are subjected to thermal stress by a heat exposure of at least 50°C. Although Paclitaxel is known to be heat sensitive, the liposomal stability and Paclitaxel loading could be preserved to a great extent under these conditions. The fast drying process and the obtained dry flow powder make this technology to a feasible alternative for the time consuming freeze-drying process.

3.5 SPRAY-DRYING WITH AN ORIFICE NOZZLE

A separate liposome formation process was still required in the so far described drying techniques prior to the drying step. Therefore, we aimed to combine the liposome formation and the drying step within one continuous process. The spray-drying concept using an online extrusion through a porous device and an orifice nozzle allowed the size adjustment of the liposomes and the consecutive drying in the same process. This combination simplifies the production process and circumvents the conventional filter extrusion process. The high liquid feed rates allowed an effective liposome formation and drying of up to 100 ml/min under preservation of the liposomal integrity.

3.6 INERT SPRAY-DRYING WITH AN ORIFICE NOZZLE

Experience from spray-drying revealed that the temperature exposure during the drying step led to a degradation of the heat sensitive drug Paclitaxel under some conditions. With the addition of organic solvents to the aqueous formulation a reduced heat capacity and therefore lower temperatures were sufficient to dry the product. The closed inert loop spray-drying system allows the spray-drying of organic solvents in a wider temperature range. Variations of solvents and solvent concentrations enabled a reduction of the drying temperature down to 35°C. The idea of the single-step liposome formation was tested in this set-up, as well. Furthermore, first evaluation studies were performed using a molecular disperse solution of lipids and excipients to overcome the MLV preparation step by ethanol injection and to simplify the production method.

3.7 SUBCRITICAL AND SUPERCRITICAL FLUID-DRYING

For setting up the subcritical and supercritical fluid-drying long process development times were necessary for finding optimum drying conditions. At working conditions above the critical point the drying process was maintained at low temperature of 40°C. Supercritical drying of aqueous liposomal formulation without the addition of co-solvents to the supercritical CO₂ was possible, but only at reduced liquid flow rates prolonging the process times. Drying became more effective by the addition of organic co-solvents, with best results concerning liposomal properties for acetone. Organic co-solvents are related to the risk of a reduced lipid and drug recovery, as they increase the solubility of these compounds in the supercritical phase. To overcome this, subcritical conditions were used by reducing the pressure in the system with the consequence that the mass transfer of carbon dioxide has to be significantly increased to compensate the reduced water solubility. The advantage is the preservation of both, hydrophilic and hydrophobic compounds by the subcritical approach.

4. CONCLUSIONS

The study provides a comprehensive overview on different stabilization techniques for liposomal formulations. The selection of the appropriate technology for a particular formulation can thereby be based on several considerations. If free flowable particulate bulk material is desired the spraying-technologies are preferred over lyophilization. Another advantage of spraying-based technologies is the possibility to combine the liposome formation step and the drying step within the same process. It is a prerequisite for the selection of the stabilization technique that the integrity of the liposomes is preserved with the incorporated drug after the process. Spray-drying is related to a thermal stress for the formulation but only for a short time. For heat labile drugs processes with low process temperatures, e.g. freeze-drying, spray freeze-drying, inert-spray drying or supercritical drying are most adequate. However, for technologies with a freezing step a sufficient stabilization against freezing induced stress e.g. by the selection of appropriate cryoprotectors is needed.

The goal to circumvent the time-consuming lyophilization step for the Paclitaxel containing EndoTAG[®]-1 formulation could be achieved by selecting spray-drying with a two-fluid nozzle as alternative technique. The feasibility to dry Paclitaxel containing formulations needs to be proofed for spray-drying with an orifice nozzle, inert spray-drying, sub- and supercritical drying, as well as percolative drying, which was so far

proofed only for selected model compounds. Alternatively, inert spray-drying or supercritical drying could be used as the drying temperature and with it the formation of degradation products can be significantly reduced as compared to conventional spray-drying.

ABBREVIATIONS

DOPC	1,2-dioleoyl- <i>sn</i> -glycero-3-phosphocholine
DOTAP-Cl	1,2-dioleoyl-3-trimethylammonium-propane-chloride
DSC	differential scanning calorimetry
HS-GC	static headspace gas chromatography
$M_{aa/lf}$	mass ratio of atomizing air to liquid feed
MLV	multi-lamellar-vesicles
NIBS	non invasive back-scatter technique
Oh	Ohnesorge number
PCA	precipitation with compressed anti-solvent
PCS	photon correlation spectroscopy
PI	polydispersity index
PVD	percolative vacuum-drying
PXL	Paclitaxel
Re	Reynolds number
RP-HPLC	reversed phase high performance liquid chromatography
SeD	secondary-drying
SEM	scanning electron microscopy
SCF	supercritical fluids
T_c	collapse temperature
T_{eu}	eutectic temperature
T_g	glass transition temperature
T_g^*	glass transition temperature of the maximally freeze-concentrated solution
TICT	twisted intramolecular charge transfer
T_{inlet}	inlet temperature
T_{nc}	no collapse range
T_{outlet}	outlet temperature
V_{aa}	atomizing air volumetric flow rate
VD	vacuum-drying
V_{da}	drying air volumetric flow rate
V_{lf}	liquid feed volumetric flow rate
We	Weber number
XRD	X-ray powder diffraction

LIST OF PUBLICATIONS AND PRESENTATIONS

PATENTS

M. Wiggenhorn, H. C. Pellikaan, G. Winter, Preparation of Powders Containing Colloidal Particles, WO2007065716, 2007.

M. Wiggenhorn, H. Haas, K. Drexler, G. Winter, Perculative Drying for the Preparation of Particles, EP06022538.0, 2006.

M. Wiggenhorn, H. Haas, K. Drexler, G. Winter, Liposome Preparation by Single-Pass Process, EP06023155.0, 2006.

JOURNALS

M. Hossann, M. Wiggenhorn, A. Schwerdt, K. Wachholz, N. Teichert, H-J. Eibl, R. D. Issel, L. H. Lindner, In vitro stability and content release properties of phosphatidyl-glyceroglycerol containing thermosensitive liposomes, BBA Biomembranes, 1768(10): 2491-2499, 2007.

M. Wiggenhorn, I. Presser, G. Winter, The Current State of PAT in Freeze-Drying; American Pharmaceutical Review, Volume 8 (1), 38-44, 2005.

POSTER AND PODIUM PRESENTATIONS

M. Wiggenhorn, H. Haas, K. Drexler, G. Winter, Application of Inert-Spray-Drying for the Formation and Stabilization of Liposomes, AFSIA & EFCE European Drying Conference, Biarritz, France, 2007.

M. Wiggenhorn, H. Haas, K. Drexler, G. Winter, Enhancing the Lyophilization Efficiency of a Liposomal Paclitaxel Formulation (EndoTAG-1TM), PSWC, Amsterdam, The Netherlands, 2007.

M. Wiggenhorn, H. C. Pellikaan, H. Haas, K. Drexler, G. Winter, Supercritical Fluid Drying of Aqueous Cationic Liposomal Formulations, AAPS Annual Meeting, San Antonio (TX) USA, 2006.

G. Winter, M. Wiggenhorn, Application of Spray Drying Technologies for Stabilization of Liposomes, European Conference Academy, Spray Drying- Solution for Pharmaceutical Industry, Lisbon, Portugal, 2006.

M. Wiggenhorn, H. Haas, K. Drexler, G. Winter, Spray-Freeze-Drying of a Cationic Liposomal Paclitaxel Formulation (EndoTAG-1™), Freeze-Drying of Pharmaceuticals and Biologicals, Garmisch-Partenkirchen, Germany, 2006.

M. Wiggenhorn, H. Haas, G. Winter, Spray-Freeze-Drying of Cationic Liposomal Formulation; 5th World Meeting on Pharm. Biopharm. and Pharm. Tech., Geneva, Switzerland, 2006.

M. Wiggenhorn, H. C. Pellikaan, G. Winter, Application of Near- and Supercritical Fluids to Dry Aqueous Liposomal Formulation; 5th World Meeting on Pharm. Biopharm. and Pharm. Tech., Geneva, Switzerland 2006.

M. Wiggenhorn, G. Winter, H. Haas, Application of DSC in the Development of Parenteral Formulations of Paclitaxel-derivatives for Targeted Delivery, 32nd Annual Meeting & Exposition, CRS, Miami Beach, USA, 2005.

Curriculum Vitae

MICHAEL WIGGENHORN

PERSONAL DETAILS

Date of birth: April 03, 1977
Place of birth: Kranenburg, Germany
Nationality: German

EDUCATION

03/2004 – 07/2007 PhD Thesis
Department of Pharmacy, Pharmaceutical Technology and
Biopharmaceutics, Ludwig-Maximilians University, Munich
Supervisor: Prof. Dr. G. Winter

08/2002 – 12/2003 MSc Master of Science in Biopharmaceutics
Drug Delivery and Technology
Leiden/Amsterdam Center of Drug Research (LACDR)
Leiden University, The Netherlands
Supervisors: Prof. Dr. G. Borchard and Prof. Dr. H.E. Junginger

09/2003 – 10/2003 Internship at Octoplus, Leiden, The Netherlands

09/2002 – 08/2003 Master thesis in cooperation with Delft University of Technology,
Process and Energy Department and FeyeCon D&I, Weesp
The Netherlands

09/1998 – 07/2002 Dipl Ing Pharmaceutical Engineering
University of Applied Science, Lippe and Hoexter,
Department of Pharmaceutical Technology, Detmold
Supervisor: Prof. Dr. G. Kutz

09/2001 – 05/2002 Diploma thesis at Haupt Pharma AG, Münster

07/2000 – 09/2000 Internship at Rottendorf Pharma GmbH, Ennigerloh